

**Freeform Framing:**

**High-performance Bending-active Strip Construction**

by

**Richard Aeck**

M.A., Arch., Georgia Institute of Technology, 2007

B.A., Econ., Wake Forest University, 2001

Submitted to the Department of Architecture  
in partial fulfillment of the requirements for the degree of

**Master of Science in Architecture Studies**

at the

**Massachusetts Institute of Technology**

February 2017

© 2015 Richard Aeck. All rights reserved.

The author hereby grants to MIT the permission to reproduce and to distribute publicly paper and electronic copies  
of this thesis document in whole or in part in any medium now known or hereafter created.

**Signature redacted**

Signature of Author: \_\_\_\_\_

Department of Architecture  
January 17, 2017

**Signature redacted**

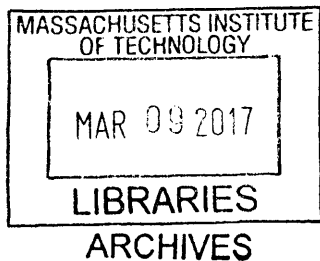
Certified by: \_\_\_\_\_

John Ochsendorf  
Class of 1942 Professor of Architecture and Civil and Environmental Engineering  
Thesis Supervisor

**Signature redacted**

Accepted by: \_\_\_\_\_

Shelia Kennedy  
Professor of Architecture  
Chair of the Department Committee on Graduate Students



**Free4orm Framing:**  
**High-performance Bending-active Strip Construction**

by  
**Richard Aeck**

**Thesis Committee**

John Ochsendorf  
Professor of Architecture and Civil and Environmental Engineering  
Thesis Supervisor

Caitlin Mueller  
Assistant Professor of Architecture and Civil and Environmental Engineering  
Guest Critic, Digital Structures and Structural Design Lab

**Free4orm Framing:**  
**High-performance Bending-active Strip Construction**

by

**Richard Aeck**

Submitted to the Department of Architecture  
on January 17, 2017 in Partial Fulfillment of the  
Requirements for the Degree of  
Master of Science in Architecture Studies

**ABSTRACT**

This thesis re-thinks conventional light frame and panelized construction methodologies employed in residential and general medium-scale construction. To do so, it investigates the flexural geometry, the structural performance, and volumetric approaches to systematizing elastically bent developable strips. Many rapidly-renewable sheet materials exist or are near market, and the local availability of flatbed machining increases with each new makerspace. Thus, this thesis proposes using simple cutting and bending operations, site-applied attachments, and granulated insulation to produce permanent, freeform, stressed-skin formwork (which is herein branded "Free4orm" strip construction). Observing only partial engagement of medium-scale building applications, this project deploys elastic bending for design diversity by developing open, pre-cut, site-assembled systems for complex structural form.

Initial contextual, typological, and geometric research exercises lead to an experimental installation (fiber-reinforced polymer rod and shrink-wrap), to material testing (plywood, bamboo, and phenolic paper), and then to creating computational dimensional analysis tools. Different methods of assembling (tiling, hinging, linking, networking, self-straining, wrapping, staggering etc.) and "unitizing" bending-active strips are developed, tested, and ultimately combined into a prototype, "bend-up, zip-up, iron-up," methodology.

Numerical solvers and plug-ins (Strand7, Karamba, and Scan&Solve) are used for in-process analysis to inform conceptualization and to supplement theoretical predictions. Full-scale prototype "unitized, rapid-assembly" and "semi-unitized, site-assembly" specimens are fabricated and experimentally loaded to evaluate theoretical stress predictions and preliminary detailing. In the closing design exercises and demonstrations, a single-module arch and a heliotropic canopy are presented. This project explores different possibilities for using flexure to create cost-aware dimensional variation in residential building systems in order to enable passive functional articulation and increase access to surface-active architecture.

*Active bending; Advanced framing; Bamboo; Building systems; Construction; Developable; Elastica; Extreme ironing, Freeform; Panelized; Plywood; Prefabricated; Segmented shells; Stressed-skin panels; Structural Insulated Panels.*

Thesis Supervisor: John Ochsendorf  
Title: Class of 1942 Professor of Architecture and Civil and Environmental Engineering

## DEDICATION

For  
**People and Variety**

*Entities ranging from atoms and molecules to biological organisms, species, and ecosystems may usefully be treated as assemblages, and therefore as entities that are products of historical processes.*

**[Delanda 2006, after Deleuze]**

*Because glass is stiff and rigid in its own plane, we were able to use the glass plane to restrain the mullion.*

**[Rice 1994]**

*If anything emerges to cut up, I'll go anywhere anytime.*

**[Matta-Clarke 1975]**

*Everything made for the greatest number is ugly, dreadful, misleading, and fraudulent.*

*That is what I think is so serious.*

**[Prouvé 1971]**

## **ACKNOWLEDGEMENTS**

The author would like to thank the Thesis Committee in particular, others directly contributing to this work, and those helping indirectly by sustaining my idealism over the years for which I am deeply grateful.

### **Collaborators**

Keldin Sergheyev and Yundong Yang \*

### **Contributors, Special Thanks**

Keyan Rahimzadeh, Justin Lee, Jamie O'Kelley, Anthony Kantzas, Carl Solander, and to my patient family Antonin Aeck, Frank Hull, Molly Aeck, and Jim Hull.

### **Thanks Also**

Shunji Ishida, Jean-Francois Blassel, Nader Tehrani, Bruce Nichol, Marc Simmons, Monica Ponce de Leon, Richard Gluckman, Richard Taylor II and III, Tristan Al Haddad, Franca Trubiano, Nat Oppenheimer, Minh Man Nguyen, Sophie Pennetier, Paul Ehret, Andreas Schnubel, Brandon Clifford, Kyoung-Hee Kim, Chris Dewart, Stephen Rudolph, Kirk Turner, Leonard Lowery, Robert Bricker, and Nathalie Lewis.

\* Over the course of the project, two individuals collaborated regularly for extended periods and made some important contributions. In spring and summer 2016, Keldin Sergheyev contributed technically by coding the computational elastica tool and helping to expand the detailed analysis workflows located in appendices C and E. In fall 2015, Yundong Yang contributed creatively and physically on an installation as part of an elective studio.

# CONTENTS

<b>Abstract .....</b>	<b>3</b>
<b>Dedication .....</b>	<b>4</b>
<b>Acknowledgements .....</b>	<b>5</b>
<b>Contents .....</b>	<b>6</b>
<b>1. Introduction.....</b>	<b>7</b>
1.1 <i>Construction Methodology</i> (Macro)	
1.2 <i>Detached Motivation</i> (Detached)	
1.3 <i>Problem Statement</i> (1Q-to-3P)	
1.4 <i>Problem – Construction</i> (2D, Conceptual)	
1.5 <i>Problem – Geometry</i> (2D-to-3D, Material)	
1.6 <i>Problem – Performance</i> (2D-to-3D, Material, Operational, Structural)	
<b>2. Literature .....</b>	<b>19</b>
2.1 <i>Literature – Construction</i> (Light frame, Panelized, Prefabricated)	
2.2 <i>Literature – Geometry</i> (Elastica, Ruled, Developable)	
2.3 <i>Literature – Performance</i> (Material, Operational, Structural)	
<b>3. Methodology .....</b>	<b>52</b>
3.1 <i>Methodology – Virtual</i>	
3.2 <i>Methodology – Rational</i>	
3.3 <i>Methodology – Evolutionary</i>	
3.4 <i>Methodology – Experimental</i>	
<b>4. Analysis .....</b>	<b>60</b>
4.1 <i>Analysis – Construction</i>	
4.2 <i>Analysis – Geometry</i>	
4.3 <i>Analysis – Performance</i>	
<b>5. Results.....</b>	<b>87</b>
5.0 <i>Results – Kerfed, Reinforced, Indexed Box-beam</i> (GEN.0)	
5.1 <i>Results – Kerfed, Reinforced, Friction-fit Panel</i> (GEN.1)	
5.2 <i>Results – Unitized, Rapid-assembly Method</i> (GEN.2)	
5.3 <i>Results – Semi-unitized, Self-assembly Method</i> (GEN.3)	
5.4 <i>Results – Combined Results</i> (GEN.4)	
<b>6. Discussion.....</b>	<b>99</b>
<b>7. Conclusion .....</b>	<b>112</b>
<b>8. Demonstrations .....</b>	<b>116</b>
<b>References .....</b>	<b>127</b>
<b>Index – Figures .....</b>	<b>133</b>
<b>Index – Tables .....</b>	<b>138</b>
<b>Index – Variables .....</b>	<b>140</b>
<b>Index – Equations .....</b>	<b>143</b>
<b>Appendix – A (Assumptions).....</b>	<b>149</b>
<b>Appendix – B (Basis of Design).....</b>	<b>155</b>
<b>Appendix – C (Calculations).....</b>	<b>161</b>
<b>Appendix – D (Data, Logs).....</b>	<b>170</b>
<b>Appendix – E (Elastica).....</b>	<b>174</b>

# 1. INTRODUCTION

In this *Chapter*, the first *Section 1.1 – Construction Methodology* establishes the research topic, describes document organization, and expands on the thesis vision and objectives. The following *Section 1.2 – Detached Motivation* addresses the detached home and examines related contextual motivation. Subsequently, *Section 1.3 – Problem Statement* introduces and describes the multi-objective design problem.

## 1.1 Construction Methodology

### Methodological Context



**Fig. 1.1 Conventional Construction – Methodologies: (a.) Light frame; (b.) Panelized.**

*Methodological origination; both conventions developed “pre-digital,” and their fundamental assumptions are static.*

[Photos: by Author; Borson 2014]

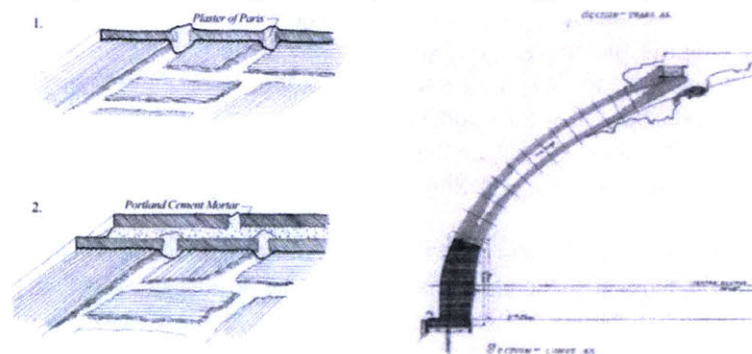
*Conventional. (Construction)* Today, the most commonly employed methods for constructing homes and similarly sized structures in North America still combine different material classes on site: those processed directly into dimensional lumber (e.g., studs or joists) and those processed further into sheet materials (e.g., laminated-veneer or sheathing products). Historically, the U.S. population increased tenfold from the 1790 to the 1870 census [Gauthier 2002] creating a housing problem. This rapid-expansion, inefficiency in milling lumber, joinery requirements, the lack of skilled labor, transport, and the resulting cost of *timber framing* were fundamental to generating the demand for more accessible and economical construction alternatives. Among the many contemporaneous technological means being introduced – such as the machine-made nail, the circular saw, the edger, the planer, and the steam-powered sawmill [Armstrong 2012] – was the capacity for the commercial production of dimensional lumber. With resources still abundant and lumber increasingly affordable, light frame construction methodology developed both of and for the challenges of America. Examples of the specific method *balloon framing* have been identified that suggest its emergence in the early 1830s [Gideon 1952], and other claims as much as 30 years earlier were encountered.

Important to the current project is the underlying conceptual logic of why light frame construction methodology developed, which was to address an absence of means, a specific need. Also relevant is that it continued to evolve following the subsequent 1832 documentation [Sprague 1983] and that its success was based on simple connections, strength through redundancy, and increased material efficiency and portability [Armstrong 2012]. Similarly, the commercialization of sheet materials in the form of plywood following World War 1 was a catalytic change in method input mechanical properties – one which ultimately contributed to the early 20th century evolution of light frame construction from board-sheathed *balloon framing* to plywood-sheathed *platform framing* [ICS 1905; Youngquist 1977], and inspired the focus on construction methodology in this thesis.

*Architectural. (Geometry)* The historical evolution of methods, along with the evident economy of using *ruled surfaces* [Pottmann et al. 2015; 2007, ch.9] specifically developable strips to approximate complex form [Flory & Nagai et al. 2012; Schiffner & Leduc 2012] and a “field-of-bricks” exercise in an experimental 2015 masonry studio (Ochsendorf & West), influenced the decision to pursue volumetric “fields-of-strips” for medium-scale building applications. Implicit in the declared focus on bending-active developable strips is increased cost- and construction-awareness, as discussed in *Section 3.2*. Beyond practical and cost considerations, a building system’s capacity for geometric variation can create value architecturally, ecologically, economically, spatially, and structurally. A related sentiment was expressed in a letter by artist Gordon Matta-Clark: “a simple cut or series of cuts acts as a powerful drawing device able to redefine spatial situations and structural components” [Diserens 2003]. Likewise, the current project prioritizes cutting and chooses flatbed (multi-axis) CNC equipment to maintain viability across existing and entry-level equipment to retain the option of *self-assembly* (in the sense of do-it-yourself). It also adopts the principle no small-bit operations to reducing machine time with large-bit feed rates. Other project principles and constraints are represented in *Chapter 3 Methodology* and the final basis of design (BOD) is documented in *Appendix – B*.

*Flexural. (Geometry)* To clarify at the outset the integral concept of *active bending*, the archer’s bow is a simple example of a closed, active system that employs bending within the elastic range (or controlled flexural bending) to develop, store, and release strain energy to perform a function. Whether fully drawn or only strung, at the scale of a longbow or child’s toy, the resultant flexural geometry of the bow is predictably an *elastica curve* (or its generalized derivative when sectional properties vary). The portable bow may appropriately be described as a *bending-active* structure because it is “composed of curved beam or shell elements which base their geometry on initially straight or planar configuration” [Knippers et al. 2013; 2011]. Both the kinetic bow and the installation herein would be classified as “behavior based” design approaches since they have in common an empirical, elastic deformation process as opposed to a distinct structural type [interpreting Lienhard et al. 2013].

*Structural. (Vision)* In place of the familiar bow, now imagine flat, renewable sheet materials extending beyond a discrete plane and the strain energy retained instead of released. The captured energy is re-purposed to “stress-stiffen” [Takahashi 2015, p.31] at the level of the assembly and continuous hinges between neighboring strips blocked from rotation targeting global performance. This structural premise is common to many of the prototypes developed in the course of this project. It also introduces one of the challenges for bending-active systems: how to approach stiffening and stabilizing them sufficiently for combined loads and service? With respect to structure type, this thesis focuses on stressed-skin panels and segmented shells, and philosophically it promotes methodology as the design space with the most potential to affect what we build. A historical example of methodological innovation is the ingenious tile vaulting method below which evolved over time. In the version shown, quick-setting plaster of Paris is used for initial placement and adjustment of a starter course of sufficient strength to serve as a bed for the Portland cement mortar and the subsequent tile course (or courses, as shown in *Figure 1.2b*).



**Fig. 1.2 Guastavino Construction – Mature method: (a.) First steps; (b.) Vertical section.**

*Methodological evolution; double-shell approximation of complex structural form via layering and staggering tiles.*

[Image: Guastavino Gompamy 1904; Source: Ochsendorf 2010, p.125; p.160]



For a bending-active segmented shell, without the benefit of plaster or mortar to accommodate error accumulating from fabrication or placement, this would need to be accommodated at the joints. However, it could be managed by manipulation of the interlayer connections or attachments (addressed further on) before holding fabrication of the closure panels. Relative to conventional stressed-skin panel construction, the thesis vision is attachment-stiffened multi-layer construction with thinner material, and only point connections between layers.

*Theory. (Project)* Hypothesized is that by developing post-digital building systems with details that anticipate geometric variation and by fine tuning the amount of prefabrication (e.g., using attachments to optimize site-assembly), economical high-performance freeform structures become achievable. The theoretical product – site-assembled permanent formwork – would first be placed, then seamed, and for more extreme climates foamed from the interior before all hold-offs are applied. Ultimately, the cavity is completed with granulated fill blown-in through fill ports. For longer span roofs or multi-story exterior envelopes, reinforcing laminations would be built-up to the interior only to the required thickness. This is conceptually similar to the Guastavino section above (*Figure 1.2b*), but with the reinforcing layers occurring at mid-span. Both horizontal and vertical applications, ranging from freeform roofs and walls to atypical deployments, are intended. Chapters 4 and 5, and the related workflows located in *Appendix – C* and *Appendix – E*, provide insight into the performance potential of networked strip and strip-integrated assemblies, geometry, analysis, and management of post-buckled bending-stress.

*Method. (Concept)* Conceptually, the strip construction methodology proposed delaminates and slices the structural insulated panel (SIP), both linguistically and literally, into renewable, economical, site-assembled plate structures. The closest methodological analogue is stave construction used in cooperage and boatbuilding where members of significant thickness are tapered and bent to produce watertight single-layer shells. For terrestrial construction assuming layers to come, the edge-to-edge joinery is less of a life safety hazard.

*Goal and Objective. (Project)* With an overall goal of contributing to moving us beyond linear sticks and planar sandwiches the project objective becomes more affordable complex structural forms producible on the widest variety of available (or even portable) flatbed CNC mills. This self-imposes simplicity and is conceptually similar to how *light frame construction* gained popularity [Allen & Iano 2014, p.173; AWC 2001; Youngquist 1977], which was by improving general access with manageable-scale inputs, accessible tools, and fasteners in opposition to joinery-dependent *heavy timber construction* [Armstrong 2012; Neufert 2000, p.36, fig.3].

*Methodology. (Project)* Regarding methodology in general, initially this thesis engages the problem of economical surface-active alternatives with topical reviews, followed by preliminary research exercises/experiments/simulations, and ultimately with formal load testing of prototypes. Effectively, the various typological, methodological, and analytical research served as fuel for design development.

*Organization. (Document)* Following this introduction (*Chapter 1*), this thesis provides literature reviews for conventional construction, geometry- and performance-related topics (*Chapter 2*), and then design and load test methodologies (*Chapter 3*) using project examples. The next chapter documents research experiments (*Chapter 4*) and reports on iterative full-scale prototyping and testing (*Chapter 5*). After discussions of the experimental results, the methodological findings (*Chapter 6*), and the project contributions (*Chapter 7*), demonstrations of the different component methods are presented (*Chapter 8*), including a combined working methodology. The final semi-unitized GEN.4 zip-up, iron-up strip system (*Section 8.4*) is a methodological response to the limited capacity for geometric variation that is characteristic of conventional construction.

## 1.2 Detached Motivation

### Detached Context



**Fig. 1.3 Detached – Motivation: (a.) Sameness epidemic; (b.) "Same as it ever was."**

*The homogeneity of detached homes in suburban Las Vegas and a similar sentiment expressed in digital noir.*

[Photo: Burtynsky 2007; Image: Sagmeister 2008]

*Detached. (Residential)* When viewed at a distance, one of the most familiar negative externalities, the mesmerizing homogeneity of American single-use suburbia (Figure 1.3a) is revealed. The story of the single-family detached home is one of space framed and design outcomes constrained by input tectonics, by building system and material properties, by variable local, regional, and socio-economic factors. Wherever one's threshold for repetition, dwellings are personal constructions and more often than not a relatable scale. As extensions of the primitive hut (e.g., Rondelet's 1833 stick- interpretation of Vitruvius) [Zwerger 2012], they are arguably the fundamental unit of architecture, rendering the systems that make them the natural choice for applying our still relatively new digitally-enhanced capabilities. Closer in, the virtual suburban isometric above (Figure 1.3b) is conspicuously uninhabited and an effective critique, down to its well-ordered flowers.

*Snout House. (Detached)* Questioning the present formula and seeking alternatives in technology, the current project pursues plate structures able to counter this placeless-ness in the belief that we can do better than more suburban "snout houses" [de Botton 2006] (i.e., prominent multi-car garages and overbuilding lots), where winding the roads are often employed to relieve the monotony. That conventional panelized and other modular prefabricated methodologies will remain relevant for many applications is not in doubt, however there will also be pre-cut, site-assembled systems after platform framing. This project takes initial steps toward that and is intended to demonstrate the application potential of post-digital capacities at the methodological level rather than a singular elixir for all challenges of detached suburbia. The portability of component parts and assemblies – made from and replaceable with locally available materials and equipment – was important in to the conceptualization of the prototypes herein.

Reviews of the performance of the detached home and other application-specific reviews are addressed in Section 2.3– *Performance*, and the fundamental preliminary point is the technological capacity (i.e., material, modeling, simulation, and milling) presently exists for us to revisit some of the deep-seated methodological assumptions and conventions of residential building systems. Our academic and geometry processing communities are hard at work on annual materially-driven installations for pedagogical and large-scale commercial ends respectfully, while at home we continue to build in the past. This is particularly troubling with housing problems developing on multiple continents, and the pursuit of open and accessible building systems able to respond to context will be increasingly important. Anticipating even just the modes of urbanization as local and variable, there will be a need for residential construction able to respond to atypical, infill, and other challenging sites.

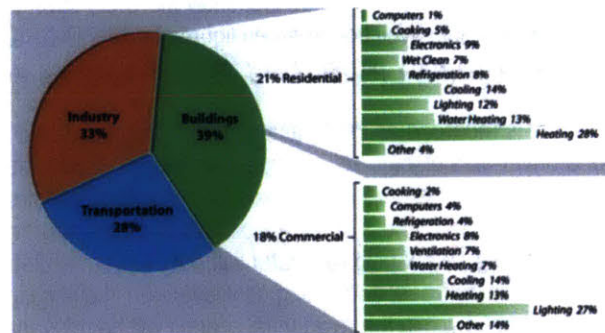


**Fig. 1.4 Detached – Motivation: (a.) Rapid-urbanization; (b.) Car-centric culture.**

*Encroachment of the São Paolo favelas and congestion in Atlanta, where the commuter river exceeds nature's.*

[Photos: Meneghini 2004; CL-ATL 2012]

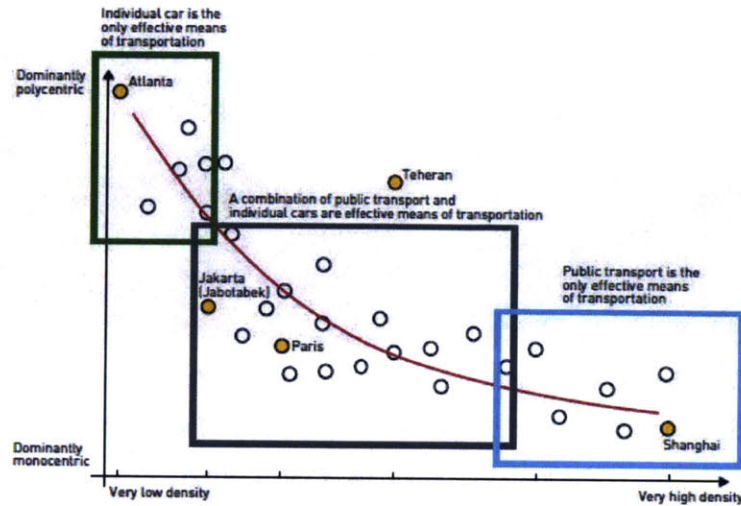
*Population.* Projected global population growth is 2.5 billion by 2050 with 90% in Africa and Asia [UNICEF 2014; UNEP 2013, p.29], and the hazards of mismanaged rapid urbanization are already observable in many places. In whatever modes urbanization is locally manifest, somewhere along the periphery of any 2050 megacity (i.e., cities over 10 million) [NGS (Zwingle) 2002], the mid- and low-rise density will still give way to accretions of attached, semi-detached, and detached homes. If the present extremes in Rio de Janeiro or São Paolo (*Figure 1.4a*) are leading indicators, this will not be predominantly vertical, and for polycentric cities it may more-closely resemble the rhizomatic character of Rocinha or Morumbi favela that is represented above [UN-WUP 2014, p.1–4; UN-Habitat 2016]. Although conceived in response to status quo residential construction in the developed world, climate- and location- specific solutions for the developing world are intended. Certainly, the rapid-assembly method proposed further on could have disaster-relief or humanitarian aid applications. To respond to site-specific context, such variations could feature the same networked plate structure approach, detailing strategies, and functional formal articulations, but use post-consumer or other local waste-mined inputs.



**Fig. 1.5 Detached – Motivation: Buildings Share of Primary Energy Consumption. (U.S.)**

*Within the "22.5% Residential" share, three of the top four categories relate directly and one indirectly, to envelope.*

*Detached.* Assuming global population and CO<sub>2</sub> levels continue on their present trajectories [NOAA-1a & -1b 2016], and that buildings in the U.S. remain the largest share of primary energy consumption [DOE 2012; fig. EIA 2006], developing higher performing, renewable building systems (ideally frame-less future construction) will be increasingly important. The figure above clarifies residential consumption, and the latest data from the 2010 SEDS (State Energy Data System) shows an increase to 41.1% attributable to buildings with residential up to 22.5% of the total, which is 54.7% relative to commercial. Also noted, is the latter value seems to exclude consumption related to the industrial-use and transport involved, as well as the CO<sub>2</sub> emissions. As discussed further on, within the residential segment the detached home is the principal operational energy offender, however it is one within reach to improve.



**Fig. 1.6 Detached – Motivation: Transport Effectiveness in Polycentric Cities. (Global)**

*Above, the relationship between spatial structure and the effectiveness of public transport.*

[Sources: Bertaud 2004; EIA 2012]

*Transport.* The increases in density that will be seen in North America may feel more naturally occurring, but rational investment in public transport has proven not to be (offered as an Atlanta native). Falling within the green rectangle above (*Figure 1.6*), and including other studies dating back to the prescient early 32-city look at density and per capita petroleum use [Newman & Kenworthy 1989], examples of U.S. cities consistently ranking as transport-efficiency or land-use challenged are: Houston, Atlanta, Phoenix, Detroit, Oklahoma City, Denver, Los Angeles, San Francisco, Washington, and Dallas. To the author, more active regulation of investment seems more appropriate than FTA incentives (e.g., grants or matching federal funds) alone for remediation of dominantly car-centric/polycentric cities and successfully manage new urban growth. Hopefully the U.S., having developed via such a rich pageant of rail, will soon manage its second act. Well documented figures by UNEP-GRID Arendal encountered in [Douglas et al. 2011] and [Bertaud & Malpezzi 2003] provide many related infographics and details in this area.

*Cases.* Whether the early 21st-century is recorded as the "glass age" that Corning would have [Morse & Evenson 2016], a renewable energy age or a driver-less electric vehicle age, increasing the performance of the future leaking boxes into which we pump air [Stein et al. 2006] is one of the cases for post-digital construction methodology. Another is that with the efficient precision of CNC and a change input assumptions, a wide variety of passive functional articulations become possible (e.g., managing rainwater without tapered insulation, creating heliotropic roof forms for PV arrays, cutting a few less existing trees, deepening cantilevers on challenging sites, or all of the above). Also, post-digital solutions proving successful within the residential context will be relevant for general medium-scale applications. As we wait for printable, cast- or grown-in-place structural wood and myco-boards [Ecovative 2014] to arrive, to the author, engineered wood, bamboo or even phenolic paper sheet materials are more accessible than what's required for cementitious [Contour Crafting 2014] or cellular-polymeric [Branch Technology 2014] options. The corresponding primer located in *Section 2.3 Analysis – Performance* provides relevant information about detached homes; it and the subsequent observations motivated selecting all-sheet-material systems as the object of and vehicle for this research.

## Industrial Context



**Fig. 1.7 Conventional Construction – Pre-process is constraining:**  
**(a.) Portable sawmill; (b.) Industrial laminator.**

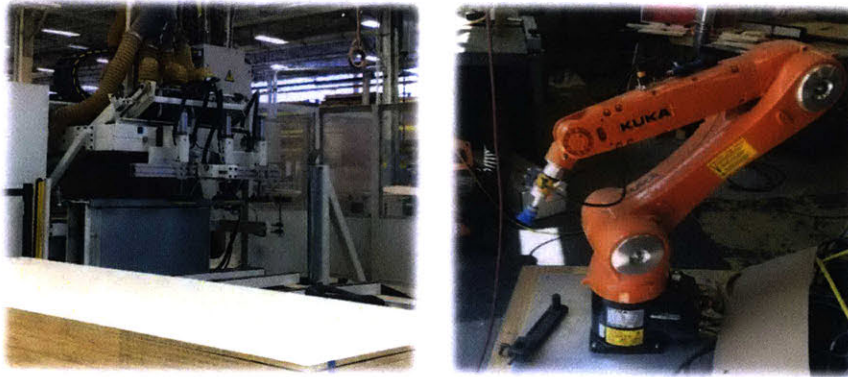
*Self-imposed constraints; the conventional pre-processing assumptions of both industries involve specialty equipment, prioritize feed rate, transport (itself or units), and disincentivize methodological evolution.*

[Photos: Wood-Mizer; by Author]

*Industry.* In the United States, modified 19th century light frame and 1970s panelized methodology are both commonly used for residential and general medium-scale construction. Today's technological innovations are being deployed for industrially prefabricated components (e.g., the I-joist or trussed-joist) to extend conventional systems as opposed to the pursuit of new possibilities. Both the material inputs and the specific methods themselves are complex, and abridging the DeLanda in the *Dedication*, they are entities "that are products of historical processes"; not simply chronological, but evolutionary. This quote comes from a description of the related initial development of the theory of assemblages [Deleuze & Guattari 1987]. For each building system above, layers of constraints are identifiable from entrenched supply-side production and distribution methodologies to material properties and demand-side nostalgia. DeLanda also characterizes *assemblage theory* nearby saying "the theory was meant to apply to a wide variety of wholes constructed from heterogeneous parts." The parts and wholes of the conventional systems above are well-documented and are recapitulated as primers insofar as is necessary to contextualize the research. Commercial industry of course is and will always be glad to help add more parts and layers, or to increase project size. Relative to 1973 single-family home size has increased 56%, and since 1999 it has continued to creep upward; currently it is plateauing [NAHB 2016]. The coincident general improvements in envelope construction and technology call into question whether these are may in fact be having an enabling effect on home size.

Certainly, the demand for conventional systems and our continued enthusiasm for historical styles do not appear to be fading yet. Nevertheless, there is considerable territory between the orthographic status quo and fully custom, one-off engineering solutions. A related study based on 2014 survey of construction (SOC) data focused on single family indicates modular and panelized/pre-cut homes were up sharply especially in the Mid-Atlantic and East North Central [NAHB 2015, p.3–5] region at 9% of new starts. While only 3.2% nationally, the proof of market penetration supports the call for re-engagement of residential construction. At a time concerned with life cycle assessment (LCA) of material inputs, with on-demand "taskers," Fordist assumptions like rolling lamination seem archaic. As far as system-built alternatives go, the development of variable-depth composites assuming a foamed-in-place structural core could be its own thesis. No longer is it necessary for non-standard propositions to carry such premiums or that their production be any further away than a neighborhood makerspace or home-improvement kiosk. If pre-1940 Sears can ship 75,000 kit homes [Thornton 2002] and Ikea can traffic in all manner of do-it-yourself (DIY) goods, it seems reasonable to expect affordable, personalizable construction from the rising tide of CNC-equipment, home improvement retail, and maker spaces.

## Technological Context



**Fig. 1.8 Post-digital Construction – Pre-process is de-constraining:**  
**(a.) Self-loading, flatbed, 5-axis mill; (b.) Water-resistant, 6-axis robot.**

*“The shift to a digital paradigm is the most fundamental technological shift humanity has probably ever encountered.”*

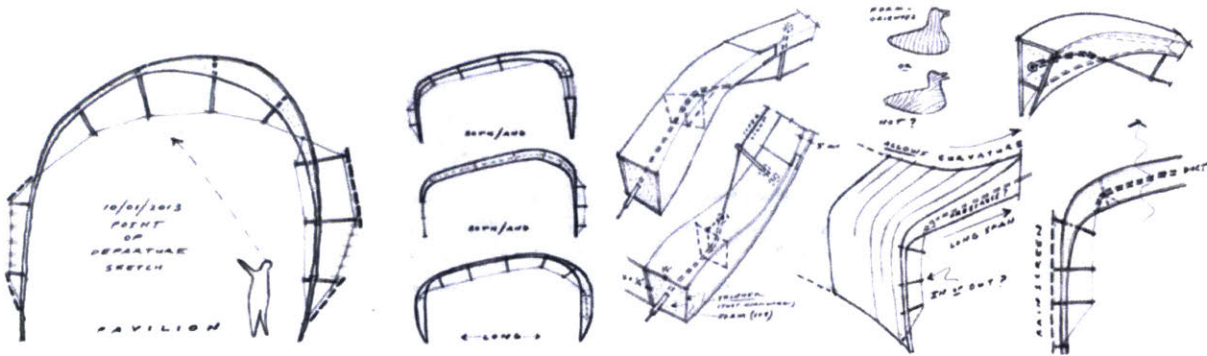
[Photos: by Author; Quote: Kolarevic 2003]

*Technology.* Precision machining has loosened the seams to the extent that repeatable, renewable, non-standard surface-active construction is not only possible but expected. More than a decade after Kolarevic's assertion about the digital shift (above), specialty multi-axis Computer Numerical Control (CNC) equipment is already in-use for diverse applications. There are self-loading, self-cleaning, multi-axis subtractive mills (*Figure 1.8a*). Examples vary from benchtop water-resistant robots (*Figure 1.8b*) and automation of assembly with pneumatics to other innovative forms of additive manufacturing – glass, cellular, welding [Klein 2015; Branch Technology 2015; MX3D 2014]. Yet in residential projects such equipment is more-often employed for the custom cabinetry or stereotomic surfacing foam block for one-off ornaments instead of engaging the way we build.

This so-called "liberation technology" is not exclusive to fabrication. Strategic methodologies like the systematic integration of modeling and simulation in Virtual Design and Construction (VDC) reduce the agency of methods towards more aware design and delivery processes. It is with this in mind that this research advocates redeploying contemporary technology and methodology beyond obvious piece- and object- level applications (e.g., hastening the imitation of historical styles, mass customizing modernism, or churning out and residential micro-texture and blobs) and instead focusing these at the system-level where the greater potential to create meaningful variety exists. There is considerable remaining territory between the orthographic extremes of the status quo and fully customized, one-off engineering solutions.

We are “post-digital” now, as was declared pre-millennium [Negroponte 1998]. Embodied and operational energy performance are increasingly prescribed by code and incentivized by certification for the exterior envelope as political support grows for ecological awareness. While the performance (structural and thermal) of glass- and carbon-fiber reinforced composites is compelling, both are inherently non-renewable and labor intensive. One needs to work with either material once to discover the challenges of modification. These materials require specialized environments which increase, rather than reduce, shop-dependence. While the occasional thermoformed-glass “Shell & Shadow” tram canopy [Nordpark Railway 2007] or stealthy carbon-fiber nest [Bankside Paramorph 2009] are welcomed, the notion of scaling either brings to mind endearingly awkward historical contradictions such as the Lustron homes, which – no matter how they were dressed – could not overcome their fundamental “metal lunchbox” character. These observations about construction methodologies, industry assumptions, and technology provide context for both where we are today and for the multi-objective problem addressed by this thesis. To contextualize the problem statement, the motivating question for selecting the specific problem is posed.

### 1.3 Problem Statement



**Fig. 1.9 Concept Sketches – Point of departure.**

*Variable-depth box-beam and panel systems with integrated cable-trusses.*

[Aeck 2013]

#### **Question of Methodology**

How can the combination of *virtual design*, *pre-rationalization*, *evolutionary design*, and the efficient precision of *computer numerical control* (CNC) machining be focused at the methodological level to create new possibilities for the most-common scale we build?

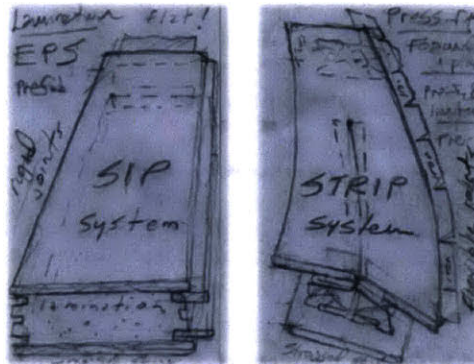
**This thesis sets out to solve three distinct but interrelated problems in order to engage this question and to develop a methodological response addressing the absence of post-digital alternatives to conventional medium-scale construction. These problems are:**

- **The Construction Problem**
- **The Geometry Problem**
- **The Performance Problem**

The three problems are described further in *Section 1.4– Construction*, *Section 1.5– Geometry*, and *Section 1.6– Performance*. This tri-partite structure is employed where possible throughout to clarify the different scopes. The corresponding literature reviews for each problem are located in *Section 2.1*, *Section 2.2*, and *Section 2.3*.

## 1.4 Problem – Construction

(2D, Conceptual)



**Fig. 1.10 Concept Sketches – Construction: (a.) SIP system; (b.) STRIP system.**

*Re-thinking stressed-skin and structural insulated panel (SIP) systems with today's means and tomorrow's methods.*

[Aeck 2014]

### **Problem of Construction**

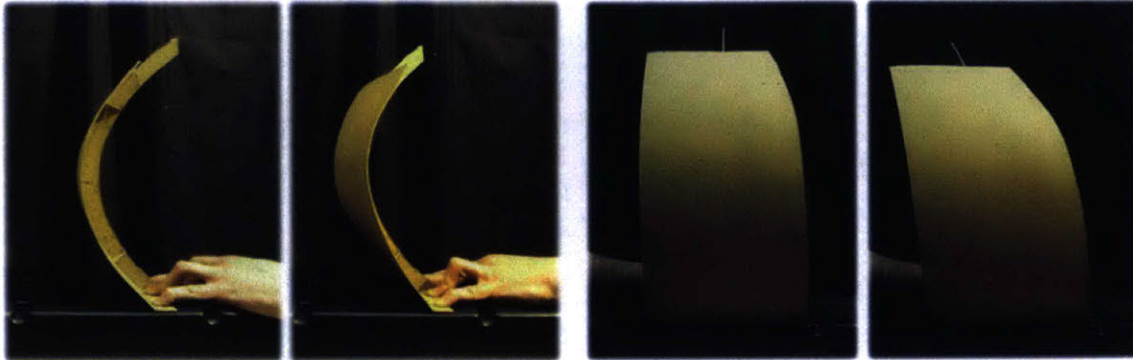
Within conventional, open building systems, design outcomes are constrained by both the site-assembly of orthogonal, piece-level standards in *light frame construction* and by the off-site unit-level lamination in *panelized construction*. There is a need for economical alternatives with the capacity for geometric variation, and by extension, personalizable construction.

**How can we generate curvature in panelized building systems using flatbed CNC cutting operations (2D) and create plate joinery to challenge conventional assumptions?**



## 1.5 Problem – Geometry

(2D-to-3D, Material)



**Fig. 1.11 Study Model – Cylinder to Conoid: (a.) Section; (b.) Elevation.**

*Transforming a cylinder into a conoid by manipulating the sixth points in section/elevation about a central flexural stiffener with a monofilament tie.*

[Aeck 2015]

### **Problem of Geometry**

De-constrained now by virtual modeling, computing, and machining technology – and given the evident relative economies of elastic bending – the emergent geometric problem is both methodological and material-driven.

**How can we transform flat/planar (2D) sheets into volumetric (3D) freeform surfaces and clarify the geometric limit states for the relevant sheet materials?**

## 1.6 Problem – Performance

(2D-to-3D, Material, Operational, Structural)



**Fig. 1.12 Study Model – Strips: Renewable, High-performance, Stressed-skins.**

*Staggering blocks the local strip and global assembly axis-of-rotation; point-connections reduce thermal bridging.*

*Pre-attached seams and site-applied attachments enable transport of curvature.*

[Aeck 2015]

### **Problem of Performance**

With the objective of specific, configure-to-order, site-assembled methods – repeatable as opposed to custom-engineered one-off solutions – the problem of performance in system-built construction becomes the iterative development and analysis of the geometric, material, operational, and structural performance of the prototypes as represented by the revised, multi-objective problem below.

**How can we systematize developable strips (2D) cut from renewable sheet materials for deployment as self-assembled, high-performance, volumetric (3D) structural forms for medium-scale building applications?**

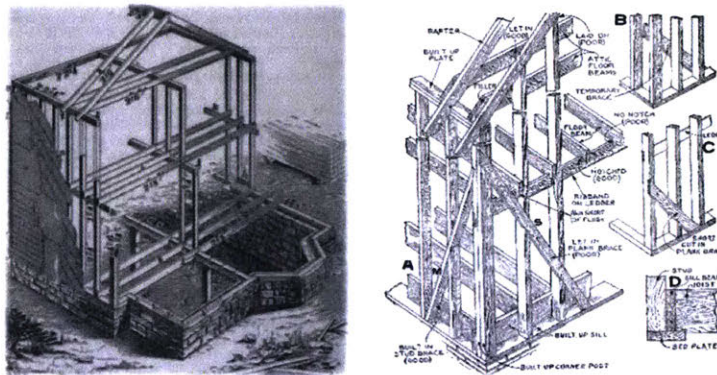
*Forms for Homes – in the geometric sense; Forms for Foam – in the literal sense.*

## 2. LITERATURE REVIEW

This *Chapter* reviews relevant history, fundamental properties, preliminary analysis, and contemporary research related to medium-scale construction, geometry, and active bending in order to contextualize the design response that follows in this thesis. It is organized by stated problem into *Section 2.1 – Construction*, *Section 2.2 – Geometry*, and *Section 2.3 – Performance*.

### 2.1 Literature – Construction

#### Construction – Light Frame



**Fig. 2.1 Light Frame – Then: Balloon framing (a.) 1899; (b.) 1923.**

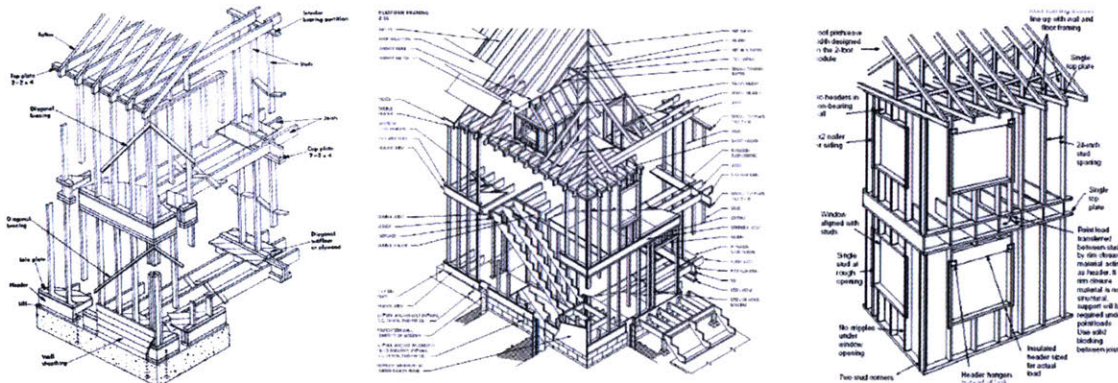
*Democratizing; the innovation of light frame construction is its relative simplicity, economy, and accessibility.*

[Sources: ICS 1899, p.222; Graham 1923]

The basis for the initial and enduring popularity of wood light frame construction lies in its relative economy and simplicity. The tools involved are accessible and the parts are portable – a stack of material, a box of nails, a hammer, a saw suitable for cuts-to-length or modifying-cuts – and soon a structure is underway. Documentation of pre-industrial board-sheathed or post-industrial plywood- and flakeboard-sheathed methods are widely-available and usually presented together across the range of references reviewed [Allen & Iano 2014; AIA 2008; Ching 2008; Neufert 2000, Reiner 1981] and guidebooks [Thallon 2008; Heldmann 2006; Jones 1986]. Likewise, industry and research publications [BSC 2010, BSI-030; TFG 2005; FPL 1999, ch.16-1] also include both to contextualize recommendations for optimization.

In addition to the well-documented life safety and flame spread considerations referenced in the Introduction to this thesis, other advantages contributed to the evolution from balloon to platform framing, including the elimination of board sheathing, the reduction in blocking and girts, and the adoption of let-in bracing [Youngquist 1977, Armstrong 2012]. The last three are consistent in that they all are labor-related externalities of commercial plywood, and cost considerations come into focus further on. Also noted in the evolution of light framing is its ongoing extension and hybridization via a wide-range of engineered component-level substitutions in direct competition with the original, typical, piece-level dimensional lumber discussed above. Such hybridization is not exclusively methodological or material. For example, component-level substitutions are common in multi-family housing. Likewise, system-level hybridization – such as parking-deck podium buildings and other mixes of protected and unprotected constructions – are also increasingly popular strategies for extending light framing vertically.

The wood light frame construction we know today is versatile; however, it is not so versatile as post-digital, site-assembled structures born of the increased capacities of today's modeling and machining could be.



**Fig. 2.2 Light Frame – Now: Platform framing (a.) 1981; (b.) 2008; Advanced framing (c.) 2014.**

*Optimizing, substituting, and layering; removing all studs in the cavity without cellular foam is a conceptual goal.*

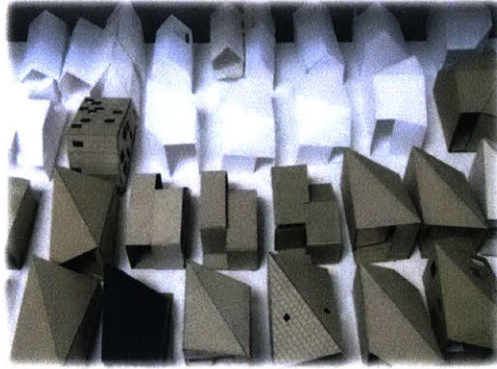
[Sources: Reiner 1981, p.131; AIA 2008, p.41; DOE 2016 after BSC 2010]

A review of the contemporary effort to revise platform framing known as *advanced framing* (or OVE; *optimum value engineering*) as represented in recent industry and government literature [APA 2014; DOE 2016] revealed various recommendations for material efficiency and thermal performance. One of the more surprising was that carbon steel connector plates, clips, and structural tees [Thallon 2008, p.74-75, fig. A–D; BSC 2010, BSI-030] were presented as typical details. The rationalization of stud spacing from 16" to 24" on center and the majority of the recommended revisions do improve material efficiency, although the global stud layout and fenestration are often uncoordinated and partial implementations are common. In addition, going from a double to a single top-plate is likely an optimistic degree of stud-and-joist coordination to expect throughout a project of any complexity.

One conceptual objection seems appropriate because measures that reduce thermal bridging, reduce board footage, or improve atypical detailing are incremental improvements, not solutions. No matter how many studs we eliminate or how much supplemental insulating sheathing we apply, repetitive, continuous, 1.5" studs in the cavity will remain a thermal flaw of the construction type. Some analogous thermal vulnerabilities in panel construction are: the intermediate stiffeners, the typical interface splines, and the atypical continuous thermally bridging interfaces.

During a recent research visit to a production facility, a regional SIP manufacturer commented on the popularization of insulated headers, declaring them their second most popular product. In these components, the conceptual response is evident and the fact that what amount to heavy SIPs have a reliable beachhead within light frame methodology was a welcome realization. Another telling point offered at parting was: "Remember, we can laminate just about anything."

Increases in frame-factor are to an extent inevitable at structural interfaces; however, in less structurally sensitive conditions the continuous built-up splines usually can give way to surface splines. Ultimately, atypical conditions will exist as depicted by the right jamb of *Figure 2.2a*, and at some point every design encounters the reality of either system-, assembly-, component-, or piece-level properties (see *Appendix – A*). The architectural representation is filtered through them, and while-well suited for orthographic accretion or subdivision of interior space, both light frame and panelized construction methodology approach their bicentennial and centennial respectfully. Thankfully, we have progressed some distance beyond the machine-made nail and the steam-powered sawmill.



**Fig. 2.3 Light Frame – Now: Study model variation.**

*Design encountering systemic properties at Architecture Research Office  
 What alternatives have become possible in our post-industrial present context?*

[Photo: ARO 2011, Richard Barnes]

These summary methodological properties and observations, a result of the literature review, are included as a primer.

**Table 2.1 Light Frame – Properties.** (of Typical)

<i>Method – Production:</i>	Off-site Prefabrication; Industrialized milling into dimensional lumber (Typ.).
<i>Method – System, Macro:</i>	On-site, Open system; Piece-level assembly direct or into sub-assemblies (Typ.).
<i>Method – Assembly, Micro:</i>	On-site, Direct and Tilt-up (Manual, Typ.) or Pick-up (Crane/Joist, Atyp.).
<i>Build – Typical:</i>	0.438" Sheathing (Ext.); 2"x 6" Studs (16" o. c., Typ.); 0.5" Gypsum (Int.).
<i>Cost – Typical:</i>	\$200/ft. <sup>2</sup> Floor area (Avg.); \$10.94/ft. <sup>2</sup> Surface area (Avg.).

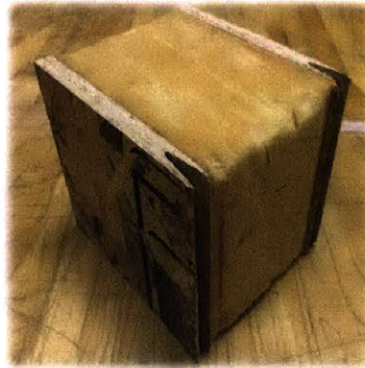
**Notes:** (a.) Surface area: [Meis 2015].

**Table 2.2 Light Frame – Observations.** (of Typical)

O1:	Orthographic inputs are constraining. (i.e., piece-level tectonics limit design and spatial outcomes.)
O3:	Basis of popularity is relative accessibility, economy, portability, simplicity. (e.g., less joinery and waste.)
O2:	Advanced framing is multi-objective optimum value engineering. (i.e., material, structural, thermal.)
O4:	Supplemental exterior insulation is remediation. (i.e., industry happy to sell more layers.)
O5:	Thermal bridging is an operational performance flaw. (ergo, conceptual objective: <i>no studs in the cavity</i> .)

**Notes:** (a.) *The innovation of light frame construction was its method which developed of the newly industrial context and had many application-specific advantages.*

## Construction – Panelized



**Fig. 2.4 Panelized – Then: Structural Insulated Panels. (SIPs)**

*Innovating; responding to the oil crisis.*

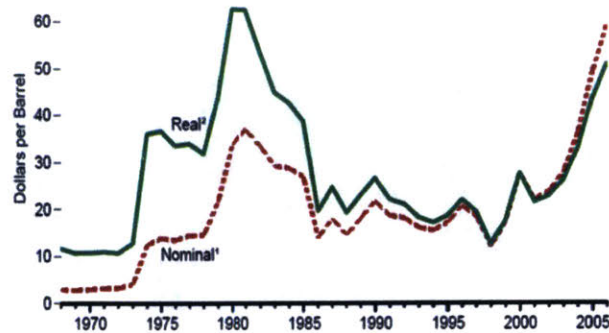
In the United States, most early commercial insulation such as Cabot Quilts [1923] and Cellotex [Bynum 2001] targeted integration into existing building systems or remediation. Wright's intuitive 1936 3-ply cavity panels at the original Usonian, the Jacobs House, unitized stressed-skins [Moe 2014, p.155, p.169–170], and his former apprentice Dow [1952] later introduced the foam core SIP that is now the most common. Yet structural insulated panels (SIPs) as we know them today did not begin to gain popularity until the 1973 oil and 1979 energy crises [EIA 2006]. Apart from automation, effective franchising, and optimization (i.e., detail revision or material substitution), the fundamental assumptions of SIP methodology are yet to evolve appreciably due to the "digital-shift." Typically, laminated-composite SIPs are still produced on semi-automated Fordist lines using hot-wire foam cutters, adhesives, and fixed rollers. These rollers (*Figure 1.7b*) are a significant constraining factor for variable-depth panels as is the practical challenge of efficiently transporting curved parts. The industry response is familiar: As with the Model T's one color, the consumer can acquire any shape so long as it is flat (cylindrical SIPs are presently manufactured).



**Fig. 2.5 Panelized – Now: Self-palletized and Transport-ready. (SIPs)**

*Palletizing; SIPs methodology is optimized for packing; Simply attach feet, straps, shrink-wrap, and a shipping label.*

In its present form, panelized construction frequently results in orthographic outcomes derivative of its prefabricated planar modules, tilt-up site-assembly, and orthographic panel-to-panel spline joinery. It also assumes consistent, self-imposed constraints specific to lamination and specialty equipment in a controlled environment. The typical SIP is a laminated composite of 0.4375" [11mm] oriented strand board (OSB) with either an expanded or extruded polystyrene (EPS or XPS) rigid foam core – ranging between 5 and 8 inches in thickness. At this point, the fundamental application of lamination is holding SIPs back. Revisiting this assumption and adjusting the amount of prefabrication are seen as a first steps to extending and increasing their relevance.



**Fig. 2.6 Panelized – Origins: U.S. Dollars per Barrel.**

"The total additional cost of using SIPs can be derived from my research as being 10% greater on average..."

[Source: EIA 2006; Quote: Meis 2015]

These summary methodological properties and observations, a result of the literature review, are included as a primer.

**Table 2.3 Panelized – Properties.**

**(of Typical)**

<i>Method – Production:</i>	Off-site Prefabrication; Industrialized lamination of EPS foam and OSB (Typ.).
<i>Method – System, Macro:</i>	Off-site, Closed system; Piece-level assembly into panels (Typ.).
<i>Method – Assembly, Micro:</i>	On-site, Tilt-up panel (Manual, Typ.) or Pick-up panel (Crane/Joist, Atyp.).
<i>Build – Typical:</i>	0.438" OSB (Ext.); 6" Rigid foam (EPS/XPS); 0.438" OSB (Int.).
<i>Cost – Typical:</i>	\$160/ft. <sup>2</sup> Floor area (Avg.); \$9.05/ft. <sup>2</sup> Surface area (Avg.).

**Notes:** (a.) *Atypical conditions are challenging (and complexity prohibitively so).*

(b.) *Modification in cavity requires engineering (i.e., HVAC, Plumbing, or Recessed lights).*

(c.) *Noxious wire cutting (Misc.); Oversize lag screws (Misc.).*

(d.) *Surface area: [Meis 2015].*

**Table 2.4 Panelized – Observations.**

**(of Typical)**

O1:	Orthographic panels are constraining. (i.e., unit-level tectonics limit design and spatial outcomes.)
O2:	Basis of popularity is relative assembly, material, and operational performance (e.g., less labor; wood.)
O3:	Industrialized lamination is a self-imposed constraint. (i.e., limits post-consumer recycling; modification.)
O4:	Styrene is a material flaw. (i.e., non-biodegradable plastic monomer derived of natural gas or petrol.)
O5:	Uniform-depth is a geometric performance flaw. (ergo, conceptual objective: <i>better</i> or <i>no rigid foam.</i> )

**Notes:** (a.) *A project conceptual objective is elimination of the self-imposed lamination constraint.*

## Construction – Prefabricated



**Fig. 2.7 Prefabricated – Then: (a.) Radial-futurism; (b.) Mechanical-idyllic; (c.) Structural-expression.**

*Innovating with post-war industrial capacity to address a pronounced need.*

[Sources: Fuller 1944-48; Lustron 1949; Prouvé 1951]

Atypical relative to today's two most common open methodologies, prefabricated construction efforts have endured in both the design and public consciousness due to their pragmatic re-purposing of inflated post-war production capacities and idealist spirit. They are included here for contrast, and the quality unifying the best of mid-20th century prefabricated systems is their experimental character. Each example above strained against modular repetition in some specific way, endeavoring to disrupt the dominant constraints of Fordist production with variety. By necessity, these tended towards proprietary closed versus open systems, but the house was a vehicle for innovation. However, kit or system-built houses have not proven to be a societal cure-all, and fully-prefabricated modular and panelized solutions have tended to display a temporal character. Renewable, post-digital prefabricated construction with increased capacity for variation offers something more and the range of medium-scale building applications targeted are detached and semi-detached homes, duplexes, infill townhouses, and mixed-use housing hybrids.



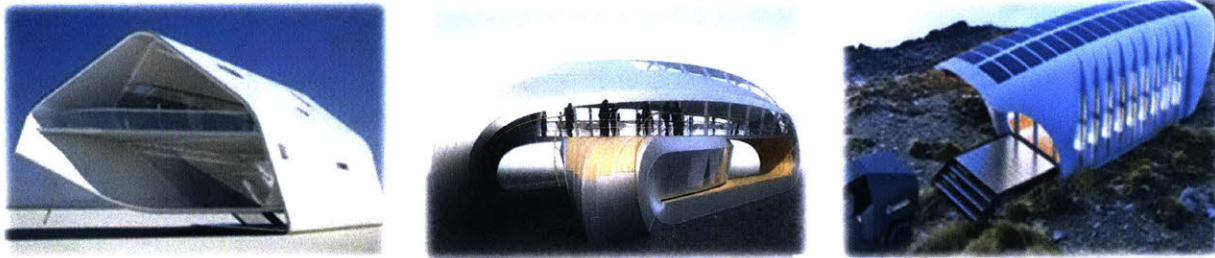
**Fig. 2.8 Prefabricated – Now: (a.) Packable-materialist; (b.) Retro-modernist; (c.) Marketable-modular.**

*Flatpak re-materializing panelized; Taliesin Mod-Fab renewing De Stijl; Blu Homes \$365/ft.<sup>2</sup> modular Breeze.*

[Sources: Lazor Office 2005; Timmerman 2012; Blu Homes 2013]

All well-developed divergences from the status quo alternatives are welcomed by the author, but critically the present prefabricated resurgence (or "rehab for prefab," affectionately) seems more a materially-warmer, proprietary, configure-to-order modernism versus a genuinely new methodology of increased capacities and digitally-enhanced methods [Aeck 2007]. Despite the breadth of contemporary offerings – aside from an atypical outlier here or there – the same old struggle of what can be achieved with an orthogonal structural system plays out repeatedly. This is not to suggest that geometric variation is some kind of cure-all. Rather, simply that in whatever post-digital industrialized alternatives eventually challenge light frame and panelized construction, that detailing for geometric variation should be developed as typical from conception. "The paradise offered by the Culture Industry is the same old drudgery" [Adorno & Horkheimer 1998, p.142].





**Fig. 2.9 Prefabricated – Future: (a.) California Roll; (b.) Boat, Loire River; (c.) AMIE 1.0.**

*Prefabricated futures: (a.) Cutting and Bending; (b.) Cutting, Bending, and Twisting; (c.) Cutting and Printing.*

[Sources: Daniel 2012; Heatherwick 2012; SOM 2015]

These summary methodological properties and observations, a result of the literature review, are included as a primer.

**Table 2.5 Prefabricated – Properties.**

**(of Typical)**

<i>Method – Production:</i>	Varies: On/Off-site Prefabrication (Typ.).
<i>Method – System, Macro:</i>	Varies: Site-built; Modular; Panelized/Pre-cut (Typ.).
<i>Method – Assembly, Micro:</i>	Varies: Frame; Modular Unit; Panel (Typ.) or Modular Block (Atyp.).
<i>Build – Typical:</i>	Varies: All-ply./Wood; Cold-formed steel; Glass/Carbon-fiber/Other (Typ.).
<i>Cost – Typical:</i>	Site-built: \$84/ft. <sup>2</sup> ; Modular: \$76/ft. <sup>2</sup> ; Panelized & Pre-cut: \$70/ft. <sup>2</sup> (Avg.).
<i>Size – Typical:</i>	Site-built: 2,457 ft. <sup>2</sup> ; Modular: 1,722 ft. <sup>2</sup> ; Panelized & Pre-cut: 2,786 ft. <sup>2</sup> (Avg.).

**Notes:** (a.) *Source data:* [US Census 2014]

**Table 2.6 Prefabricated – Observations.**

**(of Typical)**

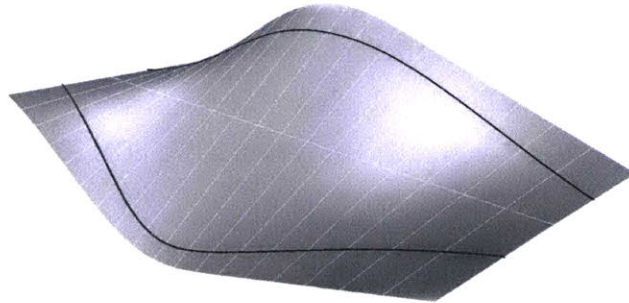
O1:	Conceptual repetition; materialist re-making of modernism (Internet prefab is virtual catalog house.)
O2:	Innovation focused on substitution, optimization, or viral appeal. (Selling reduced construction.)
O3:	Post-war prefab did not save the world, but was a vehicle for innovation. (Selling spirit of independence.)
O4:	Open and Self-assembly are democratizing. (Self in the sense of do-it-yourself or personalized.)
O5:	Atypical for single-family homes to be designed by an architect. (5%)

**Notes:** (a.) *Project focuses is open, pre-cut, site-built systems; designing for local production and assembly.*

## 2.2 Literature – Geometry

The relationship between geometry and construction is fundamental in that graphic representation and description are required to communicate architectural ideas for execution. This section provides application-specific background, and then reviews related geometric history and contemporary research.

### Geometry – Architectural



**Fig. 2.10 Architectural – Surfaces: Ruled Developable.**

*Cutting/Trimming; (a.) Cylinders, (b.) Cones, and (c.) Tangent Surfaces of a Spatial Curve.*

*Architectural. (Geometry)* The moment a designer begins to negotiate between the exterior envelope and program to influence a space geometry transcends construction and subjective aesthetics. As expressed at the outset in reference to cutting, within digitally manufactured, sheet material based systems with details that anticipate variation is the capacity for a greater range of spatial organization. Such a capacity could just as easily be used with restraint, for specific function, or within the conventional, as opposed to the indulgent sculptural expressionism that initially comes to mind. Entire neighborhoods of subtle berm-like green roofs and mid-rise urban facades inclined for daylighting with delaminating entrance canopies are a few fond daydreams. The perceived open question relative to architectural geometry is how within *ruled developable* [Pottmann et al. 2007, p.535] can we realize curved surfaces from flat, not only economically and renewably, but also multi-layer which are relevant to residential construction. Also, what from among the contemporary research in the geometry processing community can inform or help in doing so, and to what end?

Of the latter, formal articulation for either passive function or contextual adaptation – e.g., solar optimization, rainwater management, or simply an incrementally changing wall following a property boundary – are but a few of the possibilities. The geometric Beltline Treehouse [2014] from Tardio & DeReuil is a recent example of a spatial organizing strategy where the functional articulation is to avoid mature trees, as it cantilevers and extends down a wooded slope (although the means of doing so was largely scrap steel). Such strategies would translate well to with pre-cut system-built constructions. With the immediate context on site, the material type, and the practical means all consistently variable, perhaps the one area where there can be is geometry, where there are a number of possible solutions.

Returning to the stated problem of creating curved surfaces and the cost-aware, multi-layer approximation of freeform objective, an initial architectural concern with such surfaces is the visibility and the aesthetic presence of the discretization in the sense of Pottmann et al. [2007, ch.19, p.672].

Generally, this thesis employs ruled surfaces that have zero Gaussian curvature, which can likewise be mapped isometrically without distortion or "unrolled" onto a single plane. Inspired by several marine applications (sails and hulls) the D.LOFT plug-in (which allows *developable lofting* with optimization and parameters for control lofting) from

the "EvoluteTools" was used to produce both the different virtual and physical study models and test specimens. The specific choice to focus on conoids and tangents of a spatial curve strips for discretization is partly a response to conventional use of triangulated and intensity of perturbed subdivision planar quad (PQ) mesh approaches produce complex freeform structures (independent of the latter's usefulness). Ultimately there are always situation-specific concerns, and where an individual or entity is positioned on the design side, delivery side, or as a consultant somewhere between, schedule and profit-motive frequently render which will be espoused predictable.

This section opened with a virtual model of a ruled surface in abstraction (*Figure 2.10*) to represent the surface class of geometric solution proposed, and accomplishing this at full scale in physical form usually achieved one of the following ways: (1.) by approximating, discretizing, faceting, or segmenting, (2.) by deforming material inputs permanently with heat, steam, immersion, a vacuum- or pressing to positive molds, (3.) by casting-in-place or off-site in negative forms, (4.) by additive printing, (5.) by subtractive milling, or (6.) by bending within the elastic range. The proposal uses (1.), (2.), (5.), but it is the evident economy of the latter (6.) bending, that brings us to flexural geometry.

This table summarizes a few of the specific geometric references related to the systems developed in this thesis.

**Table 2.7 Geometry – Topics & Advances.**

**(of Review)**

Curves

Freeform, Curve [Pottmann 2007, p.255 f-f]

Surfaces

Freeform, Deformation [Pottmann 2007, p.469 f-f]  
 Freeform, Surface [Pottmann 2007, p.361]  
 Ruled [Pottmann 2007, p.311 f-f; 370, 634]  
 Ruled, Developable [Pottmann 2007, p.546]  
 Ruled, Warped [Pottmann 2007, p.311]  
 Ruled, Rotational (hyperboloids) [Pottmann 2007, p.289 f-f; 342]  
 Rotational/Translational [Pottmann 2007, p.305, f-f; 365, 557, 636]  
 Rotational Hyperboloid, use in Arch [Free4orm]  
 Union of developable strips [Free4orm]  
 Cylindrical; Cones/Conoidal [Free4orm]  
 Tangents of a Spatial Curve [Free4orm]

Methods

Developable Lofting [Evolute, D-Loft]  
 Geometry Analysis Tool [Front & Free4orm]  
 Elastica Analysis Tool [Free4orm]

**Notes:** (a.) *This is a list of application-specific list of topics and references.*

Geometry – Flexural

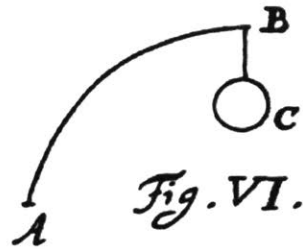


Fig. 2.11 Flexural: The elastica.

An early representation posing the elastica problem.

[J. Bernoulli 1691]

*Flexural. (Geometry)* The elastica is ubiquitous in nature, in our construction, and in everyday life. In the same way the sine curve is a named function, based on its shared relationship with the pendulum, other periodic functions and simple harmonic oscillators, a case can be made that the elastica curve should take its place among the other fundamental classes of curves; among them sinusoids, arcs, parabolas, and catenaries.

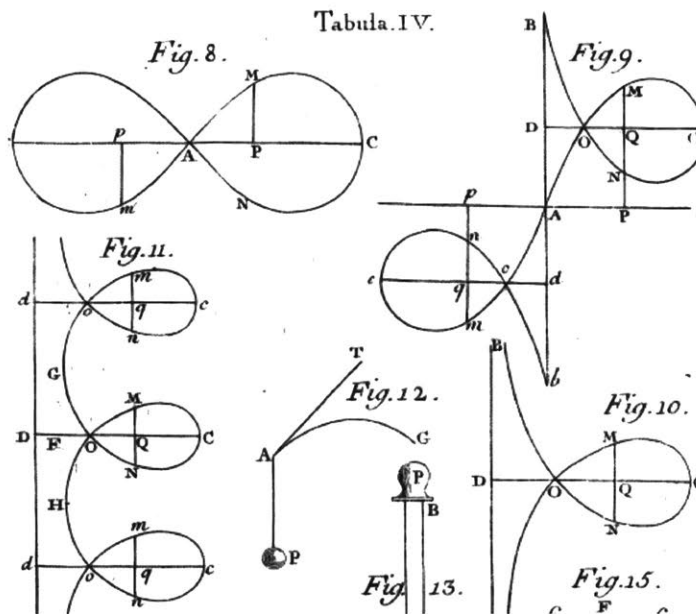
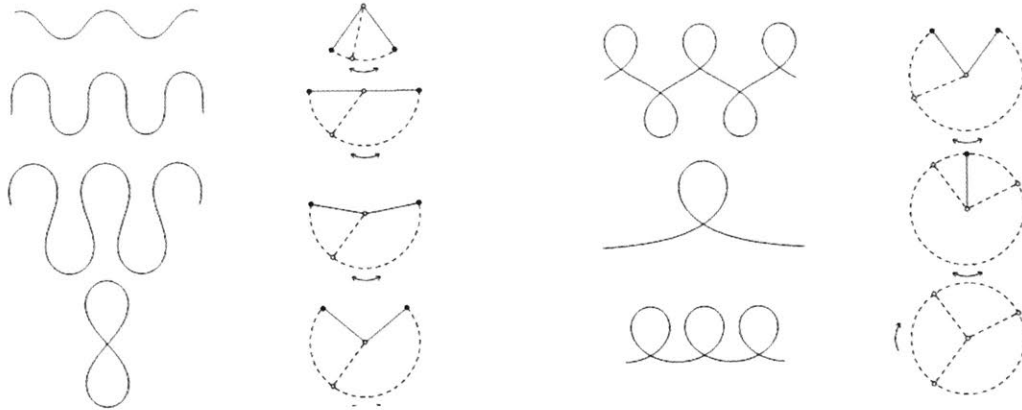


Fig. 2.12 Flexural: The elastica.

A similar figure found in Euler's Tabula IV; line segment AT above is interpreted as representing the tangent of AG.

[Euler 1744, after D. Bernoulli]

It is the solution to a differential equation that cannot be expressed as a finite sum of elementary functions. The fact that it does not have an analytical solution and is challenging to analyze, is no different from the sine. The elastica and pendulum as represented on the next page have the same differential equation, and the first challenge taken up in the analysis of the elastica later in Section 4.2 was to plot and analyze it, both empirically and numerically.



**Fig. 2.13 Flexural – Context: Elastica and Pendulum.**

*Beyond flexural relevance the elastica in plan also represents the greater or upper range of the pendulum in section, as represented by the 2nd and 4th columns.*

[Djondjorov et al. 2007]

**Table 2.8 Geometry – Observations.**

**(of Review)**

O1:	The elastica is ubiquitous.
O2:	The pendulum and water droplet are solved with small-angle approximation.
O3:	The elastica represents the upper range of the pendulum, and sine represents the lower.
O4:	The first Bernoulli solution was for the rectangular/perpendicular elastica.
O5:	The geometric objective of the project is clarifying and enabling active bending at the residential scale.

**Notes:** (a.) *Arc splines employed infinitesimally can represent any known sufficiently for fabrication but Elastica splines seem a potential alternative.*

## 2.3 Literature – Performance

In general use *high performance* signifies a position relative to some normative "other," which in architecture is frequently convention, and the distinction made most often to do with either structural or overall energy efficiency. This section reviews residential energy consumption, clarifies the "cost-aware," material, operational, structural, and financial high performance ideal pursued in this thesis, and then application-specific performance research.

### Performance – Residential

After its proportional representation (*Figure 1.5*), a look at the history of the total primary energy consumption in the U.S. shows consistent growth from 1983 to 2000, followed by fluctuation generally at or below 100 QBtu [EIA 2013]. Relative to 1983 (72.97 QBtu) and similar to 2000 (98.81 QBtu) the 2013 data represents a 33% percent change. The recent projection by fuel type of what may happen [EIA 2017, p.5, fig.9] suggests relatively modest 5% to 2040, with petroleum first, with natural gas replacing coal, and with renewable sources coming on line. Fossil fuels will continue to as primary, but code- and commercially-driven improvements in efficiency, the residential sector there are positive indications of changing market preferences that "those houses and structures that deliver increased energy efficiency have become in-demand for both traditional detached and attached home buyers as well as commercial property buyers" is of course welcomed [DOE 2008].

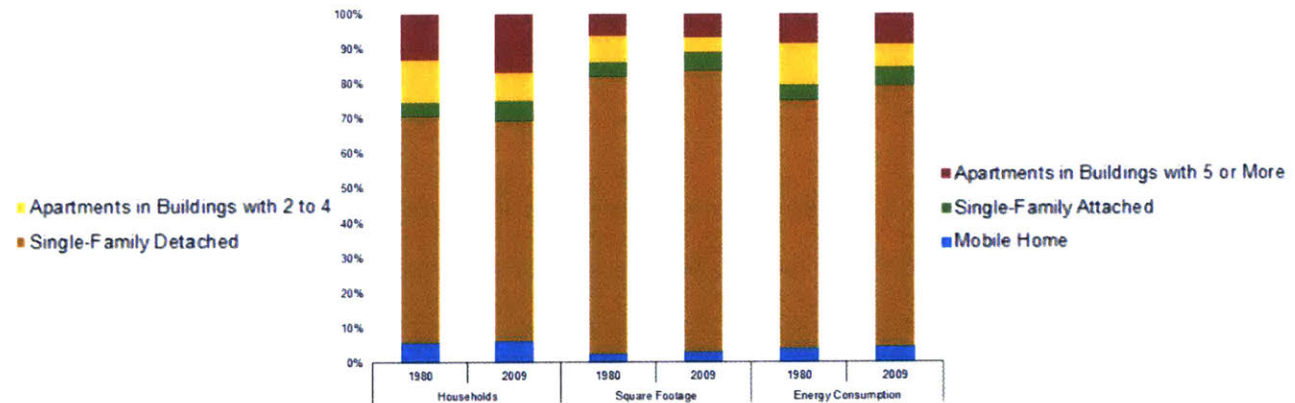


Fig. 2.14: Energy use – By Home Type. (U.S.)

[EIA 2015; data: RECS 2009, 1980]

Investigation of the historical proportions of residential energy consumption by home type confirms single family homes the majority as by far, clarifies the market history, and supports the declared focus of attention. The figure above comparing 1980 and 2009 indicates movement away from duplex and smaller-scale apartment living towards larger multi-family development. This, and the increased share of *single-family attached* units do not appear to represent changes in preferences for single-family generally, and perhaps not at all, if some of the attached and mobile home increases were a temporary effect of the financial crisis. Apparently significant is that the decrease from approximately 70% to 69% of detached single-family households came with a 5% increase to 80% of the total residential demand. Following the historical increase from 1950 (1,065 ft.<sup>2</sup>) to 1973 (1,660 ft.<sup>2</sup>), and jump in average single-family by 2013 (2,598 ft.<sup>2</sup>) detached are fundamentally larger than the other types [U.S. Census Bureau 2013, data]. With only a slight proportional decrease, the disproportionate increase in demand seems to reflect the further creep of their average size. Some lag in efficiency improvement as compared other types is assumed, but given nearly thirty years of improvement in glazing systems, and the commercialization of many *blown-in* and *spray polyurethane foam* (SPF) products for remediation, it seems less likely to be just aging housing stock showing itself.



**Fig. 2.15 Type – Residential: Detached. (Typ.)**

These preliminary general properties and observations relevant to detached homes, a result of the literature review, are included as a primer.

**Table 2.9 Detached – Properties.**

**(of Typical)**

Type	Description	Detail	Source
Externalities:	Smog/Poor air quality Sprawl/Polycentric Urban Transport/Energy Civic Externalities	(CO <sub>2</sub> levels: Full record and Recent ) (Spatial structure and Transport) (Per capita reduction strategies) (Sprawl, Justice, and Citizenship)	[NOAA-1a & -1b 2016] [Bertaud et al. 2003] [Lefèvre 2009] [Williamson 2010]
Trends:	Size Creep Urbanization Rapid Urbanization Temp. Anomalies	(2200 ft. <sup>2</sup> → 2600 ft. <sup>2</sup> ) (+2.5 Billion: 90% in Africa and Asia) (Suburban → Urban divide) (Decade: +0.74 °F, or +0.41 °C)	[NAHB 1999–2015] [UN-WUP 2014] [Thompson 2013] [NOAA-2 2016]
Related:	Energy, Buildings Energy, Transport Energy, Industry	(41.1%, <u>excludes</u> industry, some transport) (28.1%) (30.8%)	[EIA 2012] [DOE 2010, BEDB]

**Notes:** (a.) 2015: Mean floor area: 2600 ft.<sup>2</sup>; Median floor area: 2200 ft.<sup>2</sup>

[NAHB 2015]

(b.) 1999: Mean floor area: 2200 ft.<sup>2</sup>; Median floor area: 2000 ft.<sup>2</sup>

(c.) 2010: The Residential share of Total U.S. Primary Energy Consumption is 22.5% and increasing.

**Table 2.10 Detached – Observations**

**(of Typical)**

O1:	Single-use, car-centric, anachronistic.	(Is present single-family detached really the dream?)
O2:	Orthographic inputs limit geometric variation.	(Assumptions: top-down; Tectonics: bottom-up.)
O3:	Emotionally-charged, personal.	(Gable icon is intertwined with linguistic subject of home.)

**Notes:** (a.) Solar potential of detached roofs gaining traction e.g., Mapdwell, Google's imitation, Solarcity.

## Performance – Material



**Fig. 2.16 Material – Renewable: (a.) Bamboo grove; (b.) Laminated bamboo, Soy-based resin.**

*Proposing engineered bamboo for renewable plate structures due to the potential of this rapidly renewable grass, the forecast Africa/Asia population growth, and its coincidentally relevant natural range.*

[Photos: Hoffman 2011; Plyboo 2014, by Author]

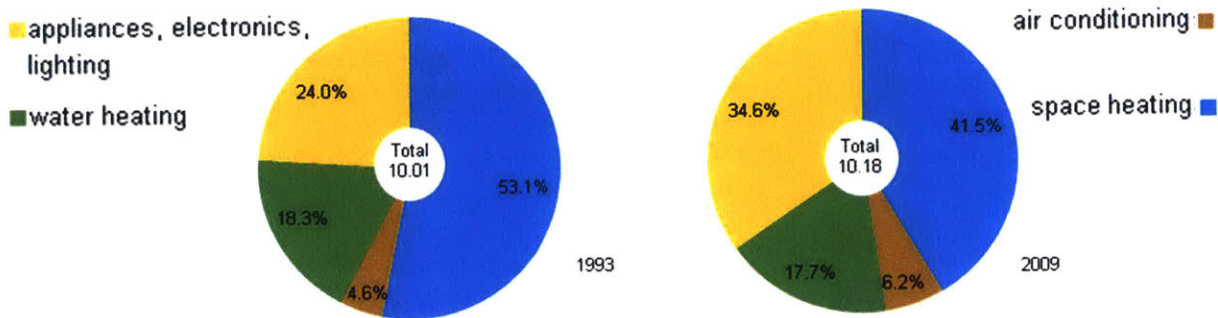
*Mimicking nomads, architects who design for lightness achieve inventive solution as they explore using less material with greater strength. This recognition of the dynamic natural cycles of a project's site and context, and the design of spaces that offer people, as the users of architecture, a direct connection to those cycles is an equally important strategy toward reinventing construction with a deeper ecological purpose.*

[from *The Cook, the Prospector, the Nomad and their Architect*. Gang 2010]  
Re-inventing Construction 2010; ed. Ilka & Andreas Ruby, p.169–170



**Performance – Operational**

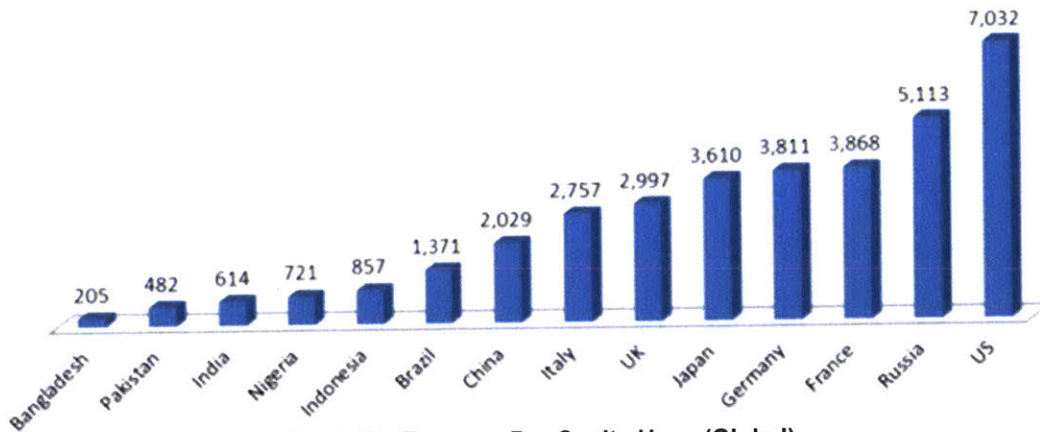
Taking a closer look at the distribution of end use in the home over time, it appears envelopes are improving, but demand is changing, likely driven by use of consumer technology.



**Fig. 2.17 Energy – Residential End Use. (U.S.)**

Total consumption is appreciably the same, but the improvement in heating efficiency appears offset by increases in appliance, and air conditioning use. [Source: EIA 2009]

While the fact that heating-related consumption is clearly down is positive, and suggests envelope related energy intensity is in decline by household is encouraging trend, we are running air more gadgets, air conditioners, and the U.S. remains the largest consumer of energy in the world [World Bank 2011].



**Fig. 2.18: Energy – Per Capita Use. (Global)**

As was mentioned earlier, the trend toward more efficient residential construction is being driven by more stringent codes, but also by the typical consumer’s desire for lower energy costs. For general behavioral context above is the global per capita consumption showing other developed countries far below that of the U.S.

These preliminary operational comparisons, a result of the literature review, are included as a primer.

**Table 2.13 Properties – by Component.**

<u>Component</u>	<u>U-factor</u>	<u>R-value</u>	<u>Source</u>
<i>Ceiling</i>	U0.026	R38.5	[IECC T R402.1.1 & .3]
<i>Wood-framed Wall</i>	U0.057	R17.5 (R20 cav. or R13 frame + R5 cont.)	[IECC T R402.1.1 & .3]
<i>Basement Wall</i>	U0.059	R10 continuous (or R13 framed)	[IECC T R402.1.1 & .3]
<i>Floor</i>	U0.047	R21.2 (R19)	[IECC T R402.1.1 & .3]
<i>Fenestration, U-factor:</i>	U0.35	R2.85	[IECC T R402.1.1 & .3]
<i>Fenestration, Glazed:</i>	U0.40	R2.50	[IECC T R402.1.1 & .3]
<i>Skylight, SHGC</i>	U0.55	R1.81	[IECC T R402.1.1 & .3]
<i>Slab</i>	U0.065	R15.4	[IECC T R402.1.1 & .3]

**Notes:** (a.) *Project operational energy focus: thermal performance and infiltration.*

(b.) *Source:* [Ching et al. 2012, p.256]

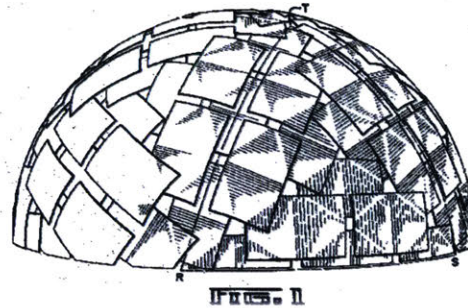
Performance – Structural: History & Context



**Fig. 2.19 Domes: Functional Articulation.**

[Source: Mitchell 1990, p.227]

*Domes. (History)* The sections above (*Figure 2.14*) of the Pantheon [CE 125], St. Peter's [CE 1590], and St. Paul's [CE 1711], illustrate historical evolution of domes from single shell, to double shell, and ultimately to a thin-/functionally-articulated **double shell**.



**Fig. 2.20 Segmented Shells: Self-strutted Geodesic Plydome.**

[Source: Fuller 1957, U.S. Patent 2,905,113]

*Plydomes. (History)* Fuller's fabulous, visionary, self-strutted Plydomes were early celebrations of the high material tensile capacity, but relatively low-stiffness of a still young commercial product (*see Figure 1.12*). As structurally and materially relevant as they are, these and many dome deployments of the time display an indifference (belligerence) towards the realities of occupancy. Were a person to "roam home to a dome" [DCMM 2012], it an undifferentiated igloo at the end of a subdivision really how we live and does the microwave or television go in the center?



**Fig. 2.21 Segmented Shells: Duck-Work.**

[Photo: Gaffney & Nguyen 2014, by Author]

*Plydomes. (Recent)* Several projects have adapted Fuller recently, the most successful of which is probably *Duck-Work* installed at the Boston Society for Architects in 2014 which according to its designers Sean Gaffney and Christina Nguyen, "invents a new type of wood construction which integrates the tools used to bend the wood directly into the assembly itself." While this may not be exactly the case, *Duck-Work* is relevant as a multi-layer plywood system that used elastic bending and commercially available hardware. The installation was notably uniform-depth, appeared limited the bending radius of 0.5" material, and employed dense "laid-up" interlayer blocks with prominent through bolting. As detailed, with the heads of the doubly-washed fasteners on the top surface, the nuts accessible from below, and with Fuller's characteristic gaps, the resulting surface fall short of the ideal.

*Shells. (Context)* Another obligatory stop is the various mid-20th century thin-shell efforts, surface-active structures from Felix Candela, whose functional articulation of fundamental hy-par typologies (e.g., anti-clastic saddles) and aggregations thereof continue to endure and amaze. Although their elegance and craft represented geometric technical progress, arguably thin-shell construction has proven to be most relevant for singular program (i.e., it is as inefficient at partitioning space as it is structurally efficient) and conventional secondary systems are common within.



**Fig. 2.22 Cast-in-Place Shells: Capilla de Palmira Cuernavaca.**

*A cast-in-place, thin-shell, complex structural form.*

[Source: Candela 1958]

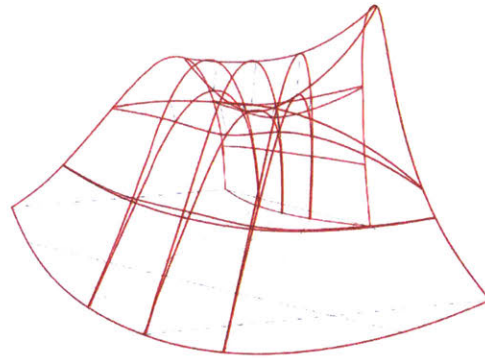
*Cast-in-Place Shell. (Context)* Backing away from the literal 1:1 mapping of span and program (which is appropriate in some cases and has produced many fine hangars, hockey rinks, and houses of worship), promoted instead is the systematic combination of surface types to economically increase spatial variety, structural performance and organizational flexibility – not just formal variation. Below the imprint of singly-curved strip falsework can be seen.



**Fig. 2.23 Cast-in-Place Forms: Stata Center.**

[Photo: by Author]

## Performance – Structural: Topics & Advances



**Fig. 2.24 Virtual Model: N51 Horn-fort Installation.**

*Mixing different tied, adjustable and closed components to target specific geometry.*

[Aeck & Yang 2015]

*Active Bending.* Structures which may be appropriately described as bending-active, a welcome descriptor introduced in the *Construction Manual for Polymers + Membranes* [Knippers et al. 2011], are those involving the systematic flexural bending of originally straight or planar inputs within the elastic range – also known as elastic deformation or simply flexure. A detailed conceptual example clarifying the concept of active bending is provided in paragraph four of the introduction. The above image (*Figure 2.18*) is an oblique view of the final 3D model for the *MIT Horn-fort* installation with its triple adjustable bending-active arch core. Its lateral system is a mix of adjustable linear, closed coupled, and tied fiber-reinforced polymer (FRP) rods.

The architectural and structural relevance of active bending and what led to it becoming one of the primary investigations in this project is its inherent economy. Among the most-relevant contemporary research efforts exploring or highlighting the potential of active bending are those studies surrounding the well-documented 2010 ICD /ITKE Research Pavilion, the 2011 AA/ETH Pavilion at Science City [Castle 2012] and the 2012 Marrakesh Umbrella [Lienhard 2014, Dissertation]. Multiple detailed analytical efforts by Lienhard & Knippers [2013; 1, 2] and most-recently, the plate structure specific exploration from Schönbrunner & Schleicher [2015; 3], are both compelling. Beyond direct structural relevance, these make detailed contributions to the collective understanding and evince the increasing popularity and potential of still relatively-new, stress-stiffened structure methodology. Each influenced this project in some specific way. For instance, the approach-based (behavior, geometric, and integrated) classification system as well as several metrics are adopted herein [Lienhard et al. 2013]. Other built material-driven efforts, such as the thin-shell Winnipeg "warming huts" from Patkau Architects [Jeska & Pascha 2015] and the recent La Cigarra Entry Pavilion also bear mentioning.

The clear majority of bending-active projects to date are adaptive-kinetic, form-active, brise-soleil, or they prioritize other temporary applications (e.g., 2014 ICD/ITKE; 2015 MIT Horn-fort). The current project gravitated towards investigating surface-active structures considering these as having more potential medium-scale applications. Admittedly, only brief engagements of glazing interfaces, fenestration, and thermal-optimization were possible during *GEN.1* of this multi-objective research (see also *Section 8.1*). After this and a review of panelized literature, improving on the status quo of using continuous studs in the cavity became a theme maintained throughout [Schleicher et al. 2015]. At this point, it seems appropriate to address the usage of "high-performance," which is meant to imply complementary material, operational, structural and fiscal analysis performance

Thus far, in bending-active and related architectural geometry discourse, a large number of surface active installations and pavilion exist. But the fundamental problems of permanent building applications such as the weatherline, insulation, and glazing seem to remain at arm's length. The majority of the projects cataloged in

Analysis (Table 3.3) involve active bending. However a few (e.g., PH = dovetail Menges) included for other relevant aspects do not. It is appropriate that the parade of predominantly single-material, self-similar screens marches on, given the context of temporary, experimental structural research with a pedagogical mandate. This is much more the domain of Erwin Hauer [Continua 2004] than the house next door. Also noted as beyond the scope of this static bending-active focused effort, is the potential for bending-active systems for kinetic direct shading, and rain screen façade applications. The same hindsight critique holds for the author's initial collaborative plywood and bending-active efforts (Plywood Delaminations 2005 & Change-of-State, 2006) and other contemporary research at the Georgia Tech Digital Building Laboratory (Space Index 2006) – the latter two tending towards polymers and geometric-material exploration over the practical or sustainable.

It is this conceptual concern, as well as revisiting a previous Luan box-beam scheme, which lead to the initial paper strip study models, the subsequent behavior-based research Case Study 1 (3.1), and the initial exploration of networked active bending through a linear-active, typologically hybrid installation. Along these same lines, speculative mechanical testing of existing sheathing products was performed to establish a baseline for experimental, renewable, engineered bamboo, wood-based, or engineered-wood materials for which there is proven existing demand.

**Table 2.14 Structural – Observations: Active bending. (Misc.)**

O1: General:	Examples interesting, but non-renewable and inappropriate for houses/housing.
O2: General:	Cost-aware functional articulation with freeform.
O3: Historical:	Linear elements/Discrete members (rods, stick, reeds, poles)
O4: Historical:	Uniform-depth Grid-shells (from Otto)
O5: Academic:	Typically Structural-pedagogical Focus (weatherline <u>not</u> engaged)
O6: Academic:	Typically Single-material, Self-similar Modules, Structural Primitives (shells, domes, arches)
O7: Industry:	Friction-fit + Self-assembly Systems with Simple Connections
O8: Industry:	Deployable, Portable, Temporary, Active Structures (tents)

**Notes:** (a.) *Is the potential of active bending more than niche?*

In *Form-Finding and Design Potentials of Bending-Active Plate Structures*, the authors assert that sheet materials such as “plywood, metals, plastics, and ... polymers,” exhibit the dual properties of flexibility and high-tensile strength. These two behaviors are a “perfect match” for bending-active structures, enabling “elements to undergo large elastic deformations and to resist high stresses before failure.”

The American co-authors of the article found in *Modelling Behavior* (53-63) are Simon Schleicher, assistant professor at UC Berkley’s College of Environmental Design (CED) and Andrew Rastetter, a Structural Engineer at BuroHappold Engineering. Their partners from the Institute of Building Structures and Structural Design (ITKE) at the University of Stuttgart, Stuttgart, Germany are R. La Magna, A. Schönbrunner, N. Haberbosch, and J. Knippers who participated in the design and construction of the ICD/ITKE research pavilion at the University of Stuttgart. Their work cites Lienhard et al. 2014 which describes the importance of flexibility and high tensile strength and the associated advantages for the design of “bent static and kinetic structures.” Consider the following three system advantages of bending-active plate structures as asserted by Schleicher et al. (collectively “the authors”):

- Structures can be constructed from “simple planar parts.”
- Fabrication with conventional flatbed processes is inexpensive.
- Assembly does not require skilled labor or auxiliary formwork.

Despite such advantages, the authors point out a “major challenge” with the design of bending-active plate structures, which is the inherent difficulty to “assess their structural behavior and to accurately anticipate their deformed geometry.”

To address this challenge, the Schleicher study borrows two design methodologies from previous studies: (1) geometry-based, and (2) integrated design methodologies (Lienhard et al. 2013). The study uses Buckminster Fuller’s “Self-strutted Geodesic Plydome” to illustrate the geometric-based approach and the ICD/ITKE Research Pavilion to reference the integrated approach.

To address the major challenge highlighted earlier – the ability to accurately predict deformed geometry and structural performance – the Schleicher study suggests two categories of digital simulation tools: (1) Real-time physics-based simulations of the kind “available for common CAD environments such as the Kangaroo Physics plugin for Rhinoceros® software, and (2) Finite element simulation (FEM) programs such as SOFiSTiK®.”

As evidence and examples, the authors employ case studies. The first case study titled “Effective Pinching” examines the benefits of single-curvature from bending thin plates. Triangular façade plates are determined by simulations in Kangaroo Physics to be optimal, and openings inside the triangular modules are pinched together “to provoke global deformations in a plate. By trimming the module’s edges, this guarantees the “module will fit into a symmetric façade tessellation.”

The second case study is titled “Mutual Reinforcement.” This case study illustrates “how flat plates can be bent into a doubly curved, multi-layered structure.” The structure features two desirable characteristics: light weight and substantial load-bearing capability. This is done by “pleating,” which is a structure analogous to corrugated cardboard. Individual plates are ventilated with holes and slits – this allows for global double curvature that is rare for a continuous plate. The plates are stacked and offset leading to a following layer covering and strengthening the first layer. A FEM simulation determines the degree of deformation.

The third case study is titled “Functionalized Instability.” This case study emphasizes a “form-giving strategy” and speed of assembly. Two ring-shaped components and two “longer undulating strips” are made from flat sheet material. The rings and undulating strips feature mortise and tenon joints for ease of connection. The ring ends are pulled together, forming a conical frustum. These cones fit into the undulating strips, acting as spacers. The cones

are pushed through until they “snap into an equilibrium position.” This process “locks” the components together, resulting in a double-layered adaptable “sandwich structure that can be applied to both synclastic and anticlastic shapes.”

The authors' case-study approach is appropriate and presents variable examples in order to cover stepped possibilities. The reader moves from a simple single-curvature single-plate bending-active case study to a double-curvature, multi-layered case study. Finally with the third case study the authors show practical and even exciting applications of bending-active plate structures. The study concludes by predicting a rich design space that predicts beautiful, efficient, strong and lightweight design applications of bending-active plate structures.



Takahashi 2015 asserts that the composites “material adaptability” takes them to a new level of possibility. This material adaptability allows supports customization and dimensional variation. One example of this is the Flectofin project, a hinge-less flipping mechanism based on the lateral torsional buckling of thin plates. Fibre composites “allow for different functionalities into load-bearing structural elements.” For example, the entrance pavilion of the Novartis campus in Basel, Switzerland was built with structural, physical, and architectural functions in mind.



Fig. 2.25: Composites – Novartis: This entrance pavilion was built with GFRP panels.

*Sandwich panels in which “multiple functions were integrated together, such as structural functions, physical functions, and architectural functions.”*

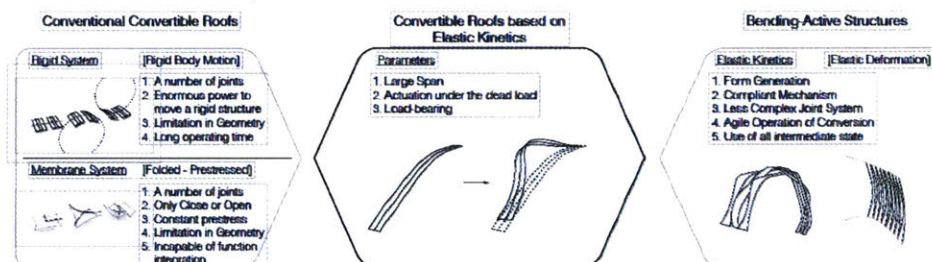


Fig. 2.26 Structural – Takahashi:

Compares convertible roofs with kinetic bending-active alternatives.

*When these systems are put side-by-side, the advantages of the proposed alternative are evident.*

Next, Takahashi has an investigation focused on plate structures where “the deformation of initially flat or slightly curved plates that bridge horizontal distances by single span”. He states that plates have “inherent load bearing capacity, especially against surface loadings.” The guiding principle here is that the plate is in “equilibrium between external forces and internal forces.” The process by which we search for a “state of equilibrium” is called “form finding.” And to inform his form-finding, Takahashi develops knowledge of key parameters such as the “thickness, stiffness, curvatures, stresses, forces, deflections and so on, in order to clarify underlying principles and address critical problems.”

On the most relevant areas is where Takahashi [B2, p.28–30] unpacks the relationship between structural height and other parameters in in detail and points out that “given a plate with a rectangular cross section  $bb \times h$ , the moment-curvature relation is” the following:

$$\frac{1}{r} = \frac{M_B}{EI} = \frac{12M_B}{E \cdot b \cdot h^3}$$

Takahashi explains the following relationship between properties:

As the cross-sectional area also linearly increases, the axial stress  $\sigma_{N_B}$  by the axial force  $N_B$  increases the square of the height.

$$\sigma_{N_B} = \frac{N_B}{A} = \frac{N_B}{b \cdot h} \propto h^2$$

Takahashi states that the "bending stress has a linear increase as the height increases," and next researches the effect of a dead load.

$$\begin{aligned} N_G &\propto h \\ \sigma_{N_G} &= \frac{N_G}{A} = \frac{N_G}{b \cdot h} \propto 1 \end{aligned}$$

"The axial force or thrust force  $N_G$  increases as the thickness increases. The plate thickness increase helps reduce the dead load effect with a quadratic effect."

Takahashi also writes, "a scale factor is denoted by  $s$  and base dimension parameters by a subscript zero (e.g.,  $x_0$  for a dimension parameter  $x$ ), and in addition assume "scale" alone means a scale change in all dimensions."

The curvature-bending moment relation is described as follows:

$$\begin{aligned} \frac{1}{sr_0} &= \frac{M_B}{EI} = \frac{12M_B}{E \cdot sb_0 \cdot (sh_0)^3} \\ M_B &\propto s^3 \end{aligned}$$

The bending stress is shown below:

$$\sigma_{M_B} = \frac{E \cdot sh_0}{2 \cdot sr_0} \propto 1$$

Next, Takahashi explains the common structural problem of scaling by stating, "The combination of normal compression stress and the deflection are malicious especially for bending-active structures due to their nonlinear nature of instability." On the subject of instability, from theories of nonlinear mechanics, positive stresses "are proved to increase the overall stiffness of a structure with geometric stiffnesses; this is called the *stress-stiffening effect*." He observes that, "negative stresses in a structure are known to destabilize the structure and its orthogonal deflections to trigger instability, leading to buckling failure modes (e.g., Euler buckling)."

One property that Takahashi singles out [p.26] is the "thickness of the bending-active plate." He asserts that bending-active plates should have as much thickness as possible. The cost of the thickness will be cubically related on the actuation force. Traditionally trusses, thickening layers, internally stiffening, or stiffening cable elements were used to give a structure additional thickness. Takahashi decides on cable structures as the most feasible. Takahashi writes, "For those reasons, bending-active plates actuated by tension cables are hypothesized to be a novel load bearing elastic kinetic plate throughout the research and examined for their structural performance, in comparison to regular thin plates." The figure on the next page [p.32, fig. 28 therein] is an excellent overview of main forces such as stress and bending:


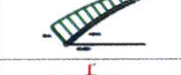
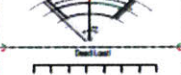



	Bending	Thickness $h$	Variable: span $s$	Thickness	Scale
Moment required for bending		$M \propto \frac{E \cdot h^3}{12 \cdot r}$	$M \propto \frac{E \cdot h^3 \cdot s^2}{12 \cdot r}$	$M \propto h^3 \cdot s$	
Normal stress due to bending		$\sigma = \frac{M}{I} \cdot y$	$\sigma = \frac{M}{I} \cdot y$	$\sigma \propto h^2 \cdot s$	
Flexural stress due to bending		$\sigma = \frac{M}{I} \cdot y$	$\sigma = \frac{M}{I} \cdot y$	$\sigma \propto h \cdot s$	
Axial force from dead load				$M \propto h \cdot s^3$	Destabilise
Axial stress from dead load				$\sigma \propto 1 \cdot s$	
Deflection from dead load				$\delta \propto h^{-3}$	

Fig. 2.27 Structural – Takahashi: Comparison of principal forces.

Such as stress and bending.

He then observes that in bending-active structures and infrastructure, the deformation property requires displacement control where internal forces, reaction forces and all the other displacements are correspondingly adjusted to fulfil those displacement inputs. Force control is a control method “where the internal forces and displacements figure out their configuration solely based on the force inputs, i.e. displacement controls require a certain mechanical mechanism that compellingly positions the displacement, while force controls can simply increase forces as the deformation goes.”

Thrust force and actuation are two forces that cause the bending-active plates to deform. The two important factors are a) destabilization of a structure due to the increase of normal stresses and deflections, and b) the control of necessary force inputs, in order for the structure to stably conduct its actuation.

Under a dead load, during the bending of an elastic plate, these two thrust forces affect the “movable supports to be considered, a thrust force due to bending and one from the dead load.” As a result, bending forces are necessary to be “larger than the dead load thrust for a stable motion of bending-active plates under the effect of dead load.” It appears that a plate with cables exerts an amount of force that dominates the thrust force. Takahashi’s studies revealed huge benefits with the use of cables which are as follows:

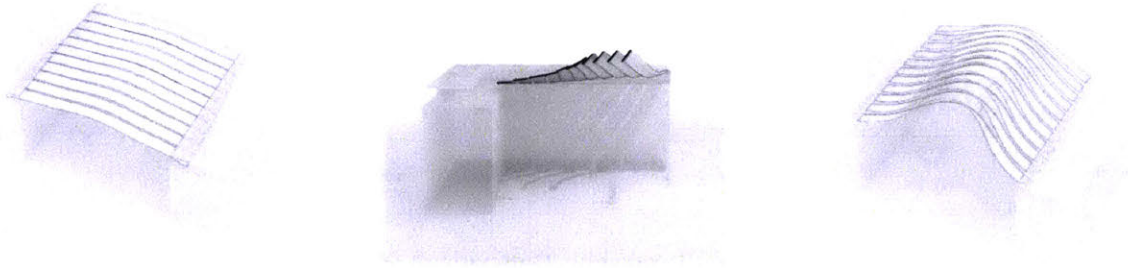
*The studies have clarified the effectiveness of introducing cables; bending of a plate by a cable can dominate the thrust force balance over the one from the dead load, allowing for stable bending actuations by a force control rather than displacement control, and thus can further decrease the thickness within a range that does not induce instability by normal stresses.*

The other type of bending-active plate is plates cantilevered by cables. The cable is connected all over the plate with sets of perpendicular joints that allow for the cable to transfer the force from the tip of the plate to the root support. Takahashi writes that, “the challenges were in the equilibrium finding among dead load, actuation cable force, and internal forces in the beginning, especially for the cases of the cable-cantilevered plates and the torsional plates.”

Next, Takahashi studies load-bearing behavior. He writes that bending-active plates must perform consistently throughout different deformation “steps.” During all steps of deformation, the structures must resist “severe external

loads such as wind loads.” Further a plate with cables “considerably decreases the magnitude of deflection,” and avoids the “snap-through buckling” that occurs in structures without cables.

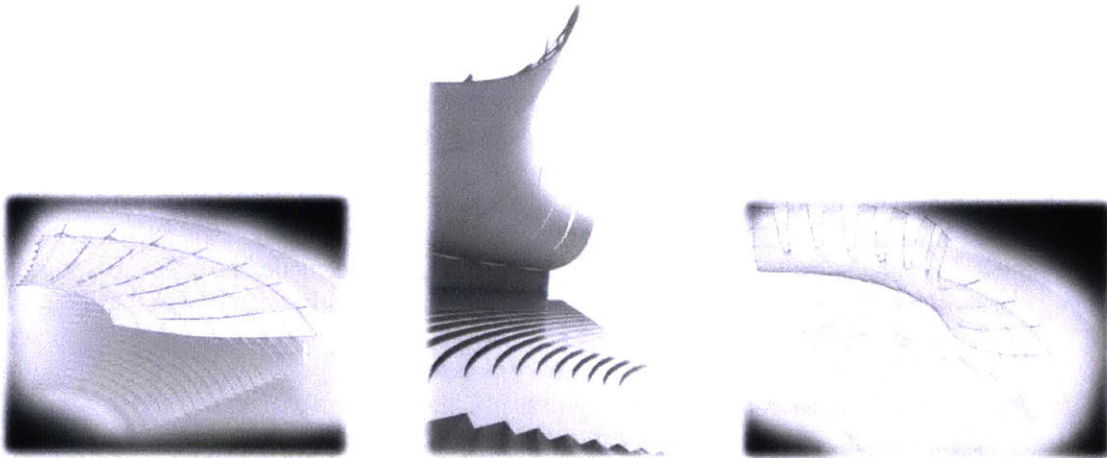
The illustration below shows the use of bending-active plates with “torsional deformation.” The plate angles are “moved from flat to inclined by means of torsional rotation. This allows for a unique light transmission control and the use of any given intermediate configuration.”



**Fig. 2.28 Structural – Active Bending:** Illustration of kinetic applications for bending-active plates.

*Torsional deformation involved in a roof structure that bridges the gap between buildings.*

The introduction of cables allows the bending-active plates to roll up for light transmission, and to straighten and cantilever as a shading device. These cantilever devices are ideal for open-air applications where “the roof needs to be supported from behind so as not to interfere the audience’s sight.”



**Fig. 2.29 Structural – Functional Articulation:** Introduction of cables allows the bending-active plates to:

(a.) Cantilever as a shading device; (b.) Roll up; (c.) Splay for light transmission.

Takahashi’s research explores the use of elastic kinetic structures as load-bearing systems. He found that the introduction of cables to bending-active plates have been proven to be “effective both for a stable actuation and to give rigidity against external wind loads.”

The recent paper from Julian Lienhard and Jan Knippers titled *Considerations on the Scaling of Bending-Active Structures* studies the scaling effects which that are relevant to problem of performance. In it some uncomplicated “systems are studied by means of dimensional analysis and FEM parameter studies to clarify at which power each influencing factor effects scaling. Based on these findings some more complex structures are studied for their scalability.” This is addressed later on by Takahashi [2015, p.26 & 27].

The authors define the term bending-active as “curved beam and surface structures that base their geometry on the elastic deformation of initially straight or planar elements.” Today, instead of the physical models used in the past, analysis is typically based on Finite-Element-Modelling (FEM). The architect or software user inputs geometrical and mechanical variables valued primarily for their relationship to each other and not their individual values. “Self-weight” factors are defined and used to simulate dead load deformation.

The authors write that the “scalar jump” from a physical model to a medium scale structure was successful. In the paper, the authors plan the scalar jump “from a medium model to a large scale structure. By doing this, they plan to fathom the scaling limits of various forms of bending-active structures.” The authors assert that “scaling is concerned with the power-law relationships between two or more variables of a system.” On one side of the equal equation is deformation and the other stability. The other side features load and mechanical properties. A *self-similar* system is one that has variables that are independent of the system’s dimensions.

The authors state that the following common effects should be considered in the scaling of building structures:

**Table 2.15 Common Effects: Scaling Structures.**

(after Lienhard 2013)

E1:	Dimension effect:	Cubic increase of mass with scale.
E2:	Load Effect:	Quadratic increase of surface area leads to quadratic increase of surface load.
E3:	Size Effect of Material:	Probability of material defects increases with size, whereas the influence of material defects increases for small size specimens.
E4:	Height Effect:	Exponential growth of wind-speed with height combined with quadratic growth of wind-load with speed.
E5:	Dynamic Effects:	Wind induced vibration, etc.

**Notes:** (a.) See also: [Takahashi 2015, B2, p.28]

The authors assert that for their paper, only mass and load will be considered. Their initial studies focused on the elastica arch in which the elastic deformation curve crosses a single span in its post-buckling state. Section 2.2, Euler described the shape of these curves in *Des curves Elastics* in 1744. The residual stress in an elastically deformed beam can be determined by the Euler-Bernoulli law which states that the bending moment ( $M_y$ ) is proportional to the change in curvature as shown in Calculations. We can write the residual bending stress as an expression of the cross-sectional height  $h$ , the Modulus of Elasticity  $E$  and the Curvature  $1/r$ .

Dimensional analysis combines the variables of a system into dimensionless groups.

*The Buckingham Pi-Theorem states that the relations in any physical system can be described by a group of  $n-r$  Pi-terms, in which  $n$  is the number of variables and  $r$  the number of basic dimensions therein (rank of the dimensional matrix).*

In mechanics, the authors state that the "basic dimensions are mass, length and time. In the following considerations on static behavior, force has been chosen by the writers as a fourth basic dimension. The exact form of the functional relationship has to be empirically obtained by a set of experiments in which the Pi-terms are systematically varied." Another of the authors' most relevant figures is as follows:

Investigating the deflection for a given elastica curve of span  $L$  stiffness  $EI$  and the line load  $qz$  and excluding the influence of mass and residual axial force we may derive the following functional equation:

$$U_z = f(L, E, I_y, q_z)$$

5 Variables:  $U_z, L, E, I_y, q_z$

2 Dimensions: [mm], [N]

The dimensional Matrix is:

	$U_z$	$L$	$E$	$I_y$	$q_z$
[N]	0	0	1	0	1
[mm]	1	1	-2	4	-1

Fig. 2.30 Structural – Elastica: Deflection.

[Lienhard et al. 2013]

The authors admonish: "it must be remembered that the stiffness of a lightweight structure does not rely only upon elastic stiffness, but also topological arrangement and geometric stiffness. Along with residual bending stress, there is a considerable amount of residual axial force  $N$  in a bending-active system, e.g., the nonlinearly distributed axial compression force in the post buckling state of an elastica curve." They then make the preliminary conclusion that: "Bending-active systems are self-similar if dead load plays a minor role and axial force is not destabilizing."

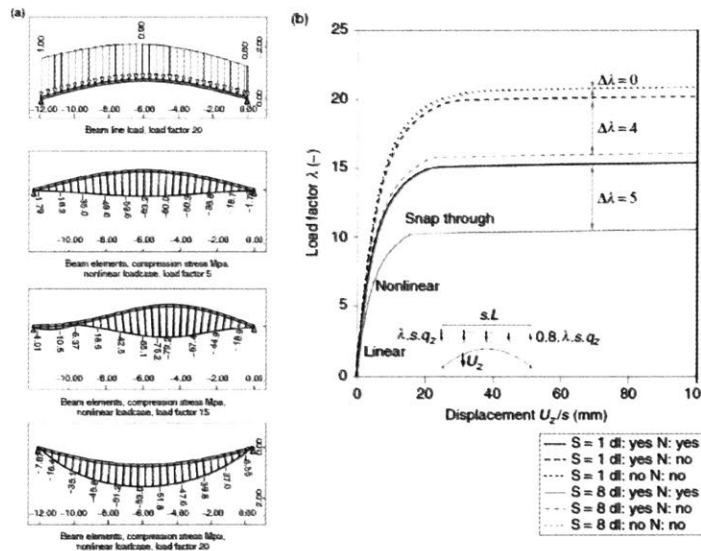
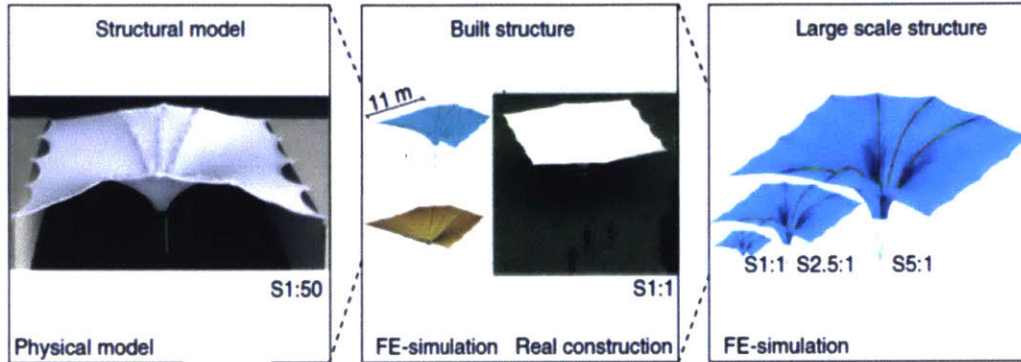


Fig. 2.31 Structural – Lienhard: The authors describe this figure as:

(a.) "Asymmetrical line load on the elastica curve showing compression stress and deformation to the point of snap-through buckling.

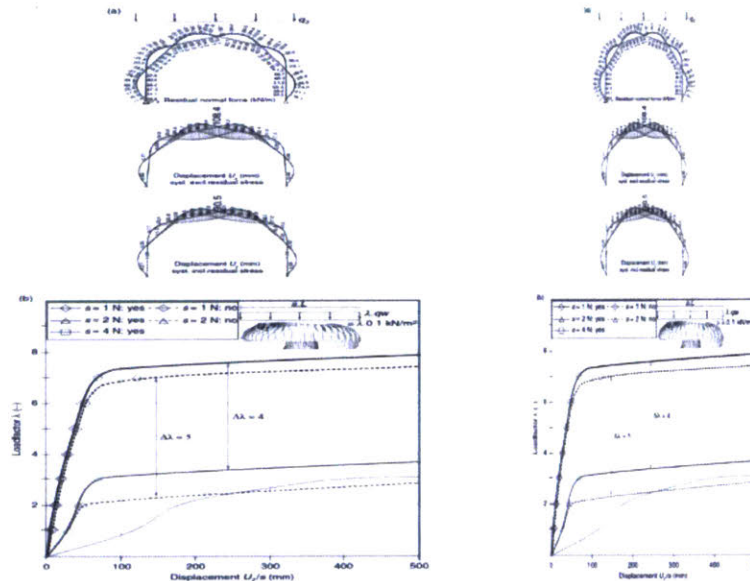
(b.) Load deflection curve of elastica curve with 15%  $f/L$  ratio at two scales; showing linear, nonlinear and snap through failure range."

To verify the above, the authors organized three case studies. At the Research pavilion ICD/ITKE 2010, residual tension stress resulted in an increase in geometrical stiffness; however, the advantageous influence of residual tension stress to the system is reduced over time due to enhanced relaxation of timber.



**Fig. 2.32 Structural – Lienhard: Study of various models of the Marrakech Umbrella. (2011)**

The authors explain that the above was designed by students for an outdoor plaza space at an architecture school in Marrakech, Morocco. The funnel shape was designed to minimize anchoring forces. The umbrella had a bending-active support structure for the free edges of the membrane which proved to be a very efficient solution. This structure highlights the possibility of using active bending in hybrid form.



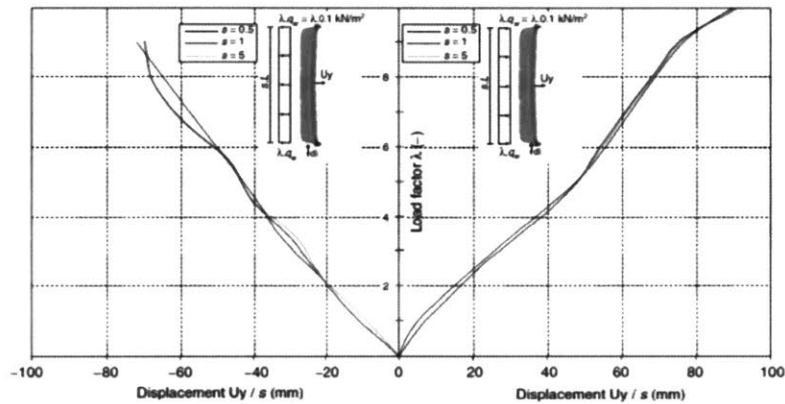
**Fig. 2.33 Structural – ITKE 2011: Pavilion**

(a.) Displacement  $U_z$  of a coupled arch section showing 17% stiffness increase including bending induced stress.

(b.) Load deflection curve of the research pavilion at different scales.

Bending-active structures where the system is stabilized by the elastic beams that, in turn, are restrained by the membrane surface.

The Flectofin® forms a reverse deformation when an external mechanical force is applied. The lamella supports are 2.2 m long and 0.25 m deep. They are made out of GFRP and produced in a vacuum bagging process. This system suggests that the above assumptions of dead load and stability only, being the limiting factors for scalability of bending active structures, may be generalized.



Load deflection curve of the Flectofin® Lamella at 3 different scales, for a given wind- suction and pressure-load case.

**Fig. 2.34 Structural – Marrakech: Load deflection curve of the Flectofin® Lamella.**

*Three (3) different scales, for a specific wind-suction and pressure-load case.*

*Kinetic Shading.* For the theme pavilion of EXPO Yeosu, Korea 2012, an elastic kinetic façade shading system inspired by the Flectofin® was built. Covering a total length of 140 m and varying in height between 3 and 14 m it was designed to withstand the very high wind loads at the Korean coast, proving the applicability of this system for large scale structures.

A FEA analysis of the scaling of bending-active structures is dependent on the significance of dead load and stability. As an important influence on the stability, it could be shown that residual compression stresses are destabilizing and tension stresses are stabilizing due to nonlinear stress-stiffening effects (see example of ICD/ITKE pavilion and Flectofin®). The consideration of axial forces in the geometrical stiffness is therefore of particular importance and may be used advantageously for the scaling of bending active structures.



M. Collins, B. O'Regan, and T. Cosgrove, in *Potential of Irish Orientated Strand Board in Bending Active Structures*, engage in a comparative study of orientated strand board (OSB) and solid timber. Three parameters central to their study are the following:

- Strength to stiffness ratio,
- Flexural stiffness of commercially available sections,
- Variability of material and section properties.

The researchers discovered that OSB was appropriate for smaller grid-shells (doubly curved structures) with relatively tight radii, and cite two categories of grid-shells: (a.) bending active and (b.) bending inactive.

**Bending active:** "the structural elements have to bend considerably to give the structure its shape, a type of bending pre-stress."

**Bending inactive:** "describes a structure whereby the structural elements do not need to bend to give the structure its shape. A typical bending inactive structure would be a truss, portal frame or a geodesic dome."

The authors state that their study is "focused on identifying the potential of OSB for use in high-end structural applications such as bending active grid-shells." Their stated objectives are as follows:

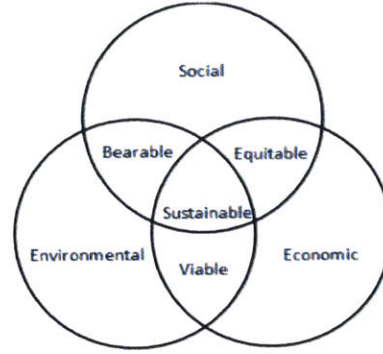
**Table 2.16 Structural – Collins, O'Regan & Cosgrove: Six objectives. (after Collins et al. 2015)**

O1:	To identify unique characteristics associated with bending active structures with implications for design.
O2:	$E/f_m$ ratios.
O3:	Flexural stiffness of available sections.
O4:	Variability.
O5:	To investigate if an engineered timber is more suitable and sustainable than solid timber for bending active grid-shells.
O6:	To assess the sustainability of constructing a large scale grid-shell in Ireland using two specific lumber products (native and non-native) in terms of reduced environmental and asocial impacts with lower costs.

**Notes:** (a.) *The authors found that in terms of the  $f_m/E$  ratio is more suitable for bending active grid-shells than any softwood solid timber. But the  $f_m/E$  ratio is not enough to make a decision "on a suitable material for use in bending-active grid-shells."*



Fig. 1 Savill Garden Gridshell



**Fig. 2.35 Structural – Grid-shell (a.) Savill Garden; (b.) Three pillars of sustainable development.**

"The longitudinal (life cycle) boundary established for this study was from the harvesting the timber in the forest to the construction of the structural roof skeleton. The primary indicator for this study was economy (cost). This included the volume of material, time, processing, and transportation and environmental metrics included the energy inputs for each process, emissions, water and waste. The social metrics included health and safety, aesthetics and the potential for Irish industry. The code regulation petition anticipated would require policymaking, legislation, and governance." Adapting the authors' figure yields:

**Table 2.17 Structural – Comparison: Longitudinal & Associated boundaries. (after Collins et al. 2015)**

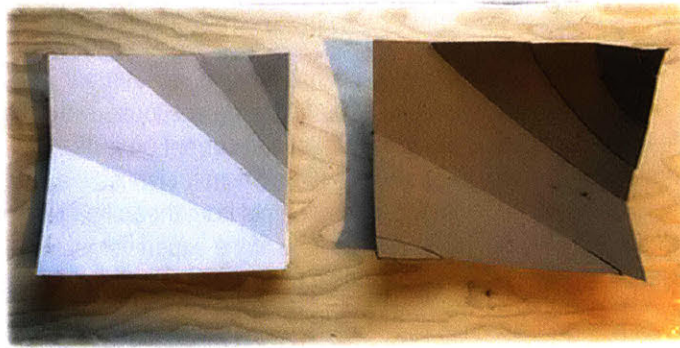
<p>The longitudinal boundary for the assessment of grid-shell constructed from imported UK larch has the steps at right.</p>	<ol style="list-style-type: none"> <li>1.) Harvest from forest</li> <li>2.) Transport to sawmill</li> <li>3.) Saw into laths</li> <li>4.) Transport to processing facility</li> <li>5.) Finger jointing</li> <li>6.) Transport to site</li> <li>7.) Scarf jointing</li> <li>8.) Construct grid-shell</li> </ol>
<p>The associated boundary using OSB has the steps at right.</p>	<ol style="list-style-type: none"> <li>1.) Harvest from forest</li> <li>2.) Transport to factory</li> <li>3.) Process into sheets</li> <li>4.) Saw into strips</li> <li>5.) Transport to site</li> <li>6.) Splice jointing</li> <li>7.) Construct grid-shell</li> </ol>

**Notes:** (a.) For input pre-processing.

The authors' findings are: "Economically the high quality larch members would be costly only if used for a project in Ireland. OSB is produced at a substantially lower cost. Environmentally, the larch solid timber has less of an impact on the environment than OSB. As far as social impact, the OSB production is located in Ireland, and the larch timber is grown in the UK, and has to be imported at a cost." The authors' two conclusions from the study are as follows:

- "Engineered timber is a more suitable and cost effective material for use in grid-shells."
- "OSB is suitable for use in grid-shells, notably smaller span grid-shells with high curvatures."

## Performance – Financial



**Fig. 2.36 Financial – Cost-aware: Cylindrical & Conoidal.**

*Study models: economical approximation of double curvature with offset-able developable strips.*

*The museum board used in the initial attempt was too thick, but the thinner chipboard stayed twisted.*

This summary of building system financial properties, a result of the literature review, is included as a primer.

**Table 2.18 Financial – Properties.**

**(Various)**

<i>Detached – Avg. Total Price:</i>	\$383,179 (Lot excluded); \$289,415 (Construction).	[NAHB 2015]
<i>Detached – Avg. Cost, Structure:</i>	\$63,077 (21.8%, Insulated; Arch & Eng.)	[NAHB 2015]
<i>Detached – Avg. Cost, Floor:</i>	\$159/ft. <sup>2</sup> as Floor area.	[NAHB 2014]
<i>Light Frame – Avg. Cost, Surface:</i>	\$9.05/ft. <sup>2</sup> as Surface area.	[Meis 2015]
<i>Panelized – Avg. Cost, Surface:</i>	\$10.94/ft. <sup>2</sup> as Surface area.	[Meis 2015]

**Notes:** (a.) *Detached, Area:* 2400 ft.<sup>2</sup>; *Site-built:* 2,457 ft.<sup>2</sup>; *Modular:* 1,722 ft.<sup>2</sup>; *Panelized & Pre-cut:* 2786 ft.<sup>2</sup>

(b.) *Detached, Floor:* \$159/ft.<sup>2</sup>; *Site-built:* \$84/ft.<sup>2</sup>; *Modular:* \$76/ft.<sup>2</sup>; *Panelized & Pre-cut:* \$70/ft.<sup>2</sup>

(c.) *References:* [NAHB 2015, Adapted]

### Single Family Price and Cost Breakdowns

Total Finished Area: 2,802 ft.<sup>2</sup>  
 Total Cost (100%): \$468,318

### Key

Site work. (5.6%): \$16,092; Foundation (11.6%): \$33,447; Framing (18%): \$52,027; Cladding (7.2%): \$20,717; Insulation (2.2%): \$6,467; Drywall (4.1%): \$11,744; Major systems (13.1%): \$37,843; Arch/Eng.(1.6%): \$4,583.

### 3. METHODOLOGY

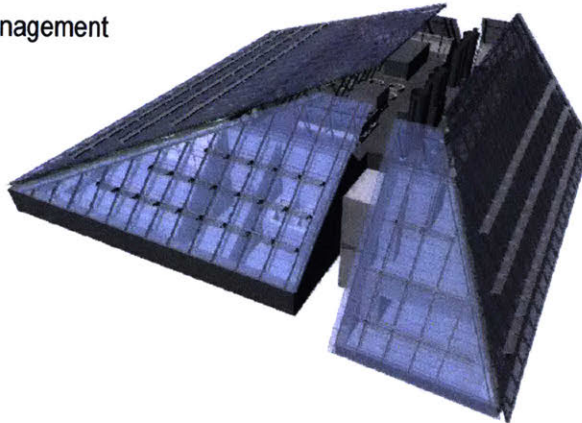
This *Chapter* is organized by the general methodology type into *Section 3.1 – Virtual*, *3.2 – Rational*, *3.3 – Evolutionary*, and overview *Section 3.4 – Experimental*. The first three sections review the fundamentals of different design methods involved referencing process images from past and current projects. With much of the preliminary analysis and formal testing prototype-specific, *Section 3.4 – Experimental* clarifies the load test methods that were used. Descriptions of specific procedures, specimens, and excerpts from theoretical and numerical analyses are included in the report-style *Chapter 5 Results*. After discussions of the experimental results and findings, method-defining examples, developmental studies, and downloadable tools are presented in *Chapter 8 Demonstrations*.

#### 3.1 Methodology – Virtual

##### Virtual Design & Construction

Introduced in a Fischer and Kunz CIFE technical report [2004] then developed as a guideline by working paper #093 [Khanzode & Fischer et al. 2006], Virtual Design and Construction (VDC) implies “the use of multi-disciplinary performance models of design-construction projects” [Fischer & Kunz 2004]. It involves five core principles:

- Model-based analysis
- Engineering modeling
- Business/Strategic management
- Visualization
- Economic metrics



**Fig. 3.1 Virtual Design – Multi-objective: Harvard Art Museums.**

*A central, evolutionary, detailed model was utilized for design development, presentation, simulation, and validation of conventional 2D documentation. Fabricator coordination was reduced with model-generated sectional overlays.*

[RPBW 2011]

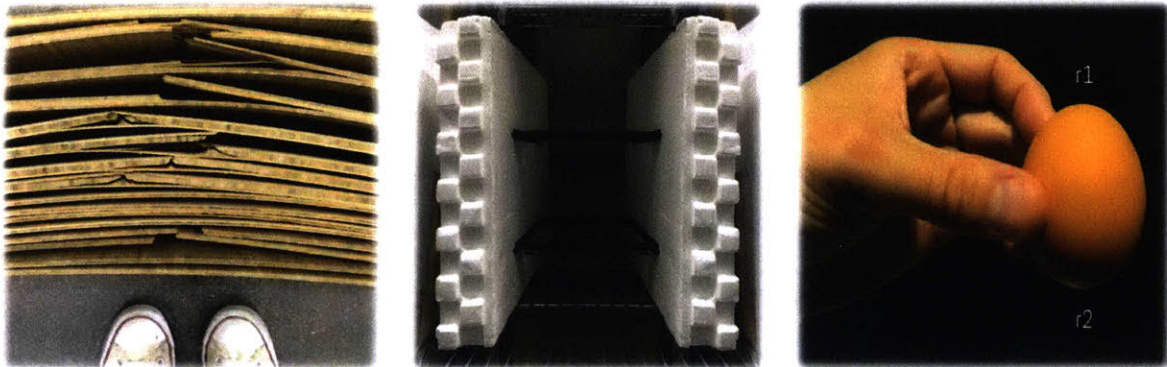
The current MIT project applied all five VDC principles if branding qualifies as business/strategic management. Also on the subject of commercialization, the 4 in “Free4orm LLC” is a reference to time – the x-axis in the measurement of operational energy. Acting also on the specific CIFE suggestion that all projects set and track “process performance parameters” [Kunz & Fischer 2012, p.26], each thread fed back into another (architecturally, technically, and economically) in our iterative application of VDC. This with concurrent physical experimentation, seemed to result in a greater certainty about detailing than that experienced in practice. Open questions tend not linger when there is feedback. What is clear is VDC-based production of scale models and tabletop mock-ups contributed significantly until results for the full scale specimens became the primary developmental influence.

## 3.2 Methodology – Rational

### Rationalized Design

Within the context of architectural geometry, different "design approaches" for realizing freeform surfaces were recently described as (1.) *non-rationalized*, (2.) *pre-rationalized*, (3.) *post-rationalized* and were discussed referencing built examples from Evolute-RFR collaborations. Therein the term "construction-aware" is used to advocate for the integration of construction and manufacturing considerations in the earliest delivery phases with the expressed objective of de-constraining architectural design space. This pragmatic strategy and the stipulated, rigorous engagement of geometry are fundamental to each of these three specific methods.

In keeping with this strategic methodology the current project experiments with the extension of pre-rationalization to engage the conceptual scope in order to address usually-excluded architectural scope. Herein, pre-rationalizations have been systematically grouped by scale, by specificity, and by motive as (1.) Macro: concept-, ideal- or logic-driven; (2.) Micro: method-, principle, or constraint-driven; and (3.) Nano: technical means-, detail-, or data-driven.



**Fig. 3.2 Pre-rationalization – Macro: Concepts.**

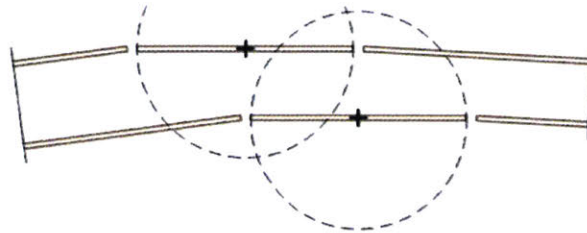
(a.) Material awareness; (b.) New types from old; (c.) Strength in geometry;



(e.) Digital and Renewable; (f.) Friction-fit over fasteners; (g.) Prototype-driven process.

Fundamentally, a non-rationalized approach independently generates or describes the intersection or division of the design surface, which the RFR example used arc splines to do. By contrast, a pre-rationalized approach involves conceptual limits like to the describable surface classes (translational, rotational, or developable). A post-rationalized approach is usually criteria-based approximation and discretization or functional optimization of an existing surface.

The figures below represent pre-rationalizations from the current project. The distinction between concepts and principles was made to separate ideas from rules. Similarly, the one made between principles and constraints was intended to represent the virtual/physical divide. As there was no existing design surface the *GEN.4* proposal was developed to reflect the results of the material testing. The properties of the available equipment, dimensions of material inputs, and the logical constraints were all considered pre-rationalizations and the in-process results which became pre-rationalizations are presented in *Section 6.1*.



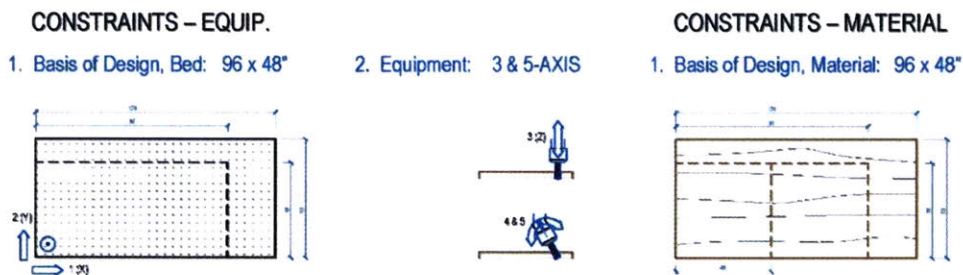
**Fig. 3.3 Pre-rationalization – Micro: Methods.**

*Strength in Geometry: Sectional blocking of the individual axis of rotation and assembly hinge lines.*

- |                                          |                                                    |
|------------------------------------------|----------------------------------------------------|
| 1. ONLY SHEET MATERIAL INPUTS            | (2D, engineered wood or panel products)            |
| 2. ONLY CUTTING / CONTOURING OPERATIONS  | (2D, eliminate surfacing to reduce machine time)   |
| 3. ONLY SMALL-BIT OPERATIONS             | (2D, 1/8" bit kerfing feed rate sub-optimal)       |
| 4. MINIMIZE CLAMPING, GLUEING, FASTENING | (screws, or brads & glue if mechanically fastened) |
| 5. MINIMIZE MATERIAL WASTING             | (circle / triangle-packed attachment details)      |

**Fig. 3.4 Pre-rationalization – Micro: Principles.**

*Primary top-down constraints*



**Fig. 3.5 Pre-rationalization – Micro: Constraints.**

*Primary bottom-up constraints; inputs and equipment.*

Although the workflow was sequential (e.g., first establish the material's "behavior-based" geometry, next generate an informed design geometry, and then compare or validate with numerical simulation) and drawing on *2.2 Literature – Geometry*, a fundamental "integrated approach" can be claimed [Lienhard et al. 2013]. The preliminary "behavior-based" geometric analysis performed for Forest Stewardship Council (FSC) certified AC plywood corresponding with this approach is located in *Section 4.2 Analysis – Geometry*.

#### CONSTRAINTS – MISC.

1. Assembly, Humidity: 8% MIN.
2. On-site, Trade Coordination: ACTIVE
3. On-site, Access: INTERIOR
4. Manufacturer, Zip-Tie: PANDUIT
5. Manufacturer, Seam Tape: ROBERTS

#### CONSTRAINTS – TRANSPORT

1. Trailer, Size: PH
2. Palette, Size: PH
3. Packing, Sequence: PH

**Fig. 3.6 Pre-rationalization – Nano: Constraints.**

*Secondary bottom-up constraints; environmental, labor, and logistical.*

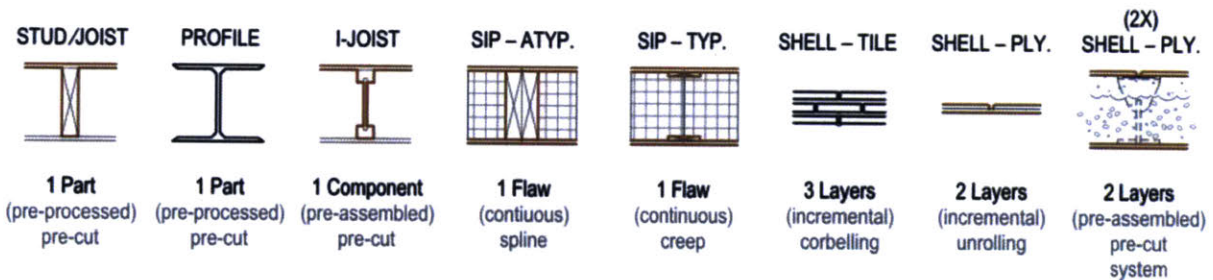
In post-rationalization, usually the technical challenge has to do with (1.) reconciling a pre-existing conceptualized geometric aesthetic for a building's appearance with the means of production, (2.) optimizing that production, or (3.) value-engineering to bring a project into viability. In the current project, the advance logging of constraints included here evinces enthusiasm for the present themes and methods employed in architectural geometry, but this also relates to assemblage theory as clarified by the Manuel DeLanda quote in the *Dedication*. An previous discussion of properties, capacities, and their relevance to architecture can be found in the author's similarly-themed initial research project *Cannoli Framing & Turnstijl Houses* [Aeck 2007].

### 3.3 Methodology – Evolutionary

#### Evolutionary Design

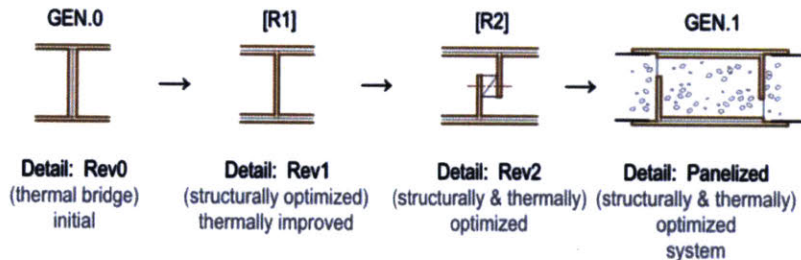
As an architectural design strategy, evolutionary design in the sense of bio-inspired Darwinian natural selection [Holland 2010] can be found in the journal *Revue Générale de l'Architecture* in the 1860s, which appears to have introduced the term "Organic Architecture" [Collins 1965]. In the 20th-century, the same term was appropriated in *The Natural House* [1954] in which Wright can be found campaigning against dormers and attics. It appeared again around the advent of the digital shift in *The Evolution of Designs* as part of a historical review of the biological analogy in architecture as "methods in design analogous to the processes of growth and evolution in nature" [Steadman 1979, 2008]. Though it is not specifically addressed in the most recent update of the latter, Lynn's 1997-2001 Embryological House is a further example of bio-inspired design for the purpose of exhibiting unlimited variety.

Today, with the advancement of post-digital numerical analysis and computational methodology, complexity and evolutionary design have come to refer to a design process that "rejects the recognition of final or ultimate forms in favor of a continuum of evolutionary forms. Such forms are continually renewed either by the influence of external dynamical forces or through the unfolding of endogenous processes of growth and mutation" [Holland 2010]. A local example, the early evolutionary computational tool "Genr8" developed by MIT's Emergent Design Group used an evolutionary approach to design because it "allows an architect or designer to both grow and evolve three dimensional digital forms or surfaces" [Hemberg et al. 2008]. It was in this spirit and that of later efforts by Axel Killian [2006] and by Phillippe Block [2005] that the downloadable computational tool included herein was developed. Like some of the structures proposed, this project employed a hybrid of virtual, rationalized, and evolutionary prototype-driven design methodology on the way to of developing the GEN.4 proposal. The beginning of that development was the evolutionary functional optimization illustrated below by Figure 3.8, which depicts the sectional transformation from the GEN.0 box-beam to an early version of the staggered GEN.3 semi-unitized method.



**Fig. 3.7 Evolution – Structural.**

*Structural comparison of some relevant types.*

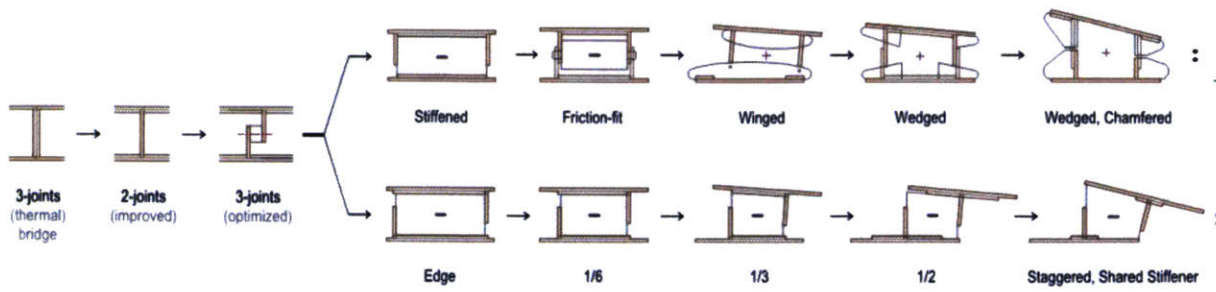


**Fig. 3.8 Evolution – Functional.**

*Functional optimization of the initial GEN.0\_Box detail → early staggered-stud GEN.1\_Panel system.*

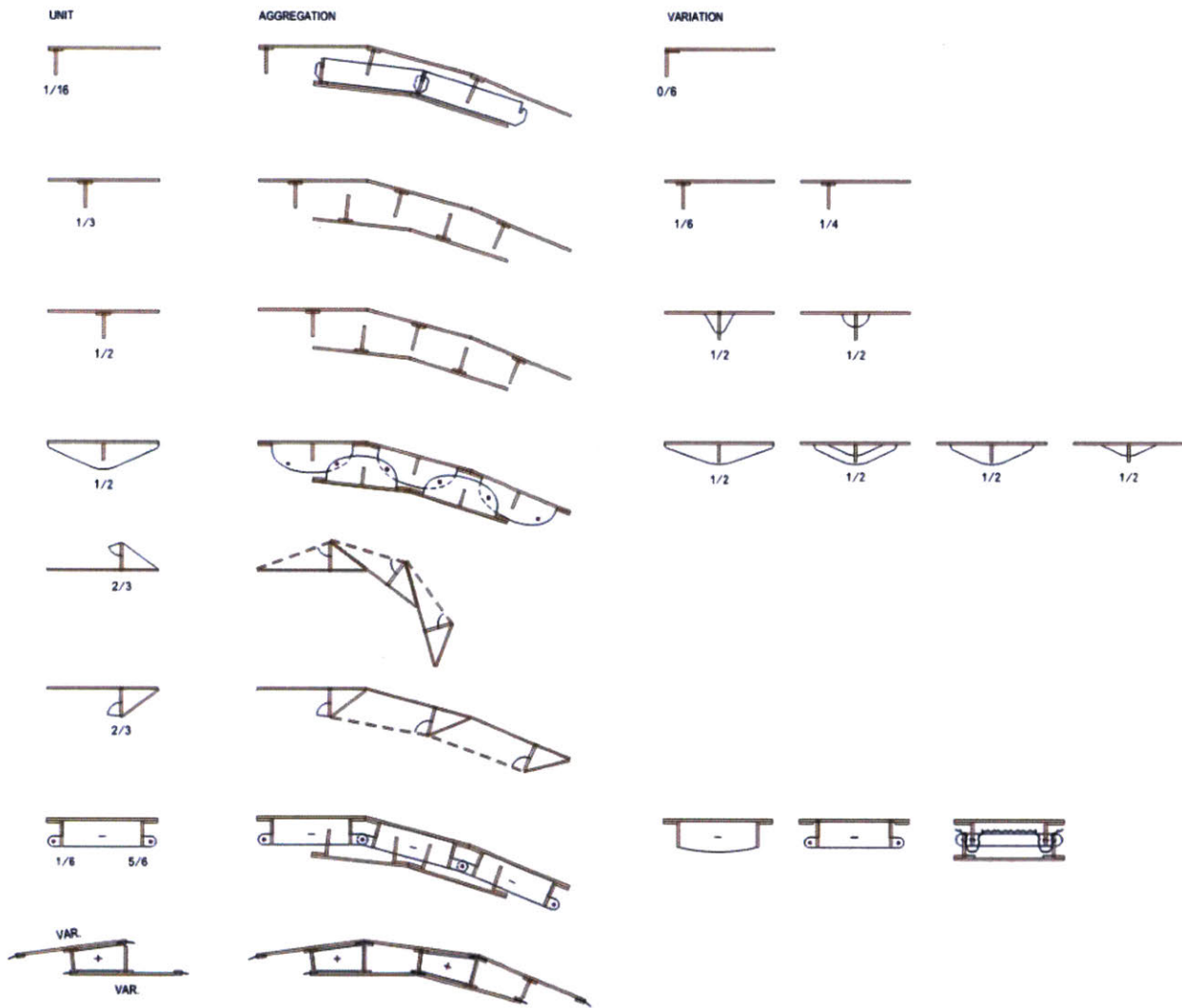
*(1.) Maximize extreme fiber, (2.) Minimize thermal bridging; (3.) Optimize hinge/edge detail access.*





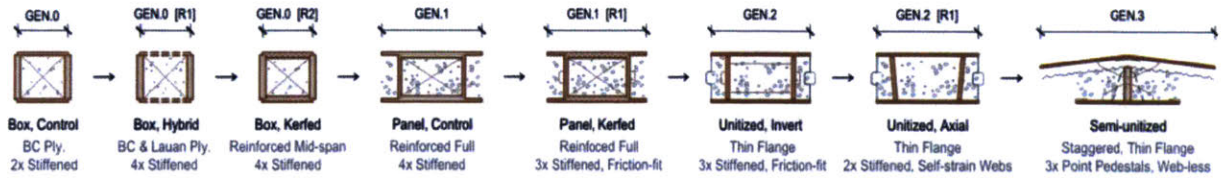
**Fig. 3.9 Evolution – Exploratory.**

*Experimental evolutionary history for late GEN.2 and early GEN.3. The webs detach, and then begin to move.*



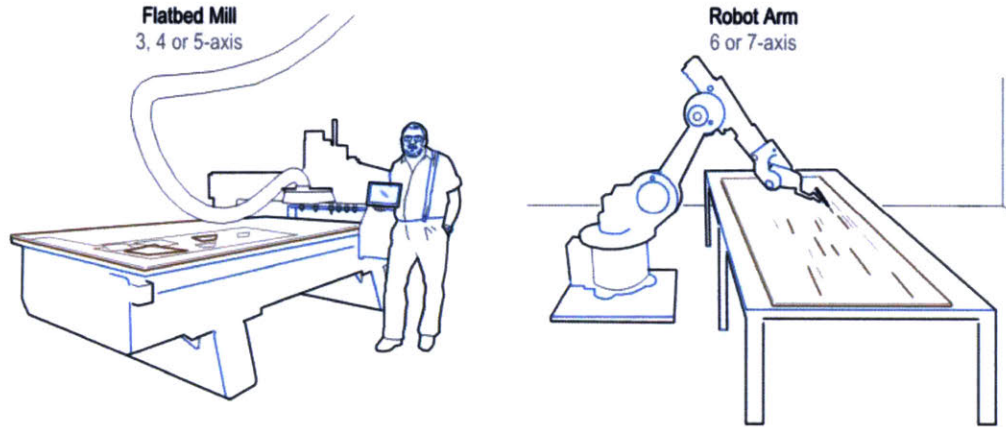
**Fig. 3.10 Evolution – Developmental.**

*Developmental evolution for GEN.3 method. Column: (1.) Unit; (2.) Aggregation; (3.) Variation.*



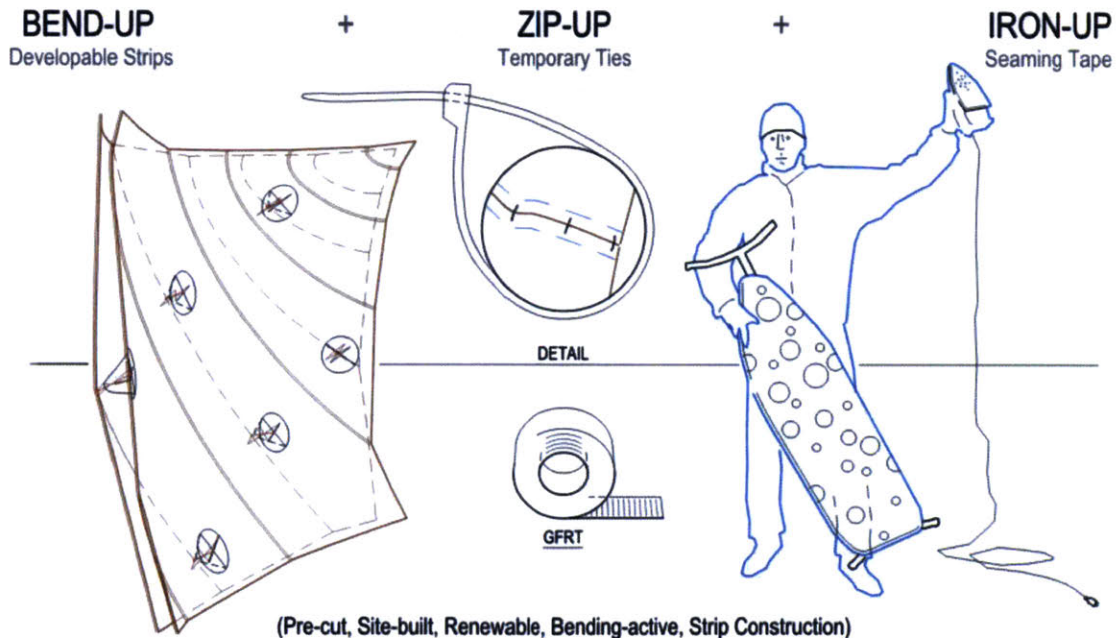
**Fig. 3.11 Evolution – Generational.**

*Typological evolution from the initial GEN.0\_Box → GEN.1\_Panels → GEN.2\_Utilized → GEN.3\_Semi-unitized.  
Evaluating box-beams, stiffening and recessing webs, optimizing thermal performance and staggering strips.*



**Fig. 3.12 Evolution – Capacities.**

*Within the varied properties of new equipment exists the capacity to extend residential construction.*



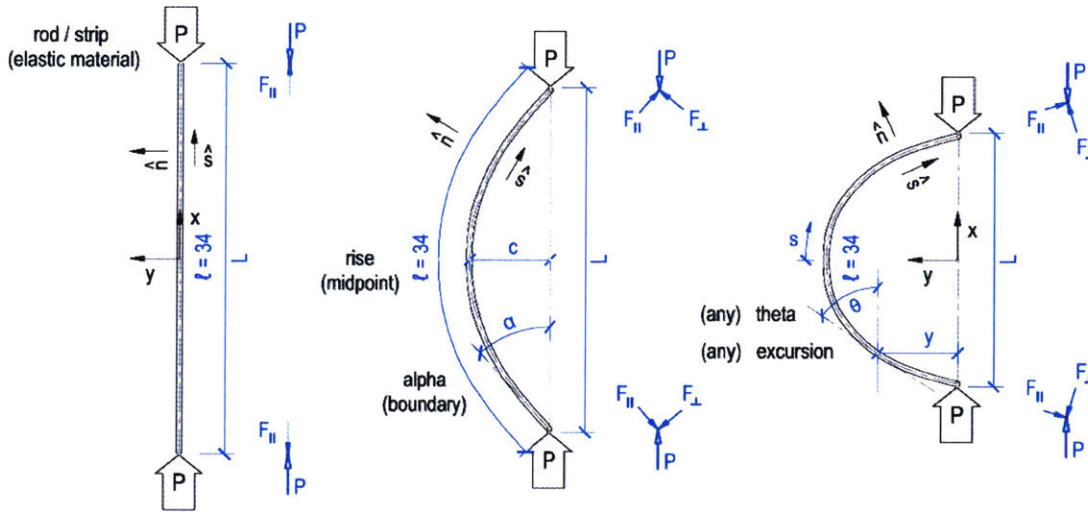
**Fig. 3.13 Evolution – Methodological.**

*Methodological alternatives resulting from changes in modeling and machining technology.*

### 3.4 Methodology – Experimental

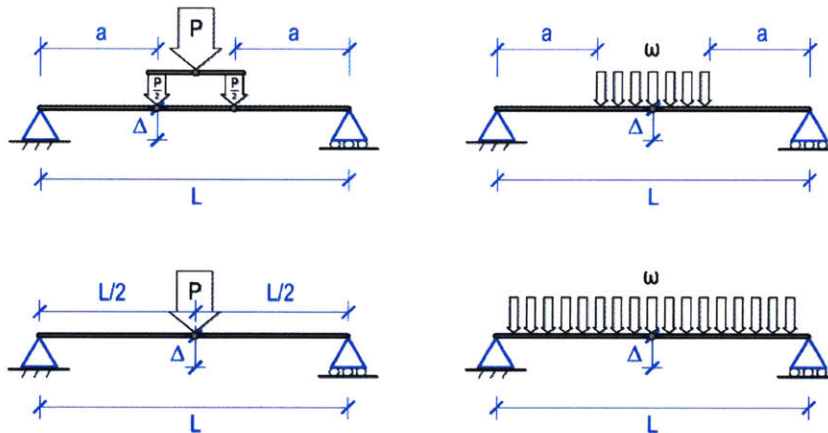
#### Experimental Loading

Detailed descriptions of each system, specimen, and procedure are provided within *Chapter 5–Results*. The dimensional analysis workflows used to generate the theoretical predictions are located in *Appendix E–Elastica*.



**Fig. 3.14 Experimental – Loading: Strips.**

See also: *Appendix – E.*



**Fig. 3.15 Experimental – Loading: Beams.**

*Appendix – C:* (a.) 4-point Flexural, (b.) Partial-Span Uniform Distributed (PSUDL)  
(c.) 3-point Flexural, (d.) Uniform Distributed (UDL)

The equipment used in four of the five load tests was a 60 KIP [413.68 MPa] Baldwin hydraulic press retrofitted for numerical control. Also, four 4"x 6"x 60" hollow steel sections (HSS) at 0.38" were added to extend its bed. Test-specific theoretical analysis workflows (*Appendix – C*) were required because of the inverted specimen curvature and the atypical loading of the *GEN.3* specimen and scale. Similarly, the following analysis of construction precedent documents application-specific research subsequent to the general topical research.

## 4. ANALYSIS

This *Chapter* is again organized by stated problem. The initial *Section 4.1 – Construction* provides supplemental application-specific precedent analysis and is organized by topic. The following *Section 4.2 – Geometry* summarizes preliminary geometric research, and the final *Section 4.3 – Performance* presents preliminary testing and mock-ups.

### 4.1 Analysis – Construction

#### Construction – Detached



**Fig. 4.1 Construction – Conventional: I-Joists.** | **Fig. 4.2 Construction – Conventional: Trussed-joists.**

*The integration of prefabricated components in conventional construction.*

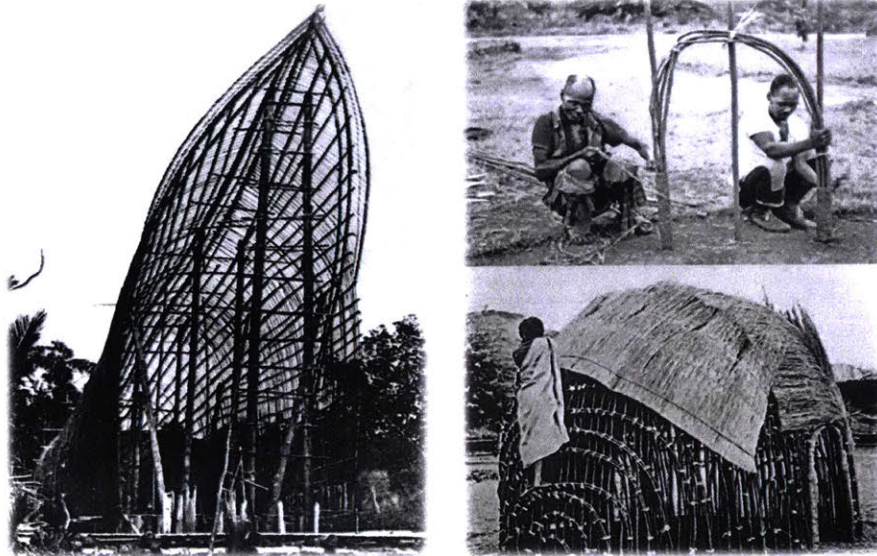
**Table 4.1 Detached – Comparisons: Methods**

**(Then vs. Typical)**

<i>Method:</i>	<i>Balloon</i>	<i>Platform</i>
<i>Class:</i>	Braced frame (Typ.).	Sheathed frame (Typ.); Braced (Atyp., Temp.)
<i>History:</i>	Pre-industrial, 1800-1930s; New continent, sawmills → New method/type; Heavy timber to Light wood frame.	Post-industrial, 1914-Present; New materials → Changes method/type; Balloon to Platform frame.
<i>Specifics:</i>	Continuous vertical members; Floor joists fixed directly to vertical studs; Let-in (1"x 4") diagonal bracing;	Discrete vertical members; Floor joists fastened to a header; Redundant partial bearing at (2"x 4") top plate.
<i>Fasteners:</i>	Nail, hand-made.	Nail, machine-made.
<i>Pros:</i>	Relative simplicity and economy; Interconnectedness, stiff.	Relative simplicity and economy; Flame-spread resolved; Reduced-labor.
<i>Cons:</i>	Thermal bridging; Sheathing is labor-intensive. Sub-floor stops at studs (Typ.). Blocking at floor often omitted; Flame spread. Long verticals increasingly scarce;	Thermal bridging; Sheathing is industrialized. Sub-floor continues under studs (Typ.). Blocking at floor inherent. Short verticals available and manageable;

**Notes:** (a.) *The revision of platform framing is known as advanced or optimum value engineering (OVE) framing.*

## Construction – Empirical



**Fig. 4.3 Construction – Empirical: Haus Tambaran. | Fig. 4.4 Construction – Empirical: Bantu Grass.**

*Both structures use light, redundant, bending-active members to produce curved, uniform-depth grid-shells.*

[Photos: Rudofsky 1965, New Guinea; Knuffel 1973, South Africa]

A “Haus Tambaran” from the Sepik province of Papua New Guinea (*Figure 4.4, above*) is both inspirational and inspired. In this hybrid structure, bamboo poles and both light horizontal and heavy vertical timber framing are employed. Translated from the English creole language *Tok Pisin*, this means “spirit house,” which is a sacred, communal structure used for ancestral worship. The lateral ladder frames provide access from the interior and serve to support a hanging vertical infill straw-thatch mat. Conceptually, mixing of types becomes significant later for the installation, and its interior approach to access differs from the next pure grid-shell example.

The bundled Bantu “grass” huts of KwaZulu-Natal, South Africa (*Figure 4.4, above*) are typically *acacia mearnsii* or grey poplar. The top photo in shows the beginning of construction at the sinking of sharpened 30cm “starters” and the bottom photo the application of fine woven mats nearing completion. This shelter featured 228 structural members and represents approximately 40 days of remote material gathering. The hut construction sequence was described initially by Knuffel [1973] and most recently by Jarzombek’s [2013] *Architecture of First Societies*. The bundling enhances and high-redundancy assures structural performance but also results in a friction exterior access system – as is revealed by the bottom photo.

## Construction – Methodological

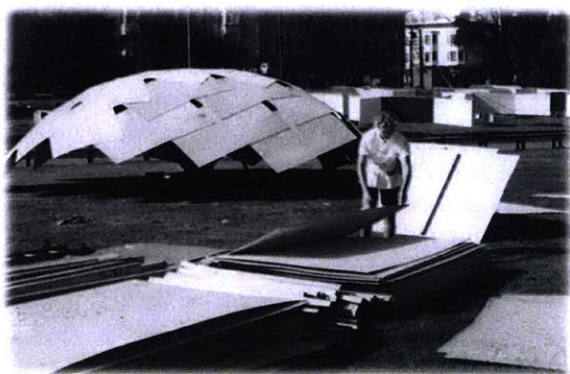


**Fig. 4.5 Construction – Steamed: Canoe.** | **Fig. 4.6 Construction – Stave: Workboat.**

[Photos: by Author; Boats & Rice 2014]

Similar in process to Thonet café chair, *Figure 4.5* depicts a steam-bent canoe sub-frame by Skip Willis encountered during a visit to Bronze Craft Foundry in Charlottesville, VA. The suspended frame brought to mind innovative wartime aviation construction, such as the bag-molded fuselage and notched spline joinery of the "Timber Terror", an all-plywood fighter-bomber. [Bonnier 1943].

Similar to barrel construction, *Figure 4.6* is wet-bent stave construction – a steam-less, traditional method employed for Mekong River Delta work boats. Using a starter jig and minimal lateral attachments planks are rough cut and joined centrally, the longitudinal tapering is then executed in place. The edge-to-edge shaping produce the lateral curvature, resulting in a rib-less, frame-less boat hull.



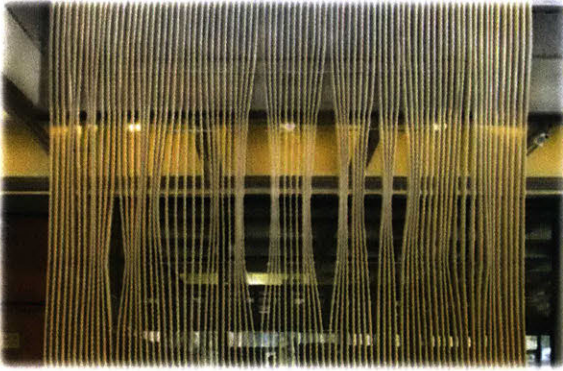
**Fig. 4.7 Construction – Stave: Candela Formwork.** | **Fig. 4.8 Construction – Sheet: Fuller-Moore Plydome.**

[Photos: Juan Guzman 1958; Moore Family Collection 1957]

Encountered at a 2012 Columbia University symposium, *Figure 4.7* is a construction photo of surface-active formwork – that could itself be the finished product – for the cast-in-place, thin-shell Restaurante Los Manantiales in Xochimilco, Mexico. Both structures are shells, but the Candela is temporary falsework and closer to the stave construction shown on the following page. Also notable is that T.E. Moore (figure right) consulted with Candela on several occasions in relation to his own long-span thin-shell efforts.

Courtesy of Thomas E. Moore's sons Charles and Hugh, *Figure 4.8* is Washington Square in San Francisco, CA. Moore (1908-1970) was an early "Plydome" contributor and architect of many innovative and long span shells. He maintained a collaboration with Buckminster Fuller following the 1950 International Design Conference, building an experimental concrete dome in 1953. A co-founder of Shell Structures, Inc. in 1955 with engineer Hugh Hyder. In 1960, Moore and Fuller developed and built a concrete geodesic "Dogbone" dome prototype.

## Construction – Post-digital: Installations



**Fig. 4.9 Strips – Tensioned: Plywood Delaminations. | Fig. 4.10 Strips – Stress-stiffened: A Change of State.**

*Rapunzel; offsetting strips (architectural active bending). Calamari; polymer strips (structural active bending).*

[Source: Georgia Tech DBL; Ponce de Leon 2005; Tehrani 2006,]

The 2005 *(Ply)wood Delaminations* installation remains within the West Architecture Building at Georgia Tech in memory of Dean Thomas Galloway. Conceptually a high-back bench, it is a uniform-depth, vertical aggregation of 0.5" [12mm] Birch providing appropriate seating for visiting critics. Between the base and initial intermediate anchorage, there are atypical bending-active "gathered" conditions. The eighty (80) continuous 4.0" deep ribs are aligned with the bush-hammered concrete rails behind them – a detail developed after observing humidity affecting the laser-cut scale model.

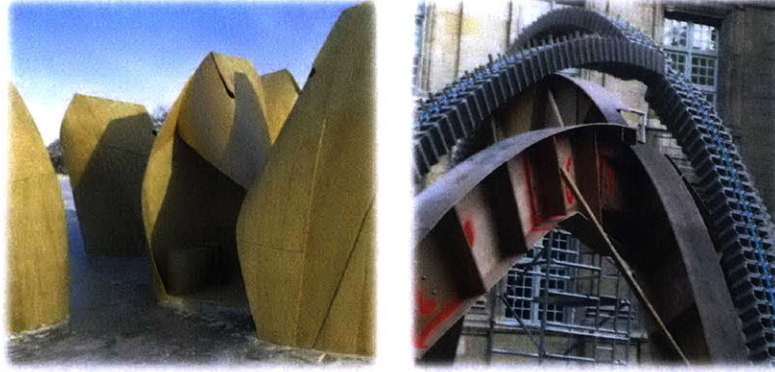
The 2006 *A Change of State* Installation was also made possible in conjunction with the Thomas W. Ventulett endowed chair. Conceptually an expression of material organization (and counterpoint), it was a variable-depth horizontal assembly of 0.125" [3mm] polycarbonate also generating from a bench. From densely stacked sheets, it expanded around existing concrete structure before shredding and twisting into a bending-active stressed-stiffened condition to enable the "leap" depicted above. After leaving the ground, it anchored to a lateral concrete beam before cantilevering in its final corrugated state.



**Fig. 4.11 Strips – Study Model: A Change of State.**

*3-strip module: Opacity change and Pre-deformation of sheet material with a geometric target.*

[Photo: by Author 2005]



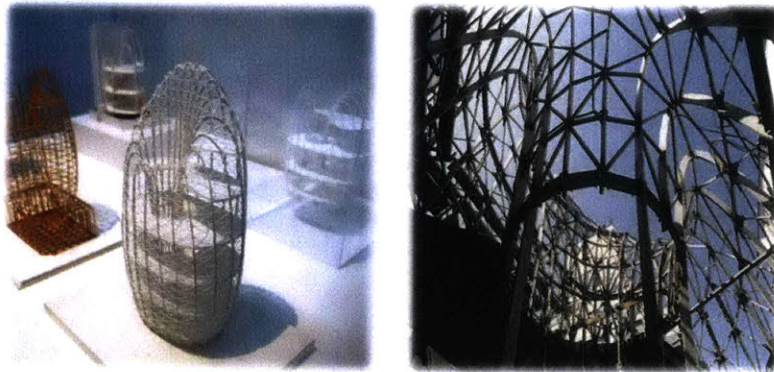
**Fig. 4.12 Sheets – Shelter: Thin-shell Plywood. | Fig. 4.13 Sheets – Centering: Post-tensioned Masonry.**  
*Bending-active, uniform-depth, thin-shell. – Compression-only, uniform-depth, arch, variable-depth Falsework.*

[Photos: James Dow 2011; Ganivet 2012, by Author]

These inviting thin-shell shelters, were clustered like a raft of plywood penguins and designed by Patkau Architects. Only two layers of 0.1875" thick flexible plywood were required to increase the use of skating trails at a (frozen) confluence of rivers near Winnipeg. An "armature which consists of a triangular base, and wedge shaped spine and ridge members" was developed for each. The architects used a full scale prototype to determine the optimum bending/deformation possible. Fields of small holes, larger cutouts, as well as the portal openings help to relieve excessive stress. At the ridges, the forms are internally stiffened for snow loads and described as a result of procedural stressing and releasing of stress. [Detail 2014, Patkau Architects 2011].

Artist Vincent Ganivet commonly employs CNC falsework and wooden "wedges" between various types of off-the-shelf masonry units. The units are restrained as required internally or externally with ratcheting straps. "A large part of [his] work is based on the mathematical figure of the catenary (the transcendental curve describing the form of a hanging chain suspended from its ends and acted upon by uniform gravitational force – its own weight. By varying the angles subtended by the wedges, Ganivet can tighten or loosen the degree of curvature assumed by his sculptures." The process adjustability is similar to what was achieved with Guastavino's initial Plaster of Paris and Portland Cement steps. Also, "after his installations are over, the masonry units can be recycled for further use" [Lambert 2011].



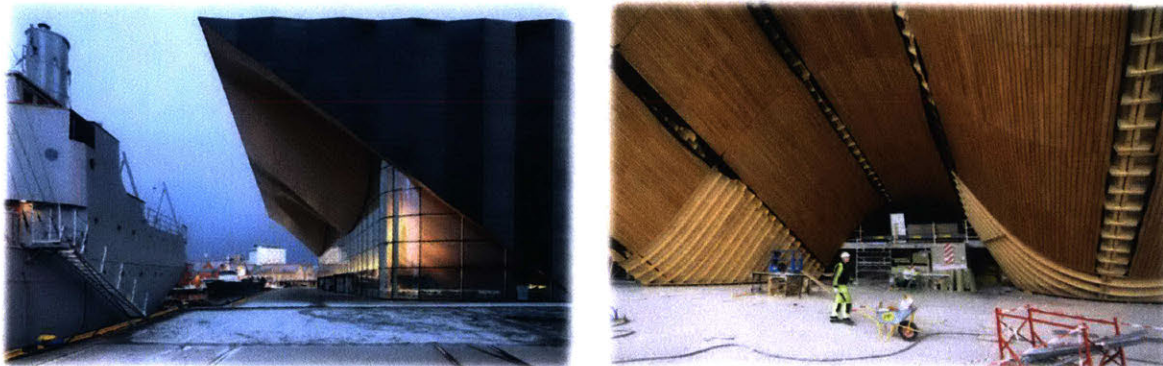


**Fig. 4.14 Post-rationalized, Post-digital – Natural Ellipse: (a.) Exterior oblique; (b.) Sub-frame detail.**

*Fiber-reinforced polymer (FRP) with radial/lateral floor system diaphragms and internal sub-frame.*

[Photos: EDH Endoh 2003; Ikeda 2008]

This forward-thinking 24-ring elliptical stressed-skin of vertically-oriented composite sheets was assembled on-site from prefabricated parts. The individual sheets were fastened to an elaborate laser-cut, carbon steel sub-frame. While the Natural Ellipse's geometric structural performance and fire resistance are compelling, its reliance on carbon-intensive fiber-reinforced polymer composites is not considered sufficiently sustainable for general detached residential applications. Likewise, its "white-out" minimalism plays well as an formal anomaly, but at scale this would quickly become as anonymizing as its form is unique. The outer bands of the four floor plates (*Figure 4.14a*) are tension rings that restrain the continuous surface-active perimeter wall. Joists radiate from the columnar core to brace the bands, and above the fourth floor discrete supplemental cross bracing is employed (*Figure 4.14b*).



**Fig. 4.15 Post-rationalized, Post-digital – Kilden Theatre: (a.) Exterior oblique; (b.) Sub-frame detail.**

*Significant pre-rationalization, but also dependence on concealed sub-frame.*

[Photos: ALA Architects 2013]

This inviting sloped façade of 21mm oak planks in Kristiansand, seems ALA Architects' undulating response to Grafton Architects' Bocconi University in Milano. The 37,700 ft.<sup>2</sup> CNC-milled design feature was post-rationalized by Zurich-based Design to Production, improves acoustical performance of the foyer, and was reportedly around \$140 ft.<sup>2</sup>, [Næss 2009]. To enable the boards to be cut to size, the twist of every single component had to be reduced to a flat plane. The grooved glue-laminated timber beams and the CNC-fabricated screw holes defined the exact position of every board" [Jeska & Pascha 2015].

### Construction – Post-digital: Mockups

(1 of 2)

As developmental research to test working assumptions or scale model observations many table-top mockups of details were produced by extracting geometry from the 3D model. These served as initial material compatibility spot-check assembly checks or "fit ups." With a compressed schedule, they became portable objects for tinkering and outside-the-shop references for detailing.



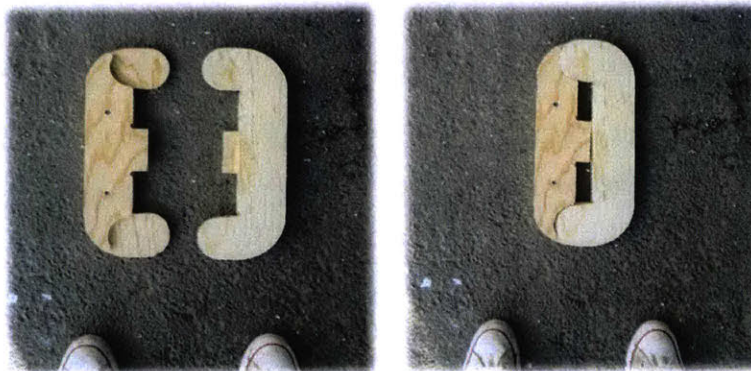
**Fig. 4.16 Mockups – GEN.0\_Strap Anchor [PRE].**

*Caution, mockups. This preliminary strap anchorage assumed local reinforcing splines top and bottom (not shown).*



**Fig. 4.17 Mockups – GEN.3\_Pedestal [R0].**

*Friction-fit, nest-able detailing (i.e., triangle-packing).*

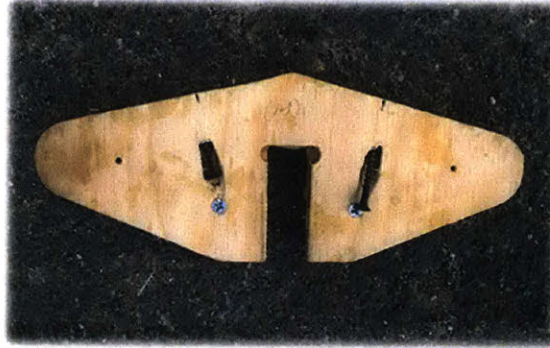


**Fig 4.18 Mockups – GEN.3\_Linkage [R0]: (a.) Open; (b.) Closed.**

**Construction – Post-digital: Mockups**

(2 of 2)

The top figure represents the initial interlayer wedge detail and the two intermediate process figures show the typical application of a wedge. The size and shape of the parts in the bottom figure are based on the smallest that would maintain vacuum and the optimization of sheet layout. The fundamental assumption of this kind of friction-fit detailing is that it can produce compact sub-assemblies which can be pre-assembled with only the main strips shipped flat.



**Fig. 4.19 Mockups – GEN.3\_Wedges [R0].**

*Intermediate, friction-fit wedge attachment, pre-drilled holes.*



**Fig. 4.20 Mockups – GEN.3\_Hinges, Method: (a.) Strips only; (b.) Strips with Wedge.**

*Initial darting template, edge splines, and joint seaming in progress.*



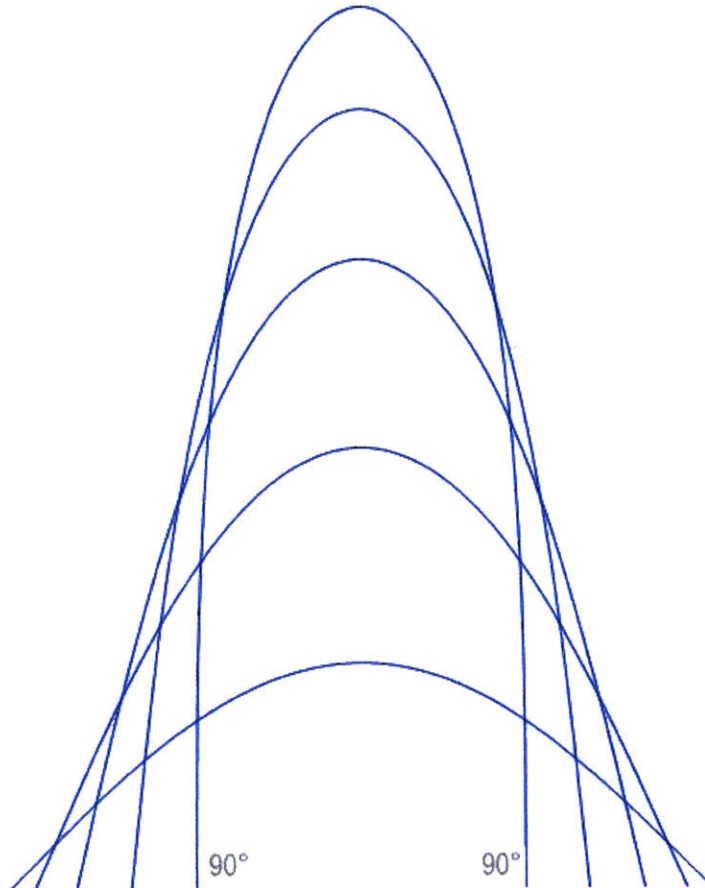
**Fig. 4.21 Mockups – GEN.4\_Pedestal [R2].**

*Friction-fit, nest-able detailing (i.e., circle-packing).*

## 4.2 Analysis – Geometry

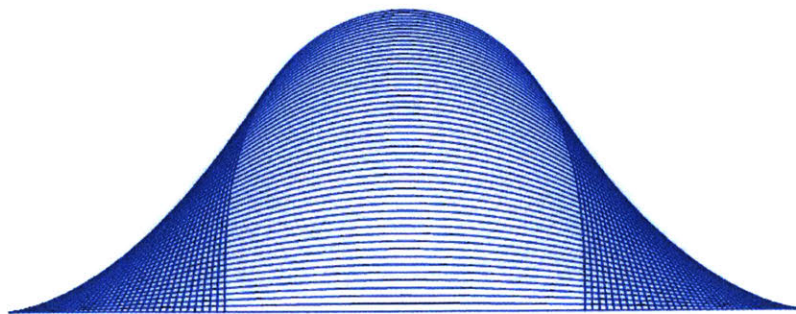
### Geometry – Curve: Pre-test

The initial objectives in these computational elastica analysis pre-tests were (1.) to understand the curve and (2.) to develop the means to clarify the minimum radius of the strip pre-test and tests.



**Fig. 4.22 Pre-test – Elastica: (a.) Increasing length.**

*Just after the  $90^\circ$  or 'rectangular elastica' is where maximum occurs and the elliptic modulus is  $(k)$  "special  $k$ ." This is before both ends touch at the lemniscate, and the means to these two radii are provided in Appendix – B.*

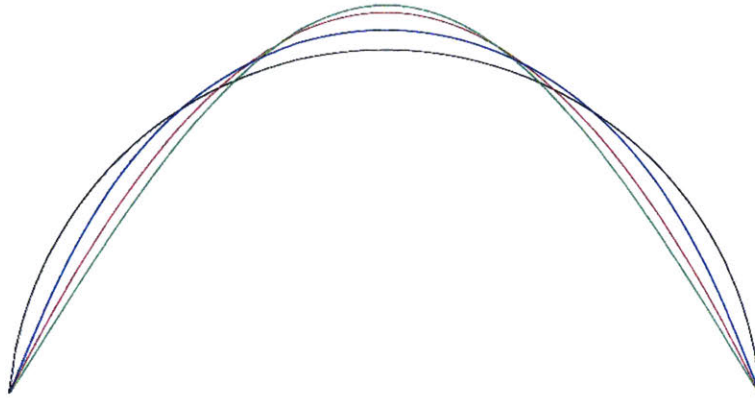


**Fig. 4.22 Pre-test – Elastica: (b.) Static length.**

*The "lesser range" of the elastica is that below the rectangular or rectangular elastica.*

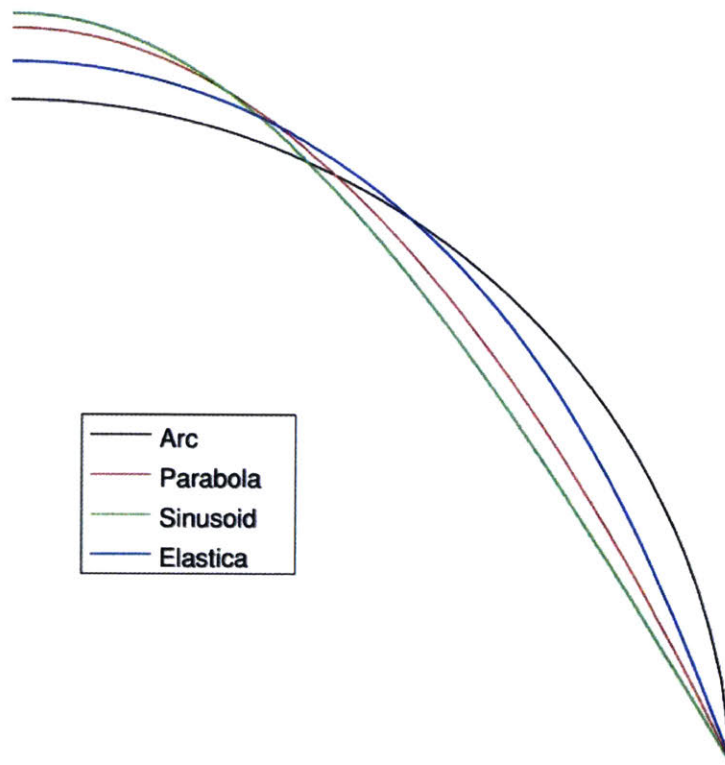
### Geometry – Curves: Pre-test

These first two studies focus on the lesser range of the elastica curve because of its relevance to panels with reduced webs or only point connections, and the Matlab–Octave tools which were developed subsequently have many potential applications – more precise geometric prediction, more accurate prediction of fabrication stresses, and with minimal modification, the flexural geometry resulting from tied assemblies.



**Fig. 4.23 Pre-test – Comparisons: (a.) Type.**

*Comparing an arc vs. parabola vs. sinusoid vs. elastica curve. The arc underestimates the minimum radius.*



**Fig. 4.23 Pre-test – Comparisons: (b.) Type, Detail.**

*The degree and minimum radius vary, but the order is consistent in the range most relevant to panel systems (i.e., above the rectangular elastica).*

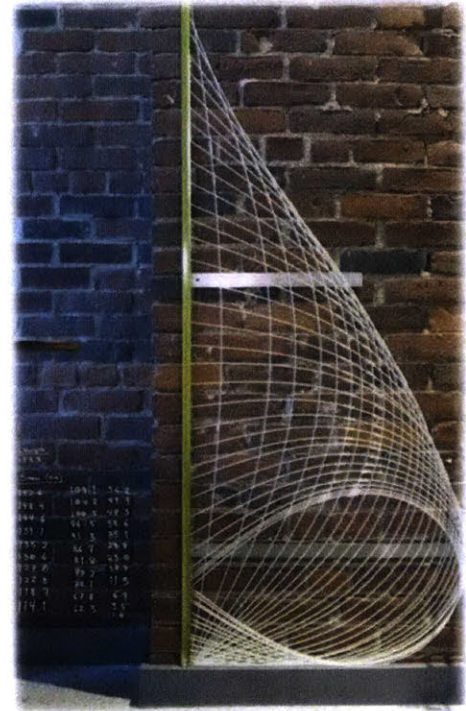
## Geometry – Rod: Pre-test

### Overview

Preliminary data was necessary for computational analysis to accurately clarify the actual minimum rod radius, so photos of a 60" fiber-reinforced polymer (FRP) rod were taken at thirty-four (34) positions. A 0.125" diameter rod was used with 0.44 mm galvanized wire, and 0.375" long brass sleeves were applied at each end – slotted to allow the span and rise to be recorded consistently. In Photoshop™, lens correction was applied, and the post-processed images were used as underlays to generate polyline elastica curve approximations for comparison with pre-test arc approximations. Infinitesimal arcs were pulled snapping to the dense polyline approximations to estimate the mid-point (MP) minimum radius. This composite figure documents the attempt and increased curiosity for further elastica analysis.

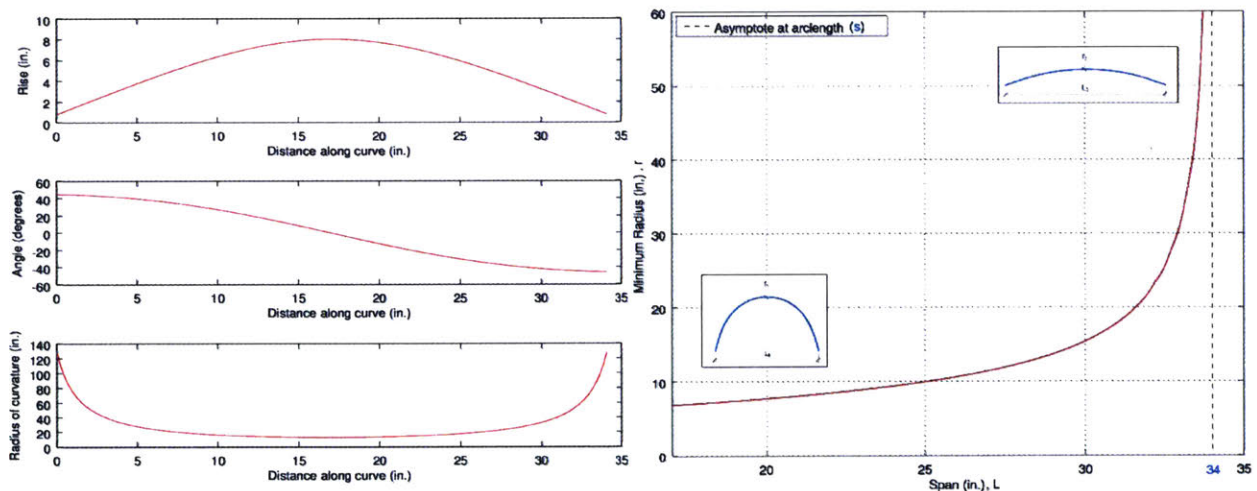
### Objectives

- (1.) To provide preliminary span-to-radius data for generating rise-to-radius empirical correlations for stress analysis.
- (2.) To inform the development of an experimental, computational tool for the non-analytical integration of elliptical integrals. The Matlab-Octave script generates the elastica mid-point minimum radius ( $e$ ) for any given rod length ( $\ell$ ) and displacement (detailed in Section 8.4).



**Fig. 4.24 Pre-test – Elastica: Photos.**

Generating data (Appendix–D) for tool creation.



**Fig. 4.25 Pre-test – Elastica:**

**(a.) Distance Along Curve (in.) vs. Radius (in.); vs. Angle (deg.); vs. Rise (in.);**

*Clarifying the behavioral and dimensional properties of the elastica.*

**(b.) Span (in.),  $L$  vs. Minimum Radius (in.),  $r_{min}$ .**

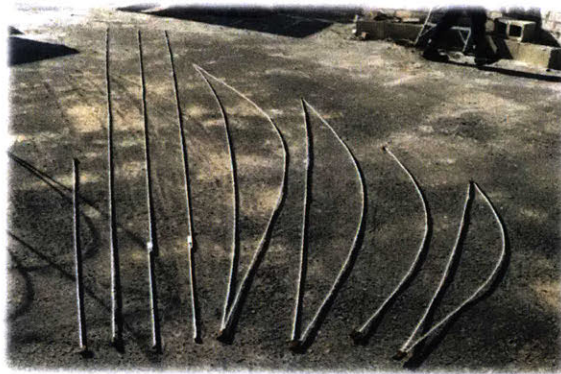
*As geometry the relationship is scale-less. Anticipating the strips test, this elastica pre-test used arclength,  $\ell$ : 34".*

Geometry – Rods: Coupled



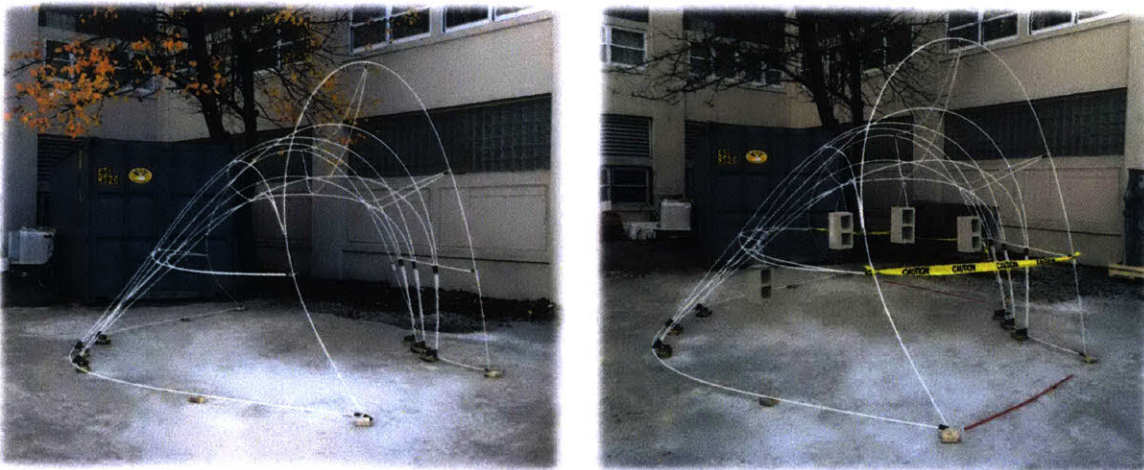
**Fig. 4.26 Coupled – Study model: Arch.**

*Developing bending-active components: adjustable ties and details allow accurate global geometric control.*



**Fig. 4.27 Coupled – Components: by Type.**

*Assembling bending-active components: linear, linear-adjustable, coupled, and tied.*



**Fig. 4.28 Coupled – MIT Horn-fort: (a.) Dimensional; (b.) Structural.**

*Testing approximation of specific form by indexing points and networking bending-active components.*

*Each-arch tested was stable at P: 175 lbs. with  $\Delta$ : 1.0".*

### Geometry – Rods: Test

This recent variable-depth, unitized, "networked, bending-active" installation was developed in an experimental masonry studio and was originally conceived as a rapid means of creating a volumetric "guide for the mason's hand" (Ochsendorf & West 2015). After a study model pre-test, the structure was constructed by indexing points along the rods and in space and applying closed lateral components and ties. Detailed manual dimensional analysis revealed interior nodes were generally within 1" of their target height and exterior edge splines within 2.25".



**Fig. 4.29 Test – MIT Horn-fort – Dimensional: Pre-digital.**

*Collecting plumb bobs.*



**Fig. 4.30 Test – MIT Horn-fort: Shrink-wrap.**

*Wrapping a variable-depth, unitized, "networked, bending-active" structure.*

[Aeck & Yang 2015]

Wire configurations were tuned and subsequently shrink-wrapped using common office binder-clips. Part form-active geometric experiment and part structural test balloon for the surface-active proposals that follow, its relevance is the componentized bending-active strategy for achieving target geometry. First, a free-form target surface was generated in Rhino via an independent process. Then rod lengths were extracted via variable offsetting and intersecting surfaces. Connections were made with paired 3" sleeves, 0.063" pins, and 0.5" [12.7] FRP-rods.



**Geometry – Strip: Pre-test**

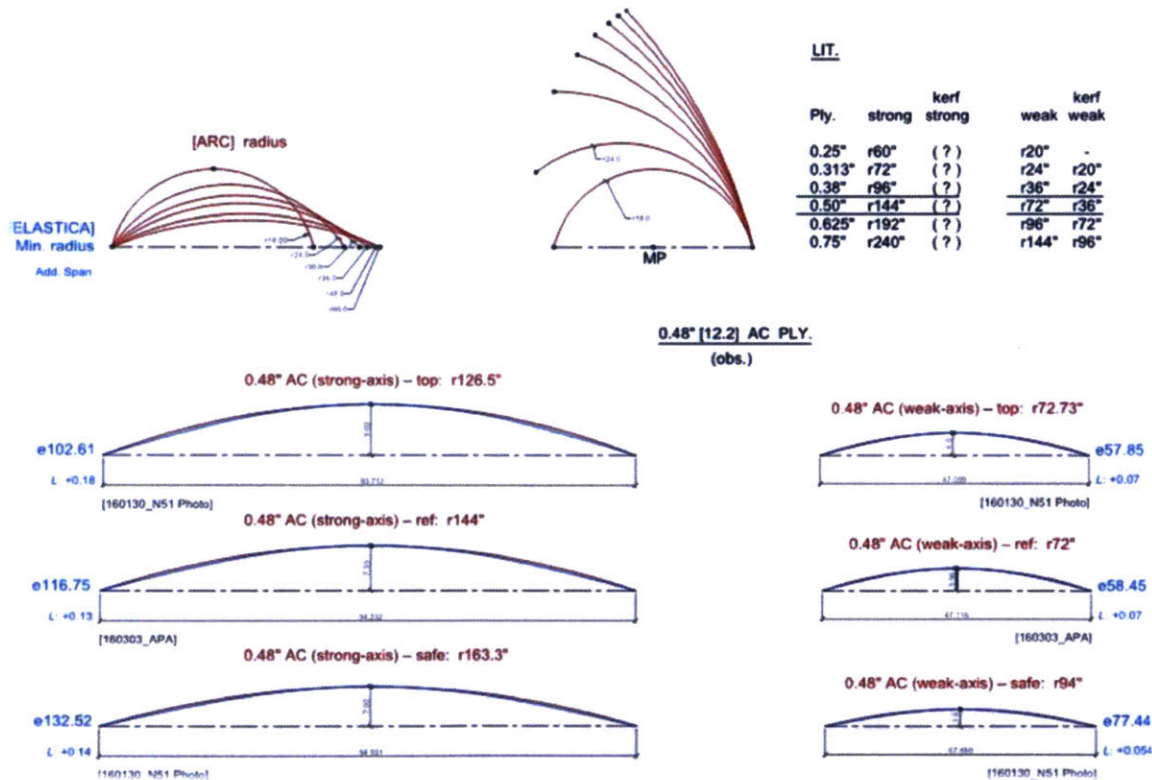


**Fig. 4.31 Pre-test – Plywood.**

Gathering data for rise (c); this behavior-based pre-test involved three thicknesses (0.3125", 0.36", and 0.48").

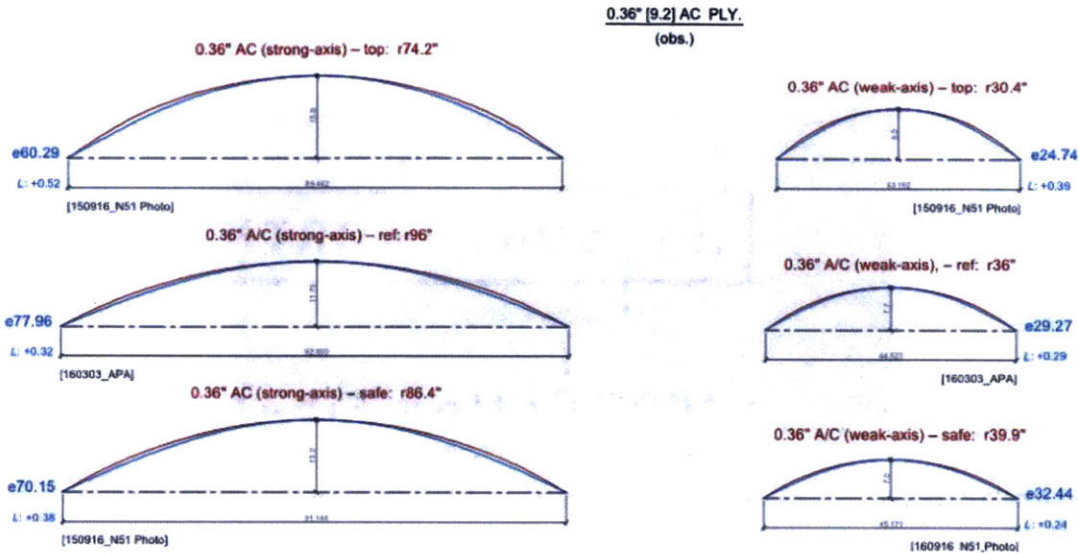
Overview

This initial empirical study (all that was originally intended) field measured the rise at different locations for nominally 0.5" [12.7] and 0.375" [9.5] AC plywood (Ply.). By iteratively scaling the span, regenerating and measuring the arclength, the red arcs were created to estimate the min. radius and evaluate the published values. Subsequently, the blue theoretical elastica curves and radii for the rise were plotted and added to represent the error (Table 4.2). The values below marked "lit" or "ref" are the industry published values, "top" and "safe" are project values.



**Fig. 4.32 Pre-test – Plywood: Arc (approx.) vs. Elastica (the.) for 0.48" Strips.**

Checking the 0.48" ply. published values for minimum radius and quantifying the error in arc approximation of flexure.



**Fig. 4.33 Pre-test – Plywood: Arc (approx.) vs. Elastica (the.) for 0.36" Strips.**

Checking the 0.36" ply. published values for minimum radius and quantifying the error in arc approximation of flexure.

**Table 4.2 Pre-test – Plywood: Arc (approx.) vs. Elastica (the.).**

**(Moisture: 8%; Units: in.)**

(Specimen) AC Plywood Thickness –	(r) Arc Radius	(c) Arc Rise	(L) Arc Span	(e <sub>c</sub> ) Elastica Radius (min.) from Rise	(%) r/e <sub>c</sub> -1	(e <sub>L</sub> ) Elastica Radius (min.) from Span	(%) r/e <sub>L</sub> -1
0.48 Ply., ½96 (strong, top)	r126.5	c9.0	L93.72	e102.61 (c9.0)	23.3	e98.70 (c9.34)	28.2
0.48 Ply., ½96 (strong, lit.)	r144	c7.93	L94.23	e116.75 (c7.93)	23.3	e112.13 (c8.25)	28.4
0.48 Ply., ½96 (strong, safe)	r163.3	c7.0	L94.59	e132.52 (c7.0)	23.2	e125.72 (c7.37)	29.9
0.36 Ply., ½96 (strong, top)	r74.2	c15.0	L89.46	e60.29 (c15.0)	22.3	e57.78 (c15.61)	28.4
0.36 Ply., ½96 (strong, lit.)	r96	c11.75	L92.05	e77.96 (c11.75)	23.1	e74.74 (c12.23)	28.5
0.36 Ply., ½96 (strong, safe)	r86.4	c13.0	L91.14	e70.15 (c13.0)	23.2	e67.25 (c13.53)	28.5
0.48 Ply., ½48 (weak, top)	r71.3	c4.0	L47.10	e57.85 (c4.0)	23.2	e56.56 (c4.16)	28.3
0.48 Ply., ½48 (weak, lit.)	r72	c3.96	L47.12	e58.45 (c3.96)	23.2	e56.10 (c4.12)	28.3
0.48 Ply., ½48 (weak, safe)	r94	c3.0	L47.48	e77.44 (c3.0)	21.2	e73.25 (c3.17)	28.3
0.36 Ply., ½48 (weak, top)	r30.4	c9.0	L43.19	e24.74 (c9.0)	22.9	e23.67 (c9.36)	28.4
0.36 Ply., ½48 (weak, lit.)	r36	c7.71	L44.52	e29.27 (c7.71)	23.0	e27.98 (c8.04)	28.7
0.36 Ply., ½48 (weak, safe)	r40	c7.0	L45.17	e32.44 (c7.0)	23.0	e31.10 (c7.28)	28.5

**Notes:** (a.) In the lesser elastica range, arc approximation from rise was over r (min.) by 23%; from span by 28.5%.

(b.) In the plywood pre-test, the observed r (min.) was on average 29.4% under the published value.

(c.) Key: Arc approximation; Elastica from rise; Elastic from span.

**Geometry – Strips: Coupled**



**Fig. 4.34 Strips: Coupled – Study Model.**

*Play-testing paper strip models.*

Represented above is a mechanism encountered in paper strip study models: that with only slight local manipulation of the mid-point sectional angle, significant control is gained over the global geometry of hinged strips. This became integral to the eventual *GEN.3\_Method* which uses attachments to manipulate and stiffen stressed-skins.

**Table 4.3 Strips: Coupled – Observations.**

**(to Test)**

O1:	Global geometric control mechanism by manipulating sectional angle.	(Location.)
O2:	Full scale continuous hinge construction is a detailing challenge.	(Dovetail; Kerf; Tambour.)
O3:	Local attachments could stiffen these assemblies efficiently.	(Keys, Tabs; Wedges.)

**Notes:** (a.) *Other study models support staggering coupled strips; potential branding as "splay" method.*

## Geometry – Strips: Test

### Overview

Thirty (30) strips were experimentally loaded to validate informal pre-test analysis and to obtain more precise displacement/span data for a range of commonly available materials. The retrofitted, pressure-sensitive, numerically-controlled hydraulic press provided nearly continuous empirical data for the forces being generated by bending. The relevant commercial publications found with values for some of the materials checked were APA-EWA Technical Topics [TT-003A, 2007] and the FAA Plywood Advisory Circular [43.13-1B, Table 1-2]. It was to make further use of the detailed displacement data from these specimens, to establish the minimum radius that the computational analysis and coding effort began.



Fig. 4.35 Strips: Test – Baldwin press.

### Setup

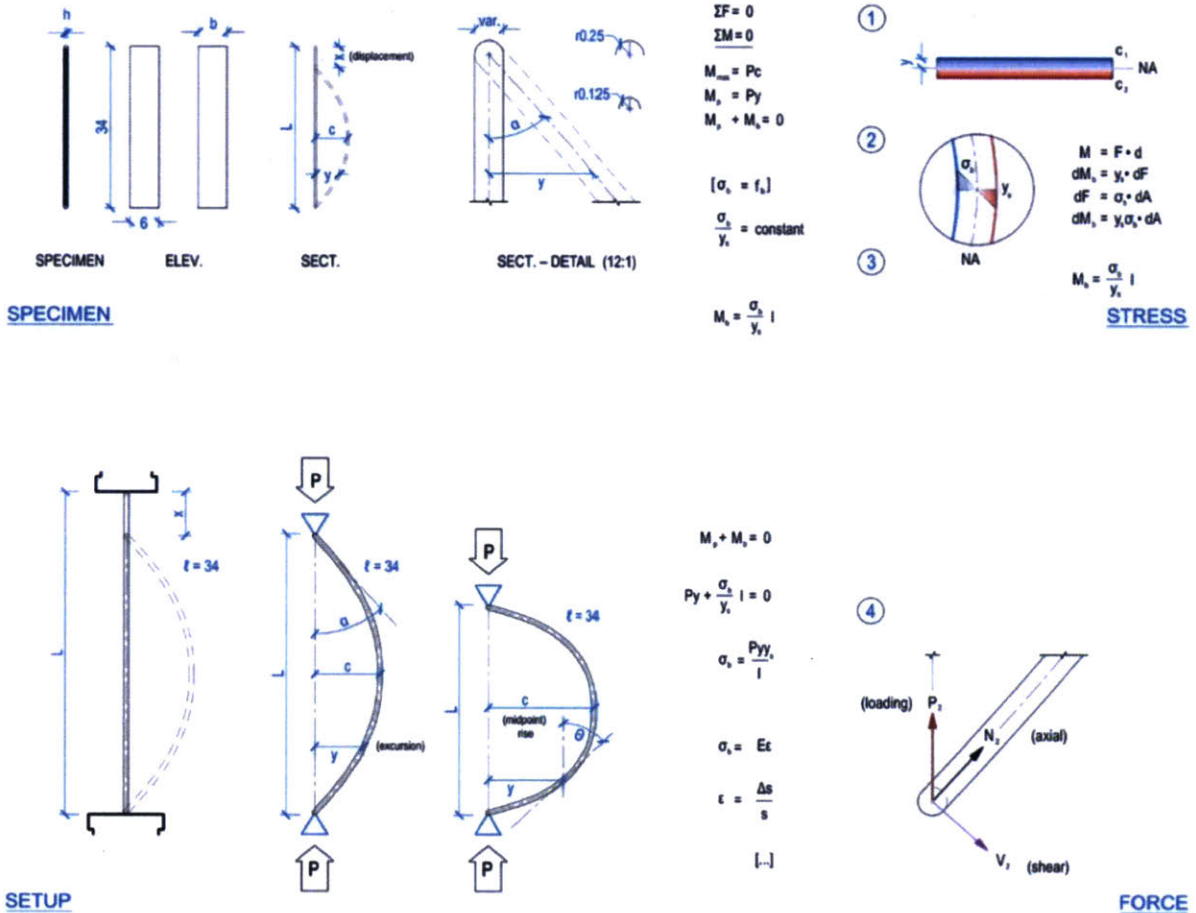


Fig. 4.36 Strips: Test – Overview.

See Figure 3.15 for detail and Appendix – E (Elastica).

Results

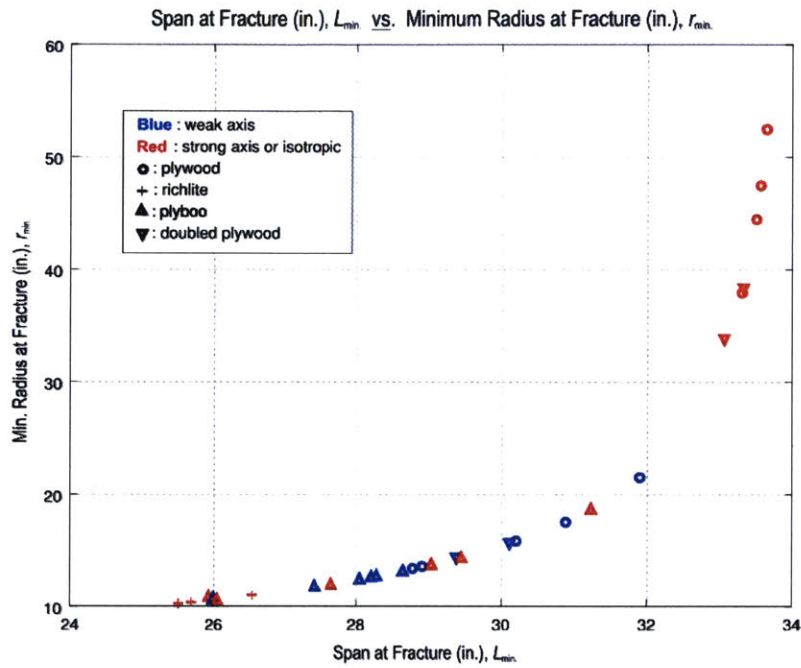


Fig. 4.37 Strips – Strong- & Weak-axis: Span at Fracture (in.),  $L_{min}$  vs. Minimum Radius (in.),  $r_{min}$ .  
 Observing spans with their theoretical minimum radius located along the Figure 4.26b curve.

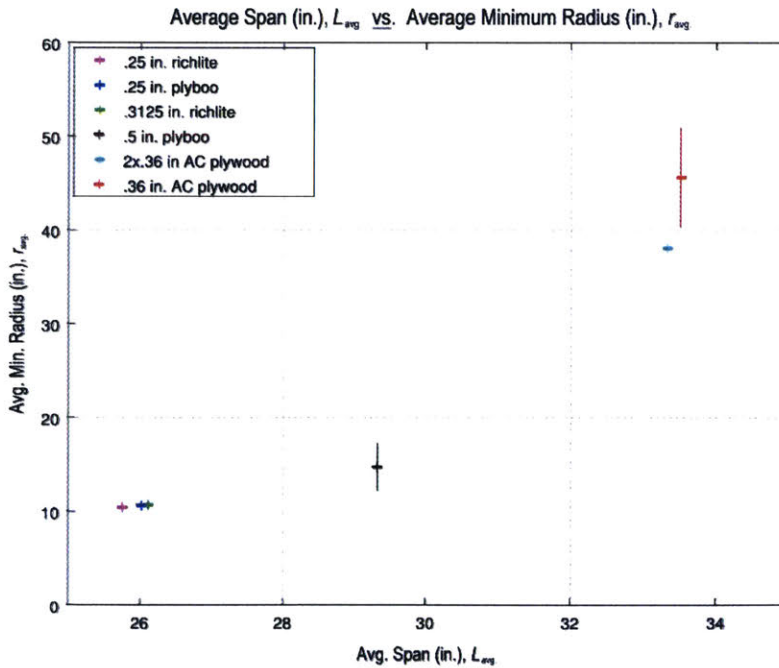
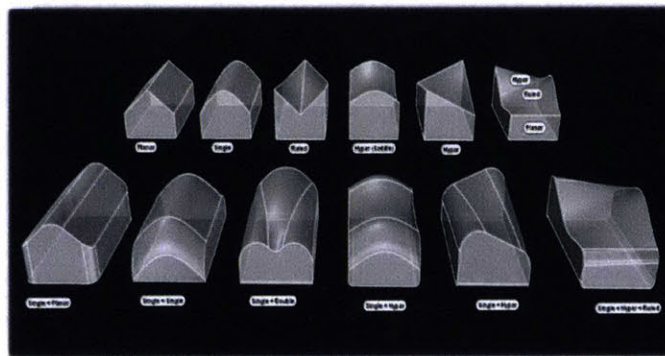


Fig. 4.38 Strips – Strong-axis: Average Span at Fracture (in.),  $L_{avg}$  vs. Average Minimum Radius (in.),  $r_{avg}$ .  
 Representing the average observed values for different materials. The laminated (2x 0.36") one failed close to 1x.

### Geometry – Roofs: Pre-test

This preliminary study assumed a cost hierarchy for different surface types with double-curvature considered the most costly, followed by single, hypar/ruled, and planar. Such considerations go to what in his 2014 lecture Mark Burry called "the big C" or "commitment to building," which is that to be implemented any solution must be describable). With this, and tactical rationalization (i.e., situational deployment of different surface types) for spatial organization, structural considerations, formal or functional articulations the preliminary study below different fundamental surface types are tested and mixed.

What is envisioned is that some multi-objective, multi-dimensional negotiation with form becomes the driver (perhaps interior program, annual rainfall, structural performance, or some factor for of each). The study below is a thread to be revisited which suggests that with a few basic operations considerable diversity can be achieved. Such thoughts begin to exceed what is possible to achieve given the prototyping objectives, but to clarify, what the proposals that follow necessarily be confined to roof forms. In the top row different types of surface curvature are inventoried, and in the each row the same basic geometry is manipulated to develop a better sense of the character/tectonic of each.

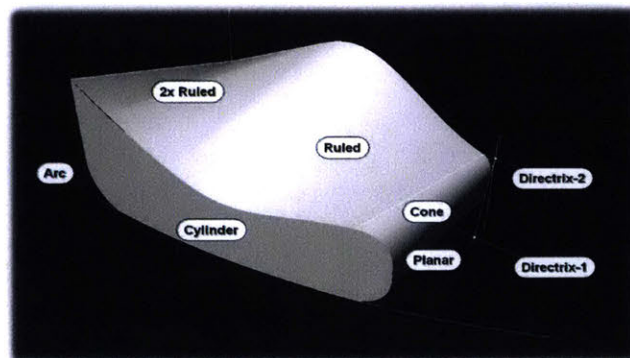


**Fig. 4.39 Geometry – Study: Roof Forms.**

Row 1: Planar; Single; Ruled; Hy-par saddle; Hy-par rotational; Hy-par ruled

Row 2: Single + Planar; Single + Single; Single + Double; Single + Hypar Saddle; Single + Hypar + Ruled

In the second image one is selected and surface types mixed, which again, could be applied to roof forms, walls, floors, or something else entirely. Likewise, it could be deliberately designed or made parametric to generate outcomes until a happy accident worth selecting/refining occurs. What we are pursuing with this is variety, but also to an extent, challenging the embedded socialized idea and iconography of the gabled roof.

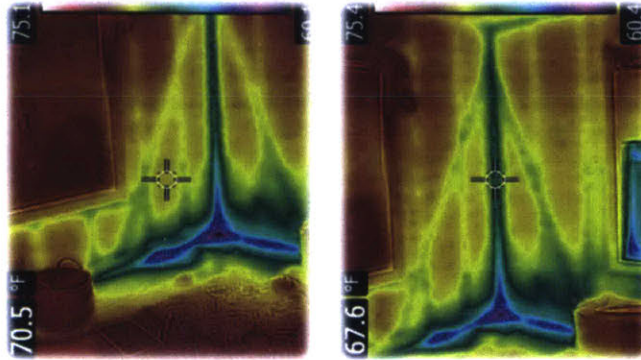


**Fig. 4.40 Geometry – Study: Roof Forms, Detail.**

*Pre-test mixing developable surface types.*

### 4.3 Analysis – Performance

#### Performance – Material



**Fig. 4.41 Material – Studs are a Factor: (a.) Cavity at 70.5 °F; (b.) Braced Multi-stud Corner at 67.6 °F.**

*Thermal bridging of vertical studs and let-in bracing in a pre-war Cambridge residence. Interface infiltration in purple.*

[Photos: by Author 2016]

These summary typological properties and observations, a result of the literature review, are included as a primer and to represent the pre-test of the *GEN.0\_Box-beam* [R2].

**Table 4.4 Material – Comparisons: Methods.**

**(1 bd. = 144 in.<sup>3</sup>)**

Method:	Light Frame – Platform	Panelized – SIPs	GEN.0_Box – All-ply.
Assembly:	On-site, Piece-level assembly.	On-site, Unit-level assembly.	On-site, Piece- and Unit-level.
Specimen:	8'x 8', 2"x 6" (2x Top plate)	8'x 8', 4.5" (Core: Rigid foam)	8'x 8', 9.0" (Reinforced & Stiff.)
Studs:	105 bd. (1.64 bd./ft. <sup>2</sup> )	20 bd. (0.313 bd./ft. <sup>2</sup> )	41 bd. (0.64 bd./ft. <sup>2</sup> )
Sheathing:	32 bd. (0.5 bd./ft. <sup>2</sup> )	64 bd. (1.0 bd./ft. <sup>2</sup> )	52 bd. (0.81 bd./ft. <sup>2</sup> )
Total:	137 bd. (2.14 bd./ft. <sup>2</sup> )	84 bd. (1.313 bd./ft. <sup>2</sup> )	93 bd. (1.45 bd./ft. <sup>2</sup> )

**Notes:** (a.) SIPs eliminate studs but fossil fuel derived rigid foam and adhesives both fundamental to the method.

(b.) 38.6% net reduction: (-53 bd.) = 80.9% studs decrease (-85 bd.); 100% sheathing increase (+32 bd.).

(c.) Reference data: [Morley 2000]

(d.) GEN.1\_Box-beams at 36" o.c. with 0.5" plywood webs, reinforced (33%) at L/3, stiffened (24" o.c.).

The material take-off pre-test for the system with the highest density, a 9"x 9" *GEN.0\_Box* [R2] spaced at 36" on center with infill panels suggested a -32% reduction relative to *platform framing* and only 10.7% increase relative to a typical 4.5" SIPs system. Reducing their spacing to 24" on center increased that by 9 bd. and only boxes 18" on center by a further 9 bd. On the following page the material usage of the different specimens are estimated

**Table 4.5 Material – Comparisons: Specimens.**

( - )

	<u>Specimen</u>	<u>in.<sup>3</sup></u>	<u>cm.<sup>3</sup></u>	<u>lbs. (the)</u>	<u>EC</u>	<u>EE</u>
Material – Volume:	GEN.0_Box	1435	23515.5	30.9	-	-
	GEN.0_Box, Hybrid:	1157	18959.9	25	-	-
	GEN.0_Box, Kerfed:	1296	21237.6	28	-	-
	GEN.1_Panel, Control:	2407	39443.8	52	-	-
	GEN.1_Panel, Kerfed:	2268	37165.9	50	-	-
	GEN.2_Unitized, Invert:	1620	26547.1	35	-	-
	GEN.2_Unitized, Axial:	2223	36428.5	48	-	-
	GEN.3_Semi-unitized:	2732	44769.5	59	-	-
	GEN.3_Arch – 180°:	9720	159282.3	209	-	-
	GEN.4_Arch – 220°:	52007	852238.7	1123	-	-

**Notes:** (a.) *References:* 1 ft.<sup>3</sup> = 1728 in.<sup>3</sup>; 1 in.<sup>3</sup> = 16.387 cm.<sup>3</sup>

(b.) *Plywood (obs.):* 0.0216 lb/in.<sup>3</sup>; *Plywood (lit.):* 0.0208 lb/in.<sup>3</sup>

**Table 4.6 Material – Comparisons: Waste.**

( - )

	<u>Specimen</u>	<u>Used</u>	<u>Scrap</u>	<u>Take-off</u>	<u>Inputs</u>
Material – Waste:	GEN.0_Nesting:	74.2%	25.8%	3421.3/4608 in. <sup>2</sup>	(1 sheet)
	GEN.1_Nesting:	86.2%	13.8%	4180.0/4608 + 1775.4/2304 in. <sup>2</sup>	(1.5 sheets)
	GEN.2_Nesting:	79.7%	20.3%	4138.2 + 3207.9/9216 in. <sup>2</sup>	(2 sheets)
	GEN.3_Nesting:	78.9%	21.1%	3175.2 + 3461.1 + 4277.0/13824 in. <sup>2</sup>	(3 sheets)

**Notes:** (a.) *This represents manual nesting to produce only what was required, but suggests 20% as basis of design at 20%. At volume and with mixed parts, estimate at least 85% seems achievable.*



## Performance – Operational

### Overview

After investigating conventional means of optimizing and remediating light frame construction and to evaluate the impact of a supplemental exterior layer of insulated sheathing on thermal performance, a basic simulation was performed. Questioning whether and to what extent a performance benefit remained, a widely-used platform Therm was employed to spot-check the viability of a typical light frame wall section (with continuous thermal-bridging studs and supplemental structural sheathing) versus an alternative strip-built section (with staggered, discontinuous construction).

### Setup

LBNL Therm (7.3); Independent generation of vector DXF sections.

### Results

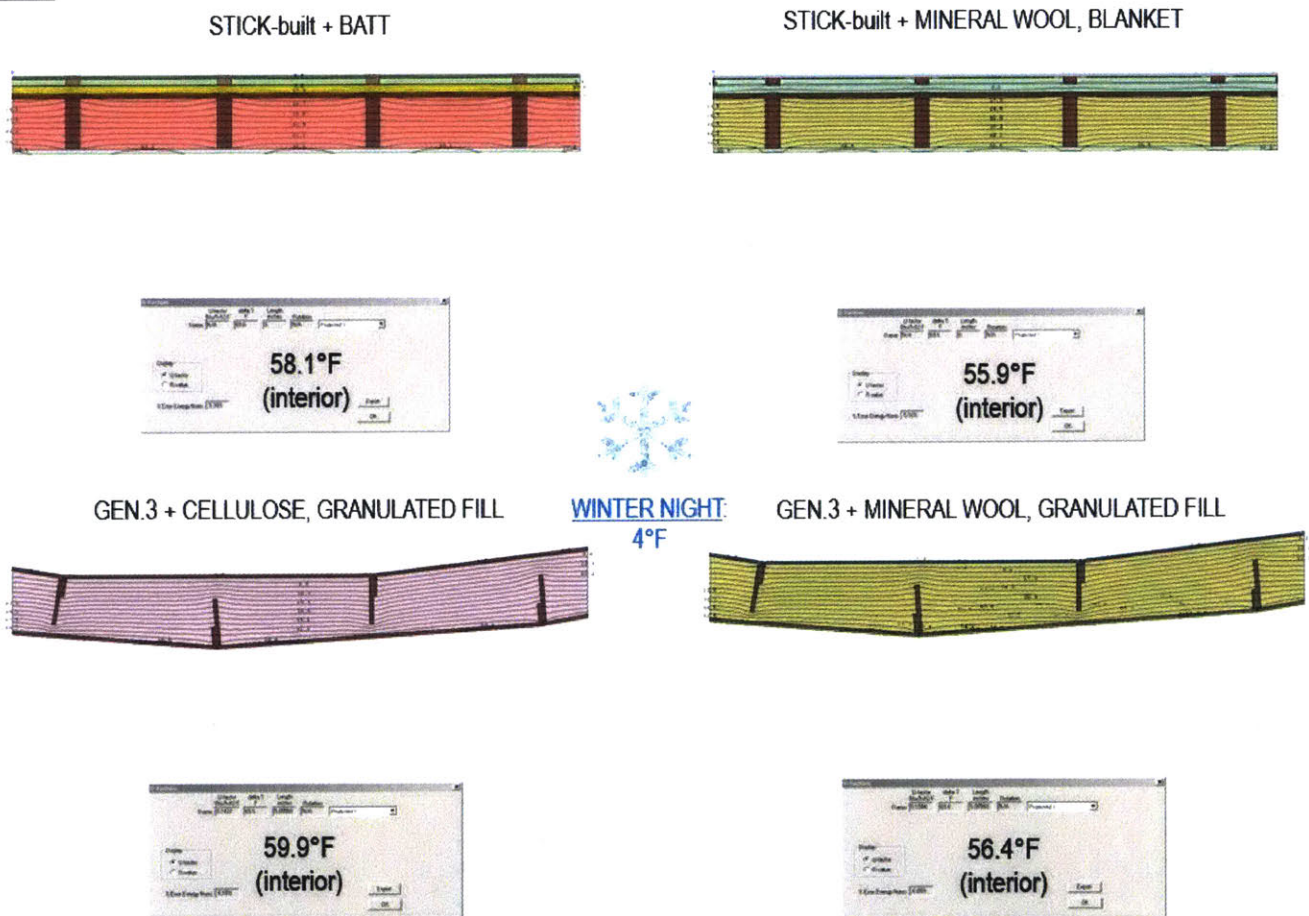


Fig. 4.42 Simulations – GEN.3\_Thermal Performance: (a.) Stick; (b.) Strip.

*The results suggest even with supplemental exterior insulating sheathing a discontinuous system with either cellulose, mineral wool, or granulated fill would outperform conventional studs by almost 2 °F. When the simulation was run without the supplemental insulation the results were just over 4 °F different, which begins to be significant.*

**Performance – Structural**

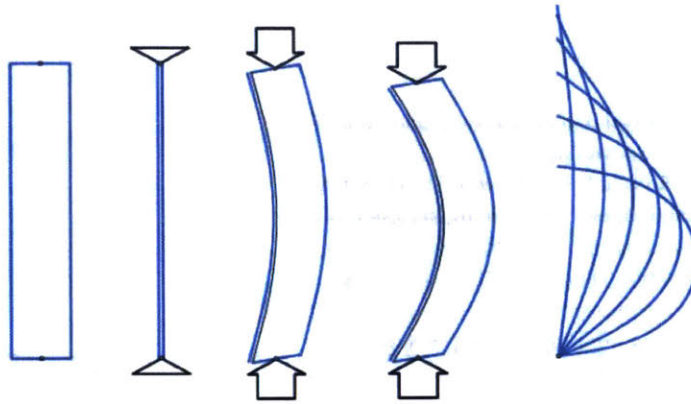
**Table 4.7 Structural – Comparisons: Methods.**

**(1 bd. = 144 in.<sup>3</sup>)**

<i>Method:</i>	<i>Light Frame – Platform</i>	<i>Panelized – SIPs</i>	<i>GEN.0_Box – All-ply.</i>
<i>Depths:</i>	2x6"; 2x8"; 2x10"; 2x12".	4.5"; 6.5"; 8.5".	9"-12" (Varies)
<i>Spans:</i>	138"; 159"; 201"; 278".	96"; 120"; 144" (>144" custom).	141" (Unreinforced at 50 psf).
<i>Total (64 ft.<sup>2</sup>):</i>	137 bd. (2.14 bd./ft. <sup>2</sup> )	84 bd. (1.313 bd./ft. <sup>2</sup> )	93 bd. (1.45 bd./ft. <sup>2</sup> )
<i>Vol. (64 ft.<sup>2</sup>):</i>	11.4 ft. <sup>3</sup> (0.18 ft. <sup>3</sup> /ft. <sup>2</sup> )	7.0 ft. <sup>3</sup> (0.11 ft. <sup>3</sup> /ft. <sup>2</sup> )	7.75 ft. <sup>3</sup> (0.12 ft. <sup>3</sup> /ft. <sup>2</sup> )
<i>Struct. only:</i>	6.7 psf	4.1 psf	4.4 psf

**Notes:** (a.) *SIPs eliminate studs but fossil fuel derived rigid foam and adhesives both fundamental to the method.*

(b.) *References: 1 bd. = 0.08333 ft.<sup>3</sup>; 0.0216 lb./in.<sup>3</sup> = 37.3 lbs./ft.<sup>3</sup>*



**Fig. 4.43 Diagram – Single strip, Bending.**

*Representation of the elastic bending of a single strip.*

These material properties, a result pre-test calculation and literature review, are included as a primer.

**Table 4.8 Structural – Comparisons: Sheets & Strips.**

(1 bd. = 144 in.<sup>3</sup>)

<i>Plywood – Nominal:</i>	0.375" (3/8", Typ.)	0.4375" (7/16", Atyp.)	0.5" (15/32", Typ.)
<i>Plywood – Observed:</i>	0.36"	0.44"	0.48"
<i>Specimen – Size:</i>	4'x 8', 48"x 96" (3-ply)	4'x 8', 48"x 96" (3-ply)	4'x 8', 48"x 96" (5-ply)
<i>Weight – Area:</i>	1.1 ft. <sup>2</sup>	1.3 ft. <sup>2</sup>	1.4 ft. <sup>2</sup>
<i>Area – Section, Sheet (4'):</i>	17.3 in. <sup>2</sup>	21.1 in. <sup>2</sup>	23.0 in. <sup>2</sup>
<i>Volume – Sheet (4'):</i>	1659 in. <sup>3</sup> (11.5 bd.)	2027 in. <sup>3</sup> (14.1 bd.)	2212 in. <sup>3</sup> (3.8 bd./ft.)
<i>Area – Section, Strip (1'):</i>	4.3 in. <sup>2</sup> [4.5 in. <sup>2</sup> ]	21.1 in. <sup>2</sup> [5.25 in. <sup>2</sup> ]	23.0 in. <sup>2</sup> [5.625 in. <sup>2</sup> ]
<i>Volume – Strip (1'):</i>	415 in. <sup>3</sup> [3.0 bd.]	507 in. <sup>3</sup> [3.5 bd.]	553 in. <sup>3</sup> [15.4 bd.]
<i>Modulus – Section, Strip (1'):</i>	0.259 in. <sup>3</sup> [0.281 in. <sup>3</sup> ]	0.387 in. <sup>3</sup> [0.383 in. <sup>3</sup> ]	0.461 in. <sup>3</sup> [0.440 in. <sup>3</sup> ]
<i>Moment – Inertia, Strip (1'):</i>	0.186 in. <sup>4</sup> [0.053 in. <sup>4</sup> ]	0.341 in. <sup>4</sup> [0.084 in. <sup>4</sup> ]	0.442 in. <sup>4</sup> [0.103 in. <sup>4</sup> ]

**Notes:** (a.) Comparing application-specific AC plywood 48" sheet and 12" strip.

(b.) Assumed density of generic plywood: 36 pcf. For OSB or COM-PLY panels add 10%.

(c.) Observed density of certified plywood: 37.3 pcf

(d.) Source of bracketed: [AF&PA 2005, NDS for Wood, Table C9.2.4]

## Performance – Structural: Strips

### Overview

Strip specimens were placed using a grooved head attachment and an engraved base target by lowering the press head incrementally. Once held, the head was backed off until no load was shown. For each material, three (3) and in most cases four (4) or five (5) specimens were tested. The results were analyzed with computational tools developed in Matlab-Octave to back-calculate the elastica geometric properties from the recorded displacements. The figure at the right (4.45) depicts one dramatic delamination observed in one of the weak-axis bamboo scrimber specimens.



Fig. 4.44 Strips – Pre-test: Weak-axis.

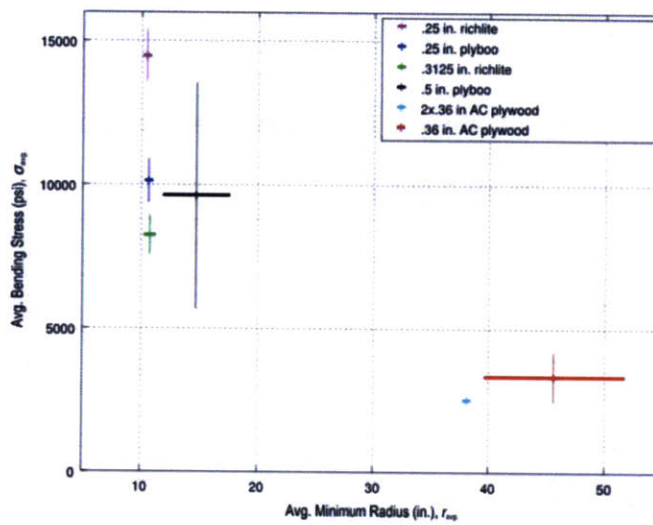


Fig. 4.45 Strips – Strong-axis: Avg. Minimum Radius (in.),  $r_{avg}$  vs. Avg. Bending Stress (psi),  $\sigma_{avg}$ .

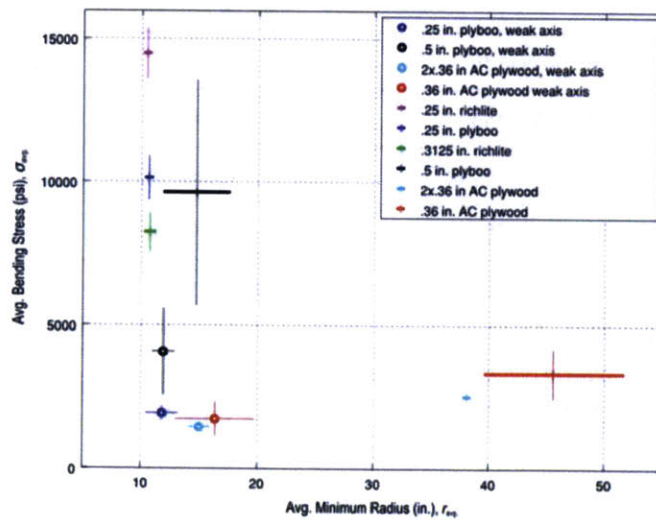
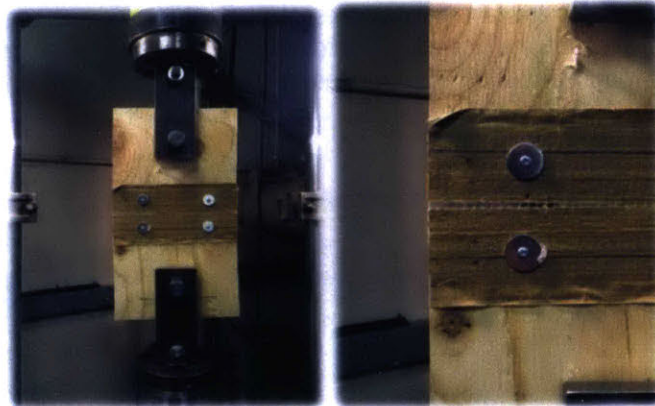


Fig. 4.46 Strips – Strong- & Weak-axis: Avg. Minimum Radius (in.),  $r_{avg}$  vs. Avg. Bending Stress (psi),  $\sigma_{avg}$ .

**Performance – Structural: Hinges**

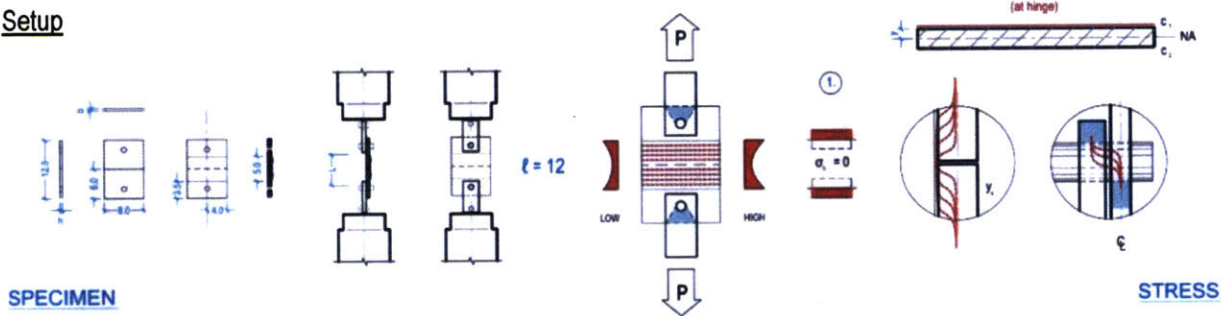
Overview

To clarify which should become the basis of design hinge, three (3) tensile tests were performed comparing two (2) cost-aware products and a (1) generic polycarbonate. The jute-fiber or burlap webbing is used in furniture upholstery and glass fiber reinforced tape (GFRT) in carpeting and flooring. To ensure a material (versus adhesion) failure anticipating conditions with local tabs where redundancy would be necessary, oversized washers and mechanical fasteners were used. The fabrication of the tensile "living hinges" was based on the existing r1" hardware for the hydraulic MST-brand equipment, which with a greater vertical range, was also used for the axial compressive tests.



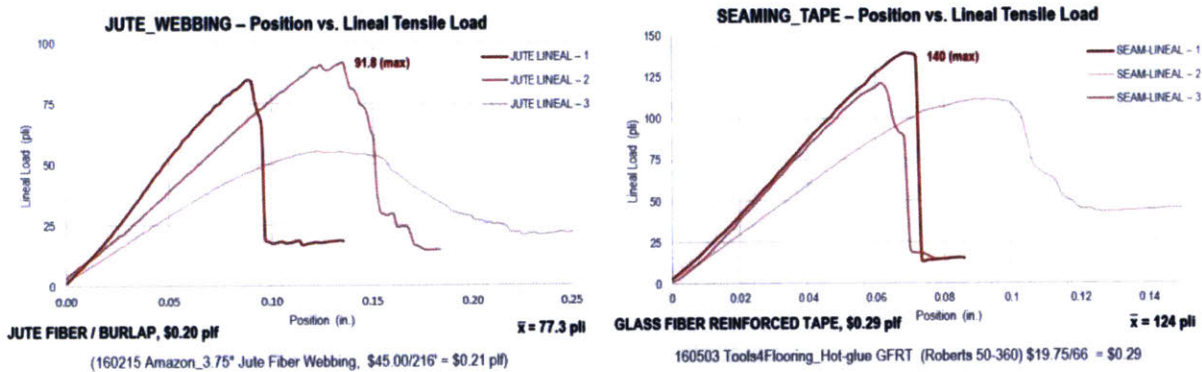
**Fig. 4.47 Specimen – Hinge: (a.) Setup; (b.) Failure Mode.**  
 Membrane fabric was considered but was many times the price.

Setup



**Fig. 4.48 Hinges – Pre-test: Overview.**

The jute fiber/burlap (77.3 plf) was 156% and the seaming tape (124 plf) was 310% better than the initial "co-poly."

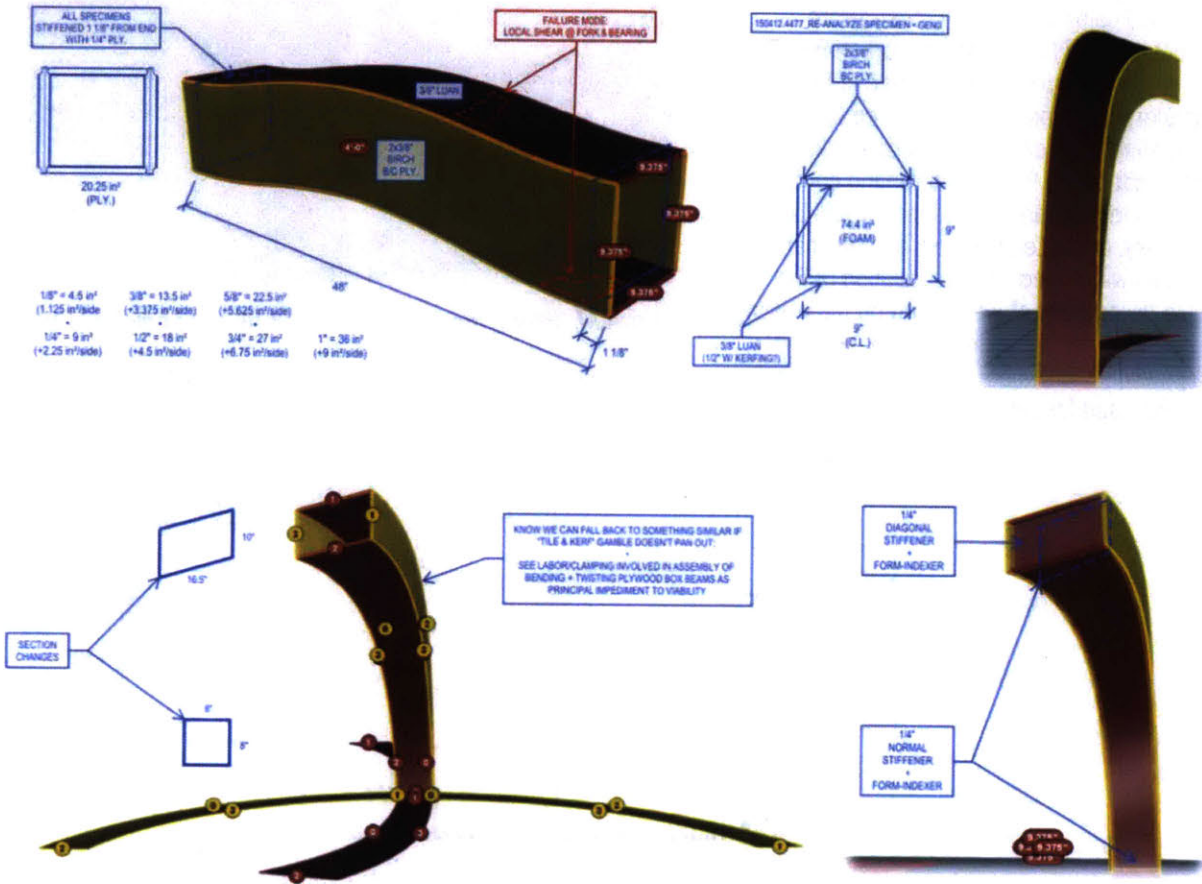


**Fig. 4.49 Hinges – Pre-test: (a.) Jute-fiber/Burlap webbing; (b.) Seaming tape, GFRT.**

The glass fiber reinforced seaming tape was 40% better than jute fiber and never failed in the full scale specimens. With the assembly end, sixth or quarter point splines as primary, ultimately the tape is a 1500 plf redundancy.

### Performance – Structural: Beams

The images and table below represent the point-of-departure analysis for two previous specimens. The relevant load test diagrams are located in *Section 3.4 Methodology – Experimental*, and the formal 4-point theoretical analysis workflow in *Appendix – C (Calculations)*.



**Fig. 4.50 Beams – GEN.0\_Box\_Hybrid: Dimensional & Theoretical Review.**

*This post-test theoretical analysis of GEN.0 is located in Appendix – B and assumed the following:*

$L$  (span): 180" (15') at 18" (1.5') on center;  $\sigma_a$ : 2,800 psi;  $E$ : 1,200 ksi

**Table 4.9 Beams – GEN.0\_Box, Hybrid [R0].**

**(BC & Luan Ply.)**

Review	Thickness (the.)	$I_x$ (eff.)	$P$ (obs.)	Assumptions
R0: GEN.0_Box, Control.	2x 0.4" (webs), 0.4" (flanges).	16.25 in. <sup>4</sup>	7,312 lbs.	BC Ply. Only.
R1: GEN.0_Box, Hybrid [R1].	2x 0.4" (webs), 0.0" (flanges).	11.29 in. <sup>4</sup>	5,380 lbs.	BC & Luan Ply.
Prediction	Thickness (the.)	$I_x$ (the.)	$P$ (the.)	
P1: GEN.0_Box, Kerfed [R2].	2x 0.4" (webs), 0.2" (flanges).	160.7 in. <sup>4</sup>	12,902 lbs.	AC Ply. Only.
P2: GEN.0_Box, Kerfed – Webs Only.	2x 0.4" (webs), 0.0" (flanges).	73.5 in. <sup>4</sup>	5,901 lbs.	AC Ply. Only.

**Notes:** (a.) *Despite internal stiffeners the failure mode of the GEN.0\_Box, Hybrid [R1] was transverse, cross-grain, punching shear at the L/3 press head and right bearing.*

## 5. RESULTS

[GEN.0, 1, 2, 3, 4]

This *Chapter* is organized by test generation into *Section 5.0 – GEN.0*, *5.1 – GEN.1*, *5.2 – GEN.2*, *5.3 – GEN.3*, and summary *Section 5.4 – Combined*. Each section is an independent experimental report on each related group of specimens and organized by stated problem. For clarity, a section (5.0) was added for the *GEN.0* box-beam so the generations and sections would be coordinated.

### 5.0 Results – GEN.0

(Kerfed, Reinforced, Stiffened Box-beam)

#### Construction – GEN.0\_System

The *GEN.0\_Box* (*GEN.0\_Box, Kerfed* [R2] in full) system was a revisionist, all-certified-plywood experiment reacting to the results of a previous project which proposed mixed-type plywood assemblies (a related pre-test study is represented in the third study in *Section 4.1*). The dimensions are identical to those of the much earlier *GEN.0\_Box, Hybrid* [R1] Lauan and BC plywood specimens with the two principal differences being (1.) kerfing and (2.) all weak-axis material orientation was used. While clearly relevant as a column, the project-specific application would be as localized ribs to extend the span for atypical low-slope flexural conditions within a larger segmented shell. This specific combination of details was chosen to establish an assembly baseline and to begin to clarify the performance potential of cable- or strap-truss integration. Also noted is the initial conceptual ideal was "glue-free," and the slower feed rate for small-bit operations proved prohibitive – resulting in an additional 22 minutes in machine time despite the repetitive linear simplicity of the kerfing.

#### Geometry – GEN.0\_Box, Kerfed (r160)

The 0.5" AC plywood *GEN.0* box-beam specimen used dense 0.2" deep kerfing on 0.75" centers to extend the minimum radius and reduce the strain energy generated from bending to minimize clamping. An r0.0625" radiused end mill bit was used to index locations for the four (4) 0.5" stiffeners, and a pocketing jig common in cabinetry and furniture was used to fasten the two (2) 0.5" vertical ribs with proprietary screws. To begin construction similarly-kerfed reinforcing tabs, or local "surface splines," were pre-attached to the top and bottom flanges at mid-span. This was done in cautious anticipation of cracks initiating from the kerfing. Four 0.0625" deep indexing kerfs were made on the outer lambs of the vertical webs to simplify locating and fastening stiffeners.



Fig. 5.1 Specimen – GEN.0\_Box, Kerfed.

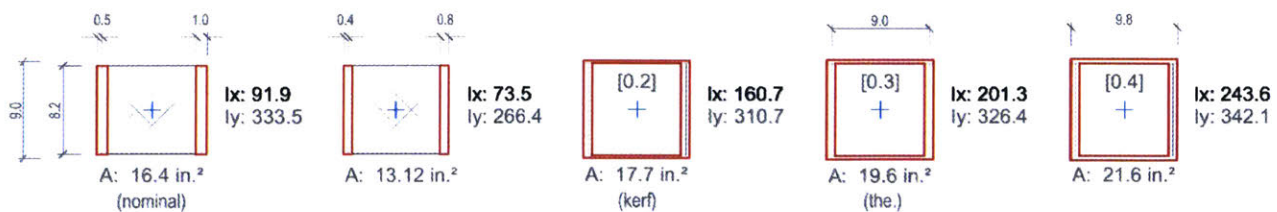


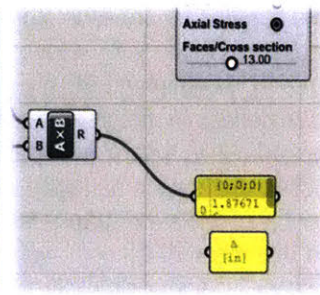
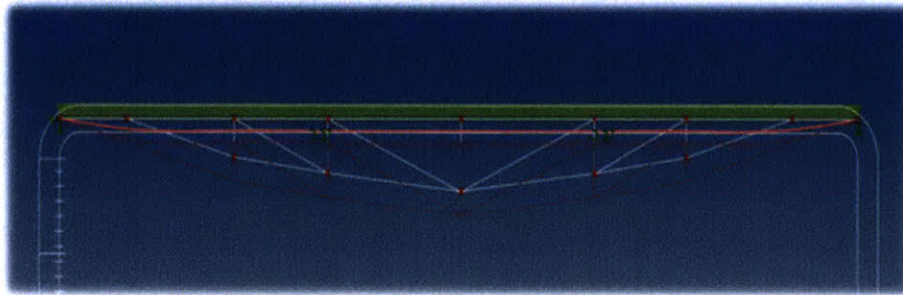
Fig. 5.2 Sections – GEN.0\_Box: Dimensional & Theoretical Properties.

**Performance – GEN.0\_Theoretical**

Assuming allowable stress values from relevant APA all-plywood beam design literature (*Appendix – A*), and using a rounded adaptation of its approach to effective depth, the following multiple theoretical predictions were made.

**Table 5.1 Predictions – GEN.0\_Box, Kerfed.**

Specimen	Thickness (the.)	$I_x$ (the.)	$P$ (the.)	(Pre-test) Assumptions
P1: GEN.0_Box – Webs & Flanges.	2x 0.4" (webs); 0.4" (flanges).	243.6 in. <sup>4</sup>	20,210 lbs.	$\sigma_a$ : 2,800 psi
P2: GEN.0_Box – Webs & Kerfed Flanges.	2x 0.4" (webs); 0.2" (flanges).	160.7 in. <sup>4</sup>	12,902 lbs.	$E$ : 1,200 ksi
P3: GEN.0_Box – Webs Only.	2x 0.5" (webs).	091.9 in. <sup>4</sup>	7,378 lbs.	$L$ : 48.0"
P4: GEN.0_Box – Webs Only.	2x 0.4" (webs).	073.5 in. <sup>4</sup>	5,901 lbs.	$H$ (total): 9.0"
P5: GEN.0_Box – Detail or Kerf Fails.	-	-	-	$h$ (web): 8.2"

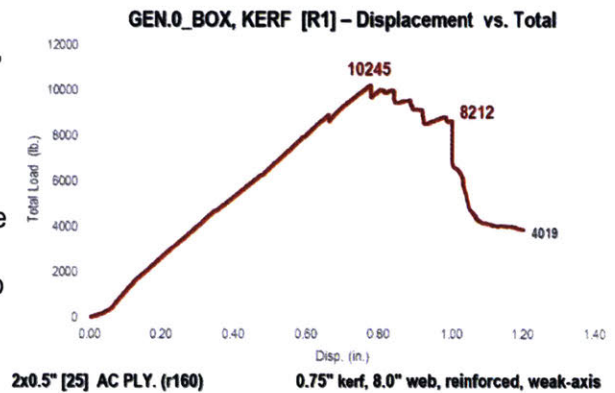


**Fig. 5.3 Simulations – GEN.0\_Box, Cable-truss.**

( $L$ : 360";  $\Delta$ : -1.23") [9.23m]

**Performance – GEN.0\_Box, Kerfed (r160)**

The kerfed box-beam specimen loaded at a rate of 0.1"/minute, showed the linear-elastic behavior anticipated, but somewhat above expectations for the weak-axis plywood baseline. The first sign of failure was audible shortly after 8,000 lbs., which became visible after the 10,243 lbs. peak – it first propagated vertically and then laterally, likely due to the weakening from the stiffener indexing line. Between the two (2) marked peaks in the figure to the right, the initial shelf from displacement 0.75" to 0.85" was the approximate duration of the vertical cracking.



**Fig. 5.4 Results – GEN.0\_Box, Kerfed.**

**Results**

$I_x$  (eff.): 18.30 in.<sup>4</sup>  
 Failure location: Web.  
 Failure mode: In-plane, cross-grain, flexural tension.  
 Pre-stress (the.): 750/2,800 psi (-26.7% of allowable)

**Assumptions**

MOR (plywood):	4,890-6,180 psi	[GTR-190]	MOR (the.):	5,535 psi	[GTR-190]
$E$ (plywood):	1,001-1,240 ksi	[GTR-190]	$E$ (the.):	1,200 ksi	[GTR-190]
$\sigma_a$ (5-ply):	3,300 psi	[APA 1998]	$\sigma_a$ (3-ply)	2,800 psi	[APA 1998]

**Notes:** The initial predictions above assumed generic isotropic versus weak-axis orthotropic properties for the plywood.  $I_x$  (eff.) used a 4-point specific, differentiated equation (A21):  $dP/d\Delta = 1/EI_{eff} \cdot x (4\alpha^3 - 3La^2/12)$



## 5.1 Results – GEN.1

(Kerfed, Reinforced, Friction-fit Panel)

### Construction – GEN.1\_System

The *GEN.1* panels were a subsequent all-plywood experiment developed with web and stiffener details to test and optimize wider assemblies. The web depth of the specimens was 9". In order to seek the upper end of the service range, both were reinforced along their full length. Similarly, the principal differences between the control and prototype are: (1.) revised kerfing, (2.) fabrication pre-stress, and (3.) strong-axis material orientation. The intended project application is as a typical a floor system, shear wall, or thermally-improved exterior wall without lamination.

### Geometry – GEN.1\_Panel, Control (r0)

The *GEN.1* control specimen used flat/planar FSC-certified AC plywood, 1.25" deck screws, 1.0" pin nails, and it was reinforced continuously over its full length to facilitate assembly. It was assumed that the web might benefit significantly from continuous support and shear transfer. Instead of light engraving to locate internal attachments, the stiffeners were located with 0.2" deep mill-indexed pilot holes. The recessed webs provide sufficient space for tabs, face splines, or other experimental panel-to-panel seaming methods.



Fig. 5.5 Specimen – GEN.1\_Panel, Control.

### Geometry – GEN.1\_Panel, Kerfed (r96)

The *GEN.1* kerfed specimen used 0.2" kerfing on 1.0" centers to reduce the minimum radius of a 0.5" sheet of plywood, and three (3) friction-fit stiffeners were located at the mid-point and sixth-points (MP and SP). Relative to the previous experiment, the radius of the prototype was reduced from r160" to r96", which is representative of the lower end of what is achievable for 0.5" plywood without H<sub>2</sub>O or kerfing beyond the neutral axis. The reinforcement was continuous over the full length, and it was assumed that either the wider kerfing or the stiffener slots would begin to erode total load capacity. The below, Strand7 numerical simulation was performed to follow up a preliminary, non-meshing, Scan & Solve study to predict the *GEN.1\_Panel* proposal at 180" and 100 psf.



Fig. 5.6 Specimen – GEN.1\_Panel, Kerfed.

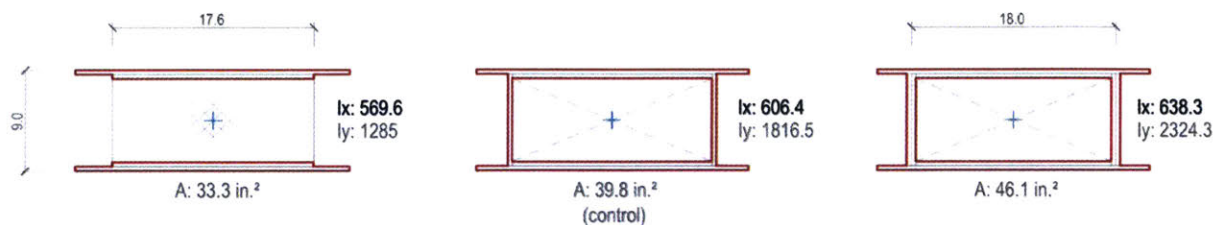


Fig. 5.7 Sections – GEN.1\_Panel: Dimensional & Theoretical Properties.

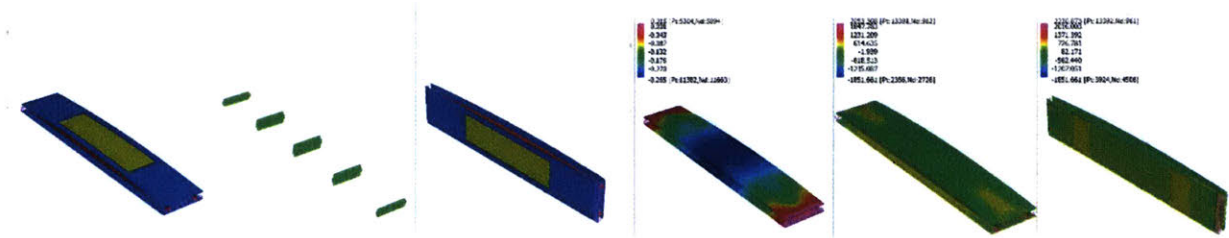
**Performance – GEN.1\_Theoretical**

Assuming allowable stress values from relevant APA all-plywood beam design literature (*Appendix – A*), and using a rounded adaptation of its approach to effective depth, the following multiple theoretical predictions were made.

**Table 5.2 Predictions – GEN.1\_Panel, Control & Kerfed**

Specimen	Thickness (the.)	$I_x$ (the.)	$P$ (the.)	Assumptions
P1: GEN.1_Panel, Control.	0.4"	606.4 in. <sup>4</sup>	50,309 lbs.	$\sigma_a$ : 2,800psi
P2: GEN.1_Panel, Control – Webs Only.	0.4"	36.8 in. <sup>4</sup>	2,954 lbs.	$E$ : 1,200ksi
P3: GEN.1_Panel, Kerfed [R1].	0.4", (0.2" eff.)	352.5 in. <sup>4</sup>	28,301 lbs.	$L$ : 48.0"
P4: GEN.1_Panel, Kerfed – Webs Only.	0.4", (0.5", $\underline{P}$ : 3685)	36.8 in. <sup>4</sup>	2,954 lbs.	$H$ (total): 9.0"
P5: GEN.1_Panel – Detail or Kerf Fails.	-	-	-	$h$ (web): 8.2"

(Pre-test)



**Fig. 5.8 Simulations – GEN.1\_Panel: Reinforced & Stiffened.**

( $L$ : 180";  $\Delta$ : -0.24")



**Fig. 5.9 Comparisons – GEN.1\_Panel, Control (r0); GEN.0\_Box, Kerfed (r160); GEN.1\_Panel, Kerfed (r96).**

*Initial load testing group photo; before and after. The order is reflected in the table below.*

**Table 5.3 Comparisons – GEN.1\_Panel, Control & Kerfed.**

(Rate: 0.1"/min.)

Specimen	Area (the.)	Pre-stress (the.)	$I_x$ (eff.)	$P$ (obs.)	Assumptions
GEN.1_Panel, Control.	39.8 in. <sup>2</sup>	0.0 % (0 psi)	23.38 in. <sup>4</sup>	7,090 lbs.	$L$ : 48.0"
GEN.0_Box, Kerfed [R2].	17.7 in. <sup>2</sup>	13.5 % (750 psi)	18.30 in. <sup>4</sup>	10,245 lbs.	$\alpha$ : 15.0"
GEN.1_Panel, Kerfed [R1].	23.5 in. <sup>2</sup>	22.5 % (1,250 psi)	13.48 in. <sup>4</sup>	7,080 lbs.	$H$ : 9.0"

**Notes:** (a.)  $I_x$  (eff.) used a 4-point specific, differentiated equation (A21):  $dP/d\Delta = 1/EI_{eff} \times (4a^3 - 3La^2/12)$

**Performance – GEN.1\_Panel, Control (r0)**

4"x 4" lengths of high-density Fir were used to elevate the control specimen above the press bed. Two 3"x 3" lengths of the same Fir were placed 12" apart to receive the longitudinally-oriented steel press head. With planar top and bottom flanges, the span was reduced 2" by the specimen sitting coplanar on its bearings. A 4-point flexural test was performed to simulate a uniformly distributed service load. The steep slope of the resultant loading curve indicates a greater rigidity than that observed in the initial *GEN.0\_Box, Kerfed* likely due to the stiffness of the change to webs with strong-axis grain and the tighter, simpler assembly. The failure mode was a controlled, flexural tension at mid-span.

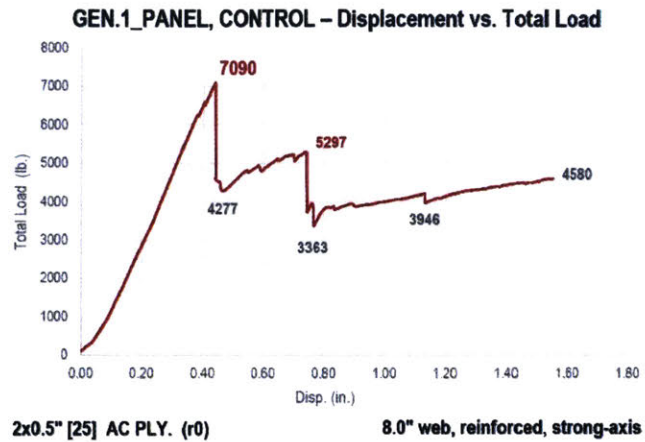


Fig. 5.10 Results – GEN.1\_Panel, Control.

**Performance – GEN.1\_Panel, Kerfed (r96)**

The setup for the second *GEN.1\_Panel, Kerfed* specimen was substantially the same aside from the bearing conditions, which were effectively linear due to the curvature. The specimen had a 48" clear span. Despite supplemental stiffening, both the shallower loading curve and its displacement nearly doubling reflect a significantly less rigid assembly. Anticipated was a mid-span failure local to the stiffener let through the web, but instead the specimen ruptured randomly 4.5" from mid-span – first on one side and then then another – suggesting material-related cause/imperfection. With the total loads within 10 lbs., the kerfing seems to have had little impact on total capacity, and thus the stiffener detailing was apparently appropriate.

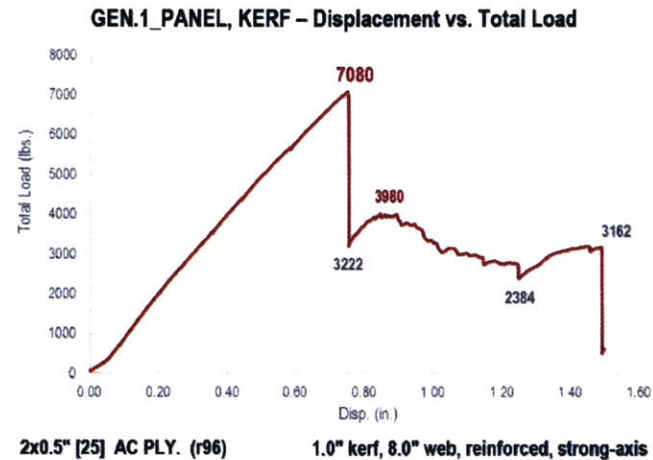


Fig. 5.11 Results – GEN.1\_Panel, Kerfed.



Fig. 5.12 Failure Modes: (a.) GEN.1\_Panel, Control; (b.) GEN.0\_Box, Kerfed; (c.) GEN.1\_Panel, Kerfed.   
 Web controlled failure at L/2; Web split at L/2 transfers to indexing; Web failure at L/3 at plug.

## 5.2 Results – GEN.2

(Unitized, Rapid-assembly Method)

### Construction – GEN.2\_System

The GEN.2 system evolved in response to the increased machine time required for kerfing and the concurrent empirical bending results (4.2). Departing from the box-girder focus on the floor system, the intent of the GEN.2 system was a rapidly deployable “voxel for insulation” best communicated by Section 8.2 – Demonstration.

### Geometry – GEN.2\_Unitized, Invert (r48)

The inverted, cylindrical, singly-curved specimen abandoned the preliminary kerfed strategy in favor of thinner 0.375" (nominal) face material bendable to a tighter radius. Although positive or low-slope applications would be typical, the GEN.2 specimen spot-checks the more severe service condition where the fabrication bending approaches the minimum radius. In the assembly, the two 0.36" (actual) faces are oriented to bend about their weak-axis and the two 0.5" webs about their strong-axis, with a single friction-fit stiffener at mid-span. The intermediate stiffener both braces the webs and facilitates assembly. Anticipating non-funicular geometries, rapid-deployment, or atypical spatial conditions, a 7,000 lbs. ratcheting strap was integrated as well.

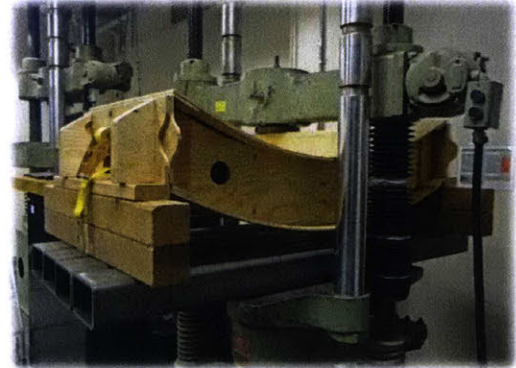


Fig. 5.13 Specimen – GEN.2\_Unitized, Invert.

### Geometry – GEN.2\_Unitized, Axial (r40)

Similar to but targeting vertical applications, this axial, conoidal (bending/twisting) specimen mixed the same FSC-certified materials, and the interior edge (figure right) achieves the r40 minimum radius. The key difference in this specimen is the webs, whose boundary slots twist slightly to remain normal to the faces and in doing so create internal stress-induced stiffness. The strap integration was included in this specimen, and leftover scraps of co-poly, a generic polycarbonate alternative used for the initial full scale “living hinges.” Prior to the jute webbing and seam tape testing presented, 0.04" co-poly was tested revealing a lineal capacity of only 30 lbs./in. and confirming the structural viability of the subsequent two alternatives.



Fig. 5.14 Specimen – GEN.2\_Unitized, Axial.

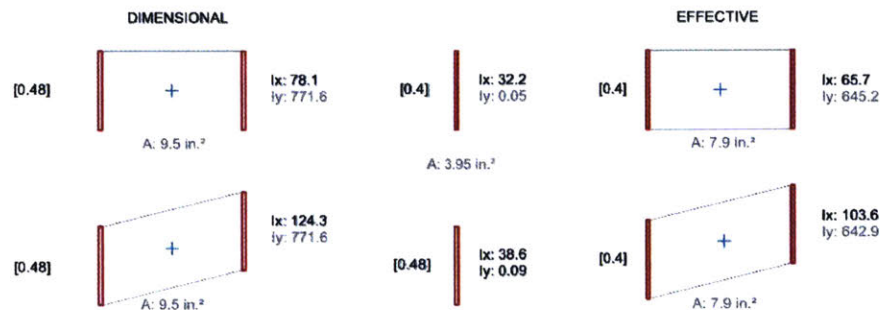
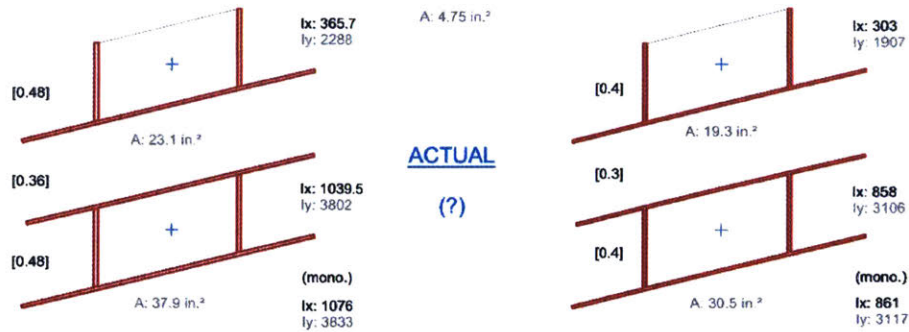


Fig. 5.15 Sections – GEN.2\_Unitized: Dimensional & Theoretical Properties. (Webs)



**Fig. 5.16 Sections – GEN.2\_Initialized: Dimensional & Theoretical. (Assembly)**

*Web theoretical predictions were closest to the experimental actual.*

**Performance – GEN.2\_Theoretical**

**Table 5.4 Predictions – GEN.2\_Initialized, Invert & Axial.**

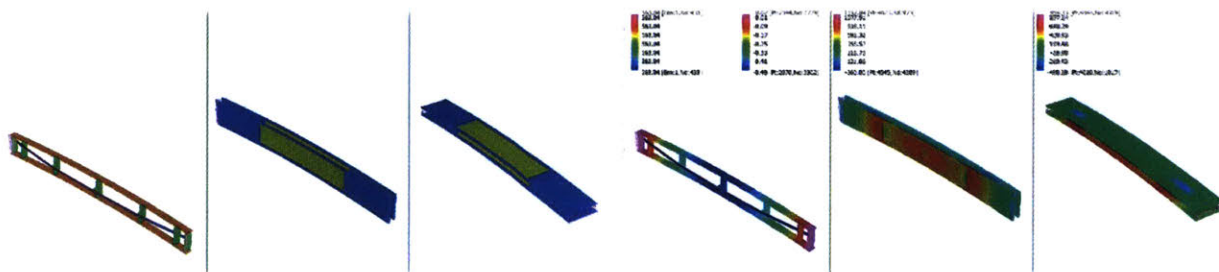
**(Pre-test)**

Specimen	Thickness (the.)	$I_x$ (the.)	$P$ (the.)	Assumptions
P1: GEN.2_Invert – Dimensional.	0.48", 0.36"	368.1 in. <sup>4</sup>	20,450 lbs.	$\sigma_a$ (5-ply): 3,300psi
P2: GEN.2_Invert – Effective.	0.4", 0.3"	312.1 in. <sup>4</sup>	17,339 lbs.	$\sigma_a$ (3-ply): 2,800psi
P3: GEN.2_Invert – Webs & Flange.	0.4", 0.3"	165.2 in. <sup>4</sup>	9,178 lbs.	$E$ : 1,200ksi
P4: GEN.2_Invert – Webs Only.	0.4"	78.1 in. <sup>4</sup>	4,339 lbs.	$H$ (total): 9.0"
P5: GEN.2_Invert – Web.	0.4"	39.5 in. <sup>4</sup>	2,194 lbs.	$h$ (web): 8.4"
P6: GEN.2_Invert – Detail or Hinge Fails	-	-	-	$L$ : 48.0"

**Invert:** (a.)  $I_x$  (eff.) used a 3-point, differentiated equation (A29):  $dP/d\Delta = 48E_{eff.}/L$ .  $I_x$  (eff.): 15.76 in.<sup>4</sup>

P1: GEN.2_Axial – Dimensional.	0.48", 0.36"	1,039.5 in. <sup>4</sup>	6,975,863 lbs.	$H, B$ : 10.7", 36.4"
P2: GEN.2_Axial – Effective.	0.4", 0.3"	858.0 in. <sup>4</sup>	5,760,626 lbs.	$H, B$ : 10.6", 36.4"
P3: GEN.2_Axial – Webs & Flange.	0.4", 0.3"	303.0 in. <sup>4</sup>	2,034,347 lbs.	$H, B$ : 10.3", 36.4"
P4: GEN.2_Axial – Webs & Flange, Offset 0.4"	0.3"	165.2 in. <sup>4</sup>	1,109,156 lbs.	$h$ (web): 9.8"
P5: GEN.2_Axial – Webs Only.	0.4"	103.6 in. <sup>4</sup>	695,572 lbs.	$H$ (total): 14.33"
P6: GEN.2_Axial – Webs Only, Offset.	0.4"	65.7 in. <sup>4</sup>	437,082 lbs.	$H$ (total): 9.8"
P7: GEN.2_Axial – Web.	0.4"	32.3 in. <sup>4</sup>	356 lbs.	$h$ (web): 9.8"
P8: GEN.2_Axial – Detail or Hinge Fails.	-	-	-	$L$ : 42.0"

**Axial:** (a.)  $P$  (the.) used (A7).  $P$  (obs.) between T6 & T7. After fasteners un-zip, parts behaved individually.

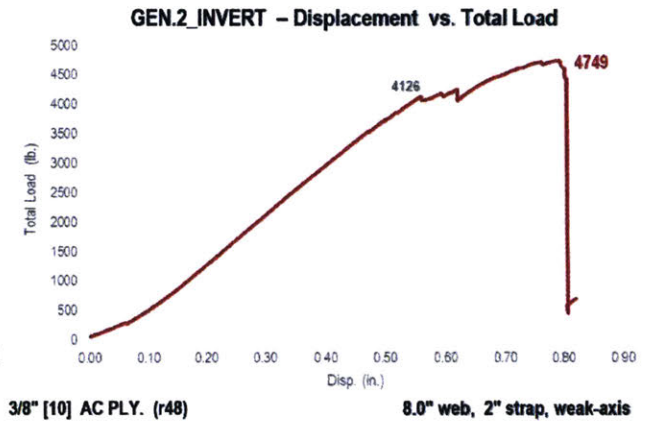


**Fig. 5.17 Simulations – GEN.2\_Initialized: Reinforced, Stiffened, & Strapped. (Low-slope)**

( $L$ : 180",  $\Delta$ : -0.49")

**Performance – GEN.2\_Initialized, Invert (r48)**

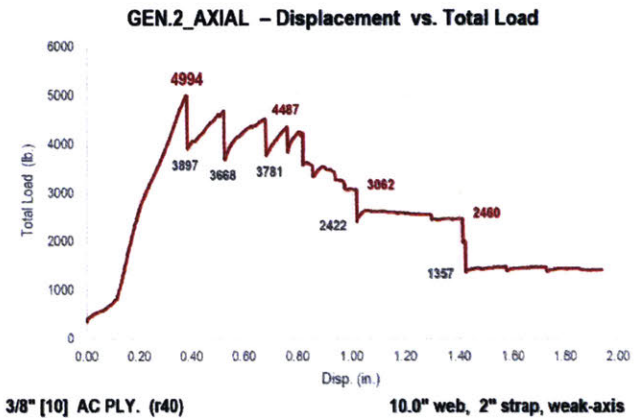
To ensure a comparable 48" clear span for the atypical inverted specimen, supplemental shear blocks were glued to the ends and redundant fasteners were applied. Because the curvature was significant enough to complicate stable placement of the spaced mid-span loading blocks, a 3-point bending test was performed. The slope of the GEN.2\_Initialized, Invert loading curve is similar to that of GEN.1\_Panel, Kerfed and the initial GEN.0\_Box, Kerfed specimen indicating consistent assembly rigidity across different generations. The failure mode of the specimen was web-rupture local to an interior plug.  $I_x$  (eff.): 15.76 in.<sup>4</sup>



**Fig. 5.18 Results – GEN.2\_Initialized, Invert.**

**Performance – GEN.2\_Initialized, Axial (r40)**

Although a different test orientation, the slope of the GEN.2\_Initialized, Axial curve is similar to the tightest-fitting GEN.1\_Panel, Control – a positive indication of a more-rigid assembly. Observable in the adjacent figure, from displacement 0.4" to 0.8", is the sequential failure of six (6) individual fasteners. Once all fasteners had torn out (un-zipped), the webs were free to buckle laterally, which they did with a slope comparable to that encountered with the individual strips' post-buckling behavior.



**Fig. 5.19 Results – GEN.2\_Initialized, Axial.**



**Fig. 5.20 Failure Modes – GEN.2\_Initialized: Details (a.) Invert; (b.) Axial.**

*In both the fasteners failed first; in (a.) at the end-cap living hinge and (b.) at the web-to-flange interface.*

The left pair of photos show the web in-plane tension rupture following the fastener failure at the co-poly "living hinge" termination bar. The right pair shows the web starting to buckle and eventual snap-through buckling; the results so far lead to a strategic realization that performance comes from forcing the bending to occur around a centroid other than that of the individual plate or strip – an initial finding which can be applied in designing these as roofs and walls.

### 5.3 Results – GEN.3

### (Semi-unitized, Site-assembly Method)

#### Construction – GEN.3\_System

The continuous longitudinal webs were eliminated in GEN.3 in favor of point connections between layers. The friction-fit "pedestal" detailing was developed to optimize assembly and reduce clamping. The initial inter-layer connection is made first with friction-fit discs until fasteners can be applied to permanently join the inner and outer layers, and thereafter remain in-place as local cantilever support. All interlayer detailing was based on circles and triangles anticipating scripted nesting on sheets, and existing "lead-in/lead-out" functionality was adapted to auto-locate fastener pockets.

#### Geometry – GEN.3 Semi-unitized (r69)

The three-strip GEN.3 specimen featured two typical pedestals located at the sixth-points (SP) and a smaller atypical mid-point (MP) post. The former were exaggerated by approximately 50% in width based on the intended out-of-context/stand-alone service. One and a half (1.5) sheets of 0.375" and half (0.5) of a sheet of 0.5" FSC-certified plywood were used (1,658.88 in<sup>3</sup> and 1,043.712 in<sup>3</sup> by volume respectively). Its 24" wide bottom flange had a minimum radius of r69.6". Using Equation (A6) for bending stress suggests 46.7% fabrication pre-stress at the far pedestal in the figure to the right and 21.9% at the r148" base of the near pedestal.



Fig. 5.21 Specimen – GEN.3\_Semi-unitized.

*Towards web-less strip construction.*

#### Performance – GEN.3\_Theoretical

Table 5.5 Predictions – GEN.3\_Semi-unitized.

Specimen	Area (the.)	I <sub>x</sub> (the.)	Pre-stress (fab.)	% (allow.)	% (MOR)
P1: GEN.3_Semi-unit. – Dimensional.	22.05 in. <sup>2</sup>	484 in. <sup>4</sup>	2,586 (r69.6, pedestal far)	92.4 %	46.7 %
P2: GEN.3_Semi-unit. – Reinforced.	44.10 in. <sup>2</sup>	970 in. <sup>4</sup>	1,216 (r148, pedestal near)	43.4 %	21.9 %
P3: GEN.3_Semi-unit. – Mid-post.	64.73 in. <sup>2</sup>	894 in. <sup>4</sup>	-	-	-

(Pre-test)

Notes: (a.)  $\sigma_o$  (3-ply), used: 2,800 psi; MOR (3-ply), used: 5,535 psi; range: 4,890 – 6,180 psi. [FPL GTR-190]

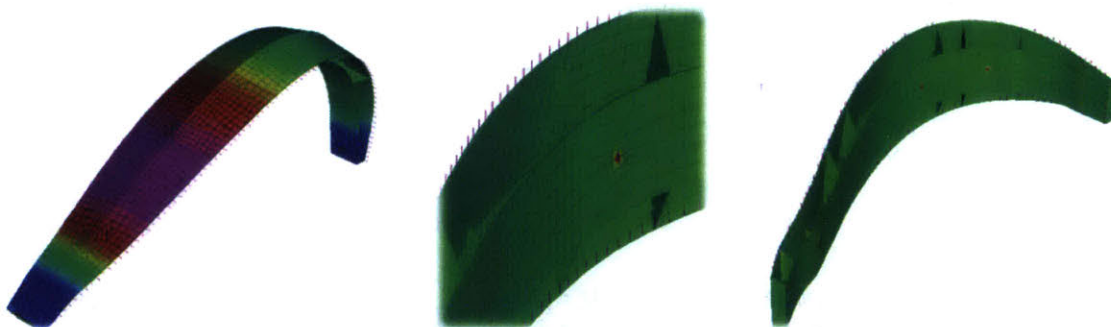
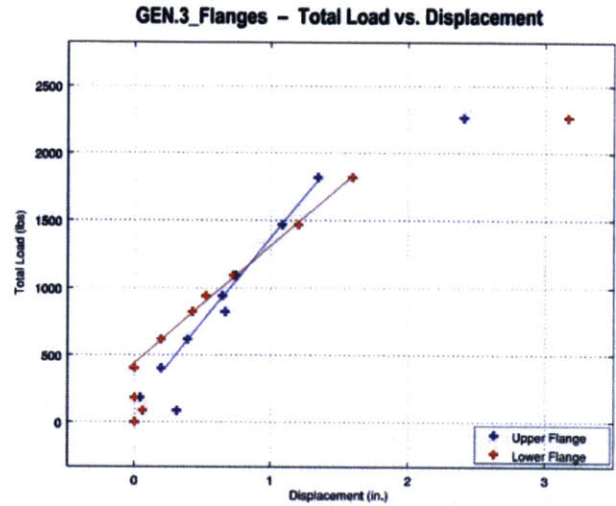


Fig. 5.22 Simulations – GEN.3\_Semi-unitized: Arch (a.) Global flexural; (b.) Midspan detail; (c.) Rotated.

*The overstressed areas local to the mid-posts are addressed by the proposed detailing.*

**Performance – GEN.3\_Semi-unitized (r69)**

Two load cells (following page) were placed based on the overall specimen length, and four (4) variable-height threaded feet were individually tuned with an analog level. The digital read out (DRO) was an International Organization of Legal Metrology (OIML) certified, Digi-weigh device, type XK3190-A12(E) [ZEMIC 2008]. To confirm its accuracy, previous specimens were weighed on separate digital equipment in the civil lab, and commercial pre-packaged raw materials of different volumes were re-weighed for comparison. Symmetrical load distribution after the placement of eight (8) concrete masonry units (CMU) was confirmed using a 2"x 10"x 120" board.



**Fig. 5.23 Results – GEN.3\_Semi-unitized: Flanges.**



**Fig. 5.24 Failure Modes – GEN.3\_Semi-unitized: (a.) Pedestal; (b.) Lower Flange; (c.) Upper Flange.**

*Figure 5.24b above shows the field-applied reinforcement at the primary pedestal interface.*

**Table 5.6 Comparisons – GEN.3\_Semi-unitized.**

**(Rate: Varied)**

Specimen	Area (the.)	$I_x$ (the.)	$I_x$ (eff.)	Pre-stress (fab.)
GEN.3_Semi-unit. – Reinforced.	44.10 in. <sup>2</sup>	970 in. <sup>4</sup>	-	-
GEN.3_Semi-unit. – Mid-post.	64.73 in. <sup>2</sup>	894 in. <sup>4</sup>	-	-
GEN.3_Semi-unit. – Typical.	22.05 in. <sup>2</sup>	484 in. <sup>4</sup>	-	-
GEN.3_Semi-unit. – Upper.	22.05 in. <sup>2</sup>	484 in. <sup>4</sup>	20.65 in. <sup>4</sup> (upper)	864 (r250, near); 900 (r240, far)
GEN.3_Semi-unit. – Lower.	22.05 in. <sup>2</sup>	484 in. <sup>4</sup>	6.56 in. <sup>4</sup> (lower)	1,216 (r148, near); 2,586 (r69.6, far)

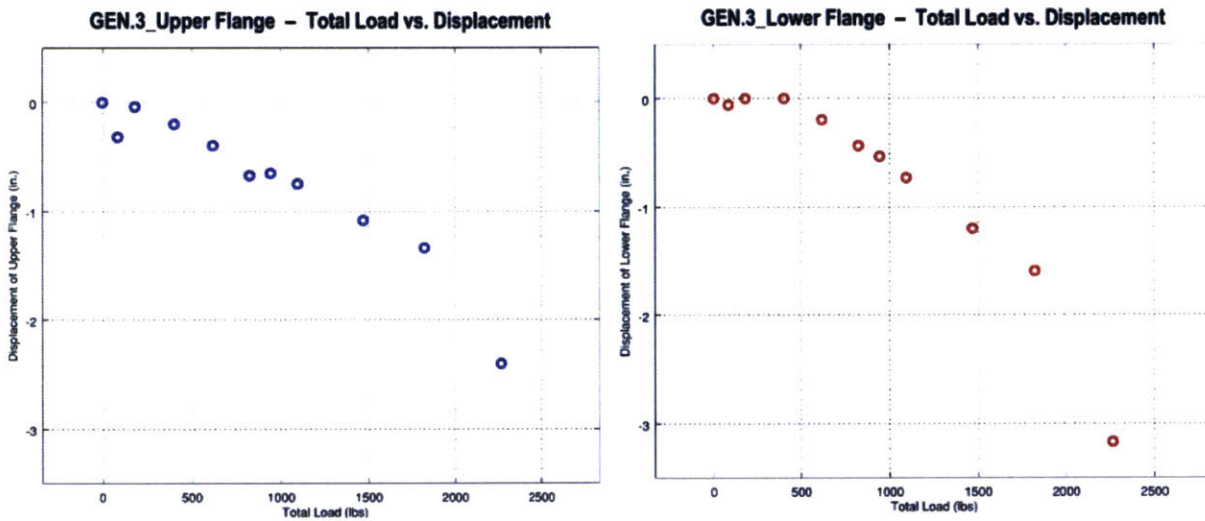
**Notes:** (a.)  $I_x$  (eff.) used a differentiated (A36):  $dP/d\Delta = (384EI_{eff})(L - 2A)/5L^4 + 48AL^3 - 168A^2L^2 + 96A^3L + 16A^4$ .  
 (b.) The increased stiffness observed in the top flange is attributed to the orientation and stiffened hinge.  
 (c.) Dimensional check was L (the.): 88.6" and L (obs.): 89.0".



**Performance – GEN.3\_Semi-unitized, Flanges**

A pre-test to 1,000 lbs. revealed rotational movement at the primary pedestal interface. To arrest this, supplemental 2"x 10"x 6" pieces of material were added on either side sufficient to receive two (2) additional fasteners. The GEN.3 specimen longitudinal pedestal laminations were mechanically fastened instead of glued and fastened, which would have avoided this field modification. At the initial rupture site in lower flange, taking into account the observed deflection, the r148" would be about r300" which equates to equates to 720 psi of pre-stress for 0.36" or 25.7% of total allowable capacity in the opposite direction of flexure. This percentage assumed a 0.36" section height and 2,800 psi [APA H815F] from the all-plywood beam design reference. The flange in-plane tension was unclear. The area loaded was 2,209.4 in<sup>2</sup> of the 3,492.8 in<sup>2</sup> total upper flange area. This amounts to 176.0 psf based on the footprint and 111.3 psf if considered to be uniformly distributed.

For the above positively curved specimen without internal webs, the flexural pre-stress from fabrication increased flange stress capacity for transverse loading by bending in the opposite direction of the global flexural deflection. Taking the flange geometrically further from its minimum radius also beneficially stress-stiffened the unit, but this increases the sensitivity of interlayer fasteners and details. For typical service conditions this increases stress capacity, but not without cost as the lower flange becomes a tie and the mid-post a tension/compression member.



**Fig. 5.25 Flanges – GEN.3\_Semi-unitized: Displacement (a.) Upper Flange; (b.) Lower Flange.**

*Move. Upper I<sub>x</sub> (eff.): 20.65 in.<sup>4</sup> & Lower I<sub>x</sub> (eff.): 6.56 in.<sup>4</sup>*

*Note that the I<sub>x</sub> (eff.) of the stiffened upper flange exceeds that of the GEN.1\_Box, Kerfed.*

## 5.4 Results – GEN.4

(Combined Results)

Table 5.7 Comparisons – Specimens

(Load Test)

Specimen	(lbs.) Load	(in.) Disp.	(in.) Min. r	Description
GEN.0_Box, Control	7,312	-0.65"	r0	0.5" BC; 08" web; 2-peak (= 6,500, 0.85" and 4,500, 1.25")
GEN.0_Box, Hybrid [R1]	5,380	-0.78"	r160	0.5" BC & 3/8" Lauan; 08" web; 1-peak (= 4,000, 1.80")
GEN.0_Box, Axial [R1]	33,000	-0.38"	r0	0.5" BC & 3/8" Lauan; 08" web. (= details same as hybrid.)
GEN.0_Box, Kerfed [R2]	10,245	-0.76"	r160	0.5" AC; 08" web; reinforced (QP); grain vert. (base = atyp.)
GEN.1_Panel, Control	7,090	-0.44"	r0	0.5" AC; 08" web; reinforced (QP); control reduced disp.
GEN.1_Panel, Kerfed [R1]	7,080	-0.75"	r96	0.5" AC; 08" web; reinforced (QP); equivalent disp.
GEN.2_Unitized, Invert	4,749	-0.79"	r48	0.38" AC; 07" web; termination bar failure. (= detail revision.)
GEN.2_Unitized, Axial [R1]	4,994	-0.38"	r40	0.38" AC; 10" web; progressive fastener failure. (= detail rev.)
GEN.3_Semi-unitized [PRE]	N/A	-2.12"	r36	0.38" AC; 08" pedestal; 18x48, parachute cord. (= pre-test.)
GEN.3_Semi-unitized	2,710	-1.60"	r69	0.38" AC; 11.5" pedestals; load: 111.3 psf. (= web-less.)
GEN.4_Semi-unitized [R1]	6,790	-3.91"	r40	0.40" LB; 11.5" pedestals; load: 100.0 psf. (= lam. bamboo.)

Notes: (a.) Simulation area (total): 12,598 in.<sup>2</sup>; area (projected): 9778.4 in.<sup>2</sup>; see GEN.#\_Weight in Section 6.3.

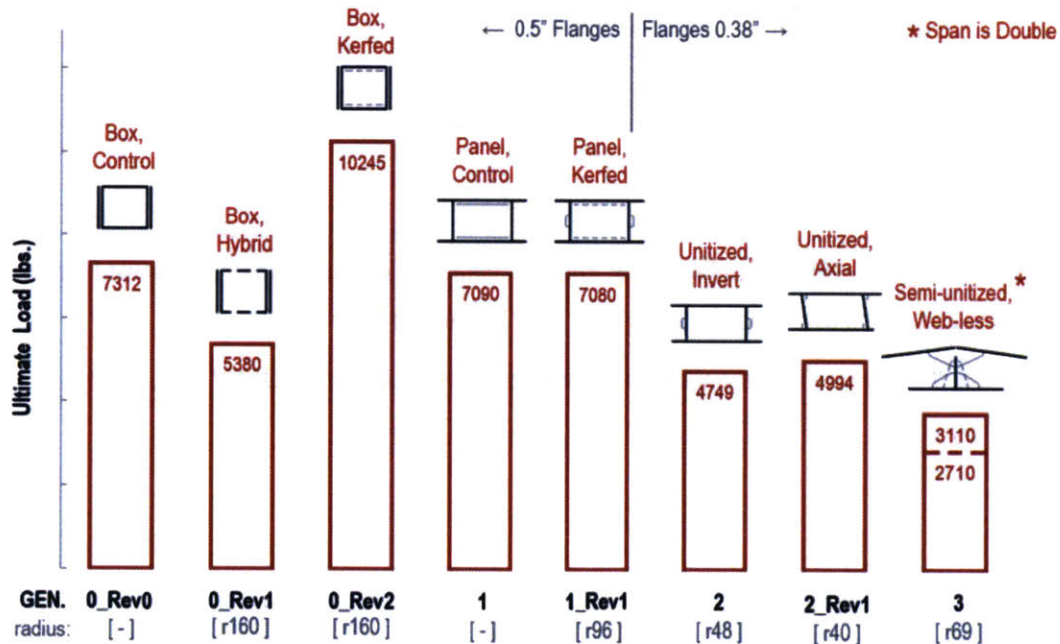


Fig. 5.26 Results – GEN.# Comparative: Ultimate Load.

For the GEN.3 specimen without internal webs the fabrication pre-stress is represented by the dashed line.

## 6. DISCUSSION

This *Chapter* is organized by stated problem into *Section 6.1 – Construction*, *6.2 – Geometry*, *6.3 – Performance*, and an additional *Section 6.4 – Project*. The first section compares the results from the prototype-driven process and presents the methodological findings from *GEN.2* and *GEN.3*. The second section compares failure mode geometry referencing a graphical overview and presents findings for each generation. The third section discusses quantitative results and performance-specific findings. The final section presents general project findings.

### 6.1 Discussion – Construction

#### Construction – Experimental: Overview

The experimental fabrication and testing produced many incremental non-quantitative results. The table below presents many of these according to the stated problems and a **general finding** for each method in bold font.

**Table 6.1 Experimental – Findings.**

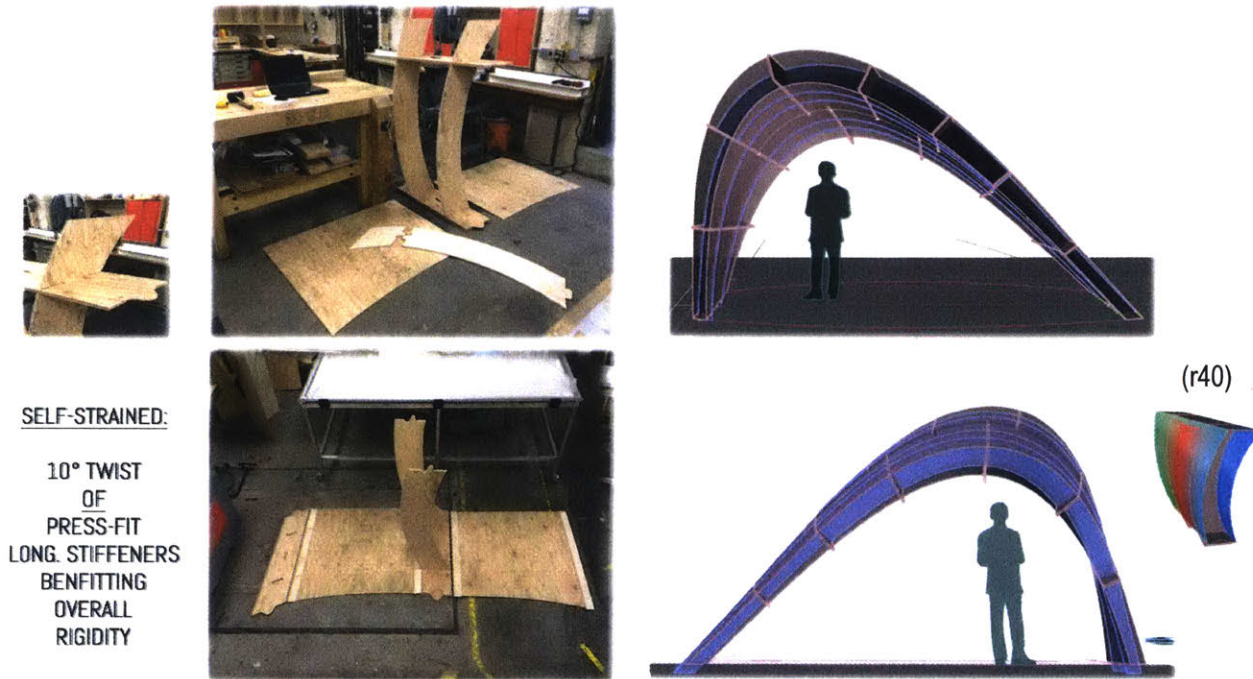
**(Fabrication & Testing)**

<i>Specimen</i>	<i>Problem</i>	<i>Findings</i>
<b>GEN.0 Box, Control &amp; Box, Hybrid [R1]</b>	<i>Method:</i> <i>Construction:</i> <i>Geometry:</i> <i>Geometry:</i> <i>Perf. Structural:</i> <i>Perf. Material:</i> <i>Perf. Material:</i>	<b>Edge joinery post-CNC is too labor intensive. Is not furniture.</b> Cove/Bullnose traveling joinery worked; added clamping. Cove/Bullnose joinery pre-test accumulated error; 0.4" over 48". 3-ply Lauan plywood was really 2-ply with a veneer core. Lauan/BC hybrid box-beam tested at 74% of all-BC plywood control. 3-ply Lauan shear was prohibitively low; will limit panel width. Lauan was non-renewable; few certified tropical hardwoods.
<b>GEN.0 Box, Kerfed [R2]</b>	<i>Method:</i> <i>Construction:</i> <i>Construction:</i> <i>Perf. Structural:</i>	<b>Box as typical is inefficient. Use it as atypical spans or columns.</b> Feed rate for small bit operations was slow; 2x-to-3x machine time. Box-beam concept was stiff; every part added to assembly time. Kerfing to bend worked perpendicular to grain; added to file prep. 3-ply BC plywood core was inferior material; grain aligned after kerf.
<b>GEN.1 Panel, Control &amp; Panel, Kerfed [R1]</b>	<i>Method:</i> <i>Construction:</i> <i>Construction:</i> <i>Perf. Structural:</i>	<b>Kerfing is 2x machine time. Friction-fit assembly is 2x faster.</b> Recessed reinforcing flange worked for seam access; added volume. Reinforcing flange helped web placement; not contributing to <i>I<sub>x</sub></i> (eff.). Pre-tests clarified fabrication pre-stress and flange residual capacity.
<b>GEN.2 Unitized, Rapid-assembly (Method)</b>	<i>Method:</i> <i>Perf. Structural:</i> <i>Perf. Structural:</i> <i>Perf. Structural:</i> <i>Perf. Structural:</i>	<b>Rapid-assembly works. Flanges prevent Webs from working.</b> Invert test webs worked; buckled flanges not contributing to <i>I<sub>x</sub></i> (eff.). Invert test showed no lateral buckling with one stiffener; try caps only. Axial test webs buckled laterally after fasteners failed; need to stiffen. Hinge co-poly width unchanged; did not see above 30 plf in either test.
<b>GEN.3 Semi-unitized, Self-assembly (Method)</b>	<i>Method:</i> <i>Construction:</i> <i>Perf. Structural:</i> <i>Perf. Structural:</i>	<b>Webs eliminated. Flanges working. Hinges &amp; Splines yet to fail.</b> Friction-fit disc worked to facilitate assembly; the pedestal key did not. Pedestal rotated; mid-point post was tension/compression member. 3-ply AC residual stress capacity was significant; span was double.

**Notes:** (a.) *Generational findings functioned as pre-rationalizations. Thin versus No webs was an open question.*

### Construction – Methods: Findings

The last two specimens tested (*GEN.2* and *GEN.3*) are initial deliverables in response to the core question and problem of methodology located in *Section 1.3 – Problem Statement*. The figures below represent the specific method developed to produce the *GEN.2* specimen, and a similar figure for the *GEN.3* specimen follows on the next page. The methodological differences and similarities are largely reducible to choices in ideological emphasis.



**Fig. 6.2 Method – GEN.2\_ Unitized, Rapid-assembly: (a.) Fit-up; (b.) Yard-arch.**

*Connecting system-built construction, elastic bending, and ironing; a renewable voxel.*

*GEN.2\_Method.* The base concept of *GEN.2* is a renewable "hollow brick" or "unitized" system, and the method is elastic deformation of pre-cut, pre-assembled, developable strips using a central, recessed, friction-fit frame.

In the *GEN.2* method, the conceptual ideal of *assembly performance* is prioritized over *thermal performance*. The physical manifestation of this design decision cuts both ways because accepting the vertical webs and horizontal caps in contact with the flanges to facilitate assembly and formation process creates lineal thermal bridges. The caps are the slotted parts to the left of the main figure, which return and receive the webs. Around 50% of the webs could be cut back for further thermal improvement without visible geometric compromise, preserving the mid-point depth. The webs shown to the right of the models above incorporate observations from the rod and strip pre-testing (i.e., precise control of the end-points with either quarter- or sixth-points used for global geometric control).

Another conceptual ideal *GEN.2* prioritizes is *geometric performance* over *structural performance* by assuming the weak-axis of the orthotropic sheet material for both flanges. In addition to their primary lateral structural role, a secondary one is they provide renewing geometric control at the top and bottom of every unit (reminiscent of mortar joints). The continuous cap boundary condition allows one person to assemble and form and minimizes clamping. The interface lap joint detail shown on both ends of the cap allows rotational adjustment in plan but blocks it in elevation. In section, assuming the details shown in *Section 8.1*, shims and any additional fasteners can be applied and the integrated strap used as a post-tensioning tendon or strap truss to allow almost any funicular "disobedience" imaginable. Ultimately, *GEN.2* is faster than *GEN.3*, and thus is presented as both "assembly- and geometrically-optimized, structurally- and thermally-improved" relative to light frame convention.

### Construction – Methods: Findings

*GEN.2–3\_Commonalities.* While both experimental methods developed involve some tactical pre-assembly of parts, a fundamental advantage of pre-cut, site-assembly methodology has over unit-level lamination is local or on-site replacement (i.e., via makerspace, cabinet shop, on-demand mobile milling truck, or drone drop). Of course, this also enables variable-depth design outcomes, and open systems simplify future modification. In the *GEN.2* method, hinges are pre-attached and parts linked prior to shipment as a flat pre-assembly with the webs and stiffeners simply bundled and banded by part. In the *GEN.3* method represented in *Figure 6.3* below, the seams are pre-attached to strips, and only the manageable scale pedestal point-connections are pre-assembled.



**Fig. 6.3 Method – GEN.3\_Semi-unitized, Site-assembly: (a.) Pre-test; (b.) Yard-arch.**

*Connecting system-built construction, elastic bending, and ironing; a segmented double shell.*

*GEN.3\_Method.* The base concept of *GEN.3* is a renewable "non-unit" or "semi-unitized" system, and the method is elastic deformation of pre-cut, developable strips using pre-assembled, pedestal point-connections and attachments (monolithic splines or laminated wedges).

In the *GEN.3* method, the conceptual ideal of *thermal performance* is prioritized over *assembly performance*. The physical manifestation of this design decision *also* cuts both ways. It eliminates the webs, resulting in "no foam or studs in the cavity" (as this became known to express the choice relative to the status quo), and it creates local thermal bridges. This was considered acceptable because the tapering parts and the slot interfaces in the pedestals and mid-posts contain the bridging to a discrete area and could be fully thermally broken with spacers or isolators.

Another conceptual ideal *GEN.3* prioritizes is *structural performance* over *geometric performance* by assuming the strong-axis of the orthotropic sheet material for the flanges. This anticipates the reduced stiffness and increased deflection resulting from the necessary elimination of webs, while targeting extreme-fiber optimization. After the elimination of the sub-frame, specific measures were developed to facilitate *GEN.3* assembly. One of these is that at the inter-layer connection, simple friction-fit discs allow the initial connection to be made until fasteners can be applied to permanently join the inner and outer flanges. Thereafter, these remain in-place as local cantilever support. Ultimately, *GEN.3* did take longer to produce than *GEN.2*, and thus is described as "assembly- and geometrically-improved; structurally- and thermally-optimized" relative to convention.

### **Construction – General: Findings**

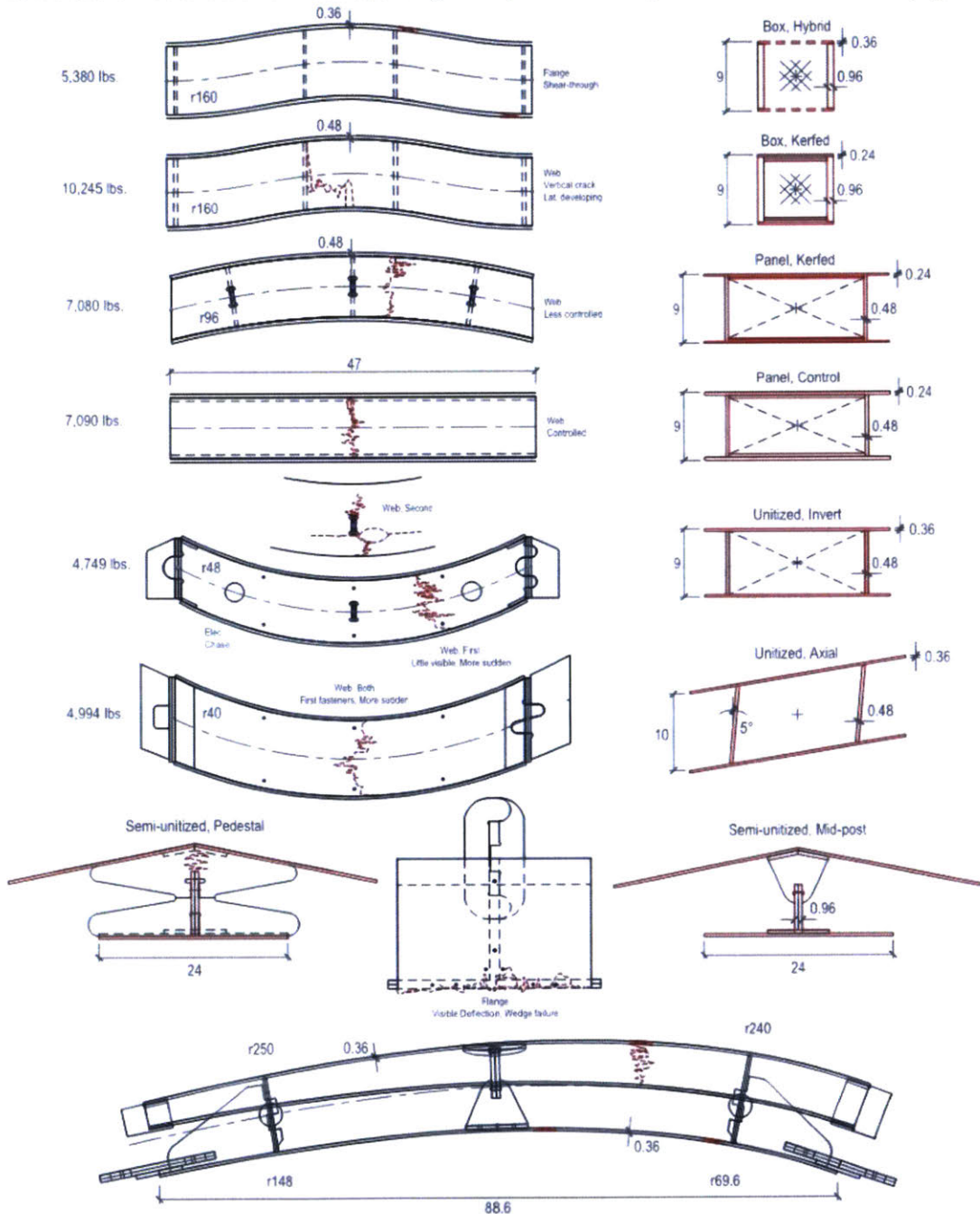
One early and apparently naïve expectation in *GEN.1* was that the theoretically tighter construction enabled by the precision of the CNC approach would be observable in performance and potentially advantageous. The observed deflections for the initial *GEN.1\_Unitsized, Control* made on a table saw, and the *GEN.1\_Unitsized, Kerfed* specimen made with a CNC-mill were significantly different. However, as the last specimen of the initial testing group to be produced, the kerfed panel on the right (*Figure 5.9*) was the tightest construction. Based on this, both *GEN.1* failing within 10 lbs. of one another, and the *I<sub>x</sub>* (eff.) comparison on the next page it does not appear the natural tightness of the construction was significant to the overall performance. That each flange of the latter kerfed specimen is already in a post-buckled state, and has been mechanically altered, seems the most likely explanation. *The GEN.1\_Unitsized, Kerfed* specimen was not de-constructed to inspect the concealed interface between the reinforcing layer and the stiffener because there were no visible signs of failure anywhere other than the web.

In terms of the resulting construction generally, *GEN.2* produces a dis-continuous cavity versus *GEN.3* continuous cavity allowed by the cruciform pedestals.

## 6.2 Discussion – Geometry

### Geometry – Specimens: Overview

This combined graphical overview of all the specimens locates and reviews the relevant dimensional properties the highlights the failure modes observed. Corresponding descriptions and interpretation follow on the next page.



**Fig. 6.4 Specimens: Overview.**

*Scale overview of specimens with failure mode location and type.*

**Table 6.2 Specimens – Findings: Failure modes.**

**(Location & Type)**

<p><b>GEN.0 Box, Control &amp; Box, Hybrid [R1]</b></p>	<p><i>General:</i> <b>Change the material and joinery.</b>  <i>Failure location:</i> L/3 in flange at right press head; L/3 local mitre joints. (Control)  <i>Failure type:</i> Transverse, cross-grain, punching shear; Local tension. (Control)  <i>Failure location:</i> L/3 in flange at right press head; L in flange at bearing. (Hybrid)  <i>Failure type:</i> Transverse, cross-grain, punching shear. (Hybrid)</p>
<p><b>GEN.0 Box, Kerfed [R2]</b></p>	<p><i>General:</i> <b>Change the grain orientation and reduce number of parts.</b>  <i>Failure location:</i> L/2 in web, developing laterally toward indexing  <i>Failure type:</i> In-plane, cross-grain, flexural tension; Interlaminar or planar shearing.</p>
<p><b>GEN.1 Panel, Control &amp; Panel, Kerfed [R1]</b></p>	<p><i>General:</i> <b>Flanges and friction-fit details not failing but kerfing is less rigid.</b>  <i>Failure location:</i> L/2 in web. (Control)  <i>Failure type:</i> In-plane, flexural tension; Controlled. (Control)  <i>Failure location:</i> L/3 in web, originated from plug. (Kerfed)  <i>Failure type:</i> In-plane, flexural tension at material flaw; Deflection. (Kerfed)</p>
<p><b>GEN.2 Unitized, Rapid-assembly (Method)</b></p>	<p><i>General:</i> <b>Unstiffened webs behave individually after fasteners fail.</b>  <i>Failure location:</i> L/3 in web. (Invert)  <i>Failure type:</i> Fastener. In-plane, flexural tension; Progressive. (Invert)  <i>Failure location:</i> L/2 in web, originated from edge fastener "pocket" detail. (Axial)  <i>Failure type:</i> Fastener. Lateral torsional buckling, then snap-through. (Axial)</p>
<p><b>GEN.3 Semi-Unitized, Site-assembly (Method)</b></p>	<p><i>General:</i> <b>Pedestals needs base like mid-post. See revised mockup.</b>  <i>Failure location:</i> L/2 in edge. (Pre-test)  <i>Failure type:</i> Flexural cracking. (Pre-test)  <i>Failure location:</i> Bottom flange at L/4, local to pedestal. (Test)  <i>Failure type:</i> In-plane, flexural tension; local shear. (Test)</p>

**Notes:** (a.) See also the [R2] pedestal revision in Section 4.1.

**Geometry – Materials: Findings**

After the plywood pre-test (*Figure 4.33*), once the elastica tool was operational, the observed rise values along with the known specimen lengths were used to calculate a more accurate theoretical minimum radius and thereafter the bending stress based on thickness. Relative to the published values for nominal 0.5" and 0.375" plywood in the APA reference, the informal pre-test suggests the observed minimum radius is on average 29.4% below the published values. For 0.5" plywood, this breaks down to 28.7% tighter at 96" (strong-axis) and only 19.6% at 48" (weak-axis). For 0.375" plywood, this breaks down to 37.2% at 96" (strong-axis) and 32.2% at 48" (weak-axis).

In the subsequent formal tests of different sheet materials, the precise press displacement data (*Appendix – D*) and the use of multiple samples make it inherently more significant. Together these provide a better indication of various material limit states, probable failure modes, and some insight into industry-published values (see also *Figure 4.33* or *Table 4.2*).

**Geometry – Tolerances: Findings**

The dimensional *fabrication tolerance* (i.e., the CNC-milling of parts) was generally negligible, aside from vacuum bed and file preparation related errors (e.g., the toolpaths flipping inside the geometry). Initially, waste material around the smaller parts was failing laterally in bending due to the lead-in or lead-out of the bit. This would shift neighboring parts, but was solved by revising layout spacing to be a minimum of one and half (1.5X) times the sheet thickness for parts under 100 in.<sup>2</sup>.



The dimensional *assembly tolerance* (i.e., the pre-assembly of component parts and attachments) generally fell within the  $\pm 0.125$ " assumptions. In the *GEN.2\_Unitized, Axial* specimen, bending or "wrapping" the pre-assembled strips over the vertical webs resulted in tapering gaps (0.38") largest local to the corner hinges. A check of the model revealed this to be a product of the four edge-to-edge gaps (0.125") sliding slightly before engaging, combined with ignoring the nominal and actual material thickness difference (0.375" and 0.36"). In the second *GEN.2\_Unitized, Invert* specimen, this was anticipated and minimized by working from the web mid-point outward toward the end-caps when connecting the webs and faces. The observed span of the interior edge of the assembled specimen measured 0.125" (45.875" versus 45.75") longer than the design span .

### **Geometry – Tolerances: Findings**

At rest and without its context, the *GEN.3\_Semi-Unitized* specimen measured 0.4" longer (89.0" versus 88.6") than its design ideal, which is primarily attributed to assembly tolerance. Plywood moisture content was observed at 6%, with no appreciable dimensional change when measured again after four (4) days in the shipping container. On the fourth day, the previous two of which had rained, its observed moisture was 8.9%. A basic check for a 96" sheet was made for this 2.9% change in equilibrium moisture which reflects an approximately 20% change in equilibrium relative humidity. Assuming the plywood average coefficient of hygroscopic expansion [FPL 2010, Wood Handbook] 0.0002 in./in. of material for 10% change in equilibrium relative humidity (RH), this would be 0.0348". For a 50% change this would be only 0.096".

Generally at levels below 50% equilibrium plywood is understood to be 20-to-50% more dimensionally stable than dimensional lumber [ibid FPL, APA, Green Modular]. At the dimensions the combined hygroscopic and smaller thermal dimensional stability of plywood is understood to be addressed with an 0.125" gap between strips. For the other two engineered sheet materials considered, laminated-bamboo and soy-based Plyboo, this would be even less.

Reference: [Zi Xuan Yu, Ze Hui Jiang, Ge Wang - 2012 - Moisture Absorption of Laminated Bamboo Composite and its Influence of Mechanical Properties, doi: 10.4028/www.scientific.net/AMM.204-208.4165; Applied Mechanics and Materials; vol. 204–208, pp.4165–4172]

### 6.3 Discussion – Performance

(by Topic)

#### Performance – Material: Findings

*Material. (Perf.)* The initial decision to investigate material between 0.5" and 0.25" was the result of industry literature review [APA, and Aircraft, Marine] and the few covert in-store pre-tests logged in *Appendix – D*. This range was judged the application-specific territory where sheet materials are thin enough for bending yet remain thick enough to serve as primary structure. By the end of the project, this had narrowed to focusing on thinner material (0.36", 3-ply) for the flanges and thicker material (0.48", 5-ply) for the inter-layer attachments and components.

**Table 6.3 Material – Specimens: by Weight**

(Data: 16.0728)

<u>Specimen</u>	<u>Rev.#</u>	<u>P (lbs.)</u>	<u>Wt. (lbs.)</u>	<u>P/Wt. (lb.)</u>	<u>Min. r (in.)</u>
GEN.0_Box, Control	-	7,312	31	235.8/lb.	r0
GEN.0_Box, Hybrid	[R1]	5,380	25	215.2/lb.	r160
GEN.0_Box, Axial.	[R1]	33,000	09	3666.6/lb.	r0 (Column details match Hybrid)
GEN.0_Box, Kerfed	[R2]	10,245	28	365.9/lb.	r160
GEN.1_Panel, Control	-	7,090	52	136.3/lb.	r0
GEN.1_Panel, Kerfed	[R1]	7,080	49	144.5/lb.	r96
GEN.2_Unitized, Invert	-	4,749	35	135.6/lb.	r48
GEN.2_Unitized, Axial	[R1]	4,994	48	104.1/lb.	r40
GEN.3_Semi-unitized	[PRE]	N/A	14	N/A	r36 (Pre-test)
GEN.3_Semi-unitized	-	3,430	29	93.44/lb.	r69.5 (58 lbs.; 46.72/lbs. at full L)
GEN.3_Yard-arch	[R1]	6,790	-	-	r69.5 (Sim. as Lam. Bamboo)

**Notes:** (a.) *The GEN.3 specimen was double the span of the others. Its 58 lbs. weight at 88.6", factored for the 47% span difference, is 27.8 lbs. and lighter than all beams aside from the one with light Lauan.*

#### Performance – Operational: Findings

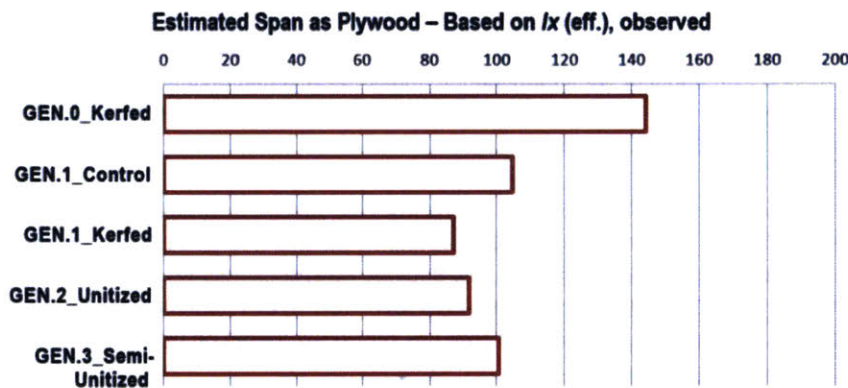
*Operational. (Perf.)* Given that the structural results discussed on the following page are not orders of magnitude apart, if these are interpreted as general parity, then thermal considerations suggest *GEN.1* as floor, *GEN.2* as wall, and *GEN.3* as roof. This is based on preliminary analysis of their respective frame reductions, and is reflected in the *GEN.4* figure. If the frame factor in a conventional SIP system is generally 1/4th that of light frame construction, as Meis' and Morley's takeoffs [2015, 2000] suggest, both *GEN.2* and *GEN.3* methods can appropriately be described as thermally-improved relative to light frame construction. At the *GEN.2* vertical webs, the estimated margin of frame reduction is still around 50% since they are rarely flush. This is further assured by the stress-stiffened or self-strained aspect of the *GEN.2* assembly discussed later in this section. At the *GEN.2* horizontal caps, the estimated frame reduction is 33%. As with the webs, cutting the back the caps is assumed, but with four structural connections occurring at this location lightening holes are shown.

**Performance – Structural: Findings**

*GEN.#\_Structural. (Perf.)* From the strip pre-tests the strength limits of available sheet-materials are clearer, and so is their probable structural performance in assemblies after three (3) full-scale specimens with 0.36" plywood flanges approaching or above the 5,000 lbs. threshold

Likewise, the failure modes through *GEN.2* were generally consistent in location (i.e., webs) and there was no real  $I_x$  (eff.) outlier among the specimens, discounting the lower *GEN.3* flange already discussed in *Section 5.3*. These along with the accuracy of the "Webs Only" theoretical predictions support the interpretation that the webs, as the relatively stiffer components due to their orientation, are seeing the stress. This goes to assembly behavior but also introduces a specific structural design problem of how to stiffen *without* webs or rigid cellular structural core. This was the challenge taken up conceptually, both in scale models and full scale prototypes, that the *GEN.3* method is designed to address.

The following two figures represent the probable span and serviceability based on the observed performance. The readiness of these assemblies "as-built" for any other application than roof is below initial expectations, however their relative performance as represented by  $I_x$  (eff.), and material economy have been established. Multiple potential design responses are possible: (1.) material change, (2.) web re-detailing, (3.) web reinforcement, (4.) flange reinforcement, and/or (5.) assembly depth increase.



**Fig. 6.6 Structural – GEN.0, 1, 2, 3 Findings: Estimated Span.**

*The estimated spans at 50 psf based on the observed  $I_x$  (eff.) are represented above.*

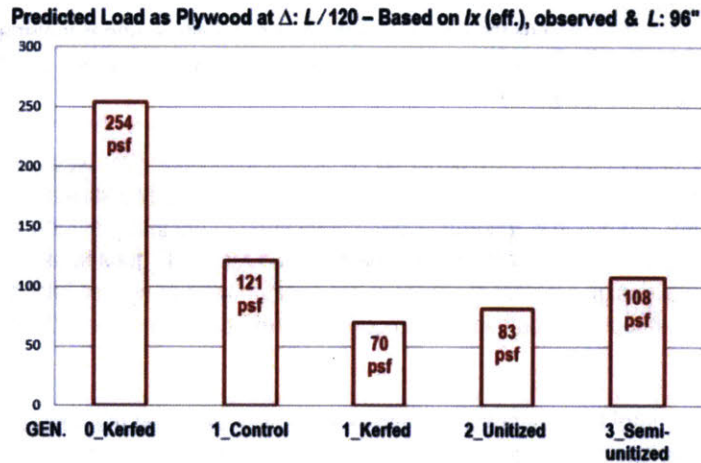
*The pre-test theoretical predictions were overly optimistic about the extent to which built-up assemblies would behave as "wholes,"*

**Table 6.4 Material – Specimens:  $I_x$  (eff.)**

**(Data: 16.0728)**

Specimen	$I_x$ (eff.) (in. <sup>4</sup> )	$\eta$ (in.)	$\Omega$ (psf)	$E$ (psi)	$1/\Psi$	$h$ (in.)	$\Omega$ (psi)	$L$ (in.)	Max. Moment (ft.-in.)	$\sigma_b$ (psi)
GEN.0_Box, Kerfed [R2]	18.30	9	50	1.2E+06	180	9	0.35	144.20	8122	1997
GEN.1_Panel, Control	23.38	30	50	1.2E+06	180	9	0.35	104.74	14286	2750
GEN.1_Panel, Kerfed	13.48	30	50	1.2E+06	180	9	0.35	87.18	9896	3304
GEN.2_Unitized, Invert	15.76	30	50	1.2E+06	180	9	0.35	91.83	10981	3136
GEN.3_Semi-unitized (Upper)	20.65	30	50	1.2E+06	180	11	0.35	100.50	13151	3502

**Notes:** *Made with  $I_x$  (eff.) from different analysis workflows, this represents if all were tested with UDL.*



**Fig. 6.7 Structural – GEN.0, 1, 2, 3\_Findings: Predicted Load.**

*Comparing applied loads at the basis of design deflection ( $L/120$ ) limit state.*

*GEN.2\_Structural. (Perf.)* At three units high, comparable to a floor-to-floor height (144"), a preliminary simulation suggested the vertical webs would need to double. With two post-buckled bending-active faces, *GEN.2* is ultimately considered to be a stressed-skin panel or semi-monocoque construction because of the extent to which the internal frame is working structurally. It is described as a method because the wrapping and elastic deformation of pre-attached component parts is a specific formation process.

*GEN.2, 3\_Structural. (Both)* Each method proposed departs from the specific assumption of lamination to a rigid foam core – at least until one with less creep is available. A known compromise with foam-core SIPs is that once the span reaches about 144" they begin to require continuous engineered splines, usually at the quarter points. Recalling a well-known early Structural Insulated Panel Association (SIPA) advertisement with a panel carrying an elephant, it is necessary to address creep in case the creature should fall asleep on its feet.

*GEN.3\_Structural. (Perf.)* Once placed with the pre-attached seams completed (ironed), the system behaves as a continuous flexural shell with its load-resisting action developed through the offset inner and outer stressed-skins. This retains only the extreme-fiber optimization of conventional SIP construction. Serving as combined shear-transfer locations and geometric control points, for typical curved panels there are three cruciform pedestals: two boundary and one intermediate. Although the shell consists of individual site-assembled units, the construction is effectively continuous with "living-hinges" intentionally staggered to misalign the axes-of-rotation. The specific advantage of this semi-unitized approach is any unit-level sectional actuation and hinge lines are naturally impeded once linked with its neighbors.

*GEN.3\_Detail. (Perf.)* A structural detail specific to *GEN.3\_Semi-unitized*, which has not been described, is the pre-attached hinges constitute local redundancy at the interfaces, sixth-point ridge wedges, and mid-point pedestal bases. The proposed detailing responds to the localized overstressed areas shown in *Figure 5.22*. This final method is distinct due to its combination of its formation process – elastic deformation, stressed flanges, and modularization strategy. Thus, it is described as a bending-active, stressed-skin, semi-unitized method.

### Performance – Structural: Findings, Arch

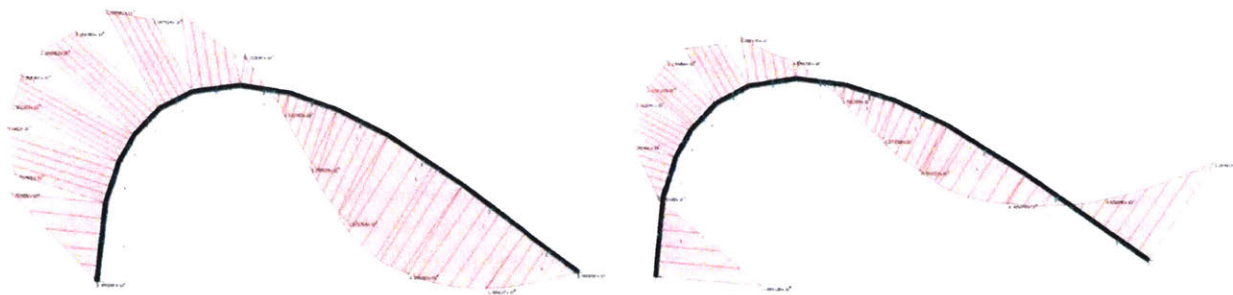
A follow up finite element analysis (FEA) simulation in Strand7 for an arch made of 0.4" plywood and 0.4" laminated bamboo was made seeking to clarify relative performance. Assuming a span of 220" [5.6m] and a 100 psf uniformly distributed load, the results indicate deflection as the probable failure mode, as represented by the composite figure below.

While the GEN.3 details and fabrication pre-stress were incorporated into the initial simulation, the stress-stiffening effect of the strain energy from bending was not due to limitations of the study. At this load level, and with increasing the system depth or adding local reinforcement both possible options, the initial study supports conceptual validity.



**Fig. 6.8 Simulations – GEN.3\_Arch: Laminated Bamboo vs. Plywood**

For L: 220" at 100 psf the failure mode was deflection. Note: plywood is underlay and laminated-bamboo is overlay.  
(Overlay  $\Delta_{LB}$ : -3.91"; Underlay  $\Delta_{PW}$ : -6.26")



**Fig. 6.9 Simulations – GEN.3\_Arch: (a.) Pinned- vs. (b.) Moment-connected supports.**

Increasing depth, adding reinforcement, changing materials, or altering boundary conditions are all possible options.

For deflected zone:  $M_{max}$ . (a.):  $-2.16 \times 10^4$  lbf-in. vs.  $M_{max}$ . (b.):  $-9.79 \times 10^3$  lbf-in.

For deflected zone: L (a.): 143.5" vs. L (b.): 111.8"

Although the initial numerical analysis indicated GEN.3 would require increased depth or additional reinforcing at  $L/3$  in either material, the deflection was 38% less for laminated bamboo. It also assumed pin-pin supports and when re-run at 50 psf was within the  $L/120$  (1.833) industrial-use threshold for roof applications [AITC 8.4.2.1] as detailed.

## 6.4 Discussion – Project

(General)

### Project – Interpretations (General)

*Method. (Project)* The significance of the methodological findings lies in their systematic questioning of conventional panelized construction methodology – either generally as the combined prototype or specifically as *GEN.2* and *GEN.3* component methods – which target internally stiffened stressed-skin panels (SSPs) and rigid-foam core structural insulated panels (SIPs), respectively.

*Material. (Project)* For greater continuity with the previous *GEN.0* and general accessibility of shop scrap plywood was used for all test specimens, and while it and bamboo scrimber are clearly relevant, laminated bamboo appears the most appropriate for extending the spans at these thicknesses. Phenolic paper is considered interesting, but was unavailable at competitive prices and no below-finish grade was available. Ultimately, in final *GEN.3* method the material (be it bamboo or plywood, or paper) is optimally located for performance – not in the cavity, bridging or impeding continuous insulation and requiring redundant layering.

*Structural. (Project)* Though self-supporting, the structural action of the final web-less proposal would rarely be exclusively that of a true arch, beam (as most of the theoretical analysis assumes), continuous vault, or column. Potential deployments of the final component method range from low-slope roofs, curved just enough to manage water run-off, to continuous vertical walls. Axial compression of wedged strips was simulated (see *Section 8.3*), but formal mechanical testing above 54" was not possible on local equipment. Especially for applications closer to that of a portal frame, the structural action would be neither exclusively flexure or compression but rather the continuous hybridization of the two, and with situational reinforcing anticipated and applied as necessary. In conditions where there is positive curvature, any fabrication pre-stress actually helps as pre-camber.

### Project – Limitations (General)

The principal limitations of the project are the scope necessarily engaged for conceptual development and some of that engaged unnecessarily for technical clarification. These and the time consumed for the installation reduced the number of full scale specimens, yet the unanticipated and varied analyses produced other findings. The variations in load test setup increased the complexity of the theoretical analysis and could have been avoided by fabricating a pivoting attachment for the hydraulic press head to keep the setup consistent (until the final generation). Nevertheless, these application- and method-specific "spot-checks" correspond to floor, wall, and roof as much as a linear evolution, and served well their intended purpose of informing the development of a unique all-sheet-material methodology (*Section 8.4*).

### Project – Future Work & Next Steps (by Problem)

Future work planned relative to the construction problem is the continued investigation and development of the final prototype methodology towards a collection of repeatable, pre-cut systems for residential use. Testing the global flexural and axial performance of *GEN.3* at full scale, the revised friction-fit pedestal detail, hinge membrane material, and split-web solutions are five specific objectives.

The rod installation and detailed engagement of the elastica were to an extent unanticipated, and they produced a tempting geometric question: Assuming wider elastically-deformed sheets and more precise analysis of both local and global elastic bending, can these be fabricated into the systems to achieve target geometries? A reprise of the installation in wood at 2x scale is one thought and a canopy sketch of the canopy for it is included in the *Section 8.4* design demonstration. Also, there appears to be no plural noun to distinguish the rods of the elastica from the curve for which a "troupe" is proposed.

The future work intended relative to the performance problem is development of an application-specific computational design or "integrated approach" for form-finding networked plate and strip assemblies – exceeding the more immediate clarification of reinforcing of double shells generally. A present idea on the supplemental reinforcement of

GEN.3 is perhaps it could anticipate the deflected form and engage or spatialize like muscle fiber at specific geometry. At the time of this issuance, the construction and geometry problems are well-engaged and proposed computational scope is left for future work, followed by comparative thermal simulations of the combined prototype.

The next steps for the project are structural simulations: (1.) a non-linear analysis follow up to quantify benefits of the staggering proposed, and (2.) a study addressing the reinforcement versus depth identified in the GEN.3 simulation for a site-specific aggregation of GEN.4.

#### **Project – Predictions & Recommendations (General)**

This project is both an expression and prediction of relevant areas of interest. There is much detailed work by others more structurally qualified as already addressed in *Chapter 2 – Literature Review*. One such example addressing the scaling and potential relevance of bending-active structures assesses their potential as "niche" and "temporary" applications. While this may be an appropriate and fair judgement at the scale commercial buildings, hopefully broader more enduring applications can become common, including residential roofs and walls.

In terms of recommendations for bending-active systems or design strategies, increased clarity about the possibilities of such approaches can be gained through pairing them with pre-rationalization and a developed framework – in this case increased conceptual-, construction-, geometry-, and performance-awareness.

#### **Project – Findings (General).**

*Interpretation. (Project)* This thesis highlights the relevance of a multi-objective, prototype-driven strategy which integrates conceptual, virtual, tactical, and geometric design methodologies as well as performance indicators. Emphasis was placed on material, geometric, and structural performance as a means of rigorously pursuing the new, but also and in hopes that we will *not simply use it to optimize* existing systems or their production. Glass and metal are well-attended to in the geometry processing community at present, both for, and a result of their commercial relevance. Encouraged is more methodological research relevant to residential roof and exterior wall applications, and an expanded definition of performance beyond minimal material structures towards a holistic "lightness" as described by Gang [2013] and detailed in *Section 2.3 Literature – Performance*.

What the general geometry processing community has achieved in the last ten years is incredible. Who wouldn't want to design glass interventions on the Eiffel Tower or elaborate nests for LVMH, but there is also tremendous potential to effect change for people in both the developed and developing world by focusing such advances on residential convention as well. Let us not be satisfied with optimization and pursue new post-digital construction methodology to challenge conventional assumptions and to extend residential construction. The proposals herein are scratches on that door. While the details or sizes will continue to evolve, the project goal of developing specific methods that combine new ingredients, yet remain relevant to people with garage or cabinetry shops and truck-bed CNC mills has been reached. A greater campaign now begins toward development for production.

## 7. CONCLUSION

In this *Chapter*, the first *Section 7.1 – Contributions* provides a comparative overview of general project contributions, findings, and analytical references. The following *Section 7.2 – Conclusions* presents specific project conclusions.

### 7.1 Contributions

Grouped by problem below in *Table 7.1* and ordered from the author's perspective are the general project contributions. Within the self-imposed constraints of commonly available flatbed CNC equipment and present related means, this thesis engaged three problems in pursuit of economical, renewable, high-performance alternatives to conventional (light frame/panelized) construction, and developed a combined prototype methodology with increased capacity for geometric variation.



**Fig. 7.1 Contributions – Methodological: GEN.4\_Method (1.) Bend-up; (2.) Zip-up; (3.) Iron-up.**

*The methodological development in response to an observed absence is considered the more significant.*

**Table 7.1 Contributions – Overview.**

**(Towards cost-aware freeform strip construction.)**

<i>Problem</i>	<i>Contribution</i>	<i>Description</i>
<b>Construction</b>	<i>Conceptual:</i>	Introduction of site-assembly, bending-active, iron-up, stressed-skin concept.
	<i>Conceptual:</i>	Development of active bending focused on renewable high-performance, medium-scale, building applications.
	<i>Methodological:</i>	Development and integration of three (3) specific methods into one (1) open prototype methodology.
<b>Geometry</b>	<i>Analytical:</i>	Creation of reusable computational dimensional analysis tools, definitions, and references.
	<i>Material:</i>	Clarification of the minimum radius/limit states and application-specific potential for different sheet materials.
<b>Performance</b>	<i>Structural:</i>	Clarification of assembly residual stress capacities, dimensional behavior under load, probable structural performance, and failure modes.





**Fig. 7.2 Contributions – Methodological: GEN.0, 1, 2, 2 (Back row); GEN.3 (Pre-test); GEN.3 (Test).**

*Responding to eighty (80) years of prefabricated SIPs with pre-cut, rapid- and site-assembly STRIPs.*

Nearly every full scale mock-up (see also *Section 4.1*) or specimen above produced some clarifying result or application-specific finding which became a pre-rationalization for the next generation or by the final prototype.

Particularly as initial specimens, the *GEN.2* and *GEN.3* load test results generally support the further development of both and the proposed evolution of internal stiffening from continuous webs to pedestals, wedges, and splines (as described in *Chapter 4* and *5*). At twice the span the *GEN.3* test was not apples-to-apples, and adding the fabrication pre-stress to that generated by the applied load seems an appropriate representation that reflects the reality of removing the webs (short of the non-linear follow-up simulation planned). Certainly one specific question at this point is if the 6 lbs. of material *GEN.3* saved relative to *GEN.2* were added back as local reinforcing, would the web-free specimen achieve parity?

For any contemplating economical approximation of freeform, be it "frame-less framing" or other adventures in bending at scale, hopefully the minimum radius reference figures, tables, and the elastica/stress workflows herein will find good use.

**Table 7.2 Contributions – Analytical.**

<b>Table 7.2 Contributions – Analytical.</b>			<b>(Re-usable)</b>
<i>Type</i>	<i>Topic</i>	<i>Description</i>	<i>Location</i>
<b>Figures &amp; Tables</b>	<i>Elastica:</i>	Distance Along Curve ( $\oint$ ) <u>vs.</u> Min. Radius ( $r$ ); Angle ( $\alpha$ ); Rise ( $c$ ).	( <i>Figure 4.25a</i> )
	<i>Elastica:</i>	Span ( $L$ ) <u>vs.</u> Min. Radius ( $r$ ).	( <i>Figure 4.25b</i> )
	<i>Elastica:</i>	Compare to other curve types, arc to elastica.	( <i>Section 4.2</i> )
	<i>Materials:</i>	Avg. Span at Fracture ( $L_{avg.}$ ) <u>vs.</u> Avg. Minimum Radius ( $r_{avg.}$ ).	( <i>Figure 4.38</i> )
	<i>Materials:</i>	Avg. Minimum Radius ( $r_{avg.}$ ) <u>vs.</u> Avg. Bending stress ( $\sigma_{avg.}$ ).	( <i>Figure 4.46</i> )
<b>Tools</b>	<i>Stress:</i>	Detailed theoretical analysis workflow for different load tests.	( <i>Appendix – C</i> )
	<i>Elastica:</i>	Detailed theoretical analysis workflow for the elastica.	( <i>Appendix – E</i> )
	<i>Elastica:</i>	Computational dimensional analysis tool.	( <a href="http://branchoff.net">branchoff.net</a> )

**Notes:** (a.) *Any future work and computational tool updates will be available at: <http://branchoff.net/free4orm>.*

## 7.2 Conclusions



**Fig. 7.3 Contributions – Structural: Active bending.**

*Assembly-level management of active bending. Resilience; releasing the strain energy after four (4) months.*

### Conclusions (Specific)

The diverse stream of incremental results from the experimental prototype-driven process highlights the value of keeping architectural thinking and making feeding back into one another. The observed assembly structural performance (as represented by the effective second moment of area  $I_x$  (eff.) and the failure modes demonstrate how even as dimensionally precise assemblies, the component parts behave less like their built-up theoretical ideal, and more according to their heterogeneous individual properties (e.g., material and grain orientation). Relative to the stated problems, the project conclusions are:

#### • Problem of Construction

How can we realize curvature in panelized building systems using flatbed CNC cutting operations (2D) and create plate joinery to challenge conventional assumptions?

*By abandoning the constraints of off-site lamination, the orthographic wire-cut rigid foam and adhesives, in favor of pre-cut, site-assembled strips linked with continuous living hinges and pre-assembled friction-fit attachments.*

#### • Problem of Geometry

How can we transform flat/planar (2D) sheets into volumetric (3D) freeform surfaces and clarify the geometric limit states for the relevant sheet materials?

*By tapering and bending ruled developable strips (which can be offset consistently to generate geometry for multi-layer applications) to produce aggregations of semi-discrete surfaces (e.g., conoidal and tangents of spatial curves) and by combining empirical and theoretical dimensional analysis of flexure, as referenced in Table 7.2.*

#### • Problem of Performance

How can we systematize developable strips (2D) cut from renewable sheet materials for deployment as site-assembled, high-performance, volumetric (3D) structural forms for medium-scale building applications?

*By developing specific integrated assembly-, geometry-, thermally, and structurally-aware methods (e.g., staggering offset-able surfaces to provide interlayer point-connections on the geodesic, inherent hinge redundancy, and control at the sixth points) in rapidly-renewable engineered bamboo or plywood, and by using bend-up, zip-up, iron-up strip methodology – which harnesses the strength in geometry and locally manages elastic bending to produce cost-aware surface-active construction without cellular foam.*

Also, through the workflows located in *Appendix–C (Calculations)* and *Appendix–E (Elastica)* the relationship between geometry and bending or fabrication pre-stress, as well as residual capacity are more clearly understood.

### **Closing Remarks**

This experimental thesis looked beyond the pre-processing of dimensional lumber and industrial lamination of conventional site-built construction towards deploying elastic bending in the form of pre-cut, hinged, developable strips for economical, approximation of freeform surfaces. Conceptually, it arrived at specific "vertical wrapping" method and a "horizontal staggering" methods and is successful in the sense that it clarifies many application-specific questions, and demonstrates with empirical evidence from full scale testing that such systems are relevant at the residential scale. The project also successfully synthesizes disparate design methodologies and highlights the value of a prototype-driven process. Ultimately, it is a proof offered to emphasize the present potential in leveraging existing post-digital capacities to begin to move on from methodological stasis in conventional medium-scale construction.

Looking now from the other side of the river, the expansion in fabrication, modeling, and simulation capacities which began in the late 20th-century has so reduced the distance between designers and production that how building systems encounter, interact with, or respond to constraints can becomes continuous and variable. This shift eases or relieves entirely many bottom-up constraints of the past, allows the agency of material, tectonic, and topological properties to become primary, and renders methods the design space with tremendous potential. As well, long-held assumptions are reasonably called in to question and should continue to be until we have methods of the present capable of performance in the greater sense, which includes dimensional variety. Like the elastica, the potential applications are ubiquitous, and with the technological means no longer missing, it is again time for even the most fundamental assumptions of conventional medium-scale construction to evolve.

As much as could be packed into this extended enjoyment against stasis has been, which along with the combined prototype methodology presented in *Section 8.4*, will hopefully inspire more discussion of possible deployments for active bending in residential construction (or other post-digital interventions and reinventions thereof).

## 8. DEMONSTRATIONS

[GEN.0, 1, 2, 3, 4]

This supplemental *Chapter* is organized by generation into *Section 8.0 – GEN.0*, *8.1 – GEN.1*, *8.2 – GEN.2*, *8.3 – GEN.3*, and *Section 8.4 – Combined*. It presents selected design demonstrations, details, pre-tests, and tools created to develop the different proposals.

### 8.0 Demonstrations – GEN.0

(Kerfed, Stiffened Box-beam)

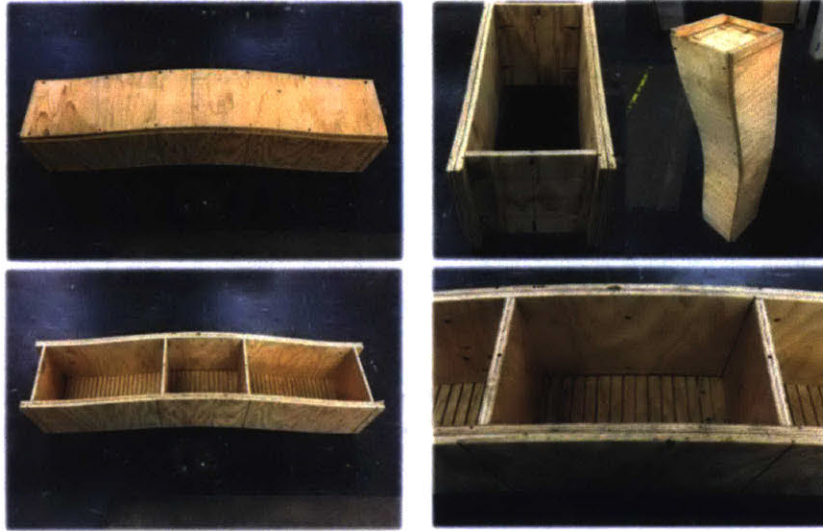


Fig. 8.0a Construction – GEN.0\_Box-beam, Kerfed [R2].

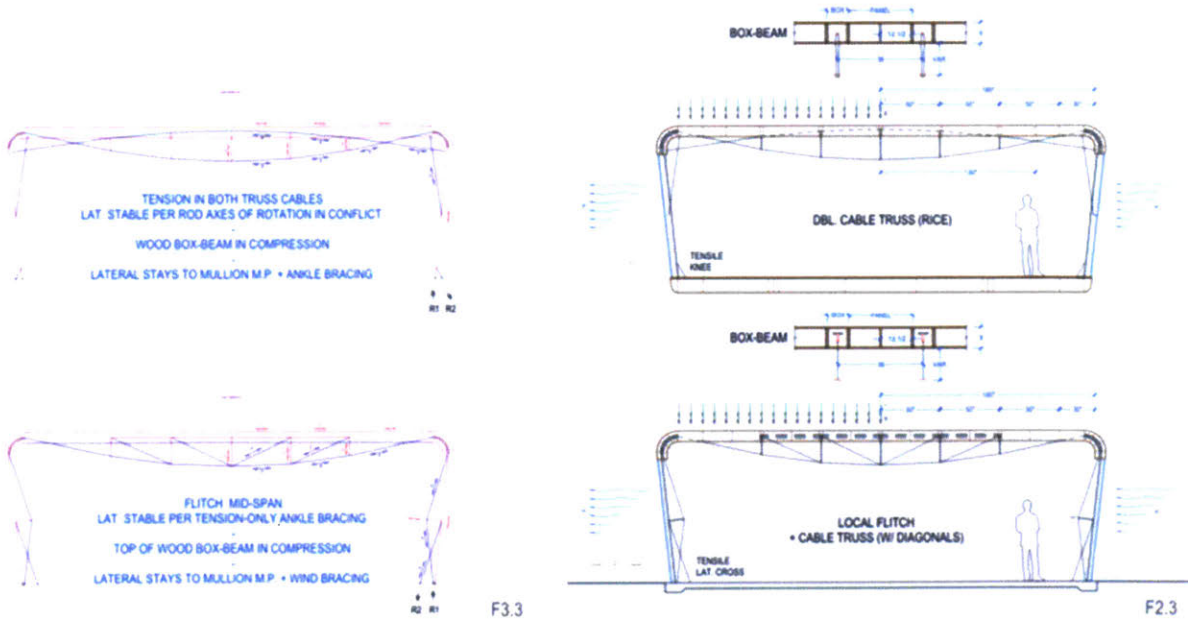


Fig. 8.0b Geometry – GEN.0\_Box-beam, Preliminary [R2].

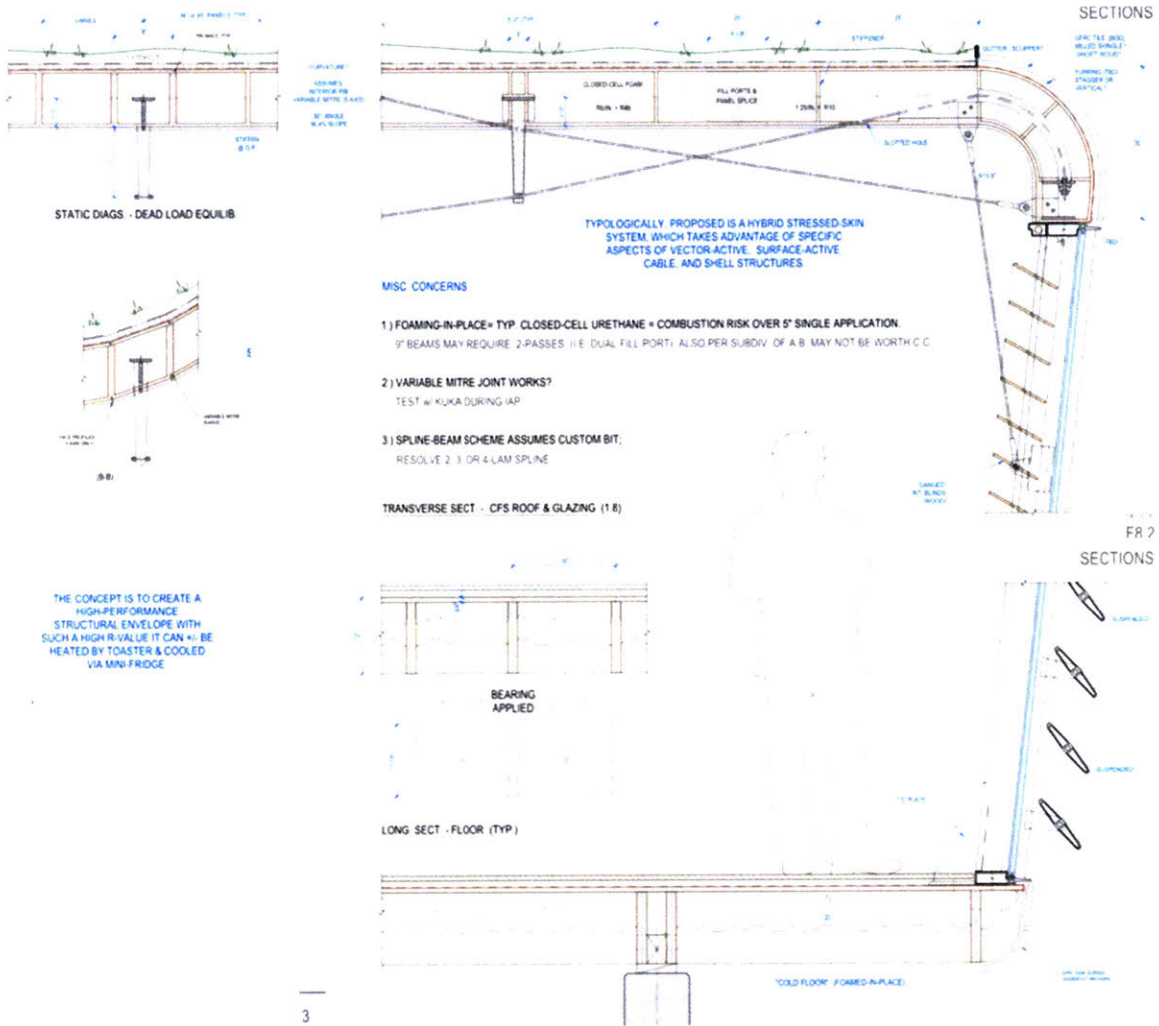


Fig. 8.0c Geometry – GEN.0\_Box-beam, Development [R2].

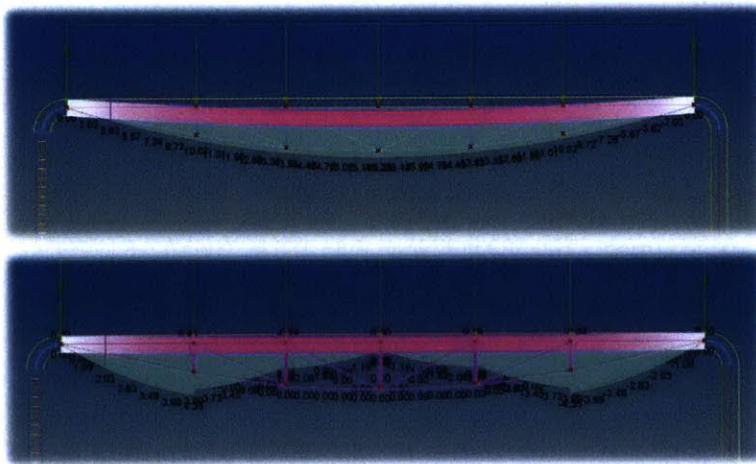
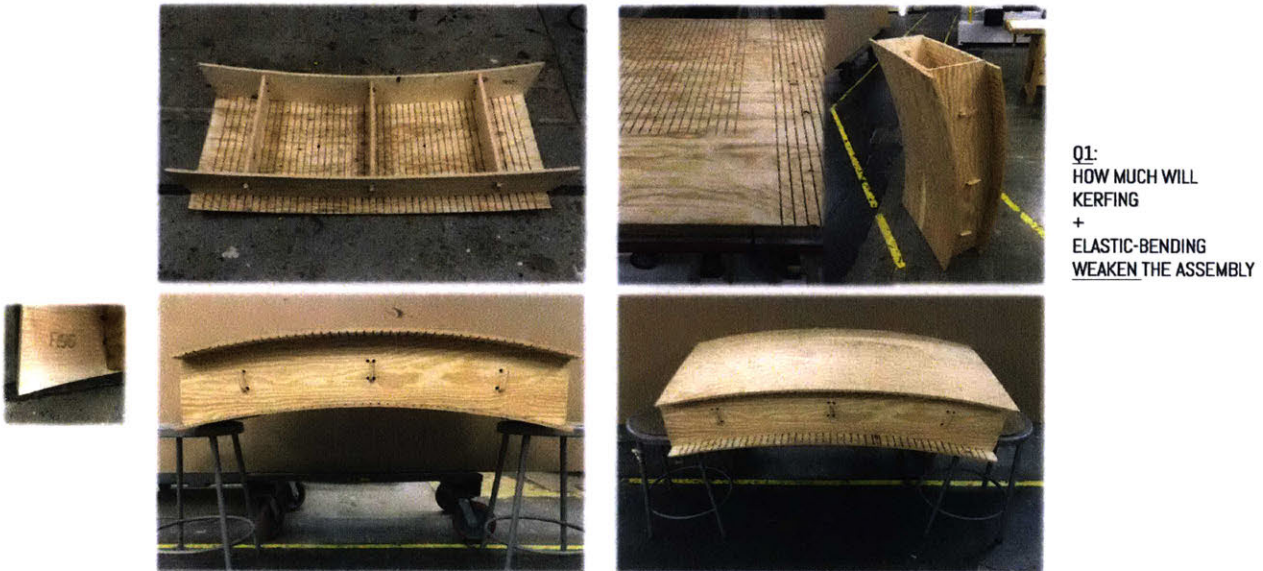


Fig. 8.0d Performance – GEN.0\_Box: Simulation, Typical vs. Spatial Beam.

Simulating; integrated cable-truss. [Karamba]

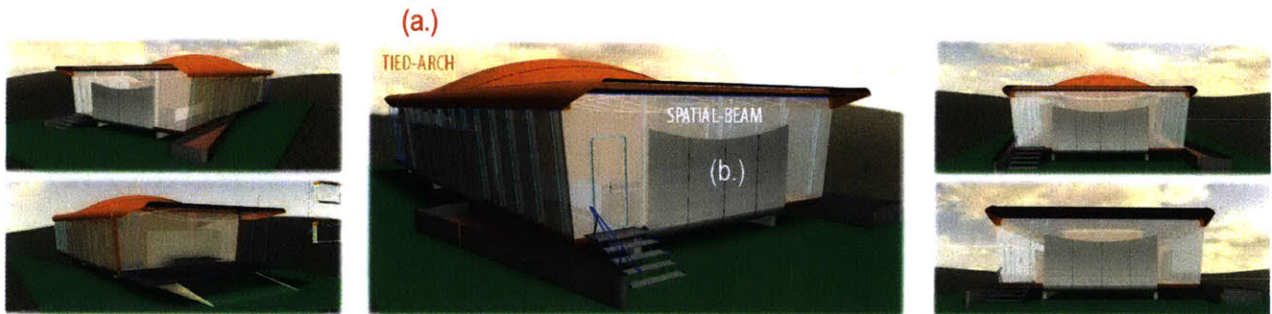
## 8.1 Demonstrations – GEN.1

(Kerfed, Reinforced, Friction-fit Panel)



**Fig. 8.1a Construction – GEN.1\_Panel: Kerfed, Detail [R1].**

*How much and in what way will the kerfing and elastic bending impact the assembly? Will the stiffener detail fail?*



**Fig. 8.1b Geometry – GEN.1\_Case Study.**

*Conceptual study: Change in structure type and action from (a.) Tied-arch to (b.) Spatial beam.*

Case study: 1,350 ft.<sup>2</sup>

(a.) Area opaque: 264,201 in.<sup>2</sup> (roof) + 194,389 in.<sup>2</sup> (floor) + 83,166 in.<sup>2</sup> (wall) = 541,756 in.<sup>2</sup> → **3,762.2 ft.<sup>2</sup>** (total)

(b.) Volume cavity: 3,762.2 ft.<sup>2</sup> x 0.66 ft.<sup>3</sup> = **2507.88 ft.<sup>3</sup>**

(c.) As closed-cell foam: \$0.75/bd. or \$9/ft.<sup>3</sup> = **\$22,570.92**

(d.) As open-cell (foam): \$0.50/bd. or \$6/ft.<sup>3</sup> = **\$15,047.28**

(e.) As R3.20 granulated fill (mineral fiber) at 2.8 pcf: \$0.20/bd. or \$2.4/ft.<sup>3</sup> = **\$6,018.91**

(f.) As R3.73 granulated fill (cellulose) at 1.15 pcf: \$0.06/bd. or \$0.72/ft.<sup>3</sup> = **\$1,805.67**

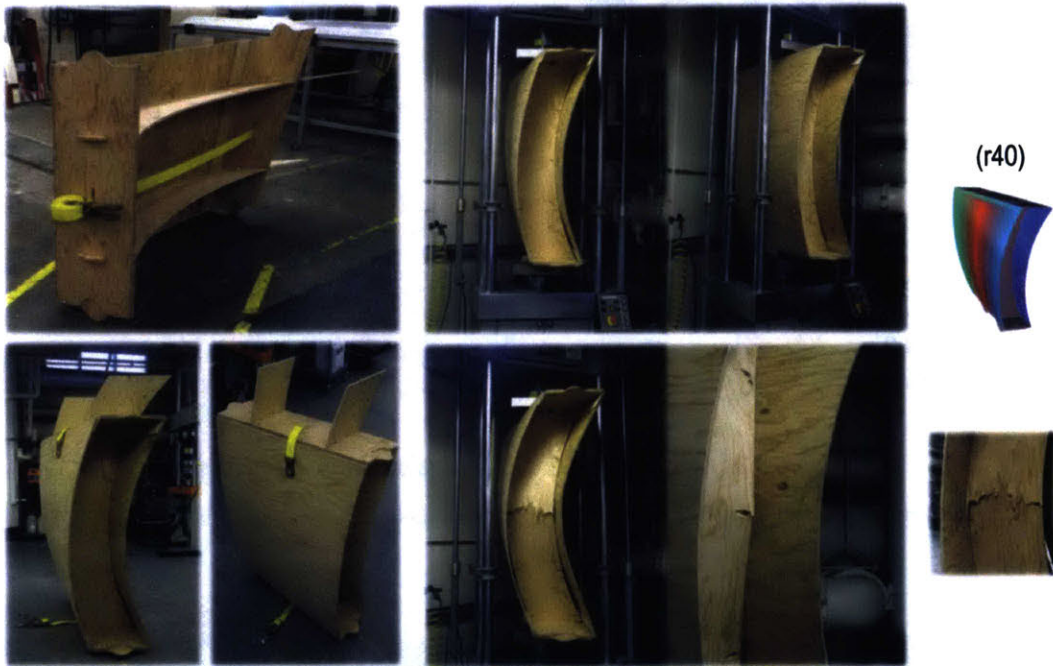
**Fig. 8.1c Performance – GEN.1\_Material Take-off.**

*Case study of closed-cell, open-cell, granulated cellulose and mineral wool suggests the economy of fill.*

## 8.2 Demonstrations – GEN.2

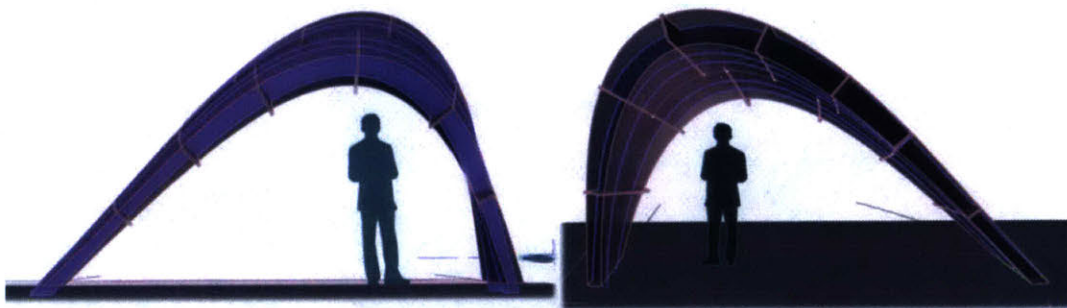
## (Unitized, Rapid-assembly Method)

The images of the *GEN.2\_Unitized, Axial* [R1] specimen below show the curvature, the self-strained webs, and the integration of ratcheting straps. These can serve the initial assembly sequence, as post-tensioning, or as a spatial strap-truss to extend the span, as represented at the bottom of the page. The primary innovation of the *GEN.2* method is its optimized assembly which is represented sequence by the sequence in *Figure 8.2d* on the next page.



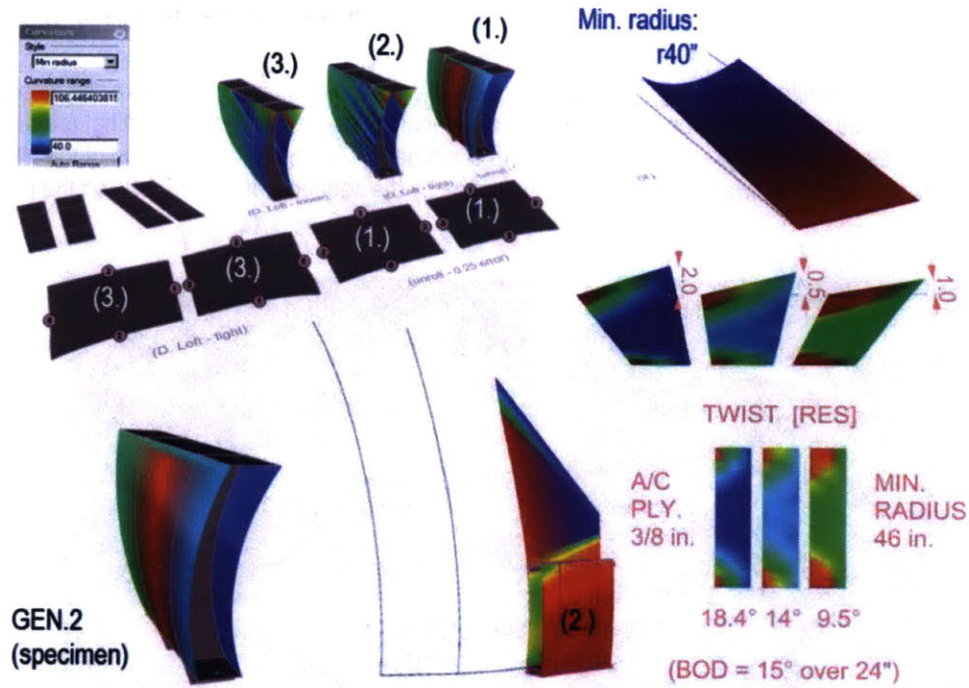
**Fig. 8.2a Construction – GEN.2\_Unitized: Rapid-assembly [R1].**

*Prioritizing rapid-assembly; the webs twist 5° to stress-stiffen the assembly.*



**Fig. 8.2b Geometry – GEN.2\_Model: Elevation & Oblique.**

*Case study: Post-tensioned vs. Strap-tensioned, arch.*



**Fig. 8.2c Geometry – GEN.2\_Analysis: Unrolling & Twisting.**

*Developmental study: (1.) Rhino Loft; (2.) Evolute, D-loft "Loose"; (3.) Evolute, D-loft "Tight."*



**Fig. 8.2d Performance – GEN.2\_Unitized: Rapid-assembly.**

*Assembly- and Geometrically-optimized; Structurally- and Thermally-improved.*

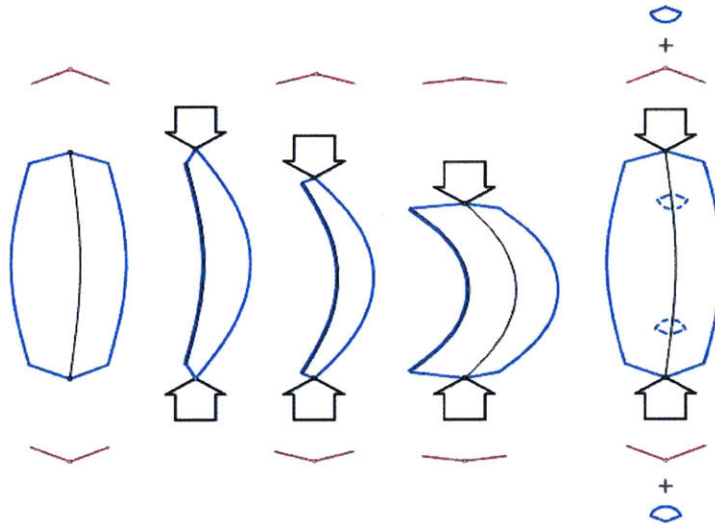


### 8.3 Demonstrations – GEN.3

### (Semi-unitized, Site-assembly Method)

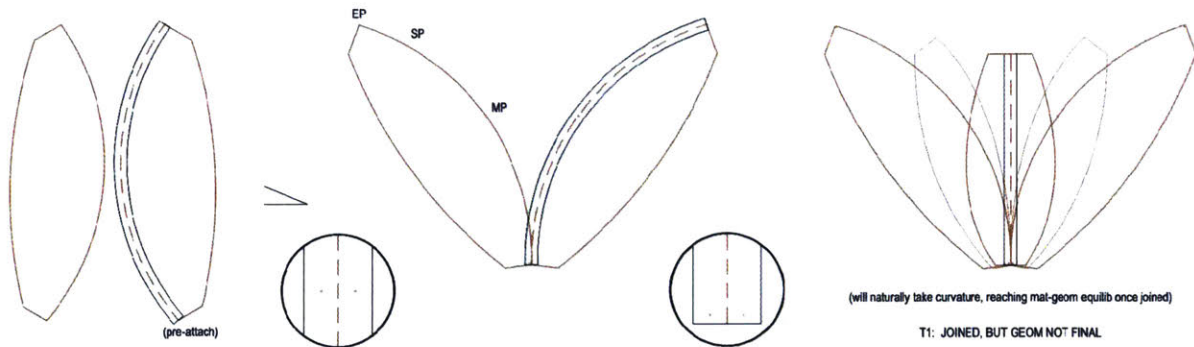
*GEN.3\_Detail.* The innovation of the semi-unitized, self-assembly *GEN.3* component method is its principled, "semi-unitized" strategy, which initially developed from observation of the mechanical behavior in the scale model, and again later in the full scale specimen.

The first principle is identify and stiffen against predictable behavior, as is illustrated for the coupled bending-active strips below. By anticipating this behavior, such assemblies may be stiffened with simple, proportionally-efficient, site-applied attachments without a sub-frame, a neighboring third, or intermediate layer as is the case in the earlier *Hybgrid*, the *A Change of State* installation, and the recent Schleicher case studies summarized in *Section 2.3*.



**Fig. 8.3a Construction – GEN.3\_Diagram: Coupled strips, Stiffened.**

The second principle is locate connections at the sixth-points so the geometry of the assemblies can be manipulated accurately, as pre-tested experimentally as a group and then by the Horn-fort installation.



**Fig. 8.3b Construction – GEN.3\_Drawings.**

The third principle is stagger strips in section so there are no continuous joints or any other the natural hinge lines. With the physical models, blocking the axes-of-rotation when combined with the elastic bending and twisting had a self-stiffening effect and resulted in rigid continuous construction.

Sequence – Core

S1: Pallets of pre-cut strips with pre-attached seaming tape and pre-assembled attachments arrive on site.

S2: Match-up the engraved labels to align pre-drilled holes for temporary zip-ties, then complete the iron-up hinge and apply upper hinge wedges and lower flange pedestals at the sixth points.

S3: Use the friction-fit discs to connect the upper and lower flanges, and then apply fasteners setting the mid-post last (and resulting in personalizable freeform strip construction versus ever more continuous studs in the cavity)

*GEN.3\_Coupled.* The studies below were follow-up using a physics engine to simulate the bending behavior of the shell. Boundary conditions restrict the shared edge of the symmetric pieces to have a rigid geometric compatibility (i.e., the shared edges are forced to stay together). A small force is applied against one of the free corners. The bending stiffness in conjunction with these boundary conditions creates the resulting shape.

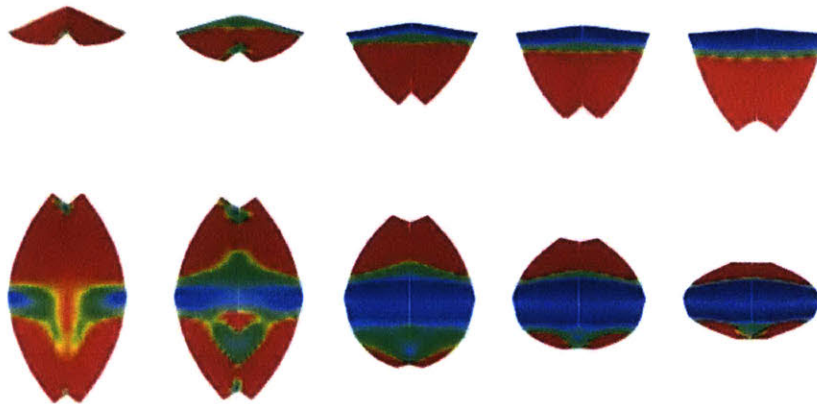


Fig. 8.3c Geometry – GEN.3\_Grasshopper: Coupled Flexural Geometry. (Tool)

*Grasshopper definition: StresStages.*

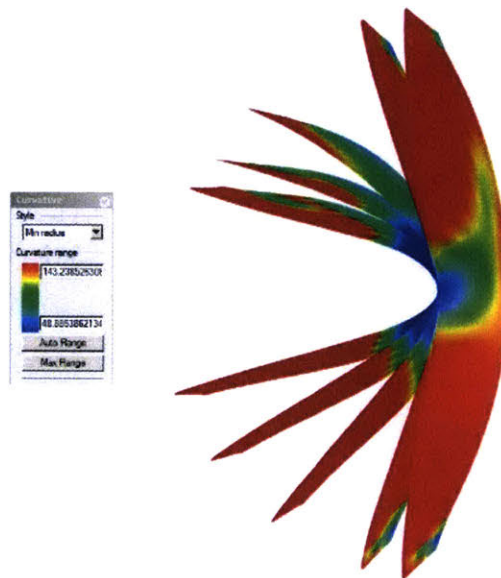


Fig. 8.3d Geometry – GEN.3\_Grasshopper: Coupled Flexural Geometry, Detail. (Tool)

*Grasshopper definition, detail: Red: r143; Blue: r48)*

Further development of the geometric *GEN.3* coupled-strip Grasshopper definition towards a multi-material version is intended, which would have many possible uses in the preliminary phases of architectural and structural design. Noted, is Keyan Rahimzadeh collaborated on this interactive tool, and it will be posted at the same link (*Figure 8.4e*) where the elastica dimensional analysis tool is once to a point where it estimates the residual stress capacity. Below, having no hydraulic presses in the lab with sufficient back-span, the larger *GEN.3* specimen had to be tested using "shop inventory." The three stages were sandbags, then barrels of water, and finally milk crates of rusty chain.



**Fig. 8.3e Performance – GEN.3\_Semi-Unitized: Load Test.**

*Assembly- and Geometrically-improved; Structurally- and Thermally-optimized.*

## 8.4 Demonstrations – GEN.4

(Combined Method)



**Fig. 8.4 Construction – GEN.4\_Study Model: Strips (a.) Elevation; (b.) Oblique.**

*Low-slope study for site-assembled, permanent, structural "Freeform-work."*

*The study model tested using continuous, notched, elastically bent webs with local, friction-fit, lateral "feet."*

**Table 8.1 Construction – GEN.4\_Method**

(Overview)

Sequence – Full

S0: Web order.	(Off-site)	S5: Transport to site.	( - )
S1: Pre-modeling & Unrolling strips.	(Off-site)	S6: Bend-up & Zip-up strips.	(On-site)
S2: Pre-cut strips.	(Off-site)	S7: Iron-up seams.	(On-site)
S3: Pre-assemble pedestals.	(Off-site)	S8: Foam-up/Fill-up.	(On-site)
S4: Pre-attach seam tape.	(Off-site)	S9: Apply furring/cladding.	(On-site)

**Notes:** (a.) See also GEN.3\_Method.

**Fig. 8.4c Construction – GEN.4\_Study Model: Detail. (1:24)**

*Staggered, multi-layer, developable strip construction.*

To automate and simplify distribution of reusable parts of the detailed elastica analysis workflow documented in *Appendix – E*, the following open-source code (*Figure 8.4d*) and terminal (*Figure 8.4e*) were created. The initial application of the code was the calculation of accurate elastica minimum radii from detailed head displacement data (versus arc approximation) for the strip specimens buckled on a numerically-controlled hydraulic press. These, along with a readme file containing step-by-step instructions, are available for download at the address below.

```

83 % In most texts, k is called 'the parameter', and
84 % k is called 'the elliptic modulus'
85
86 samples_divided_by_two = 5000; % Any positive whole number, even or odd
87
88 delta = max_t/samples_divided_by_two; % % % % % % % % DELTA
89 % The whole domain divided by an even number
90 % guarantees an odd number of elements in the discretized domain
91 % which means that -max_t/delta:delta:t will include t = 0
92 % If samples equals k, then t=0 at index = 5/2-1
93 index_of_t_equals_zero = samples_divided_by_two - 1;
94
95 min_t = -max_t;
96 ts = min_t:delta:max_t;
97
98 [sn, cn, dn, snr] = ellipj(ts, k^2);
99
100 y = c*cn; % % % % % % % % Y
101
102 Dn = dn.^2;
103
104 Dn_quad = cumtrapz(ts, Dn);
105 cum_t = ts - min_t;
106 X_at_min_t = -sn(pi/2);
107 x = (.5*c/k) .* (2*Dn_quad - cum_t) - X_at_min_t;
108
109 theta = 2*asin(k*sn); % % % % % % % % THETA
110 % Convert to degrees
111 theta_degrees = theta*180/pi;
112
113 curvature = (4*k^2/cn)*cn; % % % % % % % % CURVATURE
114 % actually negative
115 % in literature, but that's weird.
116
117 radii = 1 ./ curvature; % % % % % % % % RADIUS
118 min_radii = 0/(4*k^2);
119
120
121
122
123
124
    
```

**Fig. 8.4d Geometry – GEN.4\_Matlab-Octave: Code. (Tool)**

Version: a1.0

```

GNU Octave, version 4.0.2
Copyright (C) 2014 John W. Eaton and others.
This is free software; see the source code for copying conditions.
There is ABSOLUTELY NO WARRANTY; not even for MERCHANTABILITY or
FITNESS FOR A PARTICULAR PURPOSE. For details, type 'warranty'.

Octave was configured for 'x86_64-apple-darwin14.5.0'.

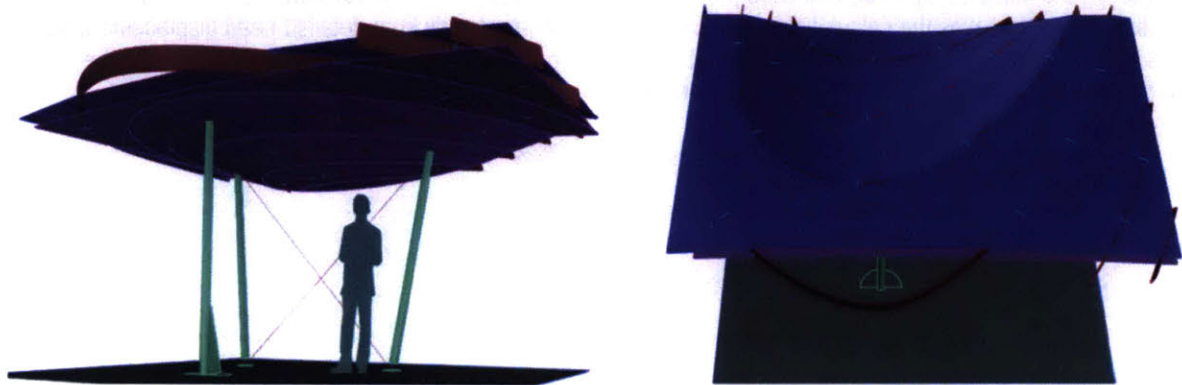
Additional information about Octave is available at http://www.octave.org.
Please contribute if you find this software useful.
For more information, visit http://www.octave.org/get-involved.html
For information about changes from previous versions, type 'news'.

>>
>> global id
>> global tests
>> elastica_func(60, 42, 30, 36, 6, '2k', 'plywood')
tests =
  scalar structure containing the fields:
  arclength = 42
  load = 60
  width = 30
  height = 0.34000
  width = 6
  I = 0.023328
  snr = 18
  material = plywood
  alpha = 1.0234
  alpha_degrees = 61.218
  elliptic_modulus = 0.52412
  rmax = 12.934
  min_radii = 11.789
  max moment = 177.21
  max bending stress = 597.0
  max shear stress = 11.790
  max compressive stress = 27.778
  max total stress = 6028.8
  min total stress = 5959.2
  experimental_MOR = 3.9276e+05
    
```

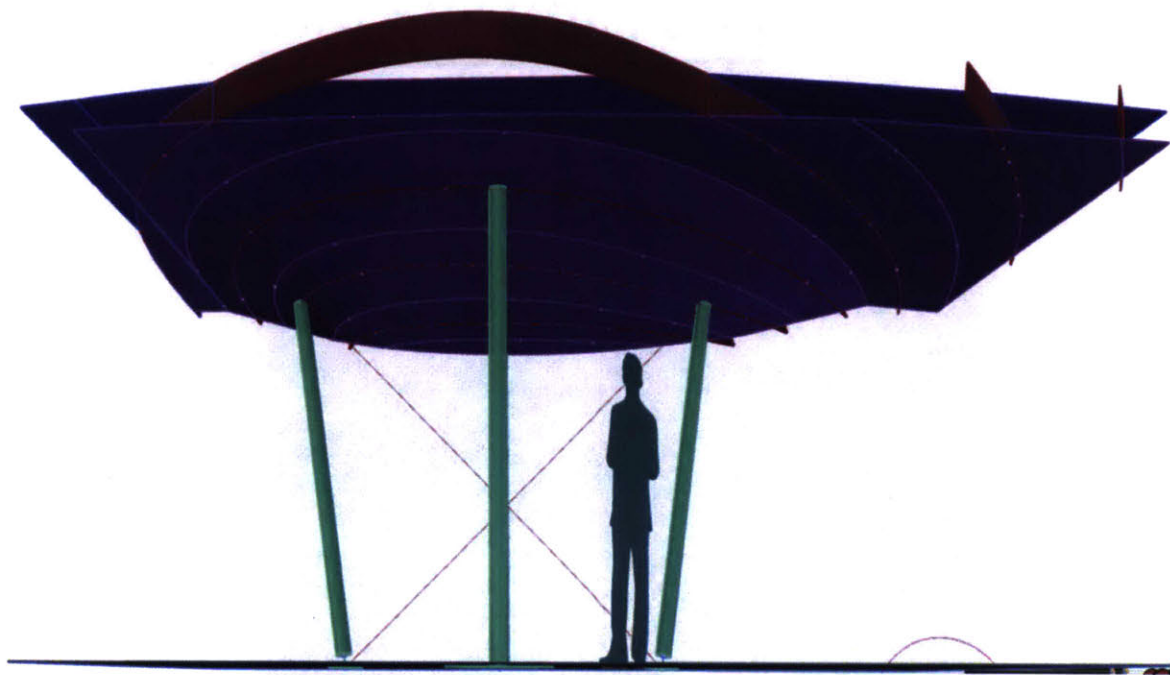
**Fig. 8.4e Geometry – GEN.4\_Matlab-Octave: Terminal I/O. (Tool)**

Downloads: <http://branchoff.net/tools>

At the time of publication, the code is provided for information purposes only and is intended only for preliminary analysis or design purposes. The alpha code has not been tested across all scales, thus it should not be used for production geometric analysis, structural design, or actual construction without redundant independent validation.



**Fig. 8.4f Performance – GEN.4\_Combined Study: Hollo-Helio Canopy (a.) Three-quarter; (b.) Aerial oblique.**  
*Hollow (no studs or foam in the cavity) and Heliotropic (passive functional formal articulation) PV Canopy.*



**Fig. 8.4g Performance – GEN.4\_Combined Study: Hollo-Helio Canopy, Detail.**  
*Site-assembled, permanent structural formwork/foamwork.*

(Fin)

## REFERENCES

### References

- Adorno & Horkheimer. 1998. *Dialectic of Enlightenment: The Culture Industry as Mass Deception*. London & New York: Continuum.
- Aeck, Richard. 2007. *Turnstijl Houses & Cannoli Framing*. 1st ed. Saarbrücken, GER: VDM Verlag Dr. Müller.
- AF&PA. 2005. "National Design Specification (NDS) for Wood Construction Commentary." Washington, DC: AF&PA American Wood Council.
- AIA. 2008. *Architectural Graphic Standards: Student Edition*. Edited by Ramsey. Hoboken, NJ: John Wiley & Sons.
- Allen, Edward, and Joseph Iano. 2014. *Fundamentals of Building Construction: Materials and Methods*. 6th ed. Hoboken, NJ: John Wiley & Sons.
- APA. 2014. "Advanced Framing Construction Guide." doi:M400A.
- Armstrong, Jim. 2012. "Lecture: The Innovation of Light Frame Construction America." Morgantown, WV: WVU.
- AWC. 2001. "Details for Conventional Wood Frame Construction." Washington, DC.
- Bayer, Eben. 2014. "Ecovative – MycoBoard." <http://www.ecovativedesign.com/myco-board>.
- Bertaud, Alain. 2004. "Tehran Spatial Structure: Constraints and Opportunities for Future Development." IRAN - NLHO, NHC, MHUD.
- Bertaud & Malpezzi. 2003. "The Spatial Distribution of Population in 48 World Cities: Implications for Economies in Transition." *Report*. doi:10.1024/0301-1526.32.1.54.
- Block, Philippe. 2005. "Equilibrium Systems." *Architectural Engineering*. MIT.
- Bonnier Corp. 1943. "Flying Plywood." *Popular Science*. doi:ISSN 0161-7370.
- Boyd & Weller et al. 2015. "Branch Technology." <http://branch-technology.com>.
- BSC (Lstiburek). 2010. "Insight Advanced Framing Undergoing Some Pretty Interesting Changes and the." Westford, MA: Building Science Corp. doi:BSI-030.
- Castle, Helen, ed. 2012. *Architectural Design: Material Computation*. London: John Wiley & Sons.
- Ching, Francis D. K., and Cassandra Adams. 2008. *Building Construction Illustrated*. 4th ed. New York: John Wiley & Sons.
- Collins, P. 1965. "Changing Ideals in Modern Architecture, 1750-1950." London: McGill Queen's Col.
- de Botton, Alain. 2006. *A Perfect Home*. UK: Channel 4 Television Corporation, Seneca Productions.
- Deleuze & Guattari. 1987. *A Thousand Plateaus*. Edited by Brian Massumi. 2nd ed. Minneapolis, MN: University of Minnesota Press.
- Diserens, Corinne. 2003. *Gordon Matta-Clark*. 1st ed. New York: Phaidon.
- DOE. 2000. "Advanced Wall Framing." *Building*. doi:26449.
- . 2012. "Buildings Energy Data Book." *Energy Efficiency & Renewable Energy Department*. Richland, WA: U.S. Department of Energy.
- Douglas, M. et al. 2011. "Are Cars the New Tobacco." *Journal of Public Health*. Oxford: Oxford Univ. Press.

- EIA. 2012. "Residential Energy Consumption Survey [RECS] (H&AC No Longer Majority).pdf."
- Fischer & Kunz. 2004. "The Scope and Role of Information Technology in Construction." *CIFE Technical Report*, no. #156: 1–17. doi:10.2208/jscej.2004.763\_1.
- Flöry, Simon, Yukie Nagai, Florin Isvoranu, Helmut Pottmann, and Wallner Johannes. 2012. "Ruled Free Forms." In *Advances in Architectural Geometry*, 56–66. Paris.
- FPL. 1999. "Wood Handbook: Wood as an Engineering Material." Madison, WI.
- Gauthier, J. 2002. "Measuring America: The Decennial Censuses, From 1790 to 2000." doi:ED468215.
- Gideon, Sigfried. 1952. "The Balloon Frame and Industrialization." In *Roots of Contemporary Architecture*, edited by Lewis Mumford, 201–205. New York: Reinhold.
- Gordon, J.E. 2003. *Structures: Or Why Things Don't Fall Down*. 2nd ed. Da Capo Press.
- Goulthorpe, Mark. 2009. "dECOi Architects." [http://web.mit.edu/mg\\_decoi/www/bankside/index02.html](http://web.mit.edu/mg_decoi/www/bankside/index02.html).
- Hadid, Zaha. 2007. "Nordpark Railway Stations." *Self*. <http://www.zaha-hadid.com/architecture/nordpark-railway-stations/>.
- Hauer, Erwin. 2004. *Continua: Architectural Screens and Walls*. New York: Princeton Architectural Press.
- Heldmann, Carl. 2006. *Be Your Own House Contractor: Save 25% without Lifting a Hammer*. 5th ed. North Adams, MA: Storey Publishing.
- Hemberg, O'Reilly, Menges, Jonas, da Costa Goncalves, Fuchs. 2008. "Genr8: Architect's Experience Using an Emergent Design Tool. In Art of Artificial Evolution." In *The Art of Artificial Evolution*, p.167–188. New York: Springer.
- Holland, B. 2010. "Computational Organicism: Examining Evolutionary Design Strategies in Architecture." *Nexus Netw J* 12 (3): p.485-495. doi:10.1007/s00004-010-0040-6.
- Huber, Benedikt, and Jean-Claude Steinegger, eds. 1971. *Jean Prouvé: Prefabrication: Structures and Elements*. New York: Praeger Publishers.
- Jarzombek, Mark. 2013. *Architecture of First Societies*. Hoboken, NJ: John Wiley & Sons.
- Jeska, Simone, and Khaled Saleh Pascha. 2015. *Emergent Timber Technologies: Materials, Structures, Engineering, Projects*. Edited by Rainer Hascher. Basel: Birkhäuser.
- Jones, Jack P. 1986. *Handbook of Construction Contracting Volume 2: Estimating, Bidding, Scheduling*. Craftsman Book Company.
- Khanzode & Fischer et al. 2006. "A Guide to Applying the Principles of Virtual Design & Construction (VDC) to the Lean Project Delivery Process." *CIFE Working Paper*, no. #093: 1–47.
- Khoshnevis, Behrokh. 2014. "Contour Crafting." *USC & USC Viterbi*. <http://www.contourcrafting.org/>.
- Kilian, Axel. 2006. "Design Exploration through Bidirectional Modeling of Constraints." MIT.
- Klein, John. 2015. "Additive Manufacturing: Of Optically Transparent Glass." MIT.
- Knippers, Jan, Jan Cremers, Markus Gabler, and Julian Lienhard. 2011. "Construction Manual for Polymers + Membranes," 296.
- Knuffel, Werner E. 1973. *The Construction of the Bantu Grass Hut*. Graz: Akademische Druck- und Verlagsanstalt.
- Kolarevic, Branko. 2003. *Architecture in the Digital Age*. New York: Spon Press. doi:10.1007/s00004-004-0025-4.
- Kunz & Fischer. 2012. "Virtual Design and Construction: Themes, Case Studies and Implementation Suggestions."



CIFE Working Paper, no. #097: p.26 (suggestions).

Laarman & Geurtjens. 2014. "MX3D: News." <http://mx3d.com/news/>.

Lambert, Yvon. 2011. *Vincent Ganivet*. Author.

Lefèvre, Benoit. 2009. "Urban Transport Energy Consumption: Determinants and Strategies for its Reduction." *S.A.P.I.E.N.S*, no. 2.3 (December). Institut Veolia Environnement.

Lienhard, Julian. 2014. "Bending-Active Structures: Form-Finding Strategies Using Elastic Deformation in Static and Kinetic Systems and the Structural Potentials Therein." Universität Stuttgart Forschungsberichte.

Lienhard, Julian, Holger Alpermann, Christoph Gengnagel, and Jan Knippers. 2013. "Active Bending, A Review on Structures Where Bending Is Used as a Self-Formation Process." *International Journal of Space Structures* 28 (3): 187–96. doi:10.1260/0266-3511.28.3-4.187.

Lienhard, Julian, and Jan Knippers. 2013. "Considerations on the Scaling of Bending-Active Structures." Edited by Christoph Gengnagel. *International Journal of Space Structures* 28 (3–4): 137–48. doi:10.1260/0266-3511.28.3-4.137.

Matta-Clarke, Gordon. 1975. "Letter, to Jerald Ordoover (Dec. 4)." Paris: EGMC Articles & Documents 1942–78.

Moe, Kiel. 2014. *Insulating Modernism: Isolated and Non-Isolated Thermodynamics in Architecture*. Basel: Birkhäuser.

Morse & Evenson. 2016. "Welcome to the Glass Age." *International Journal of Applied Glass Science*, October. doi:10.1111/ijag.12242.

Næss, Ragnar; Næss, Bjørge. 2009. "A Prestigious Project to Supply Timber?" *Norwegian Forestry Association (Foreningen Norske Lauvtrebruk)*.  
<https://translate.google.com/translate?hl=en&sl=no&tl=en&u=http%253A%252F%252Fwww.lauvtrebruk.no%252Fnews%252Fstory%252F91>.

NAHB, Dietz. 2016. "Eye On Housing: Little Change for New Single-Family Home Size." *Eye On Housing*.  
<http://eyeonhousing.org/2016/02/little-change-for-new-single-family-home-size/>.

NAHB 2015, Zhao. 2015. "System-Built Single-Family Homes in 2014."

Negroponce, Nicholas. 1998. "Beyond Digital." *Wired Magazine*, June.

Neufert. 2000. *Neufert: Architects' Data*. 3rd ed. Oxford: Blackwell Publishing.

Newman & Kenworthy. 1989. "Gasoline Consumption and Cities." *Journal of the American Planning Association* 55 (1): 24–37. doi:10.1080/01944368908975398.

NGS (Zwingle). 2002. "Megacities." *National Geographic Magazine*.

NOAA-1a. 2016. "Global CO2 Trend, Full Record (1958–2016)." Mauna Loa Observatory: U.S. Department of Commerce.

NOAA-1b. 2016. "Global CO2 Trend, Recent (2012–2016)." Mauna Loa Observatory: U.S. Department of Commerce.

NOAA-2. 2016. "Global Land and Ocean Temperature Anomalies." Mauna Loa Observatory: U.S. Department of Commerce.

Ochsendorf, John. 2010. *Guastavino Vaulting: The Art of Structural Tile*. New York: Princeton Architectural Press.

Patkau Architects. 2011. "Winnipeg Skating Shelters." *Self*. [www.patkau.ca](http://www.patkau.ca).

Pottmann, Helmut, Andreas Asperl, Michael Hofer, and Axel Kilian. 2007. *Architectural Geometry*. 1st ed. Exton, PA:

Bentley Institute Press.

- Pottmann, Helmut, Michael Eigensatz, Amir Vaxman, and Johannes Wallner. 2015. "Architectural Geometry." *Computers and Graphics (Pergamon)* 47 (November 2014): 145–64. doi:10.1016/j.cag.2014.11.002.
- Reiner, Laurence E. 1981. *Methods and Materials of Residential Construction*. Eaglewood Cliffs, NJ: Prentice Hall.
- Rice, Peter. 1996. *An Engineer Imagines*. 2nd ed. London: Ellipsis London Limited.
- Rudofsky, Bernard. 1965. *Architecture Without Architects: A Short Introduction to Non-Pedigreed Architecture*. New York: The Museum of Modern Art.
- Schiffner, Alexander, Nicolas Leduc, Philippe Bompas, Niccolo Baldassini, and Michael Eigensatz. 2012. "Architectural Geometry from Research to Practice -- The Eiffel Tower Pavilions." *Advances in Architectural Geometry 2012*, p.213-228 (eiffel).
- Schittich, Christian, and Steffi Lenzen, eds. 2014. *Holz, Wood: Best of Detail*. München: Institut für internationale Architektur-Dokumentation.
- Schleicher, Simon, Julian Lienhard, Simon Poppinga, Thomas Speck, and Jan Knippers. 2015. "A Methodology for Transferring Principles of Plant Movements to Elastic Systems in Architecture." *CAD Computer Aided Design* 60. Elsevier Ltd: 105–17. doi:10.1016/j.cad.2014.01.005.
- Schools, International Correspondence. 1905. *The Building Trades Pocketbook: A Handy Manual of Reference on Building Construction*. Edited by The Coillery Engineer Co. 2nd ed. Scranton, PA: Intl. Textbook Co.
- Sprague, Paul. 1983. "Chicago Balloon Frame: The Evolution During the 19th Century of George W. Snow's System for Erecting Light Frame Buildings from Dimension Lumber and Machine-Made Nails." In *The Technology of Historic American Buildings*, edited by H.W. Jandl. Washington, DC.
- Steadman, P. 2008. *The Evolution of Designs: Biological Analogy in Arch and the Applied Arts*. 2nd ed. Routledge.
- Stein, Benjamin, John S. Reynolds, Walter T. Grondzik, and Alison G. Kwok. 2006. *Mechanical and Electrical Equipment for Buildings*. 10th ed. Hoboken, NJ: John Wiley & Sons.
- Takahashi, Kenryo. 2015. "Spanned Flexure - Convertible Roof Systems with Elastic Kinetic Plates Actuated by Tension Cables."
- TFG. 2005. *Timber Frame Joinery & Design, Volume 2*. Beckett, MA: Timber Framers Guild.
- Thallon, Rob. 2008. *Graphic Guide to Frame Construction*. 3rd ed. Newtown, CT: The Taunton Press.
- Thompson, David. 2013. "Suburban Sprawl: Exposing Hidden Costs, Identifying Innovations," no. October: 44.
- Thorton, Rosemary. 2002. *The Houses That Sears Built*. Alton, IL: Gentle Beam Publications.
- UN-HABITAT. 2016. "World Cities Report: Urbanization and Development - Emerging Futures." Nairobi, KEN: United Nations Human Settlements Programme.
- UN-WUP. 2014. "World Urbanization Prospects: The 2014 Revision (Highlights)." New York: Dept. of Econ. & Social Affairs, Population Division.
- UNEP. 2013. "City-Level Decoupling: Urban Resource Flows." Nairobi, KEN.
- UNICEF. 2014. "Generation 2030: Africa."
- Williamson, Thad. 2010. *Sprawl, Justice, and Citizenship: The Civic Costs of the American Way of Life*. 1st ed. New York: Oxford Univ. Press.
- Wright, Frank Lloyd. 1954. *The Natural House*. 1st ed. New York: Bramhall House for Horizon Press. doi:54-12278.
- Youngquist, W. 1977. *Wood in American Life 1776-2076*. 1st ed. Madison, WI: Forest Products Research.

ZEMIC. 2008. "Digital Weighing Indicator XK3190-A12 (E)." Downey, CA: Zemic USA Inc.

Zwinger, K. 2012. *Wood and Wood Joints: Building Traditions in Europe, Japan and China*. Basel: Birkhäuser.

## References – Photo & Image

- Fig. 1.1b** Borson, Bill. "Building with Structural Insulated Panels ... or SIPs." Digital image, Panel Placement. SIPA.org. Structural Insulated Panel Association, 31 Mar. 2014. Web: 18 July 2016. <[http://www.sips.org/blog/sips-from-ajavascript:void\(0\);n-architect-s-perspective](http://www.sips.org/blog/sips-from-ajavascript:void(0);n-architect-s-perspective)>
- Fig. 1.2** Ochsendorf, John. *Guastavino Vaulting: The Art of Structural Tile*. New York: Princeton Architectural Press, 2010, p.160, fig.5.20 (custom); p127, fig.4.25 (stage 2).
- Fig. 1.3a** Courtesy of: Hasted Hunt Kraeutler, New York / Nicholas Metivier Gallery, Toronto.
- Fig. 1.3b** Sagmeister, Stefan 2008. Cover art of Byrne, David & Eno, Brian 2008. *Everything that Happens will Happen Today*. Todo Mundo. New York
- Fig. 1.4a** Meneghini, Alexandre. 2004. "Favela Morumbi: Sao Paulo turns 450: Photo of January 20, 2004." AP Photo.
- Fig. 1.4b** Creative Loafing. "Let's say the T-SPLOST fails... then what?" 07 Jun. 2012. Web: 18 July 2015. <<http://clatl.com/freshloaf/archives/2012/07/15/first-slice-71512-lets-say-the-t-splost-fails>>
- Fig. 2.1a** International Correspondence Schools. 1905. *The Building Trades Pocketbook: A Handy Manual of Reference on Building Construction*. Scranton: International Textbook Co. (edition 2, p.222, fig.6)
- Fig. 2.1b** Graham, Frank D. 1923. *Audel's Carpenter's and Builder's Guide*. New York: Theo Audel & Co. (drawing of balloon frame construction. 72 Fifth Ave, scanned by John Delano)
- Fig. 2.1b** DOE 2016 (after BSC 2010, BSI-030 Mar. 10, 2010). <<http://energy.gov/energysaver/advanced-house-framing>>
- Fig. 2.1b** ARO 2011. R House Studies. Photo: Richard Barnes. <<http://www.archdaily.com/office/architecture-research-office>>
- Fig. 2.2b** Pottmann, Helmut, Andreas Asperl, Michael Hofer, and Axel Kilian 2007. *Architectural Geometry*. 1st ed. Exton, PA: Bentley Institute Press, p.315.
- Fig. 4.3** <<http://www.boatsandrice.com/tradBoat.html#TradConstruction>>
- Fig. 3.1** Endow, Masaaki 2001. 'Natural Ellipse' Shibuya-ku, Tokyo 2000-2001 <<http://edh-web.com>>
- Fig. 4.2** ALA Architects 2016. "In Therapy – Nordic Countries Face to Face," Venice Archi. Biennale 2016. <<http://architecture.mapolismagazin.com/sites/default/files; http://ala.fi/>>
- Fig. 4.1** Moore, Thomas E. 1957, Photo of Ruth Moore in Washington Square Park, San Francisco. Courtesy of Charles and Hugh Moore

## INDEX – FIGURES

### Figures – by Chapter

- Fig. 1.1 Conventional Construction – Methodologies: (a.) Light frame; (b.) Panelized.
- Fig. 1.2 Guastavino Construction – Mature method: (a.) First steps; (b.) Vertical section.
- Fig. 1.3 Detached – Motivation: (a.) Sameness epidemic; (b.) "Same as it ever was."
- Fig. 1.4 Detached – Motivation: (a.) Rapid-urbanization; (b.) Car-centric culture.
- Fig. 1.5 Detached – Motivation: Buildings Share of Primary Energy Consumption. (U.S.)
- Fig. 1.6 Detached – Motivation: Transport Effectiveness in Polycentric Cities. (Global)
- Fig. 1.7 Conventional Construction – Pre-process is constraining:  
(a.) Portable sawmill; (b.) Industrial laminator.
- Fig. 1.8 Post-digital Construction – Pre-process is de-constraining:  
(a.) Self-loading, flatbed, 5-axis mill; (b.) Water-resistant, 6-axis robot.
- Fig. 1.9 Concept Sketches – Point of departure.
- Fig. 1.10 Concept Sketches – Construction: (a.) SIP system; (b.) STRIP system.
- Fig. 1.11 Study Model – Cylinder to Conoid: (a.) Section; (b.) Elevation.
- Fig. 1.12 Study Model – Strips: Renewable, High-performance, Stressed-skins.
- Fig. 2.1 Light Frame – Then: Balloon framing (a.) 1899; (b.) 1923.
- Fig. 2.2 Light Frame – Now: Platform framing (a.) 1981; (b.) 2008; Advanced framing (c.) 2014.
- Fig. 2.3 Light Frame – Now: Study model variation.
- Fig. 2.4 Panelized – Then: Structural Insulated Panels. (SIPs)
- Fig. 2.5 Panelized – Now: Self-palletized and Transport-ready. (SIPs)
- Fig. 2.6 Panelized – Origins: U.S. Dollars per Barrel.
- Fig. 2.7 Prefabricated – Then: (a.) Radial-futurism; (b.) Mechanical-idyllic; (c.) Structural-expression.
- Fig. 2.8 Prefabricated – Now:  
(a.) Packable-materialist; (b.) Retro-modernist; (c.) Marketable-modular.
- Fig. 2.9 Prefabricated – Future: (a.) California Roll; (b.) Boat, Loire River; (c.) AMIE 1.0.
- Fig. 2.10 Architectural – Surfaces: Ruled & Developable.
- Fig. 2.11 Flexural: The elastica.
- Fig. 2.12 Flexural: The elastica.
- Fig. 2.13 Flexural – Context: Elastica and Pendulum.
- Fig. 2.14 Energy use – By Home Type. (U.S.)
- Fig. 2.15 Type – Residential: Detached. (Typ.)
- Fig. 2.16 Material – Renewable: (a.) Bamboo grove; (b.) Laminated bamboo, Soy-based resin.
- Fig. 2.17 Energy – Residential End Use. (U.S.)
- Fig. 2.18 Energy – Per Capita Use. (U.S.)
- Fig. 2.19 Domes: Functional Articulation.

- Fig. 2.20 Segmented Shells: Self-strutted Geodesic Plydome.
- Fig. 2.21 Segmented Shells: Duck-Work.
- Fig. 2.22 Cast-in-Place Shells: Capilla de Palmira Cuernavaca.
- Fig. 2.23 Cast-in-Place Forms: Stata Center.
- Fig. 2.24 Virtual Model: N51 Horn-fort Installation.
- Fig. 2.25 Structural – Composites – Novartis: This entrance pavilion was built with GFRP panels.
- Fig. 2.26 Structural – Takahashi: Compares convertible roofs with kinetic bending-active alternatives.
- Fig. 2.27 Structural – Takahashi: Comparison of principal forces.
- Fig. 2.28 Structural – Active Bending: Illustration of kinetic applications for bending-active plates.
- Fig. 2.29 Structural – Functional Articulation: Introduction of cables allows the bending-active plates to: (a.) Cantilever as a shading device; (b.) Roll up; (c.) Splay for light transmission
- Fig. 2.30 Structural – Elastica: Deflection.
- Fig. 2.31 Structural – Lienhard: The authors describe this figure as: (a.) and (b.).
- Fig. 2.32 Structural – Lienhard: Study of various models of the Marrakech Umbrella (2011)
- Fig. 2.33 Structural – ITKE 2011: (a.) and (b.).
- Fig. 2.34 Structural – Marrakech: Load deflection curve of the Flectofin® Lamella.
- Fig. 2.35 Structural – Grid-shell: (a.) Savill Garden and (b.) Three pillars of sustainable development.
- Fig. 2.36 Financial – Cost-aware: Cylindrical & Conoidal.
- Fig. 3.1 Virtual Design – Multi-objective: Harvard Art Museums.
- Fig. 3.2 Pre-rationalization – Macro: Concepts.
- Fig. 3.3 Pre-rationalization – Micro: Methods.
- Fig. 3.4 Pre-rationalization – Micro: Principles.
- Fig. 3.5 Pre-rationalization – Micro: Constraints.
- Fig. 3.6 Pre-rationalization – Nano: Constraints.
- Fig. 3.7 Evolution – Structural.
- Fig. 3.8 Evolution – Functional.
- Fig. 3.9 Evolution – Exploratory.
- Fig. 3.10 Evolution – Developmental.
- Fig. 3.11 Evolution – Generational.
- Fig. 3.12 Evolution – Capacities.
- Fig. 3.13 Evolution – Methodological.
- Fig. 3.14 Experimental – Loading: Strips.
- Fig. 3.15 Experimental – Loading: Beams.
- Fig. 4.1 Construction – Conventional: I-Joists.
- Fig. 4.2 Construction – Conventional: Trussed-joists.
- Fig. 4.3 Construction – Empirical: Haus Tambaran.
- Fig. 4.4 Construction – Empirical: Bantu Grass.

- Fig. 4.5 Construction – Steamed: Canoe.
- Fig. 4.6 Construction – Stave: Workboat.
- Fig. 4.7 Construction – Stave: Candela Formwork.
- Fig. 4.8 Construction – Sheet: Fuller-Moore Plydome.
- Fig. 4.9 Strips – Tensioned: Plywood Delaminations.
- Fig. 4.10 Strips – Stress-stiffened: A Change of State.
- Fig. 4.11 Strips – Study Model: A Change of State.
- Fig. 4.12 Sheets – Shelter: Thin-shell Plywood.
- Fig. 4.13 Sheets – Centering: Post-tensioned Masonry.
- Fig. 4.14 Post-rationalized, Post-digital – Natural Ellipse: (a.) Exterior oblique; (b.) Sub-frame detail.
- Fig. 4.15 Post-rationalized, Post-digital – Kilden Theatre: (a.) Exterior oblique; (b.) Sub-frame detail.
- Fig. 4.16 Mockups – GEN.0\_Strap Anchor [PRE].
- Fig. 4.17 Mockups – GEN.3\_Pedestal [R0].
- Fig. 4.18 Mockups – GEN.3\_Linkage [R0]: (a.) Open; (b.) Closed.
- Fig. 4.19 Mockups – GEN.3\_Wedges [R0].
- Fig. 4.20 Mockups – GEN.3\_Hinges, Method.
- Fig. 4.21 Mockups – GEN.4\_Pedestal [R2].
- Fig. 4.22 Pre-test – Elastica: (a.) Increasing length; (b.) Static length.
- Fig. 4.23 Pre-test – Comparisons: (a.) Type; (b.) Type, Detail.
- Fig. 4.24 Pre-test – Elastica: Photos.
- Fig. 4.25 Pre-test – Elastica:  
(a.) Distance Along Curve vs. Radius; vs. Angle; vs. Rise; (b.) Span,  $L$  vs. Min. Radius,  $r_{min}$ .
- Fig. 4.26 Coupled – Study model: Arch.
- Fig. 4.27 Coupled – Components: by Type.
- Fig. 4.28 Coupled – MIT Horn-fort: (a.) Dimensional; (b.) Structural.
- Fig. 4.29 Test – MIT Horn-fort – Dimensional: Pre-digital..
- Fig. 4.30 Test – MIT Horn-fort: Shrink-wrap
- Fig. 4.31 Pre-test – Plywood.
- Fig. 4.32 Pre-test – Plywood: Arc (approx.) vs. Elastica (the.) for 0.48" Strips.
- Fig. 4.33 Pre-test – Plywood: Arc (approx.) vs. Elastica (the.) for 0.36" Strips.
- Fig. 4.34 Strips: Coupled – Study Model.
- Fig. 4.35 Strips: Test – Baldwin press.
- Fig. 4.36 Strips: Test – Overview.
- Fig. 4.37 Strips – Strong- & Weak-axis: Span at Fracture (in.),  $L_{min}$ . vs. Minimum Radius (in.),  $r_{min}$ .
- Fig. 4.38 Strips – Strong-axis: Avg. Span at Fracture (in.),  $L_{avg}$ . vs. Avg. Minimum Radius (in.),  $r_{avg}$ .
- Fig. 4.39 Geometry – Study: Roof Forms.
- Fig. 4.40 Geometry – Study: Roof Forms, Detail.

- Fig. 4.41 Material – Studs are a Factor: (a.) Cavity at 70.5 °F; (b.) Braced Multi-stud Corner at 67.6 °F.
- Fig. 4.42 Simulations – GEN.3\_Thermal Performance: (a.) Stick; (b.) Strip.
- Fig. 4.43 Diagram – Single strip, Bending.
- Fig. 4.44 Strips – Pre-test: Weak-axis.
- Fig. 4.45 Strips – Strong-axis: Avg. Minimum Radius at Fracture,  $r_{avg}$ . vs. Avg. Bending Stress,  $\sigma_{avg}$ .
- Fig. 4.46 Strips – Strong- & Weak-axis: Avg. Min. Radius,  $r_{avg}$ . vs. Avg. Bending Stress,  $\sigma_{avg}$ .
- Fig. 4.47 Specimen – Hinge: (a.) Setup; (b.) Failure Mode.
- Fig. 4.48 Hinges – Pre-test: Overview.
- Fig. 4.49 Hinges – Pre-test: (a.) Jute-fiber/Burlap webbing; (b.) Seaming tape, GFRT.
- Fig. 4.50 Beams – GEN.0\_Box, Hybrid: Dimensional & Theoretical Review.
- Fig. 5.1 Specimen – GEN.0\_Box: Kerfed.
- Fig. 5.2 Sections – GEN.0\_Box: Dimensional & Theoretical Properties.
- Fig. 5.3 Simulations – GEN.0\_Box: Cable-truss.
- Fig. 5.4 Results – GEN.0\_Box: Kerfed.
- Fig. 5.5 Specimen – GEN.1\_Panel: Control.
- Fig. 5.6 Specimen – GEN.1\_Panel: Kerfed.
- Fig. 5.7 Sections – GEN.1\_Panel: Dimensional & Theoretical Properties.
- Fig. 5.8 Simulations – GEN.1\_Panel: Reinforced & Stiffened.
- Fig. 5.9 Comparisons – GEN.1\_Panel, Control; GEN.0\_Box, Kerfed; GEN.1\_Panel, Kerfed.
- Fig. 5.10 Results – GEN.1\_Panel: Control.
- Fig. 5.11 Results – GEN.1\_Panel: Kerfed.
- Fig. 5.12 Failure Modes: (a.) GEN.1\_Panel, Control; (b.) GEN.0\_Box, Kerfed; (c.) GEN.1\_Panel, Kerfed.
- Fig. 5.13 Specimen – GEN.2\_Unitized: Invert.
- Fig. 5.14 Specimen – GEN.2\_Unitized: Axial.
- Fig. 5.15 Sections – GEN.2\_Unitized: Dimensional & Theoretical Properties. (Webs)
- Fig. 5.16 Sections – GEN.2\_Unitized: Dimensional & Theoretical. (Assembly)
- Fig. 5.17 Simulations – GEN.2\_Unitized: Reinforced, Stiffened, & Strapped. (Low-slope)
- Fig. 5.18 Results – GEN.2\_Unitized: Invert.
- Fig. 5.19 Results – GEN.2\_Unitized: Axial.
- Fig. 5.20 Failure Modes – GEN.2\_Unitized: Details (a.) Invert; (b.) Axial.
- Fig. 5.21 Specimen – GEN.3\_Semi-unitized.
- Fig. 5.22 Simulations – GEN.3\_Semi-unitized: Arch (a.) Global flexural; (b.) Midspan detail; (c.) Rotated.
- Fig. 5.23 Simulations – GEN.3\_Axial: Scan & Solve.
- Fig. 5.23 Results – GEN.3\_Semi-unitized.
- Fig. 5.24 Failure Modes – GEN.3\_Semi-unitized: (a.) Pedestal; (b.) Lower Flange; (c.) Upper Flange.
- Fig. 5.25 Flanges – GEN.3\_Semi-unitized: Displacement (a.) Upper Flange; (b.) Lower Flange.



- Fig. 5.26 Results – GEN.#\_Comparative: Ultimate Load.
- Fig. 6.1 Method – GEN.1\_Panel: Refer to Section 8.1.
- Fig. 6.2 Method – GEN.2\_Unitized, Rapid-assembly: (a.) Fit-up; (b.) Yard-arch.
- Fig. 6.3 Method – GEN.3\_Semi-unitized, Site-assembly: (a.) Pre-test; (b.) Yard-arch.
- Fig. 6.4 Specimens: Overview.
- Fig. 6.5 Structural – Specimens: by Weight.
- Fig. 6.6 Structural – GEN.0, 1, 2, 3\_Findings: Estimated Span.
- Fig. 6.7 Structural – GEN.0, 1, 2, 3\_Findings: Predicted Load.
- Fig. 6.8 Simulations – GEN.3\_Arch: Laminated Bamboo vs. Plywood
- Fig. 6.9 Simulations – GEN.3\_Arch: (a.) Pinned vs. (b.) Moment-connected supports.
- Fig. 7.1 Contributions – Methodological: GEN.4\_Method (1.) Bend-up; (2.) Zip-up; (3.) Iron-up.
- Fig. 7.2 Contributions – Methodological: GEN.0, 1, 1, 2, 2 (Back); GEN.3 (Pre-test); GEN.3 (Test).
- Fig. 7.3 Contributions – Structural: Active bending.
- Fig. 8.0a Construction – GEN.0\_Box-beam, Kerfed [R2].
- Fig. 8.0b Geometry – GEN.0\_Box-beam, Preliminary [R2].
- Fig. 8.0c Geometry – GEN.0\_Box-beam, Development [R2].
- Fig. 8.0d Performance – GEN.0\_Box: Simulation, Typical vs. Spatial Beam.
- Fig. 8.0e Geometry – GEN.0\_Box-beam, Development [R2].
- Fig. 8.1a Construction – GEN.1\_Panel: Kerfed, Detail [R1].
- Fig. 8.1b Geometry – GEN.1\_Case Study.
- Fig. 8.1c Performance – GEN.1\_Material Take-off.
- Fig. 8.2a Construction – GEN.2\_Unitized: Rapid-assembly [R1].
- Fig. 8.2b Geometry – GEN.2\_Model: Elevation & Oblique.
- Fig. 8.2c Geometry – GEN.2\_Analysis: Unrolling & Twisting.
- Fig. 8.2d Performance – GEN.2\_Method: Unitized, Rapid-assembly.
- Fig. 8.3a Construction – GEN.3\_Diagram: Coupled strips, Stiffened.
- Fig. 8.3b Construction – GEN.3\_Drawings.
- Fig. 8.3c Geometry – GEN.3\_Tool: Geometry-to-Stress.
- Fig. 8.3d Geometry – GEN.3\_Tool: Geometry-to-Stress, Detail.
- Fig. 8.3e Performance – GEN.3\_Semi-Unitized: Load Test.
- Fig. 8.4 Construction – GEN.4\_Study Model: Strips (a.) Elevation; (b.) Oblique.
- Fig. 8.4c Construction – GEN.4\_Study Model: Detail. (1:24)
- Fig. 8.4d Geometry – GEN.4\_Matlab-Octave: Code. (Tool)
- Fig. 8.4e Geometry – GEN.4\_Matlab-Octave: Terminal I/O. (Tool)
- Fig. 8.4f Performance – GEN.4\_Combined Study: Hollo-Helio Canopy (a.) Three-quarter; (b.) Aerial Oblique.
- Fig. 8.4g Performance – GEN.4\_Combined Study: Hollo-Helio Canopy.

## INDEX – TABLES

### Tables – by Chapter

Table 2.1	Light Frame – Properties.	(of Typical)
Table 2.2	Light Frame – Observations.	(of Typical)
Table 2.3	Panelized – Properties.	(of Typical)
Table 2.4	Panelized – Observations.	(of Typical)
Table 2.5	Prefabricated – Properties.	(of Typical)
Table 2.6	Prefabricated – Observations.	(of Typical)
Table 2.8	Geometry – Observations.	(of Review)
Table 2.9	Detached – Properties.	(of Typical)
Table 2.10	Detached – Observations.	(of Typical)
Table 2.12	Material – by Method.	(1 bd. = 144 in. <sup>3</sup> )
Table 2.13	Operational – by Component.	(Spot-check)
Table 2.14	Common Effects: Scaling Structures.	(after Lienhard 2013)
Table 2.15	Structural – Collins, Regan & Cosgrove: Six objectives.	( - )
Table 2.16	Structural – Comparison: Long. & Associated boundaries.	( - )
Table 2.17	Structural – Observations: Active bending.	(Misc.)
Table 2.18	Financial – Comparisons.	(Various)
Table 3.1	Pre-rationalization – Micro: Principles.	( - )
Table 3.2	Pre-rationalization – Micro: Constraints.	( - )
Table 2.3	Light Frame – Comparisons.	(of Typical)
Table 4.1	Detached – Comparisons: Methods	(Then vs. Typical)
Table 4.2	Pre-test – Plywood: Arc (approx.) <u>vs.</u> Elastica (the.)	(Moisture: 8%; Units: in.)
Table 4.3	Strips: Coupled – Observations.	(to Test)
Table 4.4	Material – Comparisons: Methods.	(1 bd. = 144 in. <sup>3</sup> )
Table 4.5	Material – Comparisons: Specimens.	( - )
Table 4.6	Material – Comparisons: Waste.	( - )
Table 4.7	Structural – Comparisons: Methods.	(1 bd. = 144 in. <sup>3</sup> )
Table 4.8	Structural – Comparisons: Sheets & Strips.	(1 bd. = 144 in. <sup>3</sup> )
Table 4.9	Beams – GEN.0_Box: Hybrid [R1].	(BC & Lauan Ply.)
Table 5.1	Predictions – GEN.0_Box, Kerfed.	(Pre-test)
Table 5.2	Predictions – GEN.1_Panel, Control & Kerfed	(Rate: 0.1"/min.)
Table 5.3	Comparisons – GEN.0, 1_Panel, Control & Kerfed.	(Rate: 0.1"/min.)
Table 5.4	Predictions – GEN.2_Unitized, Invert & Axial.	(Rate: 0.1"/min.)

Table 5.5	Predictions – GEN.3_Semi-unitized.	(Rate: Varied)
Table 5.6	Comparisons – GEN.3_Semi-unitized.	(Rate: Varied)
Table 5.7	Comparisons – Specimens.	(Load Test)
Table 7.1	Pre-rationalization – Nano: Constraints.	(Make Table)
Table 3.3	Pre-rationalization – Nano: Constraints.	(Make Table)
Table 3.3	Pre-rationalization – Nano: Constraints.	(Make Table)
Table 3.3	Pre-rationalization – Nano: Constraints.	(Make Table)
Table 3.3	Pre-rationalization – Nano: Constraints.	(Make Table)
Table 3.3	Pre-rationalization – Nano: Constraints.	(Make Table)
Table 7.1	Contributions – Overview	(Towards cost-aware freeform strip construction)
Table 7.2	Contributions – Analytical	(Re-usable)
Table 8.1	Sequence – GEN.4 Construction	(Overview)
Table A.1	Units – Conversions.	(General)
Table A.2	Strips – Radius & Stress.	(Radius: in.; Stress: psi)
Table A.3	Material – Embodied Energy.	( - )
Table A.4	Material – Thermal Properties.	( $r = 1/k$ )
Table A.5	Material – Mechanical Properties.	(1 MPa = 145.038 psi.)
Table A.6	Materials – Rates & Measures.	( - )
Table A.7	Structural – Theoretical Properties.	( - )
Table B.1	Plywood – Bending.	(Moisture: 8%; Units: in.)
Table B.2	Plywood – Twisting.	(Moisture: 8%; Units: in.)
Table B.3	Material – Efficiency.	( - )
Table B.4	Specimens – Thermal Properties.	( - )
Table B.5	Structural – Mechanical Properties.	(GEN.4)
Table B.6	Financial – Rates & Measures.	(GEN.4)
Table C.1	Pre-rationalization – Nano: Constraints.	(Make Table)
Table D.1	Pre-test – Elastica: Data.	(Units: cm)
Table D.2	Reference – Flexural: Plywood.	(Radius: in.; Stress: psi)

## INDEX – VARIABLES

### Variables

<u>Var.</u>	<u>Description</u>	<u>IMP</u>	<u>SI</u>	<u>Alt.</u>	<u>Notes</u>
$\alpha$	alpha	deg.	[rad.]	°	(Angle at boundary)
$\beta$	beta	deg.	[rad.]	°	(Angle secondary )
$c$	rise of an arch	in.	[mm]	-	(Midpoint only)
$\ell$	rod length	in.	[mm]	-	(Total rod length)
$K$	Effective length	-	-	-	(= 0.5, 0.7, 1.0, 2.0; AISC Table C-C2.1)
$k$	elliptic modulus	-	-	-	(Sq. root of elliptic parameter)
$s$	length along arc	in.	[mm]	cm	(Distance along)
$\hat{s}$	direction along curve	in.	[mm]	cm	(Unit vector, tangency)
$\zeta$	scale factor	-	-	-	(Unit-less)
$\lambda$	load factor	-	-	-	(Unit-less)
$U_z$	Deformation in global Z	in.	[mm]	cm	(Non-midpoint)
$L$	Span	in.	[mm]	cm	-
$x$	displacement	in.	[mm]	cm	-
$y$	excursion (non-midpoint)	in.	[mm]	cm	-
$r$	radius of curvature	in.	[mm]	cm	-
$h$	height of a cross section	in.	[mm]	cm	-
$b$	width of a cross section	in.	[mm]	cm	-
$E$	Modulus of Elasticity	psi	[N/mm <sup>2</sup> ]	MOE	(= $\sigma/\epsilon$ ; material constant for stiffness)
$R_m$	Modulus of Rupture	psi	[N/mm <sup>2</sup> ]	MOR	(flexural or bend strength)
$\epsilon$	strain	-	-	E vs. E	(= $1/L$ ; extension per unit length loaded.)
$\rho$	density	pcf	[kg/mm <sup>3</sup> ]	-	-
$I_y$	Second moment of area	in. <sup>4</sup>	[cm <sup>4</sup> ]	mm <sup>4</sup>	-
$S_y$	section modulus	in. <sup>3</sup>	[cm <sup>3</sup> ]	mm <sup>3</sup>	-
$\sigma$	stress	psi	[N/mm <sup>2</sup> ]	$f$	(= $P/A$ ; load per unit area.)
$\sigma_a$	stress, allowable	psi	[N/mm <sup>2</sup> ]	$f_a, f_w$	(safe or working stress.)
$\sigma_c$	stress, compressive	psi	[N/mm]	$f_c$	-
$\sigma_t$	stress, tensile	psi	[N/mm]	$f_t$	-
$\sigma_v$	stress, shear	psi	[N/mm]	$f_v$	-
$\sigma_m$	stress, combined	psi	[N/mm]	$f_m$	(applied, dead, fab. pre-stress.)
$\sigma_b$	stress, bending	psi	[N/mm]	$f_b$	(external moment.)
$\sigma_f$	stress, fabrication	psi	[N/mm]	$f_p$	(fabrication pre-stress)
$\sigma_r$	stress, residual	psi	[N/mm]	$f_r$	-
$\sigma_r$	stress, ultimate	psi	[N/mm]	$f_u$	(stress at material failure)
$q_z$	load, linear	pli	[N/mm]	$\omega$	-
$q_w$	load, wind	psf	[kN/m <sup>2</sup> ]	$\omega$	-
$F_R$	Force Axial, Residual	lbs.	[N]	-	-
$DL$	Dead Load	pcf	[N/mm <sup>3</sup> ]	-	-
$LL$	Live Load	pcf	[N/mm <sup>3</sup> ]	-	-
$SL$	Snow Load	pcf	[N/mm <sup>3</sup> ]	-	-
$\Theta$	Theta	deg.	[rad.]	$\theta$	(Between $\hat{s}$ and loading axis)
$\Delta$	Deflection	in.	[mm]	-	-
$\delta$	change in quantity	-	-	-	(Unit-less)
$u$	distance from neutral axis	in.	[mm]	-	(Fiber's distance from)

## Abbreviations

<u>Abb.</u>	<u>Description</u>		
<b>BOD</b>	Basis of Design	<b>GEN.#</b>	Generation (No.)
<b>MOR</b>	Modulus of Rupture	<b>L.B.</b>	Laminated Bamboo
<b>MOE</b>	Modulus of Elasticity	<b>o.c.</b>	On Center
<b>SIP</b>	Structural Insulated Panel	<b>s.f.</b>	Safety Factor (= $f_u/f_w$ )
<b>ICF</b>	Insulated Concrete Form	<b>R#</b>	Revision (No.)
<b>SSP</b>	Stressed-Skin Panel	<b>r#</b>	radius (No.)
<b>SPF</b>	Spray Foam	<b>Int.</b>	Interior
<b>VDC</b>	Virtual Design and Construction	<b>Ext.</b>	Exterior
<b>CCF</b>	Closed-Cell Foam	<b>Cav.</b>	Cavity
<b>CL</b>	Centerline	<b>GFR</b>	Glass Fiber Reinforced
<b>EP</b>	End-Point	<b>DRO</b>	Digital Read Out
<b>MP</b>	Mid-Point	<b>APA</b>	The Engineered Wood Association
<b>NA</b>	Neutral Axis -	<b>Ply.</b>	Plywood
<b>OCF</b>	Open-Cell Foam	<b>1-ply</b>	One Layer
<b>QP</b>	Quarter-Point	<b>3-ply</b>	Three Layer Build
<b>OVE</b>	Optimum Value Engineering	<b>5-ply</b>	Five Layer Build
<b>SP</b>	Sixth-Point	<b>Unk.</b>	Unknown
<b>ODE</b>	Ordinary Differential Equation		
<b>3DM</b>	Rhino File Format		
<b>PDF</b>	Portable Document Format		
<b>F4F</b>	Free4orm Framing		
<b>Typ.</b>	Typical		
<b>Atyp.</b>	Atypical		
<b>Var.</b>	Varies		
<b>Lit.</b>	Literature		
<b>Min.</b>	Minimum		
<b>Max.</b>	Maximum		
<b>The.</b>	Theoretical		

## Terms

<b>Object-level</b>	<b>1:</b> at the scale of the whole. (i.e., above varies; can be a house or a baluster)
<b>System-level</b>	<b>1:</b> at the scale of the system. (i.e., above unit-level)
<b>Assembly-level</b>	<b>1:</b> at the scale of the panel or modular assembly. (e.g., a single SIP, spandrel panel, or glazing lite)
<b>Component-level</b>	<b>1:</b> at the scale of the pre-assembled portable comprised of multiple parts. (e.g., a trussed joist)
<b>Joinery-level</b>	<b>1:</b> at the scale of the individual detail or interface. (e.g., a connection)
<b>Piece-level</b>	<b>1:</b> at the scale of the individual part. (e.g., a milled part)
<b>Unit-level</b>	<b>1:</b> at the scale of the assembly. (i.e., above piece-level)
<b>Part-level</b>	<b>1:</b> at the scale of the individual piece. (e.g., a milled part)

## Definitions

- Approach** 1: treating a problem in a certain way; a way of doing, engaging, or thinking about something.  
2: preliminary steps toward a purpose; general, philosophical.  
(non-prescriptive, can refer to a methodology, technique, and various other things)
- Concept** 1: an abstract generalized understanding or relationship retained in the mind.  
(from specific reasoning, experience, imagination or abstraction)
- Framework** 1: a set of concepts and/or relationships posited about a phenomenon.
- Methodology** 1: the study of methods/usage in a field.  
2: a collection of practices, procedures, and rules.  
(can be philosophical or ideological; how to teach, make, or study)
- Method** 1: a procedure for addressing or engaging; the practical means.  
2: a specific process, technique, or way of doing something. (prescriptive)
- Means** 1: the specific physical/technical means of production; the equipment; the nuts and bolts.
- Ideal** 1: axiom representing an abstract, hypothetical, or theoretical optimum.
- Ideology** 1: a system of ideas and ideals, especially those that form the basis of a theory.
- Philosophy** 1: the study of the fundamental nature of knowledge, reality, and existence.
- Principle** 1: a fundamental axiomatic assumption.
- Strategy** 1: planning towards an overall goal; dealing with specific actions. (planning)
- Tactic** 1: the actual means used in gaining an objective; the execution.
- Technique** 1: the combination of procedure and skill.
- Theory** 1: a system of assumptions, principles, and relationships that explain a specific phenomenon.  
(or set of phenomena.)

## INDEX – EQUATIONS

This *Index* contains general use equations from the different theoretical analysis workflows developed for the load tests and for the elastica, which are located in *Appendix C – Calculations* and *Appendix E – Elastica*.

### Equations – General

Arc Length:  $s = \theta r$  (A1)

Curvature:  $\kappa(s) = \frac{1}{r(s)} = \frac{d\theta}{ds}$  (A2)

Hooke's Law  
for Continuous Media:  $\sigma = E\varepsilon$  (A3)

Moment  
due to Bending:  $M_b(r) = \frac{EI}{r}$  (A4)

Bending Stress:  $\sigma_b(u) = \frac{Eu}{r}$  (A5)

Bending Stress at Extreme Fiber for Beam with Symmetry in  $\hat{r}$  Direction:

$$\sigma_b = \frac{Eh}{2r} \quad (A6)$$

Euler's Critical Buckling Load:  $P_{crit} = \frac{\pi^2 EI}{(K\ell)^2}$  (A7)

(where effective length  $K = 1.0$  for hinge-hinge/pinned-pinned or  $K = 2.0$  for eccentrically loaded columns.)

## Beams – Idealized: General Formulas

Shear Force for Beam with transverse load  $\Omega(x)$ :

$$F_v(x) = \int_0^x \Omega(x') dx' \quad (\text{A8})$$

$$\Omega(x) = \frac{dF_v}{dx} \quad (\text{A9})$$

Moment due to Load for Beam with transverse load:

$$M_P(x) = \int_0^x F_v(x') dx' \quad (\text{A10})$$

$$F_v(x) = \frac{dM_P}{dx} \quad (\text{A11})$$

Moment due to Bending in Euler-Bernoulli Beam Theory:

$$M_b = EI \frac{d^2\Delta}{dx^2} \quad (\text{A12})$$

Shear Stress:  
Average

$$\sigma_{v\text{ ave}}(x) = \frac{F_v(x)}{A(x)} = \frac{\int \sigma_v(x) dA}{A(x)} \quad (\text{A13})$$

Shear Stress:

$$\sigma_v(x) = \frac{1}{b} \int_{A_y} \frac{\partial}{\partial s} \sigma_s(s, u) dA \quad (\text{A14})$$



## Beams – Idealized: Formulas for Simply Supported Beams with Given Loading Conditions

### 4-point Flexure

Two concentrated, central, applied loads. See also *Figure S.1*.

$$\text{Load:} \quad W(x) = \begin{cases} \frac{P}{2}, & x = a \\ \frac{P}{2}, & x = L - a \\ 0, & \text{elsewhere} \end{cases} \quad (\text{A15})$$

$$\text{Total Load:} \quad P \quad (\text{A16})$$

$$\text{Reaction at each Support:} \quad -\frac{P}{2} \quad (\text{A17})$$

$$\text{Shear Force:} \quad \left(\frac{2}{P}\right) \cdot F_v(x) = \begin{cases} 1, & x \in [0, a] \\ 0, & x \in (a, L - a] \\ -1, & x \in (L - a, L] \end{cases} \quad (\text{A18})$$

$$\text{Moment due to Load:} \quad \left(\frac{2}{P}\right) \cdot M_p(x) = \begin{cases} x, & x \in [0, a] \\ a, & x \in (a, L - a] \\ L - x, & x \in (L - a, L] \end{cases} \quad (\text{A19})$$

$$\text{Deflection:} \quad EI \left(\frac{12}{P}\right) \cdot \Delta(x) = \begin{cases} f_1, & x \in [0, a] \\ f_2, & x \in (a, L - a] \\ f_3, & x \in (L - a, L] \end{cases} \quad (\text{A20})$$

$$f_1 = (3aL - 3a^2)x - x^3$$

$$f_2 = -a^3 + 3aLx - 3ax^2$$

$$f_3 = -L^3 + 3aL^2 - 3a^2L + (3L^2 - 3aL + 3a^2)x - 3Lx^2 + x^3$$

Deflection  
at press head:  
( $x = a$   
or  
 $x = L - a$ ):

$$\Delta(a) = \left(\frac{P}{12EI}\right) (3a^2L - 4a^3) \quad (\text{A21})$$

#### 4-point Flexure (continued)

Two concentrated, central, applied loads. See also *Figure S.1*.

$$\Delta(L/2) = \Delta_{max} = \Delta(a) + \delta\Delta$$

Deflection

at midspan:

$$(x = \frac{L}{2}),$$

which is max.

$$\text{where } \delta\Delta = -R + \sqrt{R^2 - \frac{(L-2a)^2}{4}} \quad (\text{A22})$$
$$\text{and } R = \frac{EI}{Pa}$$

#### 3-point Flexure

One concentrated, center, applied load. See also *Figure S.2*.

Load:

$$W(x) = \begin{cases} P & x = L/2 \\ 0 & \text{elsewhere} \end{cases} \quad (\text{A23})$$

Total Load:

$$P \quad (\text{A24})$$

Reaction

at each Support:

$$-\frac{P}{2} \quad (\text{A25})$$

Shear Force:

$$\left(\frac{2}{P}\right) \cdot F_v(x) = \begin{cases} -1, & x \in [0, L/2] \\ 1, & x \in (L/2, L] \end{cases} \quad (\text{A26})$$

Moment

due to Load:

$$\left(\frac{2}{P}\right) \cdot M_P(x) = \begin{cases} -x, & x \in [0, L/2] \\ -L + x, & x \in (L/2, L] \end{cases} \quad (\text{A27})$$

Deflection:

$$EI \left(\frac{48}{P}\right) \cdot \Delta(x) = \begin{cases} 3L^2x - 4x^3, & x \in [0, L/2] \\ -L^3 + 9L^2x - 12Lx^2 + 4x^3, & x \in (L/2, L] \end{cases} \quad (\text{A28})$$

Deflection

at midspan:

$$(x = \frac{L}{2}),$$

which is max.

$$\Delta(L/2) = \Delta_{max} = \frac{PL^3}{48EI} \quad (\text{A29})$$

**Partial-span Uniformly Distributed Load (PUDL):**

Symmetric. See also *Figure S.3*.

Load  
Distribution:

$$\Omega(x) = \begin{cases} 0, & x \in (0, a] \\ \omega, & x \in (a, L - a] \\ 0, & x \in (L - a, L) \end{cases} \quad (\text{A30})$$

Total Load:

$$(L - 2a)\omega \quad (\text{A31})$$

Reaction  
at each Support:

$$-\frac{(L - 2a)\omega}{2} \quad (\text{A32})$$

Shear Force:

$$\left(\frac{2}{\omega}\right) \cdot F_v(x) = \begin{cases} -(L - 2a), & x \in [0, a] \\ -(L - 2x), & x \in (a, L - a] \\ L - 2a, & x \in (L - a, L] \end{cases} \quad (\text{A33})$$

Moment  
due to Load:

$$\left(\frac{2}{\omega}\right) \cdot M_p(x) = \begin{cases} -(L - 2a)x, & x \in [0, a] \\ a^2 - Lx + x^2, & x \in (a, L - a] \\ -L^2 + 2La + (L - 2a)x, & x \in (L - a, L] \end{cases} \quad (\text{A34})$$

Deflection:

$$EI \left(\frac{24}{\omega}\right) \cdot \Delta(x) = \begin{cases} f_1, & x \in [0, a] \\ f_2, & x \in (a, L - a] \\ (\text{symmetric}), & x \in (L - a, L] \end{cases} \quad (\text{A35})$$

$$f_1 = (L^3 + 6aL^2 - 24a^2L + 16a^3)x + (4a - 2L)x^3$$

$$f_2 = a^4 + (L^3 + 6aL^2 - 24a^2L + 12a^3)x + 6a^2x^2 - 2Lx^3 + x^4$$

Deflection  
at midspan:  
( $x = \frac{L}{2}$ ),  
which is max.

$$\Delta\left(\frac{L}{2}\right) = \Delta_{max} = \left(\frac{\omega}{384EI}\right) (5L^4 + 48AL^3 - 168A^2L^2 + 96A^3L + 16A^4) \quad (\text{A36})$$

**Full-span Uniformly Distributed Load (UDL):**

Typical. See also *Figure S.4*.

Load:  $\Omega(x) = \omega, \quad x \in (0, L)$  (A37)

Total Load:  $\omega L$  (A38)

Reaction  
at each Support:  $-\frac{\omega L}{2}$  (A39)

Shear Force:  $\left(\frac{2}{\omega}\right) \cdot F_v(x) = -L + 2x$  (A40)

Moment  
due to Load:  $\left(\frac{2}{\omega}\right) \cdot M_p(x) = -Lx + x^2$  (A41)

Deflection:  $EI \left(\frac{2^4}{\omega}\right) \cdot \Delta(x) = L^3x - 2Lx^3 + x^4$  (A42)

Deflection  
at midspan:  
 $\left(x = \frac{L}{2}\right)$ ,  
which is max.  $\Delta(L/2) = \Delta_{max} = \frac{5\omega L^4}{384EI}$  (A43)

This appended *Chapter* contains the fundamental general assumptions, information, and values that were used in project development.

**Assumptions – Construction****(General)****Construction – Ideology (General)**Macro

- (1.) Industry has chosen to optimize the existing product and production to continue to sell what it has been.
- (2.) System-built market share is increasing, and demand for freeform renewable bamboo or wood houses will develop once the market sees it is already possible.
- (3.) High performance herein exceeds minimum material or structural considerations, and includes total cost-, material- and construction-awareness.

Micro:

- (1.) Avoiding the gluing/clamping trap will help ensure a cost-aware versus premium product.
- (2.) Avoiding the edge-joinery/furniture making trap will ensure a cost-aware versus premium product.
- (3.) Avoiding the stereotomic/surfacing machining time sink will help ensure a cost-aware versus premium product.

Nano

- (1.) As a tropical hardwood and with low shear capacity, existing Lauan "bending plywood" products are non-viable for the intended application. Related: [Schimel et al. 2001].
- (2.) With inherent high machine time from small bit feed rates, kerfing (as a strategy) and existing pre-kerfed products which command finish prices, are not cost effective for the intended application.

## Assumptions – Geometry

(General)

### Geometry – Conversion (General)

Table A.1 Units – Conversion.

<u>IMP</u>	<u>Imperial</u>	<u>SI</u>	<u>Metric</u>	<u>Alt.</u>	<u>Notes</u>
1.00 in.	lineal in.	[2.54 cm]	cm	"	(-)
12.00 in.	lineal ft.	[30.48 cm]	cm	"	(but base 12 can be divided by 2, 3, 4, and 6)
39.37 in.	inches	[1.0 m]	meter	"	(39.370078 in.)
144 in. <sup>2</sup>	square ft.	[0.092 m <sup>2</sup> ]	sq. m.	sf	(0.092903 m <sup>2</sup> )
144 in. <sup>3</sup>	board ft.	[0.0077 m <sup>3</sup> ]	cu. m.	bd.	(0.007742 m <sup>3</sup> )
1728 in. <sup>3</sup>	cubic ft.	[0.028 m <sup>3</sup> ]	cu. m.	cf	(0.028317 m <sup>3</sup> )
1.00 ft.	lineal ft.	[0.3048]	m	plf	(-)
1.00 ft. <sup>2</sup>	square ft.	[0.092 m <sup>2</sup> ]	sq. m.	psf	(0.092903 ft <sup>2</sup> )
1.00 ft. <sup>3</sup>	cubic ft.	[0.028 m <sup>3</sup> ]	cu. m.	pcf	(0.028316 m <sup>3</sup> )
3.28 ft.	feet	[1.0 m]	lineal m.	plm	(3.28084 ft.)
10.76 ft. <sup>2</sup>	square m.	[1.0 m <sup>2</sup> ]	sq. m.	psm	(10.7639 ft. <sup>2</sup> )
35.32 ft. <sup>3</sup>	feet	[1.0 m <sup>3</sup> ]	cu. m.	pcm	(35.3147 ft. <sup>3</sup> )
1.00 lb.	pound	[0.454 kg.]	kilogram	half-kilo.	(0.45359 kg.)
2.20 lbs.	pounds	[1.0 kg.]	kilogram	kilo.	(2.20462 lbs.)

Notes: (a.) 1000 psi = 1 ksi = 6.895 MPa, or 1 MPa = 0.145 ksi.

### Geometry – Rods (General)

Elliptic modulus ( $k$ ).

Lemniscate $k$ :	0.908908557548541	Lemniscate, $\alpha$ :	130.70991°	(where ends touch)
Special $k$ :	0.837452958488127	Special, $\alpha$ :	113.74426°	(where rise is maximum)
Rectangular $k$ :	0.707106781186547	Rectangular, $\alpha$ :	90.00000°	(where alpha is perp.)

Radius (min.).

$$r_{\min.} = c/4k^2. \quad k = \sin(\alpha/2). \quad (\text{min. radius: } r_{\min.}; \text{ rise: } c; \text{ elliptic modulus: } k; \text{ boundary angle: } \alpha)$$

Table A.2 Strips – Radius & Stress.

(Radius: in.; Stress: psi)

<u>Thick</u>	r240"	r192"	r144"	r96"	r72"	r60"	r48"	r36"	r30"	r24"
0.2"	500	625	833	1250	1667	2000	2500	3333	4000	5000
0.24"	600	750	1000	1500	2000	2400	3000	4000	4800	6000
0.3"	750	938	1250	1875	2500	3000	3750	5000	6000	7500
0.36"	900	1125	1500	2250	3000	3600	4500	6000	7000	9000
0.4"	1000	1250	1667	2500	3333	4000	5000	6667	8000	10000
0.5"	1250	1563	2083	3125	4167	5000	6250	8333	10000	12500

Notes: (a.) Used equation (A6) for extreme-fiber bending stress:  $\sigma_b = Eh/2r$ .

(b.) Used:  $E$ :  $1.2 \times 10^6$  psi (Initial project  $E$ : 1.0, then 1.125 avg. from GTR-190, and finally  $1.2 \times 10^6$  psi).

## Assumptions – Performance

(General)

### Performance – Material (General)

**Table A.3 Material – Embodied Energy.**

(1 MJ/Kg. = 429.92 Btu/lb.)

Type	Material	Btu/lb.	CO <sub>2</sub> /lb.	lb./ft. <sup>3</sup>	MJ/kg.	CO <sub>2</sub> /kg.	kg./m. <sup>3</sup>
Energy – Embodied:	Plywood:	6,449	0.49	33.7 – 45	15.0	1.07	540 – 720
	Plywood, Certified (FSC):	-	-	33.7 – 45	-	-	-
	Bamboo, Laminated:	-	-	42	-	-	-
	Bamboo, Scrimber:	-	-	39.1	-	-	-
	Timber:	3,654	0.21	30.0 – 45	8.5	0.46	480 – 720
	Hardwood, sawn:	3,353	-	-	7.8	-	-
	Softwood, sawn:	3,353	-	-	7.8	-	-
	Polyurethane foam:	43,637	1.58	1.87	101.5	3.48	30
	Polystyrene foam:	38,091	1.15	0.94 – 1.87	88.6	2.55	15 – 30
	Glass wool:	12,037	0.61	0.75	28.0	1.35	12
	Mineral wool:	7,223	0.48	1.50	16.8	1.05	24
	Cellulose:	404	-	2.68	0.94 – 3.3	-	43
	Aluminum:	66,638	3.73	168.5	155	8.24	2700
	Steel, stainless:	24,376	2.78	490	56.7	6.15	7850
	Steel:	8,641	0.62	487	20.1	1.37	7800
	Glass:	6,448	0.39	156.1	15.0	0.85	2500
	Brick:	1290	0.11	106.1	3.0	0.24	1700
CMU Block:	288	0.03	90.5	0.67	0.073	1450	
Mortar:	572	0.09	var.	1.33	0.208	var.	
Concrete:	477	0.07	149.8	1.11	0.159	2400	

**Notes:** (a.) Adapted [Hammond & Jones 2006] *Embodied energy and carbon footprint database, Univ. of Bath.*

(b.) References: 1 m.<sup>3</sup> = 35.32 ft.<sup>3</sup>; 1 kg. = 2.205 lbs.; 1 lb. = 0.454 kg;

### Performance – Operational (General)

**Table A.4 Material – Thermal Properties.**

(r = 1/k)

Type	Material	Btu-in./hr.-ft. <sup>2</sup> -°F	W/m-°K	Notes
Conductivity:	Lamboo-k:	0.94	0.14	(Lamboo lit.)
	Plyboo-k:	1.57	0.22	(To confirm, Shah 2015)
	Phenolic Paper-k:	1.48	0.21	(Richlite lit.)
	Plywood-k:	0.760 – 1.02	0.11 – 0.15	(Group 1 – 4; 0.8 if Unknown)
Resistivity	Lamboo-R:	1.1	7.90	(Lamboo lit.)
	Plyboo-R:	-	-	(Unconfirmed)
	Plywood-R:	1.25 – 0.98	9.1 – 6.7	(0.47 – 0.62 for 0.36" – 0.48")

**Notes:** (a.) Sources: [Plyboo; Lamboo; Richlite; Performance Panel 2015; Bam. Scrimber Pat. 2011; Shah 2015].

(b.) k = conductivity: 1 Btu-in./hr.-ft.<sup>2</sup>-°F = 0.14 W/(m°K); r = resistivity: hr.-ft.<sup>2</sup>-°F/(Btu-in.); (m°K)/W.

**Performance – Structural (General)**

**Table A.5 Material – Mechanical Properties.**

**(1 MPa = 145.038 psi.)**

<u>General</u>	(psi) <u>Compress</u>	(psi) <u>Tension</u>	(psi x 1000) <u>E</u>	(psi) <u>MOR</u>	(psi) <u>Shear</u>	(pcf) <u>Density</u>
Carbon fiber.	-	270,000	60,000	-	-	104
Steel, high strength:	-	225,000	25,000	-	11,200k	490
Steel, mild:	-	58,000 – 80,000	29,000	-	11,200k	490
Carbon fiber plastics:	-	50,000 – 150,000	-	-	-	-
Glass fiber plastics:	-	50,000 – 150,000	-	-	-	107 – 120
Aluminum, extruded:	-	20,000 – 80,000	-	-	-	168
Aluminum, cast:	-	10,000	-	-	-	168
Glass:	-	5,000 – 25,000	10,000	-	-	150 – 175
Concrete:	-	600	-	-	-	150
Egg shell:	-	1.1 (membrane)	-	-	-	65
<u>Related</u>						
Phenolic Paper, along-gra.	18,400	19,200	1,760	22,000	11,500	84
Phenolic Paper, cross-gra.	15,900	13,100	1,760	17,300	11,500	84
Lamboo, along-grain:	13,500	21,500	2,900	12,800	2,900	42
Lamboo, cross-grain:	3,050	550	2,900	12,800	2,900	42
Wood, along-grain:	1,700 (Dry)	15,000	2,000	12,500	-	32 (D. Fir)
Wood, cross-grain:	625 (Dry)	500	1,765	12,500	-	32 (D. Fir)
Plyboo, along-grain	-	3,500	148	9,100	-	39.1 (low E)
Plyboo, cross-grain	-	3,500	148	9,100	-	39.1 (low E)
Plywood, along-grain:	-	-	1,200	5,535	-	36
Plywood, cross-grain:	-	-	1,200	5,535	-	36

**Notes:** (a.) Sources: [Hunt 2003, p.95; Plyboo; Lamboo; APA] by Type.



**Table A.6 Structural – Theoretical Properties.**

The. – Avg. Span:	180"	[-]
The. – Deflection:	L/240	[-]
The. – MOE:	1,200 psi	[-]
The. – MOR:	5,535 psi	[FPL GTR-190, Table 12-1]
The. – $\sigma_a$ (3-ply):	2,800 psi	[APA H815F, p.6]
The. – $\sigma_a$ (5-ply):	3,300 psi	[APA H815F, p.6]

**Notes:** (a.) Sources: by Line.

**Performance – Financial (General)**

**Table A.7 Material – Rates & Measures.**

Financial – Light Frame

Lumber, No.2 Pine, prime.	2"x 10"x 16"	\$15.30	\$0.00 bd.	-	[Home Depot 2016]
Lumber, No.2 Pine, prime.	2"x 12"x 16"	\$14.98	\$0.00 bd.	-	[Home Depot 2016]
Ply. Sub-floor, Exterior grade.	0.75"x 48"x 96"	\$32.27	\$0.00 bd.	-	[Home Depot 2016]
Ply. Sheathing, Pine, prime.	0.468"x 48"x 96"	\$15.25	\$0.00 bd.	-	[Home Depot 2016]
Ply. Sheathing, Tongue-Groove.	0.468"x 48"x 96"	\$23.58	\$0.00 bd.	-	[Home Depot 2016]

Financial – Panelized

Premium for singly-curved.	-	-	25%, min.	-	[R-Control site visit]
SIP assembly labor.	"assembler"	-	\$60/hr.	-	[R-Control site visit]
Machinist for press, contours	"former"	-	\$120/hr.	-	[R-Control site visit]

Financial – Labor

	<u>Dim.</u>	<u>Total</u>	<u>Unit Rate</u>	<u>Mfg.</u>	<u>Source</u>
Labor, Machinist (Press)	60 min.	\$0.00	\$64/hr.	Baldwin	[MIT, Rudolph]
Labor, Machinist (CNC)	60 min.	\$0.00	\$120/hr.	Onsrud	[R-Control site visit]
Labor, Skilled	60 min	\$0.00	\$60/hr.	N/A	[Taskrabbit 2015]
Labor, Unskilled	60 min	\$0.00	\$15/hr.	N/A	[Taskrabbit 2015]

**Notes:** (a.) Sources: by Line.

This appended *Chapter* contains final application-specific assumptions, information, and values; the performance basis of design.

**Basis of Design – Construction**

**Construction – Tools & Equipment (BOD)**

Hand Tools

- Dead-blow hammer. (for friction fit. connections)
- Wood file or rasp. -
- Large snips. (for zip-ties, seam tape)
- Box-cutter. -
- Handheld shear. (for hinge redundancy tabs)
- Pry-bar, wide face. (for mistakes)
- Screw gun. -
- Bits, magnetic. (quick-change.)



**Fig. B.1 BOD – Ironing: More.**  
*Iron, retail (obs.): 354° = Also hot.*

**Construction – Manufacturers (BOD)**

Inputs

Mfg.

Notes

- Bamboo Laminated: Lamboo Technologies. (or approved Equal.)
- Bamboo Scrimber: Plyboo. (or approved Equal.)
- Plywood: APA Grade stamp, or Certified. (FSC or SFI-certified)
- Seam Tape: Roberts. (or approved Equal.)
- Zip-ties: Panduit or Flex-Cuffs. (50 lb.; UV-resist.; metal tooth)
- Glue: Franklin International. (Titebond reg., II, & III)



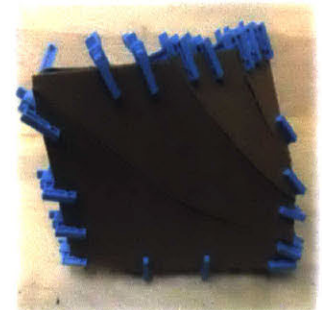
**Fig. B.2 BOD – Plywood: Group 1.**  
*Only veneer grades: N, A, and C.*

Equipment

Mfg.

Notes

- Moisture meter: General Tools & Instruments. Type: MMD4E
- Digi-Weigh: Zemic. XK3190-A12(E)



**Fig. B.3 BOD – Clamps: Less.**  
*Initial model. Full scale: Zip and Iron.*

## Basis of Design – Geometry

(GEN.4)

### Geometry (BOD)

The viability of multi-layer strip construction, especially in the case of interlayer point connections, depends on the successful management of error accumulating primarily from assembly and placement tolerances (and secondarily from fabrication tolerances and dynamic behavior). Assumed is that all of the proposed methods and details, would enable renewing quality management of dimensional tolerance at the unit-level. Some field interface adjustment has been provided for, and the extension of the elastica analysis tool for the study of the elastic bending between multiple points is also anticipated.

### Geometry – Plywood (BOD)

**Table B.1 Plywood – Bending.**

(Moisture: 8%; Units: in.)

(Specimen) AC Plywood Thickness –	( $r_{lit.}$ ) Lit. Radius	( $r_{arc.}$ ) Arc Radius	( $c$ ) Arc Rise	( $L$ ) Arc Span	( $e_c$ ) Elastica Radius (min.) from Rise	( $c$ ) Elastica Rise	( $r_a$ ) Allowable Radius (min.) at 2800 psi	(%) $e_c/r_{lit.}$
0.48 Ply., ½96 (strong, top)	r144	r126.5	c9.0	L93.72	e102.61	c9.0	ra103	-28.7
0.36 Ply., ½96 (strong, top)	r96	r74.2	c15.0	L89.46	e60.29	c15.0	ra77	-37.2
0.48 Ply., ½48 (weak, top)	r72	r71.3	c4.0	L47.10	e57.85	c4.0	ra103 (weak)	-19.6
0.36 Ply., ½48 (weak, top)	r36	r30.4	c9.0	L43.19	e24.74	c9.0	ra77 MOR?	-32.2

- Notes:** (a.) In the lesser elastica range, arc approximation from rise was over  $r$  (min.) by 23%; from span by 28.5%.  
 (b.) In the plywood pre-test, the observed  $r$  (min.) was on average 29.4% under the published value.  
 (c.) Key: *Industry Literature*, *Arc approximation*; *Elastica from rise*;  
 (d.) Bending MOE is a measure of resistance to deflection and relates to its stiffness [GTR-190, 12-2].

**Table B.2 Plywood – Twisting.**

(Moisture: 8%; Units: deg. & in.)

(Specimen) AC Plywood Thickness –	( $\theta_{lit.}$ ) Lit. Angle	( $\theta_{obs.}$ ) Twist Angle	( $\theta_{obs.}$ ) Twist Inches (in.)	( $\theta_{obs.}$ ) Twist Angle (max.)	( $r_{min.}$ ) Strip Radius (min.)	( $L$ ) Strip Span	( $r_a$ ) Allowable Radius (min.) at 2800 psi	( $b$ ) Strip Base (min.)
0.48 Ply., ½48 (strong, top)	N/A	5.0°	0.75	10°	r350	L48	r103	9
0.36 Ply., ½24 (strong, mid)	N/A	9.5°	1.0	20°	r90.5	L24	r77	6
0.36 Ply., ½24 (strong, safe)	N/A	14.0°	1.5	20°	r60.8	L24	r77	6
0.36 Ply., ½24 (strong, top)	N/A	18.4°	2.0	20°	r46.1	L24	r77	6

- Notes:** (a.) Twisting BOD for 0.36" plywood is 12° over L24" and for 0.5" plywood is 6° over L48".

## Basis of Design – Performance

(GEN.4)

### Performance – Material (BOD)

**Table B.3 Material – Properties.**

	Type	lb.C/lb.	kg.C/kg.
Material – Carbon:	Plywood:	0.487	0.221
	Timber:	0.275	0.125
	Sawn hardwood:	0.282	0.128
	Sawn softwood:	0.271	0.123
Material – Moisture:	Plywood:	6–9.8% (obs.)	
	Lamboo:	5–9% (lit.)	
	Plyboo:	5.7–7.4% (lit.)	



**Fig. B.4 Material – MC: 7-10%.**

*Equilibrium moisture content.*

**Notes:** (a.) *Group 1* (natural, not repaired): *Only veneer grades N, A, and C.*

(b.) Lamboo (D1037): 20% RH; *h* (swell): -0.13%; *L* (parallel): -0.04%, (perp.): -0.10%

(c.) Plyboo (D1037): 20% RH; *h* (swell): -0.40%; *L* (parallel): -0.09%, (perp.): -0.07%

(d.) *Sources:* [Hammond 2008; Lamboo 2015; Plyboo 2006] *by Type.*

**Table B.4 Material – Efficiency.**

	Specimen	in. <sup>3</sup>	cm. <sup>3</sup>
Material – Volume:	GEN.0_Box	1435	23515.5
	GEN.0_Box, Hybrid:	1157	18959.9
	GEN.0_Box, Kerfed:	1296	21237.6
	GEN.1_Panel, Control:	2407	39443.8
	GEN.1_Panel, Kerfed:	2268	37165.9
	GEN.2_Unitized, Invert:	1620	26547.1
	GEN.2_Unitized, Axial:	2223	36428.5
	GEN.3_Semi-unitized:	2732	44769.5
	GEN.3_Arch – 180°:	9720	159282.3
	GEN.4_Arch – 220°:	52007	852238.7



**Fig. B.5 Material – Waste: Avg. %.**

*Estimating waste per generation.*

Material – Waste:	GEN.0_Nesting:	74.2 %	3421.3/4608 in. <sup>2</sup>	(1 sheet)
	GEN.1_Nesting:	86.2 %	4180.0/4608 + 1775.4/2304 in. <sup>2</sup>	(1.5 sheets)
	GEN.2_Nesting:	79.7 %	4138.2 + 3207.9 /9216 in. <sup>2</sup>	(2 sheets)
	GEN.3_Nesting:	78.9 %	3175.2 + 3461.1 + 4277.0/13824 in. <sup>2</sup>	(3 sheets)

**Notes:** (a.) *References:* 1 in.<sup>3</sup> = 16.387 cm.<sup>3</sup>

(b.) *Plywood* (obs.): 0.0216 lb./in.<sup>3</sup>; *Plywood* (lit.): 0.0208 lb./in.<sup>3</sup>

## Performance – Structural (BOD)

### Properties, General.

The. – Avg. Span:	180"	[ - ]
The. – Deflection:	$L/240$	[ - ]
The. – MOE:	1,200 psi	[ - ]
The. – MOR:	5,535 psi	[FPL GTR–190, Table 12-1]
The. – $\sigma_a$ (3-ply):	2,800 psi	[APA H815F, p.6]
The. – $\sigma_a$ (5-ply):	3,300 psi	[APA H815F, p.6]

<i>Non-ply., Effective depth</i>	<i>Non-ply., Kerfed, Effective depth</i>
0.48" → 0.4"	0.48" with 0.2" kerf → 0.24"
0.44" → 0.36	0.44" with 0.2" kerf → 0.2"
0.36" → 0.3"	0.36" Bending Lauan ply. → 0.0"
0.313" → 0.25"	

## Performance – Structural: Plywood (BOD)

### Plywood, Minimum.

GEN.4 – Plywood: 3-ply build with > 0.1"/layer and APA grade stamp.

### Plywood, General.

GEN.4 – $\rho_{ply.}$ :	34.08 pcf
GEN.4 – $\rho_{bd.}$ :	2.83 bd.
GEN.4 – Area-wt.(0.48"):	1.40 psf; (0.44"): 1.30 psf; (0.36"): 1.06 psf.

### Plywood, Rupture Modulus.

GEN4. – MOR: 5,535 psi [FPL GTR–190, Table 12-1]

### Plywood, Allowable.

GEN.4 – $\sigma_a$ (5-ply):	3,300 psi	[APA H815F, p.6]
GEN.4 – $\sigma_a$ (3-ply):	2,800 psi	[APA H815F, p.6]

### Plywood, Effective depth (APA).

<i>Plywood, Effective depth (APA)</i>	<i>Plywood, Effective depth</i>
$t_b$ : 0.170" or 0.216" (for bending)	0.48" → 0.4"
$t_v$ : 0.280" or 0.371" (for shear & deflection)	0.44" → 0.36
E: 1,800 ksi (general)	0.36" → 0.3"
E: 1,950 ksi (with deflection; shear calcs.)	0.313" → 0.25"
	0.25" → 0.2"

### Plywood, Kerfed.

0.48" with 0.2" kerf	→ 0.24"
0.44" with 0.2" kerf	→ 0.2"
0.36" Bending Lauan ply.	→ 0.0"

**Performance – Financial (BOD)**

**Table B.6 Financial – Rates & Measures**

**(GEN.4)**

<u>Description</u>	<u>Dim.</u>	<u>Total</u>	<u>Unit Rate</u>	<u>Mfg.</u>	<u>Source</u>
Labor, Machinist (CNC)	1hr.	\$0.00	\$120/hr.	Onsrud	[MIT, N51]
Labor, Skilled	1hr.	\$0.00	\$60/hr.	N/A	[Taskrabbit 2015]
Labor, Student	1hr.	\$0.00	\$20/hr.	N/A	[Taskrabbit 2015]
Labor, Unskilled	1hr.	\$0.00	\$15/hr.	N/A	[Taskrabbit 2015]
Seam Tape	6"	-	\$0.25 plf	Roberts	[Amazon 2015]
Seam Tape	4"	\$4.62	\$0.23 plf	Roberts	[Amazon 2015]
Jute Webbing,	3.75"x 72"	\$45.00	\$0.208 plf	-	-
OSB (1 or 2?)	0.468"x 48"x 96"	\$12.58	\$0.00 bd.	-	[Home Depot 2016]
Spray Foam, Open-cell (OCF)	1 ft. <sup>3</sup>	\$5.28	\$0.44 – 0.65 bd.-	-	[Green Build. Advisor 2014]
Spray Foam, Closed-cell (CCF)	1 ft. <sup>3</sup>	\$8.40	\$0.70 – 1.00 bd.-	-	[Green Build. Advisor 2014]
Concrete, Delivered:	1 yd.	\$60.00 +	\$90.00/yd.	-	-
Concrete, Reinforced	1 yd.	-	-	-	-
Plywood, Structural:	48"x 96" x 0.48"	-	-	-	-
Bamboo; Laminated:	48"x 96" x 0.5"	-	-	-	-
Bamboo; Scrimber:	48"x 96" x 0.5"	\$48.00	\$2.00 psf	Plyboo	Web; Natural, Flat. grain
Time, Modeling:	1hr.	-	-	-	-
Time, Machining:	1hr.	-	-	-	-
Time, Pre-assembly:	1hr.	-	-	-	-
Time, Site-assembly:	1hr.	-	-	-	-

**Notes:** (a.) Source of Total is project receipts and site visits 2014 – 2016.

This appended *Chapter* presents the theoretical analysis workflows developed for an increased understanding of the different load tests.\*

## Calculations – Theoretical

**Table C.1 Theoretical – Analysis: Load Tests.**

(Units: cm)

4-point Flexure	(C-5)	<i>Derived for project use; appropriate for general use.</i>
3-point Flexure	(C-7)	
Partial-span Uniform Distributed Load	(C-8)	<i>Derived for project use; appropriate for general use.</i>
Full-span Uniform Distributed Load	(C-8)	

### Overview

#### Analytical predictions for beam performance:

The ultimate goal was to predict, by way of beam analysis, how the different specimens in each generation would behave under service conditions. As service conditions could entail any combination of dynamic loading, here it is presumed to mean simply supported with a constant duration uniformly distributed load (UDL). UDL is, of course, an industry convention as a model for service conditions. Naively, one might expect that predictions for deflection and maximum load could thus be computed quite easily by:

- Calculating theoretical second moments of area  $I$  for each specimen cross section (using, say, polylines and "AreaMoments" command in Rhino),
- Using published values for moduli of elasticity (MOE) and moduli of rupture (MOR), and
- Substituting these into the formulas for the full-span UDL, which begin with Equation (A38).

However, this approach gives predictions for performance that are between one and three orders of magnitude greater than real world test results (some have been located in results for contrast). This is believed to be due to the calculated  $I$ , which naively idealizes the assembly cross section as a continuous material, like cast metal or concrete. Unfortunately the specimens were not grown-in-place or cast molten plywood, but cut from plywood sheets and assembled with common cabinet, deck screws, or pin nails. As such, a ply five inches from the cross section's centroid does not quite bend about the theoretical centroid, but rather at some point nearer to its own internal centroid. The overall effect is that the geometric contribution to rigidity is less than anticipated by the theoretical  $I$ .

A more accurate analysis could be conducted by modeling each plywood sheet and fastener separately. Because of the complexity of such a task, it is left for future computational or numerical scope. Instead, a simpler approach is employed that resurrects 1D beam analysis.  $I$ , as second moment of area, still represents the geometric contribution to rigidity in the 1D beam equations, so an *effective* second moment of area was sought by testing each specimen.

\* Over the course of the project, two people collaborated regularly for extended periods and made important contributions. In the spring and summer of 2016, Keldin Serghyev contributed technically by coding the computational elastica tool and helping to expand the theoretical stress analysis workflows. In the fall of 2015, Yundong Yang contributed creatively and physically on the installation as part of an elective studio.

Using this  $I_{eff}$ , steps 2 and 3 of the scheme above may still be used. This section basically serves to arrange all the pieces necessary to perform that analysis. Predictions for failure load and deflection for each test are presented, followed by an extraction of  $I_{eff}$  from the experimental data.

### Test Selection

Because of the prototype-driven process, not all specimens were able to be tested identically. Most were tested as beams (transverse loading), and some were tested as columns (axial loading). This section clarifies those specimens tested as beams, as not all could be tested under identical beam load conditions. The four point flexure test was the default, but to accommodate the GEN.2 Invert and GEN.3, different conditions were necessary. Because of the curvature of the GEN.2 Invert specimen, a three point test setup was employed, and the GEN.3 specimen necessitated an open air load test because no available hydraulic press was far enough from a wall to center the specimen.

In spite of the educational variety of tests used, some of the derivations remain common to all the tests and specimens. These common derivations are discussed first, followed by the derivations and calculations specific to each testing condition. Derivations common to all tests have been marked “All tests”.

#### All tests: Calculating theoretical failure load:

In static equilibrium, the magnitude of the moment due to bending is equal to the magnitude of the moment due to the applied load:

$$M_b = M_p \quad (S1)$$

Combining this with Equation (A4), we get the following:

$$M_p = \frac{EI}{r} \quad (S2)$$

This relation is true regardless of the loading condition used, so long as  $M_p$  is replaced with a function  $M_p(x)$  that is applicable to the specific loading condition. All expressions relevant to this research, and for  $M_p(x)$ , begin with Equation (A19), which can be found in the Index – Equations. Moment due to load always includes the total load  $P$  as a factor (or can be rearranged to include  $P$ ), so some rearranging of Equation (S2) will yield a formula for the failure load as a function of the radius of curvature. If we knew the radius at failure (i.e., the minimum allowable radius), then we could stop here.

However, we are typically equipped with a value for the flexural strength rather than one for the minimum allowable radius. Therefore, we seek to clarify the relationship between total load and internal stress. Equation (S2) can be written in terms of stress if we recall from the derivation of bending moment (A5) that:

$$\sigma_b = \frac{Eu}{r} \quad (S3)$$

Using this to write a stand-in for  $r$  in Equation (S2) and rearranging, we get a standard expression for the moment due to the load in terms of the bending stress:



$$M_P(x) = \frac{I\sigma_b}{u} \quad (S4)$$

This derivation can go no further without picking a specific expression for  $M_P(x)$ , so it is left to be resumed later for each of the four loading conditions. After the particular  $M_P(x)$  is substituted in, we get an expression for the predicted failure load as a function of bending stress.

All tests: Calculating theoretical deflection of beam:

We calculate the theoretical deflection of the beam due to the external load by following the standard Euler-Bernoulli beam analysis. Again going back to Equation (S2), we recognize that for small deflections  $\Delta$ , the curvature  $1/r$  may be approximated as  $d^2\Delta/dx^2$ . This allows us to write:

$$M_P = EI \cdot \frac{d^2\Delta}{dx^2} \quad (S5)$$

To get an ordinary differential equation (ODE) in  $x$ , we substitute in an expression for the moment as a function of  $x$ . The solution  $\Delta(x)$  can be found by integrating twice:

$$\Delta(x) = \frac{1}{EI} \iint M_P(x) dx^2 \quad (S6)$$

Calculating these integrals will of course result in two constants of integration. In general (i.e., regardless of loading condition), we can make use of the following pieces of information to eliminate them:

- Both  $\Delta(x)$  and  $d\Delta/dx$  must be continuous.
- All the loading conditions used in this research were symmetric, which implies that the derivatives  $d\Delta/dx$  at  $x = 0$  and  $x = L$  have opposite sign but equal magnitude.
- Symmetry of the loading conditions also implies that the maximum deflection is at midspan, so that  $d\Delta/dx$  is zero at midspan.
- The deflection is defined as zero at the supports;  
 $\Delta(0) = \Delta(L) = 0$ .

Regardless of the loading condition, we always end up with a formula for the deflection of the beam that has the following form:

$$\Delta(x) = \frac{PL^3}{EI} G(x) \quad (S7)$$

Where  $G(x)$  is a dimensionless function of geometry that's unique to each loading condition,  $G(x)$  for each loading condition will be derived.

All tests: Effective Second Moment of Area and the Load vs. Deflection curve slope:

We may rearrange Equation (S7) and differentiate to get an expression for the anticipated slope of the load vs. deflection curve:

$$\frac{dP}{d\Delta} = \frac{EI}{L^3G} \quad (S8)$$

This slope is constant in the region where  $E$  is constant – i.e., the proportional zone. Since  $E$ ,  $L$ , and  $G$  are constants for a given specimen, loading condition, and location of deflection measurement; we presume that if we extract the slope from the experimental load and deflection data for each specimen, we can use it to instead calculate the second moment of area (appearing in the numerator) that is actually contributing to the assembly's rigidity. In other words, rearrange Equation (S8) to solve for  $I_{eff}$ :

$$I_{eff} = \frac{L^3G}{E} \cdot \left( \frac{dP}{d\Delta} \right)_{experiment} \quad (S9)$$

As touched on before, this abstraction allows us to lump all the imperfections of specimen assembly into one quantity,  $I_{eff}$ , which can then be used to make more realistic predictions about how each specimen would behave under loading conditions other than those used in its flexure test. Thus  $I_{eff}$  has the added benefit of permitting comparison of performance between specimens that were tested under different conditions.

#### 4-point Flexure

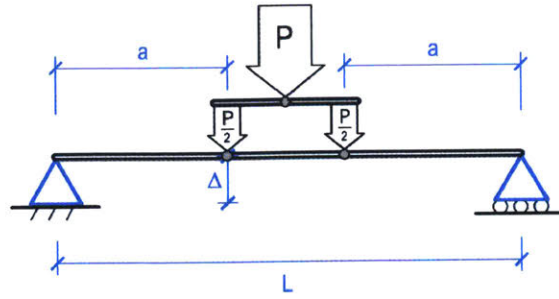


Fig. C.1 Load Test – 4-point Flexure

#### 4-point Flexure: Calculating theoretical failure load:

The four point flexure test features a larger swath of constant applied moment between two press heads, which is, of course, one of its distinguishing advantages. This can be seen in the expression for the moment in Equation (A19). Between  $x = a$  and  $x = (L - a)$ , the moment due to the load is the product of half the total load  $P$  (i.e., the load applied by one press head) and the moment arm  $a$ . Therefore, substituting into Equation (S4), we may write:

$$\frac{P}{2}a = \frac{I\sigma_b}{u} \quad (S10)$$

Then solve for the total load:

$$P = \frac{2I\sigma_b}{au} \quad (S11)$$

The most extreme fiber in tension is said to be a distance  $u_{tc}$  from the neutral axis of the cross section. We assume the member fails when the bending stress in this fiber exceeds the flexural strength of plywood, so we substitute the modulus of rupture for the bending stress  $\sigma_b$ . Thus we arrive at a prediction for the load that causes failure:

$$P_{fail} = \frac{2I \cdot MOR}{au_{tc}} \quad (S12)$$

#### 4-point Flexure: Calculating theoretical deflection of beam:

From Equation (A19), we get the moment due to the load in a four point flexure test:

$$\left(\frac{2}{P}\right) \cdot M_P(x) = \begin{cases} x, & x \in [0, a] \\ a, & x \in (a, L - a] \\ L - x, & x \in (L - a, L] \end{cases} \quad (S13)$$

Integrating this equation twice yields a formula for the deflection as a function of  $x$ , which can also be found in appendix A as Equation (A20). For  $0 \leq x \leq a$ , we get the following equation for deflection:

$$EI \left(\frac{12}{P}\right) \cdot \Delta(x) = (3aL - 3a^2)x - x^3 \quad (S14)$$

The location of maximum deflection is at midspan,  $x = L/2$ . However, in the four point tests on GEN.0, GEN.1, and GEN.2, the displacement of the press head was the actual measured quantity, which corresponds to  $x = a$ , or equivalently  $x = L - a$ , rather than midspan. We therefore only need concern ourselves with the deflection at  $x = a$ :

$$\Delta(a) = \left( \frac{P}{12EI} \right) (3a^2L - 4a^3) \quad (\text{S14})$$

Which, in the style of Equation (S7), we may write more concisely as:

$$\Delta(a) = \frac{PL^3}{EI} G(a) \quad (\text{S15})$$

Where

$$G(a) = \frac{a^2}{12L^3} (3L - 4a) \quad (\text{S16})$$

### 3-point Flexure

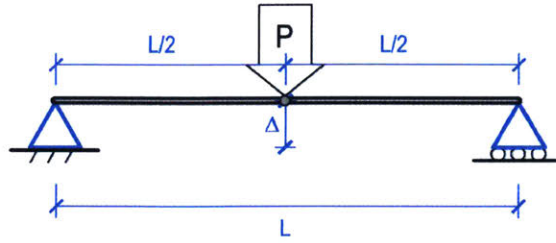


Fig. C.2 Load Test – 3-point Flexure

While the equations for the three point flexure test could be arrived at by beginning the Euler-Bernoulli beam analysis from scratch, it is much easier to simply take the limit of the four point flexure equations as the moment arm  $a$  approaches midspan  $L/2$ . Since the equations for the three point flexure test are available in most textbooks on statics, but the four point flexure equations are not, taking this limit serves more to confirm the veracity of the four point flexure equations presented herein.

3-point Flexure: Calculating theoretical failure load:

We need only take the limit of Equation (S12) as  $a \rightarrow L/2$ :

$$\lim_{a \rightarrow L/2} P_{fail} = \lim_{a \rightarrow L/2} \left[ \frac{2I \cdot MOR}{au_{tc}} \right] \quad (S17)$$

$$P_{fail} = \frac{4I \cdot MOR}{u_{tc}} \quad (S18)$$

3-point Flexure: Calculating theoretical deflection of beam:

For  $0 \leq x \leq L/2$ , we get the following equation for deflection by taking the limit of as  $a \rightarrow L/2$ :

$$\lim_{a \rightarrow L/2} \left[ \frac{2EI}{P} \cdot \Delta(x) \right] = \lim_{a \rightarrow L/2} [(3aL - 3a^2)x - x^3] \quad (S19)$$

$$\frac{2EI}{P} \cdot \Delta(x) = \frac{1}{24} (4x^2 - 3L^2)x \quad (S20)$$

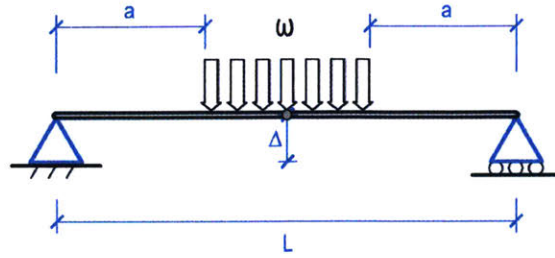
And at midspan, which is the location of the press head, the deflection becomes the familiar expression:

$$\Delta\left(\frac{L}{2}\right) = \frac{PL^3}{EI} G\left(\frac{L}{2}\right) \quad (S21)$$

Where

$$G\left(\frac{L}{2}\right) = \frac{1}{48} \quad (S22)$$

**Partial-span – Uniformly Distributed Load (PUDL)**



**Fig. C.3 Load Test – PUDL**

Partial-span UDL: Calculating theoretical failure load:

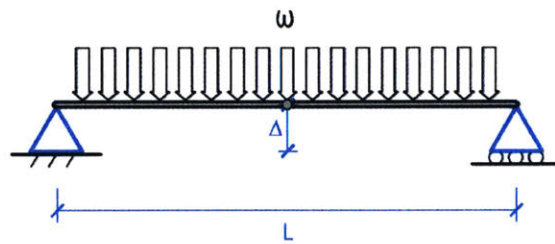
We again start with Equation (S4), and substitute in for  $x$  the second regime of Equation (A34) for the maximum moment for  $M_p$ , which occurs at midspan.

$$\left(\frac{2}{\omega}\right) M_p = (a^2 - Lx + x^2) \quad (S23)$$

$$M_p = \left(\frac{\omega}{2}\right) (a^2 - Lx + x^2) \quad (S24)$$

$$\frac{I\sigma_b}{u} = \left(\frac{\omega}{2}\right) (a^2 - Lx + x^2) \quad (S25)$$

**Full-span – Uniformly Distributed Load (UDL)**



**Fig. C.4 Load Test – UDL**

Full-span UDL: Calculating theoretical failure load:

We again start with Equation (S2), and substitute in the maximum moment for  $M_p$ , which occurs at midspan.

$$\left(\frac{2}{\omega}\right) M_p = -Lx + x^2 \quad (S26)$$

$$\frac{I\sigma_b}{u} = \left(\frac{\omega}{2}\right) (-Lx + x^2) \quad (S27)$$

# Calculations – Pre-test

DL: 20psf (Self-Wt.)  
 LL: 40psf (Residential)  
 SL: 40psf (Snow/Wind)

Density (lb./in.<sup>3</sup>)  
 Density (lb./ft.<sup>3</sup>)  
 ECC (CO<sub>2</sub>e/lb.)  
 σ (compression)  
 σ (tension)  
 σ (shear)  
 σ (bending)  
 E (M.O.E.)

	WOOD	PLY.	STEEL	6061 ALUM.	FIBER CARBON
Density (lb./in. <sup>3</sup> )	0.019	0.019	0.284	.10	.06
Density (lb./ft. <sup>3</sup> )	33 lb.	33 lb.	490.75 lb.	167 lb.	104 lb.
ECC (CO <sub>2</sub> e/lb.)	0.04	0.04	0.8	10	15
σ (compression)	1 ksi	1 ksi	25 ksi	19 ksi	20 ksi
σ (tension)	1.2 ksi	1.2 ksi	25 ksi	19 ksi	20 ksi
σ (shear)	0.6 ksi	0.433 ksi	12.5 ksi	0 ksi	10 ksi
σ (bending)	1.2 ksi	1.125 ksi	24 ksi	12 ksi	15 ksi
E (M.O.E.)	1600 ksi	1600 ksi	29000 ksi	10000 ksi	18000 ksi

**SHEAR (36" O.C.):**  
 Ry = W/2  
 18000 lb./2  
 Ry1 = 9000 lb.  
 Ry2 = 9000 lb.

**MOMENT (20' @ 36" O.C.):**  
 TW: 36 in.  
 TA: 36 in. • 240 in. = 8640 in.<sup>2</sup>  
 8640 in.<sup>2</sup>/144 in.<sup>2</sup> = 60 ft.<sup>2</sup>  
 60 ft.<sup>2</sup> • 100 psf = 6000 lb.  
 300 plf x 1.0 (S.F.) = 300plf  
 300 plf x 20 ft. = 6000 lb.  
 0.3 klf x 20 ft = 6k

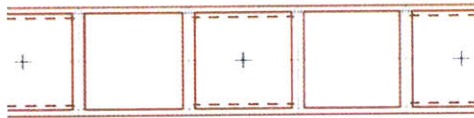
$$M_{max} = \frac{w \cdot L^2}{8} = \frac{0.3 \text{ klf} \cdot 20 \text{ ft.}^2}{8} = 15000 \text{ lbf-ft.} = 180000 \text{ lbf-in.}$$

$$M = \frac{0.3 \text{ klf} \cdot 20 \text{ ft.}^2}{8} = 15 \text{ k-ft.} \rightarrow = 180 \text{ k-in.}$$

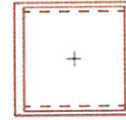
$$\sigma_{bend} = 1.2 \text{ ksi} = \frac{180 \text{ k-in.}}{S_{req}} = \frac{180 \text{ k-in.}}{1.2 \text{ ksi}_{allow}} = 150 \text{ in.}^3_{req}$$

SECT. MODULUS - SQUARE:

$$S_{square} = \frac{g^3}{6} = \frac{9^3}{6} = 121.5 \text{ in.}^3 = \text{NO (NEED COVERPLATES @ 36" O.C.)}$$



SECT. MODULUS - HOLLOW:



$$S_{net} = S_{gross} - S_{void}$$

$$S_{net} = \frac{B \cdot H^2}{6} - \frac{b \cdot h^2}{6}$$

$$= \frac{9.75 \cdot 9.375^2}{6} - \frac{8.25 \cdot 8.625^2}{6 \cdot 9.375}$$

$$S_{net} = 48.72 \text{ in.}^3 \text{ (LOW)}$$

$$I = 48.72 \text{ in.}^3 \cdot 4.675 \text{ in.} = 228.36 \text{ in.}^4 = \frac{B \cdot H^3 - b \cdot h^3}{12}$$

$$S_{net} = \frac{I}{y} \quad \leftarrow y \text{ (to N.A.)}$$

$$S_{-2x12} = 77.8 \text{ in.}^3 \cdot 4.675 \text{ in.} = 364.69 \text{ in.}^4$$

**MOMENT, ATYP. (20' @ 18" O.C.):**

TW: 18 in.  
 TA: 18 in. • 240 in. = 4320 in.<sup>2</sup>  
 4320 in.<sup>2</sup>/144 in.<sup>2</sup> = 30 ft.<sup>2</sup>  
 30 ft.<sup>2</sup> • 100 psf = 3000 lbs.  
 150 plf • 1.0 (S.F.) = 150 plf  
 150 plf • 20 ft. = 3000 lbs.  
 0.15 klf • 20 ft. = 3k

$$M_{max} = \frac{w \cdot L^2}{8} = \frac{0.15 \text{ klf} \cdot 20 \text{ ft.}^2}{8} = 7500 \text{ lbf-ft.} = 90000 \text{ lbf-in.}$$

$$M = \frac{0.15 \text{ klf} \cdot 20 \text{ ft.}^2}{8} = 7.5 \text{ k-ft.} \rightarrow = 90 \text{ k-in.}$$

$$\sigma_{bend} = 1.2 \text{ ksi} = \frac{90 \text{ k-in.}}{S_{req}} = \frac{90 \text{ k-in.}}{1.2 \text{ ksi}_{allow}} = 75 \text{ in.}^3_{req}$$

$$77.8 \text{ in.}^3 > 75 \text{ in.}^3 \therefore \text{O.K. (BARELY)}$$

TARGET for 2x9 = 180in (vs. assumed 240in)

**MOMENT, TYP. (15' @ 18" O.C.):** Avg. (2x8 & 2x10)

TW: 18 in.  
 TA: 18 in. • 180 in. = 3240 in.<sup>2</sup>  
 3240 in.<sup>2</sup>/144 in.<sup>2</sup> = 30 ft.<sup>2</sup>  
 22.5 ft.<sup>2</sup> • 100 psf = 2250 lb.  
 150 plf • 1.0 (S.F.) = 150 plf (S.F. in MOE)  
 150 plf • 15 ft. = 2250 lb.  
 0.15 klf • 15 ft. = 2.25 kips

$$S_{+2x14} = 64.15 \text{ in.}^3 \quad I_{+2x14} = 64.15 \text{ in.}^3 \cdot 4.675 \text{ in.} = 300.72 \text{ in.}^4$$

$$M = \frac{0.15 \text{ klf} \cdot 15 \text{ ft.}^2}{8} = 4218 \text{ lbf-ft.} = 50625 \text{ lbf-in.}$$

$$M = \frac{0.15 \text{ klf} \cdot 15 \text{ ft.}^2}{8} = 4.22 \text{ k-ft.} \rightarrow = 50.63 \text{ k-in.} = \frac{50.63 \text{ k-in.}}{1.2 \text{ ksi}_{allow}} = 42.19 \text{ in.}^3_{req}$$

$$64.15 \text{ in.}^3 > 42.19 \text{ in.}^3 \therefore \text{O.K. (34.2%)}$$

Fig. B.2 Beams – GEN.0\_Box, Hybrid: Pre-test Analysis.

The above pre-test analysis suggests a span of L: 180" and 18" on center is viable in bending with reinforcement.

This appended *Chapter* contains the raw data and observation logs kept for the scale model play-tests, and the full scale pre-tests, and tests.

**Data – Pre-test**

**Table D.1 Pre-test – Elastica: Data.**

(Units: cm)

#.	<i>Span (L), Elastica Min. Radius (e).</i>	
1.	[L152.6, e∞]	11. [L109.1, e42.9] 21. [L62.3, e27.5] 31. [L6.9, e18.9]
2.	[L148.4, e145.6]	12. [L104.2, e40.4] 22. [L56.2, e26.3] 32. [L3.5, e18.5]
3.	[L144.6, e105.0]	13. [L100.5, e38.7] 23. [L49.9, e25.1] 33. [L1.6, e18.3]
4.	[L139.1, e80.3]	14. [L96.5, e37.0] 24. [L44.3, e24.2] 34. [L0.0, e18.1]
5.	[L135.2, e70.4]	15. [L91.3, e35.1] 25. [L38.6, e23.3]
6.	[L130.6, e62.2]	16. [L86.7, e33.6] 26. [L35.1, e22.7]
7.	[L127.0, e57.4]	17. [L81.8, e32.2] 27. [L28.8, e21.8]
8.	[L122.8, e52.9]	18. [L77.2, e30.9] 28. [L23.0, e21.0]
9.	[L118.7, e49.3]	19. [L72.1, e29.7] 29. [L17.7, e20.3]
10.	[L114.1, e45.9]	20. [L67.8, e28.7] 30. [L11.3, e19.5]

**Notes:** (a.) *Arclength ( ℓ )*: [152.4] + [0.2] *slot of brass sleeve* = [L152.6]

**Log – Observations**

**Observations (Project)**

O1: For bending-active structures, that the GEN.2 and GEN.3 specimens were stiff, and did significant work seems sufficient for general worth. Required with active bending is detailed analysis of physics and specimens to confirm the viability and these can be gained. Inherently there are advantages in terms of geometric capacity, and disadvantages in terms of monitoring residual stress closely so what more is there to say? We begin work now on their revision for repetition and production.

O2: To understand their potential as assemblies there has also been progress, and to do the same as aggregations will require a comprehensive analysis of the global physics and specific applications. This is future geometric work to clarify at what scales they can be significant. This project focused on investigating if they could be systematized for a specific application and moves on to their architectural potential at scale. And if it helps them to catch on it will make this it easier!



This appended *Chapter* presents the theoretical analysis workflow developed for an increased understanding of the elastica.\*

**Methods – Elastica**

**Motivation**

Structural design, structural analysis, and the rating of both bending-active assemblies and structures require a detailed understanding of the physics of the individual members.

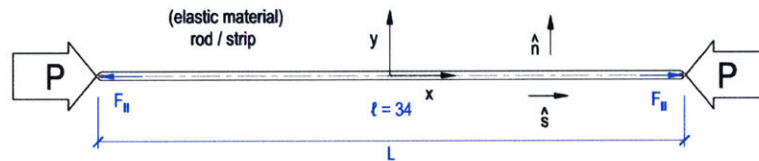
The designer is chiefly concerned with the maximum curvature (minimum radius) that a sheet of material can safely maintain, and the load (residual stress capacity that the sheet can support once it is in a post-buckled/flexural state). Or, given a form already decided upon, what material and thickness ought to be selected to safely realize that structure. For structural analysis and rating, the requirement of understanding deepens.

The effect of a distributed load across a bending-active structure requires knowledge of the stresses and strength at every point. Our goal is therefore to answer the following questions:

- What is the radius of curvature for any point in a bending-active member?
- What are the stresses at any point in a bending-active member?
- What safety limits can we impose on a bending-active member?

**Selection of a Simple Analogue**

Understanding the physics of bending-active members begins with selection of a simple analogue that exhibits only the key physics and neglects the rest. Several candidates for a simple analogue immediately come to mind: the slender column, the cantilevered beam, the simply supported beam, the simply supported chain, and finally, the purely elastic rod.



**Fig. E.1 Elastica: Unbuckled State**

Our analysis begins with the consideration of a purely elastic rod, herein called the “elastica,” and distinct from the geometric “elastica curve.” The elastica is a homogeneous cylinder of a length far exceeding than its radius, and therefore primarily a one-dimensional object with negligible mass. This is a step towards understanding bending-

\* Over the course of the project, two people collaborated regularly for extended periods and made important contributions. In the spring and summer of 2016, Keldin Serghyev contributed technically by coding the computational elastica tool and helping to expand the theoretical stress analysis workflows. In the fall of 2015, Yundong Yang contributed creatively and physically on the installation as part of an elective studio.

Stress  $\sigma$  is directly proportional to strain  $\varepsilon$ , for both positive (i.e., tensile) stresses and negative (i.e., compressive) stresses. The constant of proportionality is the elastic modulus,  $E$ , which is constant throughout the material. Thus we may write:

$$\sigma = E\varepsilon \tag{E1}$$

Because it is elastic, all deformations are completely reversible if the external load causing them is removed. This ability or property to store strain energy and deflect under load is known as resilience, which is defined as the amount of strain energy which can be stored without causing permanent damage [Gordon 2003, p.90].

This simple analogue serves well for three reasons.

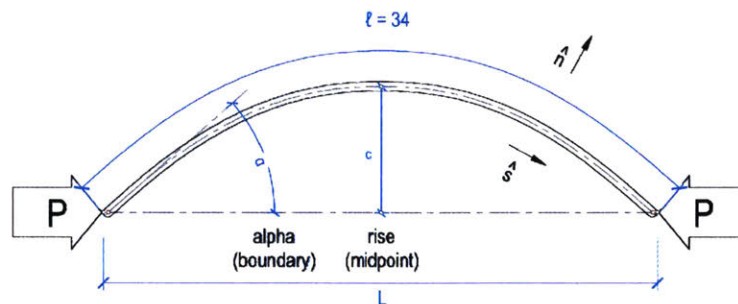
Firstly, all real materials (plywood included) are elastic up to a certain limit, and all structures in stable equilibrium have restorative forces that can be approximated by Hooke's law around the equilibrium point.

Secondly, for the materials proposed for use in bending-active structures, such as plywood, the loads applied are much larger than the static load due to the material's mass. And thirdly, while a sheet of plywood is obviously not a one-dimensional object, it can be modeled as many thin plywood elastica lined up side by side.

**Introduction to the Elastica: Setup**

Consider an elastic rod of length  $\ell$  centered on the  $x$ -axis, so that the ends are initially at  $x = \ell \pm / 2$ . Suppose that a force  $P$  is applied to one end of the rod in the  $\hat{x}$  direction, in this case by the operable head of a hydraulic press, and an equal and opposite force applied to the other end by the static bed of the press. In this configuration, the forces are collinear in what is called the loading axis, and the rod experiences pure compression.

Once sufficient force (the Euler critical buckling load) is applied, a small perturbation will cause the rod to buckle outward from the loading axis into the  $\hat{y}$  direction. Therefore, we may use  $y$  to measure the excursion of any point on the elastica from the loading axis. The function  $y = f(x)$  that describes the shape of the elastica is called the elastica curve.



**Fig. E.2 Elastica: Buckled State – 1**

In its post-buckled state, the distance from one end of the elastica to another, measured along the curve, is called the arclength  $s$ , and the total arclength is the rod length  $\ell$ . The total length of the chord between the two ends of the rod is called the span  $L$ , and the distance along this chord (which is collinear with the  $x$ -axis) is called the displacement. The point of maximum excursion is called the rise, which we call  $c$  after Euler's notation.

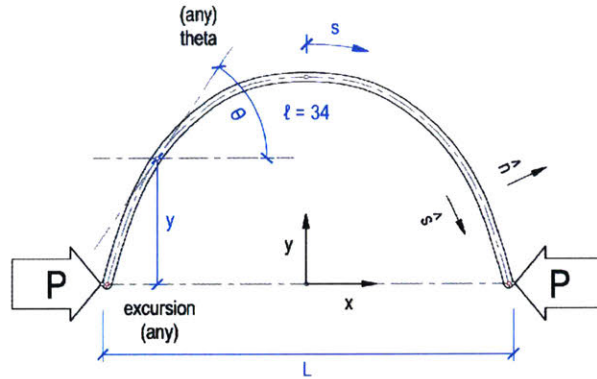


Fig. E.3 Elastica: Buckled State – 2

### Consideration of Statics Produces Differential Equation

Now that our coordinate system is established, we apply statics to arrive at a differential equation which, when solved, describes the shape of the elastica. When the force applied by the hydraulic press remains constant, the elastica settles into a constant shape. In static equilibrium, the sum of all concurrent forces and moments must be zero. We may write:

$$\Sigma F = 0 \quad (E2)$$

$$\Sigma M = 0 \quad (E3)$$

We analyze the moments, beginning with the moment  $M_l$  imposed by the load. At any point on the elastica, this moment is equal to the product of the force acting on the ends of the rod and length of the moment arm between the force and the point. The magnitude of this moment arm is just the point's excursion. Thus:

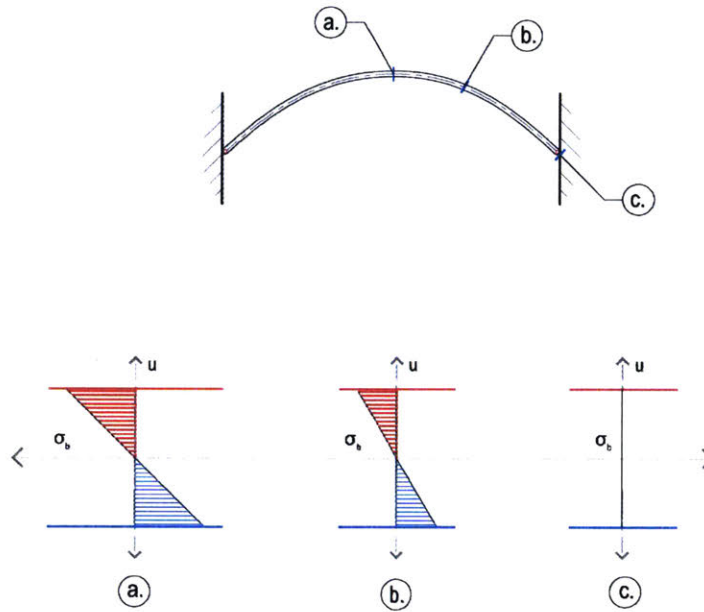
$$M_p = P \cdot y \quad (E4)$$

Next, to find the moment generated internally by the material, we focus on an infinitesimal slice of the elastica, such as *Figure E.5*, located following step (E10). At this scale, the curve is an arc of a circle, with radius  $r$  and arclength  $s$ . We assume there are some neutral surface of fibers somewhere in the middle of the rod that are neither in compression nor tension, and that it is these fibers with the arclength  $s$ , while the arclength of the other fibers are either more or less than  $s$ . For any fiber on the compression side, we see that the arclength is  $s - \delta s$ , and on the tension side, the arclength is  $s + \delta s$ . We may write:

$$s = \theta r \quad (E5)$$

$$s + \delta s = \theta(r + u) \quad (E6)$$

The flexural stress at three locations along the length is represented on the following page in *Figure E.4*.



**Fig. E.4 Elastica: Stress profile at three locations**  
(see also the detail in *Figure E.5*)

Thus, the strain of a fiber a distance  $u$  from the neutral fiber is:

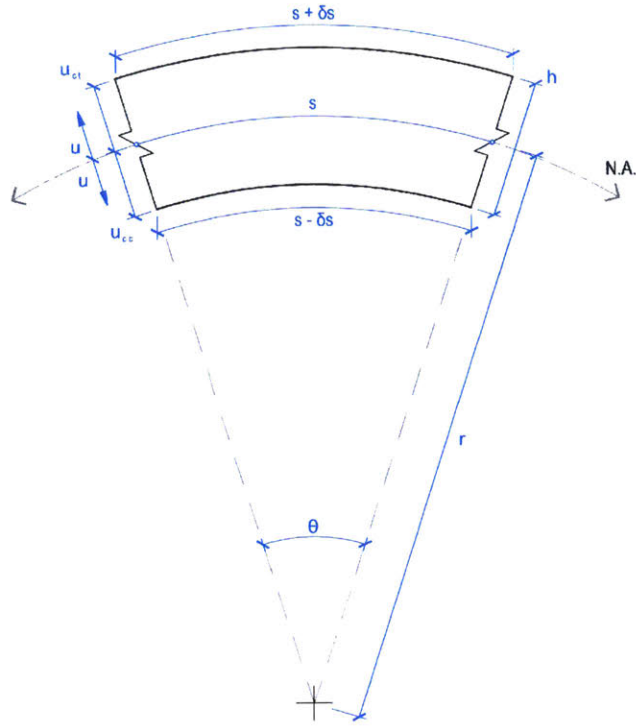
$$\varepsilon = \frac{\delta s}{s} \quad (\text{E7})$$

$$\varepsilon = \frac{(s + \delta s) - s}{s} \quad (\text{E8})$$

$$\varepsilon = \frac{\theta u}{\theta r} = \frac{u}{r} \quad (\text{E9})$$

Using Equation A3 (E1) and (E9), we may now write the stress due to bending at any point as:

$$\sigma_b(u) = \left(\frac{u}{r}\right) E = \frac{E}{r} u \quad (\text{E10})$$



**Fig. E.5 Elastica: Infinitesimal Slice and Nomenclature**  
(Detail.)

The infinitesimal bending moment at any fiber  $u$  away from the neutral fiber is:

$$dM_b = u \cdot \sigma_b \cdot dA \quad (\text{E11})$$

Thus, the total moment generated by all fibers in the rod is:

$$\int dM_b = \int u \sigma_b dA \quad (\text{E12})$$

Using Equation (E10),

$$M_b = \int u \left( \frac{E}{r} u \right) dA \quad (\text{E13})$$

But  $E/r$  is invariant within a given section of the rod, so the integral becomes:

$$M_b = \frac{E}{r} \int u^2 dA \quad (\text{E14})$$

The remaining integral is a purely-geometric parameter of the rod cross section known as the second moment of area  $I$ . Therefore, the bending moment is:

$$M_b = \frac{EI}{r} \quad (\text{E15})$$

By Equation (E4), we know that the bending moment and the moment due to loading must balance:

$$M_P + M_b = 0 \quad (\text{E16})$$

Therefore, we may write:

$$\frac{EI}{r} = -Py \quad (\text{E17})$$

This is significant because it relates the radius of curvature with the excursion of any point on the elastica.

Next we move to expressing this equation in one function. We note that Equation (E5) in differential form gives us:

$$\frac{d\theta}{ds} = \frac{1}{r} \quad (\text{E18})$$

We may now write Equation (E17) as:

$$EI \frac{d\theta}{ds} = -Py \quad (\text{E19})$$

Based on our coordinates defined in Figure (E.3) and Figure (E.5), we can get  $y$  from noting that:

$$\frac{dy}{ds} = \sin \theta \quad (\text{E20})$$

To use this fact, we differentiate Equation (E19) with respect to the arclength  $s$  and substitute:

$$EI \frac{d^2\theta}{ds^2} = -P \sin \theta \quad (\text{E21})$$

And thus we get the elastica equation:

$$\frac{d^2\theta}{ds^2} = -\frac{P}{EI} \sin \theta \quad (\text{E22})$$

This is a nonlinear second order ODE without an analytical solution. This poses an additional challenge to solving the elastica problem, and thus an extra barrier to the proliferation of bending-active structures. The prevailing attitude in structural engineering is that it's easier not to bend at all, or, failing that, bend as little as possible.

### Solving the Elastica Equation

For most engineering applications, bending is minimized, which allows us to reason that the angle  $\theta$  is small, which thus warrants replacing  $\sin \theta$  with the first term from its Taylor expansion about zero:

$$\sin \theta \approx \theta \quad (\text{E23})$$

This approximation makes the equation a familiar second order ODE, and the solution consists of sinusoids. This is a familiar path, because Equation (E22) applies to other physical phenomena, such as the angle of the undamped pendulum. Analysis of the pendulum conventionally employs the small angle approximation, and the sinusoidal solution is accepted.

This solution is unacceptable because the bending-active proposals herein exhibit angles that are too large for the small angle approximation to be valid. One might begin to approach the problem of larger angles (for bending-active members or for pendula) by trying to use additional terms from sine's Taylor expansion. But unfortunately, this quickly makes the differential equation nonlinear once again. Beléndez et al. 2007 show that an exact solution for the undamped pendulum can be expressed in terms of elliptic functions and elliptic integrals. Pacheco & Piña 2007 go through a similar analysis for the elastica. We follow the derivation in Pacheco & Piña here.

First we introduce a dimensionless arclength  $\tau$ :

$$\tau = s \sqrt{\frac{P}{EI}} \quad (\text{E24})$$

This allows us to write Equation (E22) in dimensionless form as:

$$\frac{d^2\theta}{d\tau^2} = -\sin \theta \quad (\text{E25})$$

If both sides are multiplied by  $\frac{d\theta}{d\tau}$ , one integration is possible, which gives:

$$\frac{1}{2} \left( \frac{d\theta}{d\tau} \right)^2 = \cos \theta + C \quad (\text{E26})$$

Here,  $C$  is the constant of integration. We use half-angle identities to express this as:

$$\frac{1}{2} \frac{d\theta}{d\tau} = \pm \sqrt{k^2 - \sin^2 \frac{\theta}{2}} \quad (\text{E27})$$

Where we abandon a complicated expression for  $C$  in favor of  $k$ , as  $k$  takes on significance later. Pacheco & Piña walk through additional steps necessary to arrive at the following solution:

$$\sin \frac{\theta}{2} = -k \operatorname{sn}(\tau, k), \quad (\text{E28})$$

The solution makes use of  $\operatorname{sn}$ , the Jacobi elliptic function, and  $k$  has now taken on the role of the elliptic modulus. We may rearrange to get an expression for the angle:

$$\theta(\tau) = 2 \sin^{-1}[-k \operatorname{sn}(\tau, k)] \quad (\text{E29})$$

This solves the elastica equation: Equation (E22). However, extra steps are necessary to get an answer in Cartesian coordinates. First, we make use of the following Jacobi elliptic function identity:

$$\operatorname{sn}^2(\tau, k) + \operatorname{cn}^2(\tau, k) = 1 \quad (\text{E30})$$

This allows us to express Equation (E27) as:

$$\frac{1}{2} \frac{d\theta}{d\tau} = -k \operatorname{cn}(\tau, k) \quad (\text{E31})$$

Using this fact and Equation (E19) now permits us to write a solution for  $y$ :

$$y(\tau) = 2k \sqrt{\frac{EI}{P}} \operatorname{cn}(\tau, k) \quad (\text{E32})$$

Now that we have a relation between  $\theta$  and  $\tau$ , we can also find a function for  $x(\tau)$ . First we recognize that, like Equation (E20), we have:

$$\frac{dx}{ds} = \cos \theta \quad (\text{E33})$$

As before, we use a half-angle identity, and then another Jacobi elliptic function identity:

$$\frac{dx}{ds} = 2\cos^2\left(\frac{\theta}{2}\right) - 1 \quad (\text{E34})$$

$$= 2\operatorname{dn}^2(\tau, k) - 1 \quad (\text{E35})$$

We can integrate this with respect to  $\tau$  to get:

$$x(\tau) = \int (2\operatorname{dn}^2(\tau, k) - 1) \frac{ds}{d\tau} d\tau \quad (\text{E36})$$

$$= \sqrt{\frac{EI}{P}} \left( 2 \int \operatorname{dn}^2(\tau, k) d\tau - \tau \right) \quad (\text{E37})$$

The integral of  $\operatorname{dn}^2(\tau, k)$  defines the incomplete elliptic integral of the second kind  $\mathbb{E}(\tau, k)$ , so  $x(\tau)$  can be written concisely as:

$$x(\tau) = \sqrt{\frac{EI}{P}} (2\mathbb{E}(\tau, k) - \tau) \quad (\text{E38})$$

We now possess parametric equations for  $y$  and  $x$  that together describe the solution of the elastica equation. However, our work is not yet complete, because we are not always equipped with  $E$ ,  $I$ , and  $P$ . Furthermore, we usually do not have  $k$ , since the elliptic modulus is not directly measurable.



### Restating Parameters in Terms of Known or Measurable Quantities

The elliptic modulus has a direct relationship with the angle at the boundary, which we call  $\alpha$  in accord with Euler's notation. This can be seen from Equation (E29). From properties of the Jacobi elliptic functions, we know that at the boundaries,  $\text{sn}(\pm\mathbb{K}(k), k) = \pm 1$ , where  $\mathbb{K}(k)$  is the complete elliptic function of the first kind. Thus, Equation (E29) becomes:

$$\sin \frac{\alpha}{2} = \pm k \quad (\text{E39})$$

For the remainder of the parameters, we can again follow the steps of Pacheco & Piña. First, we recognize that the rise  $c$  is the amplitude of  $y(\tau)$ . Therefore,  $y = c$  at  $\tau = 0$ . Using Equation (E32), this means:

$$c = 2k \sqrt{\frac{EI}{P}} \quad (\text{E40})$$

Another property of the Jacobi elliptic functions dictates that  $\text{cn}(\tau, k) = 0$  when  $\tau = \pm\mathbb{K}(k)$ . This is where  $y = 0$ , which is the end of the rod, so  $s$  must be  $\ell/2$ . Therefore, we may use Equation (E24) to write:

$$\mathbb{K}(k) = \frac{\ell}{2} \sqrt{\frac{P}{EI}} \quad (\text{E41})$$

Combining Equations (E40) and (E41) yields the following:

$$\frac{c}{\ell} = \frac{k}{\mathbb{K}(k)} \quad (\text{E42})$$

Also where  $y = 0$  and  $\tau = \mathbb{K}(k)$ ,  $x$  must be half the span  $L$ . Substituting these facts into Equation (E38), we get:

$$\frac{L}{2} = \sqrt{\frac{EI}{P}} (2\mathbb{E}(k) - \mathbb{K}(k)) \quad (\text{E43})$$

We can rearrange Equation (E41) and use it to get rid of  $E$ ,  $I$ , and  $P$  in Equation (E43):

$$\frac{L}{\ell} = 2 \frac{\mathbb{E}(k)}{\mathbb{K}(k)} - 1 \quad (\text{E44})$$

If only the arclength and span are known, this equation is particularly useful. Although it cannot be inverted to give  $k$  as a function of  $L/\ell$ , a guess and check method can be used. Or alternatively, many values of  $k$  and  $L/\ell$  can be tabulated ahead of time, which was the strategy implemented in the Octave/Matlab code used in this research to analyze the elastica. When  $L/\ell$  is given, the corresponding  $k$  can be looked up. The precision of the match is, of course, controlled by the table step size and the method of table interpolation used.

### Other Functions and Parameters of Interest: Curvature and Radius

Going back to Equation (E19), we can use our new understanding of  $y$  to get a function for curvature:

$$\frac{d\theta}{ds} = -\frac{P}{EI}y \quad (\text{E45})$$

$$= -\left(\frac{4k^2}{c^2}\right)(c \cdot \text{cn}(\tau, k)) \quad (\text{E46})$$

$$\frac{d\theta}{ds} = -\left(\frac{4k^2}{c}\right)\text{cn}(\tau, k) \quad (\text{E47})$$

The radius of curvature is the reciprocal:

$$r(\tau) = -\left(\frac{c}{4k^2}\right) \cdot \frac{1}{\text{cn}(\tau, k)} \quad (\text{E48})$$

We can find the point of maximum curvature, and thus minimum radius, by differentiating Equation (E47) (with respect to  $\tau$  or  $s$ ) and setting equal to zero:

$$0 = \left(\frac{4k^2}{c}\right)\text{sn}(\tau, k) \cdot \text{dn}(\tau, k) \quad (\text{E49})$$

In the domain of interest, this is satisfied at  $\tau = 0$ , which is midspan in our coordinate system and nicely confirms one's physical intuition. Therefore, the maximum absolute curvature is:

$$\max\left(\frac{d\theta}{ds}\right) = \frac{4k^2}{c} \quad (\text{E50})$$

And the minimum radius is:

$$\min(r) = \frac{c}{4k^2} \quad (\text{E51})$$

The sign is of little concern, so it was dropped. It is technically negative, which agrees with the clockwise rotation of  $\hat{s}$  in the  $xy$ -plane as  $s$  increases.

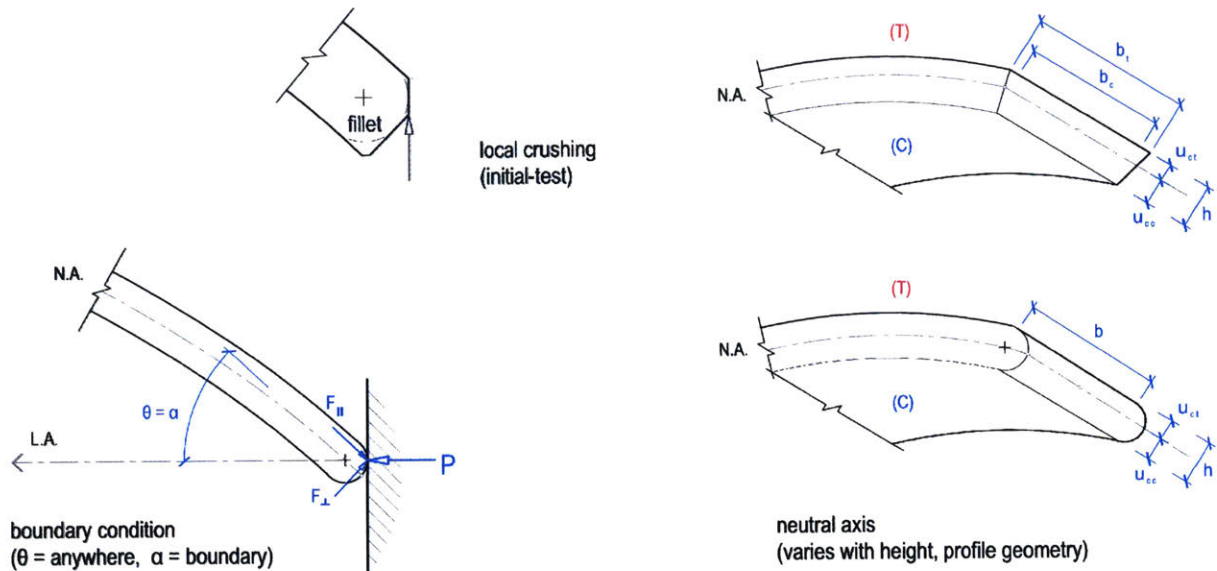


Fig. E.6 Elastica: Force  $P \rightarrow F_{||}$  and  $F_{\perp}$ , Alpha relationship

### Stresses in Bending Active Members When Modeled as Elastica

At the boundary of the elastic rod, where the external force  $P$  is applied, the angle between the rod and the  $x$ -axis is  $\alpha$ . Therefore, the reaction force parallel to the cross section of the rod is:

$$F_{||} = P \sin(\alpha) \quad (E52)$$

And the reaction force perpendicular to the cross section of the rod is:

$$F_{\perp} = P \cos(\alpha) \quad (E53)$$

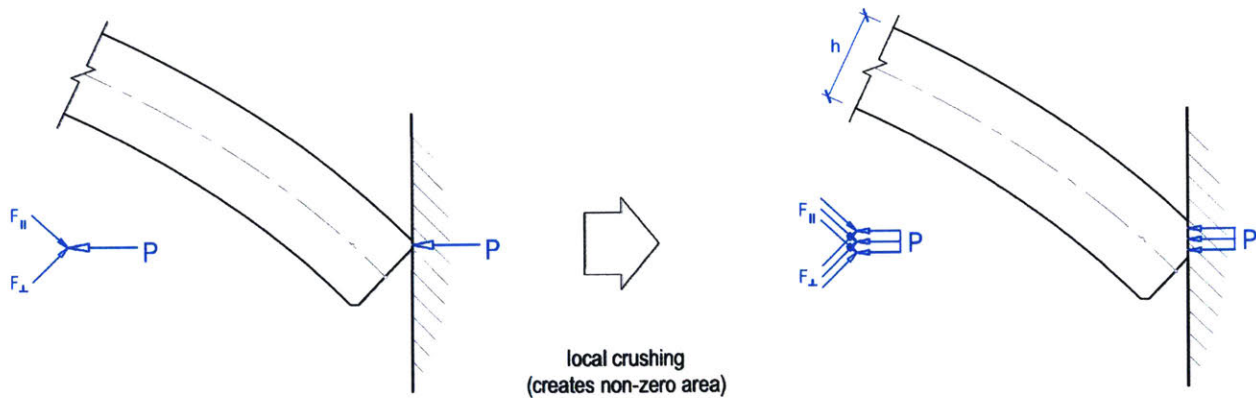


Fig. E.7 Elastica - Local Forces: (a.) Pre-test, initial and (b.) Pre-test, local crushing

If the load were perfectly concentrated along the line of contact with the hydraulic press head, then these forces would both result in shear stresses. However, in practice, the load is somewhat distributed across the edge face of the rod, due to local crushing or intentional filleting of the edges. We assume that  $F_{||}$  creates a uniform compressive stress over the area  $A$  of the face.

We are interested in the component of this compressive stress that is parallel to  $\hat{s}$  at any point along the length of the rod, which can be obtained by simply replacing  $\alpha$  in Equation (E52) with  $\theta$ :

$$\sigma_c = \frac{P}{A} \sin \theta \quad (E54)$$

According to (E22), we can rewrite this as:

$$\sigma_c = \frac{P}{A} \frac{dy}{ds} \quad (E55)$$

We can readily obtain a new expression for  $\frac{dy}{ds}$  by differentiating Equation (E32) and using the Jacobian, which is:

$$\frac{d\tau}{ds} = \frac{2k}{c} \quad (E56)$$

We thus get:

$$\frac{dy}{ds} = \frac{dy}{d\tau} \cdot \frac{d\tau}{ds} \quad (E57)$$

$$\frac{dy}{ds} = -2k \operatorname{sn}(\tau, k) \operatorname{dn}(\tau, k) \quad (E58)$$

Going back to the compressive stress, we can now write the following:

$$\sigma_c = -\frac{2kP}{A} \operatorname{sn}(\tau, k) \operatorname{dn}(\tau, k) \quad (E59)$$

From symmetry considerations, we expect the compressive stress at the midplane (i.e., the plane perpendicular to  $\hat{s}$  at  $\tau = 0$ ) to be  $P/A$

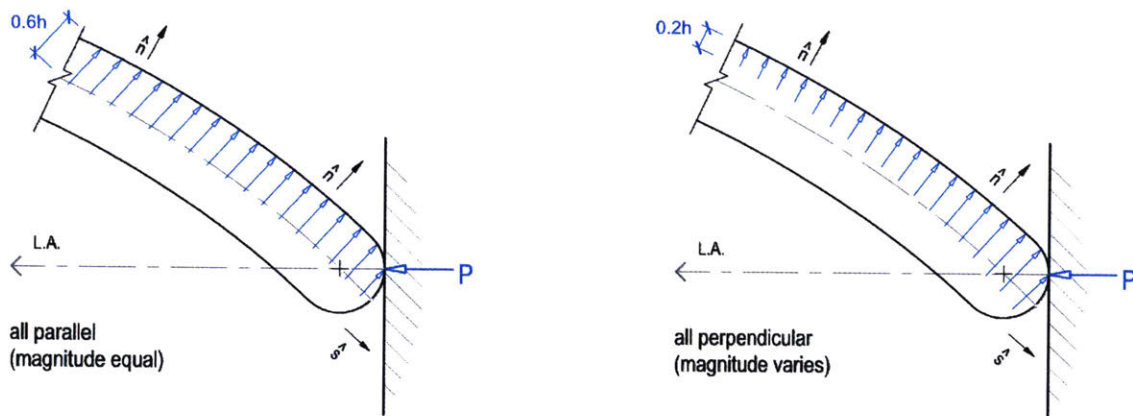


Fig. E.8 Elastica – Local Forces: (a.) Parallel, equal and (b.) Normal to Surface, reducing

Fin.